Co-agonist Regulation of Pre and Postsynaptic NMDA Receptors in the Entorhinal Cortex

Lench, Alex

Award date:
2015

Awarding institution:
University of Bath

Co-agonist Regulation of Pre and Postsynaptic NMDA Receptors in the Entorhinal Cortex

Alexander Martyn Lench

A thesis submitted for the degree of Doctor of Philosophy

University of Bath
Department of Pharmacy and Pharmacology

September 2015

Table of Contents

Figures and Tables

Acknowledgements

I would like to take this opportunity to thank all my family and friends for their help and kindness over the years. Special thanks go to my parents Teresa and Martyn, my sister Holly, my uncle Paul and my partner Georgia for all the love and support they have given me.

But the biggest thank you must go to Professor Roland Jones. During my PhD I have never had *any* doubt that I was working with the best supervisor and this time has been the most enjoyable, creative and enlightening of my life so far thanks to Roland's benevolent and nurturing mentorship.

Abstract

The NMDA receptor is a highly diverse receptor with many functions. In particular NMDA receptors present on postsynaptic spines mediate the effects of the synaptic neurotransmitter glutamate, whilst NMDA receptors present on presynaptic nerve terminals directly regulate the release of neurotransmitters. The aim of this thesis was to expand the characterisation of these two populations of NMDA receptors by examining the functional role of the co-agonist binding sites. NMDA receptors have been strongly implicated in mechanisms of cognition and also the pathophysiology epilepsy and so I have focused my study in the entorhinal cortex which is an area increasingly seen to be central to both of these phenomenon.

Initial work focussed on the endogenous regulation of the presynaptic NMDA receptors. My results indicated that the co-agonist site of these receptors was activated by D-serine and that this ligand may come from astrocytes, in contrast to the observations that others have made for postsynaptic NMDA receptors. Following this, I then characterised the effects of partial agonists of the NMDA receptor co-agonist site at each of these populations of NMDA receptors and report differential effects for the function of these receptors. Finally I then examined the effects of the co-agonist site ligands on epileptiform activity as a simple form of emergent neuronal network activity. Results from my study of co-agonist site ligands provide important new insights into the relationship between NMDA receptors and neuronal synchrony and also the mechanism of cognitive enhancement by the high efficacy partial co-agonist D-Cycloserine.

Abbreviations

aCSF	Artificial cerebrospinal fluid
AMPA	α-amino-3-hydroxy-5-methyl-4-isoxazolepropionic acid
ATD	Amino-terminal domain
ATP	Adenosine triphosphate
CA1	Cornu ammonis area 1
CA3	Cornu ammonis area 3
CICR	Calcium induced calcium release
CNS	Central nervous system
CoV	Coefficient of variation
CTD	C-terminal domain
DAAO	D-amino acid oxidase
DCS	D-cycloserine
EC50	Half maximal effective concentration
ED50	Half maximal effective dose
eNEPSC	evoked NMDAr EPSC
EPSC	Excitatory postsynaptic current
extraNMDAr	Extrasynaptic NMDAr
GFP	Green fluorescent protein
GO	Glycine oxidase
HEK	Human embryonic kidney
IEI	Inter-event-interval
IP3	Inositol triphosphate
LBD	Ligand binding domain
LTD	Long term depression
LTP	Long term potentiation
mEPSC	Miniature EPSC
mGluR	Metabotropic glutamate receptor
NMDA	N-methyl-D-aspartate
NMDAr	NMDA receptors
PDS	Paroxysmal depolarising shift

postNMDAr	Postsynaptic NMDAr
preNMDAr	Presynaptic NMDAr
SC	Subiculum
sEPSC	Spontaneous EPSC
TCA	Tricarboxylic acid
tLTD	Timing dependent LTD

Chapter 1

Introduction

1.1 Synaptic Transmission

In the late 19th century, Santiago Ramon y Cajal used the recently invented Golgi stain to demonstrate that whilst varying in shape, all neurones consist of a cell body (or 'soma') that contains the nucleus, an axon and dendrites. Neuronal membranes are perforated by ion pumps, exchangers and channels that maintain a difference in the concentration of the principal ions between the intracellular and extracellular environments. When activated, ligand-gated ion channels open allowing ions to flow through the channel pore according to their electrochemical gradient, producing a change in conductance and activation of second messenger pathways. Such changes in conductance can lead to an action potential, a large depolarisation which propagates throughout the neurone due to sequential opening of voltage gated sodium channels.

Neurones can interact with each other directly by gap junctions but more commonly by synapses. When the action potential reaches a synapse, voltage-gated calcium channels in the presynaptic terminal (the bouton or variscosity) are activated and calcium flows in triggering exocytosis of vesicles containing a neurotransmitter. The neurotransmitter then diffuses across the synaptic cleft and binds to receptors present on the spine of the postsynaptic cell to elicit an excitation or an inhibition. Released neurotransmitters also commonly act on receptors on the presynaptic terminal to produce a feedback loop and they are removed from the cleft either by degradation or by reuptake back into neurones or into glial cells. Typically, an action potential ignites at the excitable, initial portion of the axon and travels down the axon to signal other neurones and also 'back-propagates' to its own dendrites. Excitatory neurones or 'principal cells' are predominantly glutamatergic and exhibit diverse connectivity, inhibitory neurones or interneurones are predominantly GABAergic and typically have local connectivity, providing feedback and feedforward inhibition.

In the 1950s, Katz and colleagues utilised intracellular recordings from muscle fibres at the neuromuscular junction in frogs observing that without nervous activity small depolarisations were observable, occurring at random but with a

constant probability. Interestingly when the calcium concentration was lowered the size of evoked synaptic responses decreased and the probability, but not size, of these spontaneous potentials decreased. Furthermore, the evoked responses were seen to increment in steps about the size of these spontaneous events further indicating that these events represent a minimum quantity of release, and these were termed 'quanta' (see Del Castillo and Katz, 1954). Later it was shown that a quantum corresponds to the neurotransmitter contained within one vesicle (Heuser et al, 1979).

At synapses between neurones the situation is complicated by the amount of synapses occurring at varying positions and the smaller size of potentials which may not be separable from background noise. The lower access-resistance granted by patch clamp recording is useful to increase the signal to noise ratio and this technique also allows the neurone to be voltage clamped, allowing direct observation of spontaneous currents. The physiological function of these synaptic events remains unclear though it may be that they represent a synaptic noise which enhances transmission via stochastic resonance or that they are important for the development and maintenance of synapses (see Greenhill et al, 2014). Important here though, is that they provide a selective substrate for the investigation of transmitter release.

1.2 The Entorhinal Cortex

The brain consists of the brainstem (the medulla, pons, cerebellum and midbrain) the diencephalon (thalamus and hypothalamus) and the telencephalon (limbic system, basal and cerebral cortex). The cerebral cortex can be spatially divided broadly into four lobes – frontal, parietal, temporal and occipital and the functions of the cortex can be characterised as sensory, motor or associative. The cortex is made up mainly of layered neurones (lamina) and ninety percent of the cortex is neocortex, containing six layers (or having six layers during development) of which layer 4 is the main input layer and layer 5 is the main output layer. Neurones are also lined up with the neurones above and below forming functional columns. The entorhinal cortex (EC) is a non-neocortical region of the cortex located in the

temporal lobe curved around the rostral surface of the hippocampus (part of the limbic system; see. Fig. 1.2) and acts as the gateway to this structure. The EC can also be divided into 6 layers though it lacks a true cellular layer 4. The intrinsic connectivity and laminar differences in principal cell types are depicted in Fig. 1.1. Projections to the hippocampus originate predominantly from layers 2 and 3 whilst projections both to and from the neocortex are largely by layer 5 (see Van Strien et al, 2009).

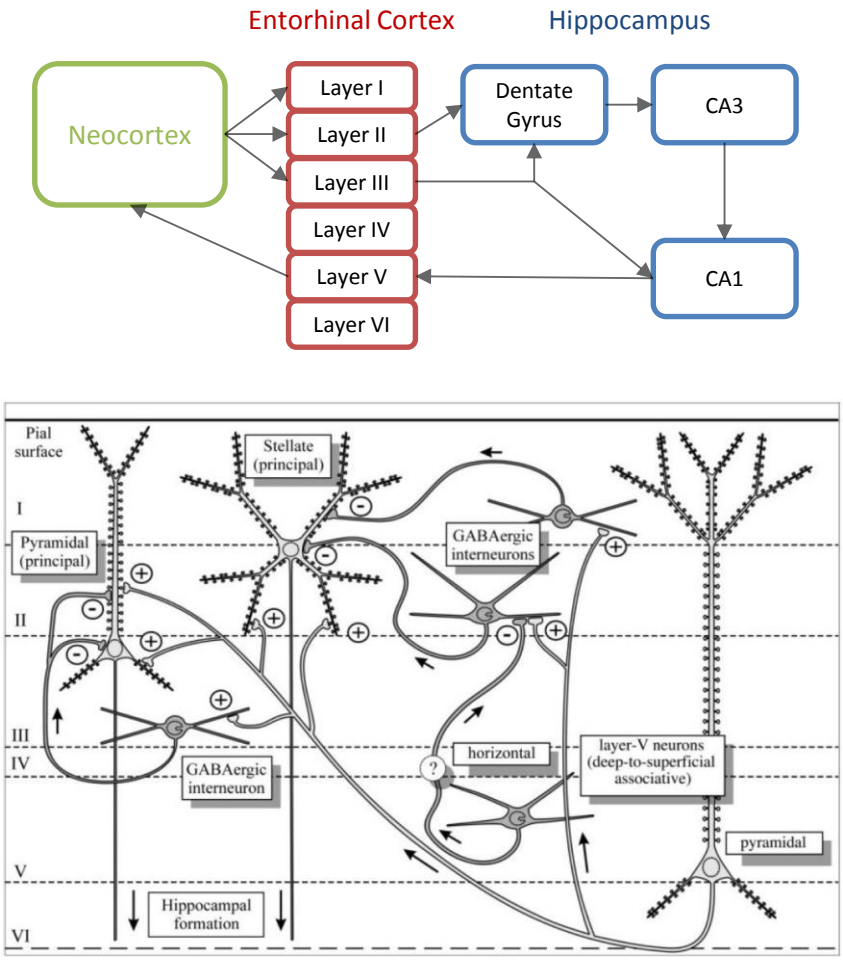

Fig. 1.1. Connectivity of the EC. The above diagram depicts the extrinsic connectivity of the medial EC. Neocortical input is largely to the superficial layers and layers II and III project to the hippocampal trisynaptic loop whilst hippocampal input and neocortical output is largely through layer V. The below diagram indicates the different cell types and morphology of each layer of the medial EC, along with their intrinsic connectivity (from van Haeften et al., 2003). Principal cells are largely pyramidal in layers III and V and stellate in layer II and exhibit high interconnectivity whilst inhibitory control is more pronounced in the superficial layers

1.2.1 The EC in cognition

Historically, two people were instrumental in linking the temporal lobe to memory. The first was Wilder Penfield, a surgeon who electrically stimulated parts of the cortex during brain surgery and found that when the temporal lobe was stimulated, patients described experiencing recollections of past experiences. The second is the famous patient H.M. who underwent a bilateral medial temporal lobe resection which resulted in extreme anterograde amnesia for declarative memory. This was significant in that H.M. retained all other cognitive functions, indicating that memory formation is a distinct process whilst the selective nature of his surgery indicated that declarative memory formation (but not long-term storage) is dependent on the temporal lobe. Imaging and lesion studies have subsequently indicated that the hippocampus and the associated cortical regions, particularly the EC, are the key elements of this memory system (Roof et al, 1993; Glasier et al, 1995; Cho and Jaffard, 1995; Kopniczky et al, 2006; Ranganath et al, 2004; Zola-Morgan et al, 1993; Maass et al, 2014). The EC is now believed to be highly important as the site of interaction with the hippocampus, directly mediating input-output with the neocortex and it may provide pre- and post-hippocampal information processing through its intrinsic connectivity (Eichenbaum, 2001; Squire et al, 2004; Dickerson and Eichenbaum, 2010).

Whilst technology has allowed cognition to be efficiently examined on the anatomical level, the functional understanding of cognition is highly limited, though some observable phenomena on both the synaptic and network levels are thought to be important. The neuronal network is a complex system and network activity is emergent. Emergence is a common but fascinating concept describing a new structure with new properties and organisation, arising from the self-organisation of another and may also account for Newtonian physics (which govern the brain), social structures and possibly even the conscious mind (see Gazzaniga et al, 2008). In a neuronal ensemble, activity alternates between complex and oscillatory/'rhythmic' behaviour. Rhythmic activity is highly dependent on principal cell-interneurone dynamics and can be of several possible frequency bands, which have a natural logarithmic ratio meaning they cannot

synchronise phases and undergo perpetual complex interactions. These oscillations can be correlated to different thinking states, and the frequency of an oscillation is thought to correspond to the length of a temporal processing window whereby information is integrated and/or propagated (see Buzsaki, 2006).

On the synaptic level, the ability for the future strength of transmission to change in response to activity, termed synaptic plasticity, is thought to represent the cellular basis of memory. In 1949 Donald Hebb postulated that if synapses strengthened in response to strong activity then the original pattern of stimulated synapses would become auto-associated forming an 'engram' which could easily be re-iterated by a later stimulus. Broadly, Hebb's mechanism represents a conceptually sound schematic and has been supported by studies demonstrating mutual molecular dependencies of synaptic plasticity and memory (see Bear et al, 2007). However, the details of the engram and how it relates to computation by networks is unclear.

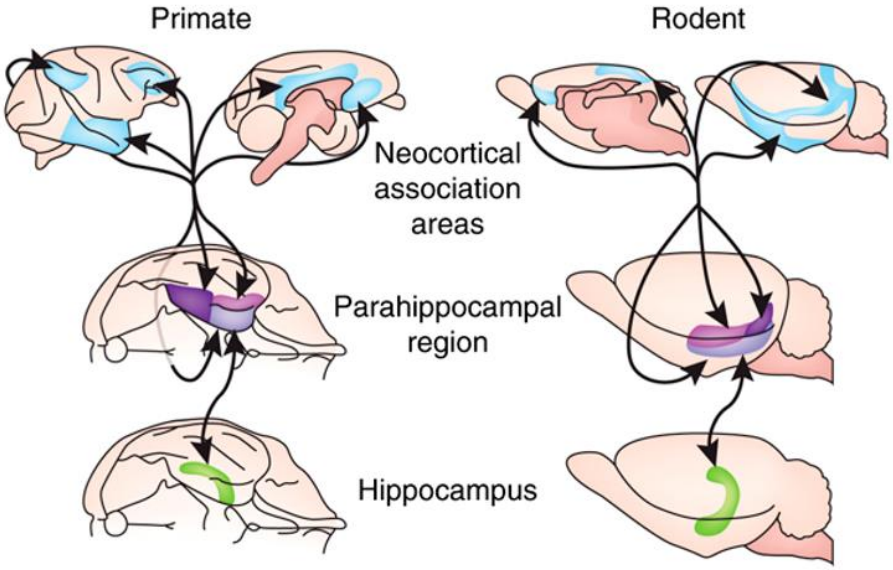

Fig. 1.2. The medial temporal lobe memory system in monkeys and rats (from Dickerson and Eichenbaum, 2010). Information from areas of the neocortex (blue) flows to, and converging in, the perirhinal cortex (purple), the parahippocampal cortex (dark purple), and the entorhinal cortex (light purple). Information from these interconnected areas leaves for the hippocampus from the entorhinal cortex, this pathway is known as the perforant path. Information is processed in the hippocampus and flows to the neocortex in a reversed manner. The parahippocampal region is located in the temporal lobe in primates but beneath the cortex in rodents.

Recently, the hippocampus and EC have been focussed on for their role in spatial navigation, which was originally discovered by the observation of hippocampal place cell which fire when a rat enters a certain part of its environment (O'keefe, 1978). Later, grid cells were identified in the EC, occurring predominantly in layer 2 (Hafting et al, 2005). These cells fire according to location according to a triangular grid and in doing so have the capacity to collectively represent the environment as Euclidean space. Though many discuss these regions as being a solely memory or navigation system, it is likely that a novel way of thinking which encompasses both functions is needed (Millivojevic and Doeller, 2013; Eichenbaum and Cohen, 2014). In their review, Buzsaski and Moser (2013) discussed several parallels between declarative memory and navigation, indicating the possibility that these share a fundamental mechanism. It is reasoned that many animals achieve navigation with much simpler systems but that the representational capacity of this system may have provided a substrate for the evolution of memory. Furthermore the EC has also been implicated in disorders of cognition including Alzheimer's disease (Stranahan and Mattson, 2010) and Schizophrenia (Prasad et al, 2004).

1.2.2 The EC in epilepsy

The EC also appears to be important in the pathology of epilepsy. Epilepsy is a clinically diverse disease characterised by recurrent and unprovoked seizures. It can be caused by genetic mutations, developmental disorders/ abnormalities or by an insult to the brain, mechanical or other, which is typically followed by a seizure free latent period before epilepsy develops. Seizures are periods of abnormal synchronous neuronal excitation and in epilepsy typically are of the scale of seconds or minutes or can be continuous in status epilepticus, and may or may not involve muscular convulsions. There is no known consistent mechanism for epilepsy apart from in the broadest sense that the normal balancing of neuronal excitation and inhibition is perturbed. Such perturbations could initiate on the level of ions, neurones, synapses or networks (Scharfman, 2007) but the diversity of epilepsy and its treatment, even within specific forms, suggests that unifying schematics may not be possible. Treatments for epilepsy typically act broadly to

redress the balance of excitation and inhibition. Whilst treatment is effective, in many cases seizures are drug refractory and so there is a clinical need for novel drugs which selectively target the underlying pathological mechanisms.

Temporal lobe epilepsy (TLE) is the most common form of adult epilepsy and multiple lines of enquiry have implicated the EC as a key region in this condition. TLE can be treated surgically with a partial temporal lobectomy and removal of the EC is particularly important to the success of this surgery (Sperling et al, 1996; Siegel et al, 1990; Fried, 1993; Goldring et al, 1992; Goldring et al 1993). Then, animal studies in vivo and in vitro have observed that epileptiform activity in the temporal lobe is commonly traced back to the EC, implicating this structure as being the site of initiation for seizure activity (Ben-Ari et al, 1981; Collins et al, 1983; Stringer, 1994; Du et al, 1995; Jones and Lambert, 1990; Avoli et al, 2002; Lopantsev and Avoli, 1998). Though the precise pathology of TLE is largely unclear, a common theory is that TLE represents a pathological replay of juvenile brain physiology which is inappropriate within the adult brain and that epileptogenesis in this condition represents the elicitation of these aberrant developmental mechanisms (see Scharfman, 2005). The development of new synapses producing abnormal connectivity is one such mechanism that may lead to enhanced synchronisation (Sloviter et al, 2006) another is the re-emergence of machinery that conveys the enhanced synaptic transmission and plasticity seen in the developing brain (Cohen et al, 2003).

1.3 NMDA Receptors

The amino acid glutamate is the primary excitatory neurotransmitter in the central nervous system acting at a family of receptors which can be broadly divided into ionotropic and metabotropic/G-protein coupled receptors. Ionotropic glutamate receptors are the NMDA, AMPA and kainate receptors and are heteromeric cation channels of which the AMPA and kainate receptors mediate fast excitatory transmission with low calcium permeability. This is in contrast to the slower responses and more complex action of the NMDA receptors (NMDAr), so named after its original specific agonist; N-methyl-D-aspartate.

1.3.1 Structure of NMDAr

Ionotropic glutamate receptors are comprised of four subunits, each of which contains four domains (depicted in Fig. 1.3.A). These are the amino (or 'N-') terminal domain (ATD) and the ligand (or 'agonist') binding domain (LBD), which are large 'clamshell-like', extracellular structures, the transmembrane domain (TMD) which consists of 3 membrane spanning helices and a re-entrant 'P-loop', and the intracellular C-terminal domain (CTD). The ATD is the site of binding for many allosteric NMDAr modulators including protons, ifenprodil and its analogues, zinc ions and polyamines, whilst the LBD is the site of binding for agonists. The TMD forms the ion channel whilst the CTD mediates interactions with intracellular proteins and is thereby thought to be important in receptor trafficking and signalling. The structure of NMDAr has been studied at the atomic level using X-ray crystallography of the isolated extracellular amino terminal domain and ligand binding domain regions (see Wyllie et al, 2013). Although the complete structure has not been elucidated, Sobolevsky et al (2009) have combined the LBD structure with more complete structural information of the

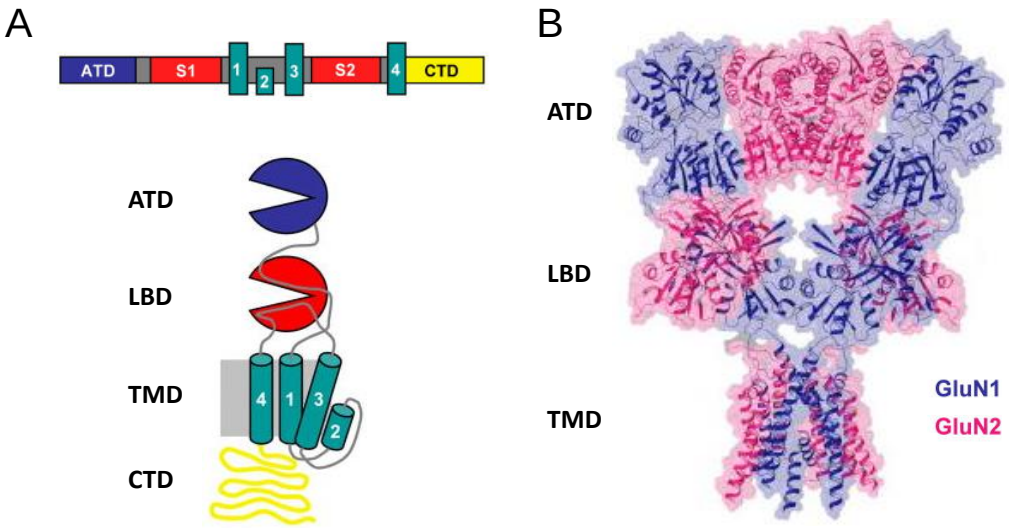

Fig. 1.3. Structure of ionotropic glutamate receptors. A – Linear structure and general schematic of an ionotropic glutamate receptor subunit. B – Model of the full NMDAr structure based on crystal structures from the GluN1 and GluN2A and GluA2 subunits. Adapted from Wyllie et al (2013), panel B originally from Sobolevsky et al (2009).

the closely related GluA2 AMPA receptor subunit to produce a putative structural model of the full NMDAr (see Fig.1.3.B).

Functional NMDAr are heterotetramers comprising two obligatory GluN1 subunits and two GluN2 subunits. Additionally two GluN3 subunits have been cloned which may be important in early development though have low homology with other subunits, and appear to have a relatively muted prevalence. Initial evidence suggested that the quaternary arrangement of the subunits was non-alternating (GluN1/GluN1/GluN2/GluN2) (Schorge and Colquhoun, 2003) but more recent studies utilising cysteine linking have indicated a 'hetero-dimer' arrangement (GluN1/GluN2/GluN1/GluN2) (Sobolevsky et al, 2009; Lee and Gouaux, 2011; Riou et al, 2012; Salussolia and Wollmuth, 2012). In the plasma membrane the NMDAr forms part of a large multiprotein complex which is thought to determine the precise signalling and downstream effects that follow ion permeation through the receptor pore. The NMDAr channel pore can pass both sodium and calcium ions into the cell, but relative calcium permeability is around tenfold higher than that of sodium (Mayer and Westbrook, 1987) and is thought to be the major intracellular signalling mechanism.

1.3.2 Regulation of NMDAr

One particularly fascinating aspect of the NMDA receptor is the large amount of endogenous regulation that it undergoes. Firstly, the NMDA receptor is unique in that it recognises both an agonist and a co-agonist, both of which are required for channel opening. GluN2 subunits contain the glutamate binding agonist site whilst co-agonist sites are located on GluN1 subunits and can be activated endogenously by glycine or D-serine. Secondly, at resting membrane potential the NMDAr channel is blocked by extracellular magnesium ions and this block is removed upon depolarisation and some synthetic compounds such as MK801, phencyclidine, memantine and ketamine also act to block the NMDAR channel producing a use-dependent and non-competitive inhibition. Extracellular zinc ions inhibit GluN2A and, at higher concentration, GluN2B containing receptors, some neurosteroids such as pregnanolone sulphate also inhibit NMDAr and the

polyamines spermine, spermidine and putrescine have complex and diverse modulatory effects on NMDAr activity (Paoletti, 2011). However, although there has been a strong interest in NMDAr regulation, the roles and interactions between the types of endogenous modulation of the NMDAr in the brain are currently unclear.

1.3.3 Diversity of NMDAr

There are four different GluN2 subunits which can be incorporated in NMDAr, termed A-D. Receptors can be diheteromeric, containing two GluN1 subunits and two GluN2 subunits of the same subtype, or triheteromeric, containing two GluN1 subunits and two different GluN2 subtypes. Additionally there are eight, regulated isoforms of the NR1 subunit arising from different combinations of three splice variants and these can also influence receptor kinetics and some pharmacological properties of the receptor, most significantly the inhibition of the receptor by protons (pH dependent inhibition).

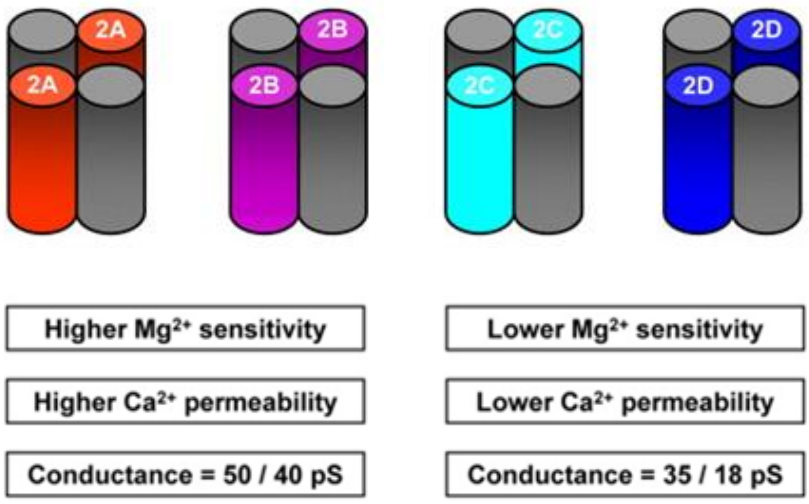

Fig. 1.4. Functional Influence of GluN2 Subunit Identity. Adapted from Wyllie et al, 2013. The function of the NMDAr is highly dependent on the GluN2 subtype present. Considering diheteromeric NMDA receptors, multiple properties are broadly separated by categorising as 2A/2B or 2C/2D containing receptors.

However, the largest determinant of NMDAr function is the subtypes of GluN2 subunits which the receptor contains. Importantly, GluN2A and GluN2B containing receptors typically have higher conductance, calcium permeability and sensitivity to magnesium blockade than those containing GluN2C and GluN2D subunits Interestingly, Retchless et al (2012) have shown that all of these three differences in pore permeation/blockade between 2A/B and 2C/D are all mediated by a difference in a single amino acid residue located in the TMD. Different GluN2 subunits have varying affinity for glutamate but interestingly the GluN2 subunit present can also determine the efficacy and affinity of ligands of the GluN1 subunit, indicating an important coupling between the GluN1 and GluN2 subunits. In addition the GluN2B-selective inhibitors ifenprodil and Ro25-6981 etc., and polyamines are thought to bind at the interface between GluN1 and GluN2 subunit ATD's, again emphasising the importance of the interaction between the GluN1 and GluN2 subunits (Karakas et al, 2011, Mony et al, 2011).

Receptor open probabilities can be calculated using single channel (microscopic) recording and are typically compared under conditions of saturating agonist concentrations. For recombinant diheteromeric NMDA receptors these values are typically 0.5 for GluN2A containing receptors, 0.1 for GluN2B and are very low (0.01-0.04) for GluN2C and GluN2D diheteromers (Wyllie et al, 2013). The deactivation of NMDA receptors is also highly dependent on subunit composition and this was extensively investigated by Vicini et al (1998), utilising whole cell patches and outside-out patches containing multiple receptors (macroscopic recordings). Here it was observed that the monoexponential decay times for diheteromeric NMDA receptor responses following brief application of a saturating glutamate concentration (synaptic like) were approximately 100ms for GluN2A, 250ms for GluN2B and GluN2C and 4s for GluN2D. Both Gielen et al (2009) and Yuan et al (2009) created and studied chimeric receptors to examine the source of these differences in NMDAr open probability and deactivation kinetics observing that both are controlled by the GluN2 ATD. This interesting finding has expanded the importance of the ATD as a key determinant in the functional properties of NMDAr subtypes.

Temporal changes in NMDAr composition are thought to be an important component of brain development, in particular is the well documented increase in GluN2A subunit expression beginning at postnatal week 2 reflecting a neurodevelopmental decrease in plasticity at this age (Sanz-Clemente, 2013, Paoletti et al, 2013). Spatial differences in NMDAr composition are seen on the subcellular, cellular (including neurones and glial cells) and brain region levels. Within the neuronal membrane, NMDA receptors can be divided spatially into three populations – presynaptic, postsynaptic and extrasynaptic. Extrasynaptic NMDAr (extraNMDAr) can be located on spine necks, dendritic shafts, or somas and may play a key role in regulating the excitability of these zones (Zhou et al, 2014). Postsynaptic and Presynaptic NMDA receptors are discussed in detail later (sections 1.5 and 1.6 respectively).

1.3.4 Clinical importance of NMDAr

NMDAr have been repeatedly implicated in epileptic pathology and many studies have observed a pathologically increased NMDAr expression in brain tissue from patients and in animal models (Ghasemi and Schacter, 2011). In addition, many NMDAr ligands modulate seizures in animals and the NMDAr is one target of the clinically used anticonvulsant felbamate (Subramaniam et al, 1995). The importance of NMDAr in the function and regulation of synapses has also lead to a huge interest in these receptors with respect to cognition (Collingridge et al, 2013). Interestingly, the only pharmacological treatment for Alzheimer's disease besides the acetylcholine esterase inhibitors is the NMDAr blocker memantine. It is thought that the dysregulation of glutamatergic synapse in Alzheimer's disease leads to constant low-level depolarisation, causing 'noisy' NMDAr activity. By virtue of its moderate potency, memantine is thought to counteract this noise whilst allowing normal transmission to take place, thereby redressing the NMDAr dysfunction (Parsons et al, 2013). The high-efficacy co-agonist site partial agonist D-cycloserine (DCS) has also been indicated to have cognitive enhancing properties. Cognitive enhancement by DCS has been demonstrated in many animal study paradigms (discussed later) and in humans though its precise effects at NMDAr in the brain are unknown, with many studies simply ascribing effects to

a pro-NMDAr action. Interestingly there is also some evidence that DCS can produce anticonvulsant effects (discussed later).

1.4 Receptor Gating and Partial Agonism

The ability of a drug to bind a receptor is termed affinity and the ability of the drug to activate the receptor when bound is termed efficacy. The term 'intrinsic efficacy' is in some instances more useful, as other factors such as receptor reserve can influence observed efficacies, though will not be used here. An agonist has 100% efficacy and thus can elicit a full response. A partial agonist has a sub-maximal efficacy and thus produces a sub-maximal response when all receptors are fully bound which for ion channels results in a sub-maximal receptor open probability (the probability of a bound receptor opening). These effects were classically described by the model of Del Castillo and Katz (1957) who were the first to give separate binding (affinity driven) and activation (efficacy driven) equilibria (Fig. 1.5). Under such a scheme the activation equilibrium would lie further towards 'active' for a full agonist than for a partial agonist.

Fig. 1.5. Classical model of receptor activation. This simple model first described by Del Castillo and Katz (1957) was the first to distinguish between receptor binding and receptor activation. In the presence of an agonist the unbound ('R') and bound ('A.R') forms of the receptor are in an equilibrium referred to with rate constants k+1 and k-1. The bound receptor is also in equilibrium with the bound, activated receptor ('A.R*') with rate constants termed α and β.

However, for some ion channels at least, the idea of a single activation equilibrium is obsolete. Several studies focussing particularly on the pentameric glycine and nicotinic receptors identified a 'conformational wave' whereby the conformation

of this receptor changes through a number of sequential intermediate shut states before becoming open. Intermediate states can be detected using single-channel recording through observation of open and shut times (i.e. how long the channel stays open/closed in each instance) in the presence of different concentrations of a ligand. Such experimentation typically involves fitting the sequences of open and shut times (durations of open periods and shut periods) to a putative mechanism and calculation of the rate constants in the reaction scheme. How well the mechanism fits the data can be judged, for example, by the ability of the fit to describe the distribution of open and shut times and the change in channel open probability (overall fraction of time the channel spends open) with drug concentration (see Colquhoun et al, 2003).

In this way, Lape et al (2008) described an intermediate agonist-bound, shut (or 'pre-open') conformation known as the 'flip' from which the receptor channel opens rapidly irrespective of what agonist is bound. Their work indicates that contrary to previously thought, it is a shift in the resting-shut/flipped-shut equilibrium towards flipped-shut that produces partial agonism. This conclusion was largely informed through the observation of brief shuttings (typically 5-10μs) which are thought to be fluctuations between the flip and open state. These closures were of similar length in the presence of full agonists and partial agonists indicating that this step was not relevant to the difference in agonist efficacies. The opening of the channel itself is a very rapid process with an indeterminably fast rise time.

The idea of the 'flip' state is also significant because an all-high affinity state allows for the appearance of cooperative binding via the Monod-Wyman-Changeux scheme which, due to its simplicity, is able to account for the abundance of co-operative binding across many proteins.. However, it may be difficult to find a unifying model for every receptor because even if receptors did indeed share the same mechanism, which may seem unlikely, different receptors may spend no appreciable time in one step giving the appearance of a different mechanism (Colquhoun and Lape, 2012). Another problem lies in explicitly linking kinetic observations of intermediate states with structural conformation changes.

1.4.1 NMDAr gating and partial agonism

Banke and Traynelis (2003) produced a kinetic model of NMDA receptor gating which suggested that GluN1 and GluN2 subunit undergo independent transitions and that partial agonists increase time spent in a single shut state associated with the bound subunit. However, the idea of independent GluN1 and GluN2 transitions may have been influenced by the idea of a non-alternating arrangement, which is no longer favoured. Alternatively, the more recent kinetic single channel analysis by Kussius and Popescu (2009) indicated the presence of five resolvable closed states and three/four open states in the gating of these receptors (Fig. 1.6). Partial agonists of both the glutamate and glycine site were seen to have broad effects on channel gating, increasing time spent in multiple closed states, in contrast to the more simple 'flip' based mechanism for partial agonists at nicotinic and glycine receptors. However, it was suggested that one of the closed states ('C2') could represent an all-high-affinity state which is arrived at in a concerted manner.

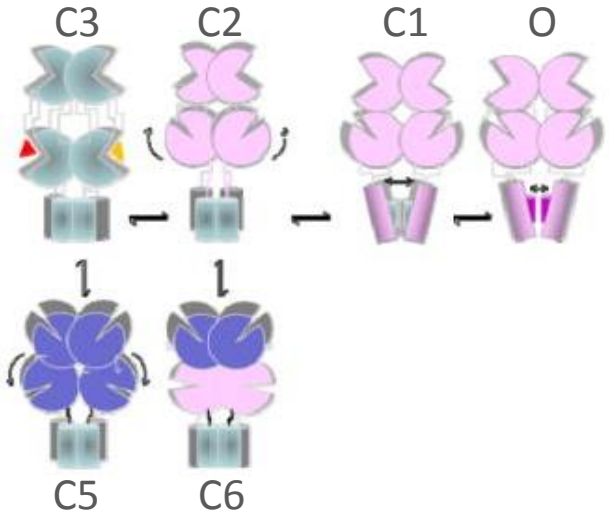

Fig. 1.6. Kinetic model of NMDAr gating (adapted from Kussius and Popescu, 2009)**.** The images depict speculative structures representing kinetically resolved gating stages. 'C' denotes 'closed' and 'O' denotes 'open'. The C3 structure is the only stage in which binding and unbinding occurs and these are not shown. C5 and C6 are long lived bound-closed stages. Open stages are represented as a single aggregate.

Interestingly, partial agonists of NMDAr also alter the decay of NMDAr macroscopic currents. These properties were extensively studied by Priestley and Kemp (1994) who demonstrated that relative to a full agonist, partial agonists of either site decrease the decay time of synaptic currents in an extent proportional to their efficacy. Kussius and Popescu (2009) indicated that relative to a full agonist, a partial agonist such as DCS will increase time spent in multiple bound/closed states including (indirectly) long-lived bound/closed (i.e. 'desensitized') states. This model also accurately predicts that partial agonists accelerate the decay of macroscopic currents resulting from prolonged glutamate application, through increasing the time spent in bound/closed states which can also transition to long-lived bound/closed (desensitized) states. More recently this scheme was seen to accurately predict changes in the decay time of synaptic-like macroscopic currents resulting from structural changes in NMDAr (Paganelli et al, 2013). In this way it appears that the sub-maximal decay time produced by NMDAr partial agonists result from the same broad reductions in channel gating efficiency that produce sub-maximal amplitude, providing a simple explanation of why the extent of both is determined by the compound's efficacy.

Some analyses have indicated that the NMDAr, alongside the AMPAr, can display different gating 'modes'. For example, Popescu and Auerbach (2003) studied single channel activity of GluN2A NMDAr observing 3 distinct gating modes which were separable by characteristic open probabilities and mean open times. The usefulness of such a scheme was shown by Zhang et al (2008), who demonstrated that modal gating can account well not only for observed variation of receptor kinetics over time, but also for biphasic decays of macroscopic currents. Under such a scheme two different gating modes, with monoexponential decays of different time constants, superimpose to produce the biexponential macroscopic decay. Zhang et al (2008) observed that gating modes change over a minute timescale, thus changes could occur to alter the distribution of gating modes before but not during the synaptic response. Kussius and Popescu (2009) were unable to rule out the possibility that changes in the proportions of gating modes contribute to submaximal open probabilities, and ultimately the understanding of the mechanism of partial agonism at NMDAr is not certain.

1.5 Postsynaptic NMDA receptors

The most well studied NMDAr are those located on the postsynaptic spine, due to their more obvious action and directly observable function. These are termed postsynaptic NMDA receptors (postNMDAr) and are well studied as having a central role in neuronal and network dynamics. PostNMDAr are thought to be highly important as 'coincidence detectors' becoming open and unblocked only when presynaptic glutamate release and back-propagation of an action potential to the dendrite are present (Bear et al, 2007). Calcium entry through the postNMDAr leads to changes in the strength of the signal at that synapse, particularly to increase the strength which is known as long-term potentiation (LTP). In the immediate period, one way in which this occurs is through autophosphorylation of calmodulin-dependent protein kinase II which can phosphorylate AMPAr, increasing their conductance. Also postNMDAr activation can lead to insertion of new AMPAr receptors into the plasma membrane.

Following release, the glutamate concentration in the synaptic cleft rapidly peaks at saturating concentration (approximately 1 mM) and is then cleared quickly by reuptake with a time constant of around 1 ms (Clements et al, 1992). Synaptic glutamate binds to postNMDAr producing a current of amplitude which will be determined by the number of receptors being activated, the receptor open probability and the conductance of the open channels (Fig. 1.7). Glutamate rebinding does not occur indicating that the time course of synaptic NMDAr currents is determined only by receptor gating i.e. the transitioning between open-bound, closed-bound and closed-unbound states (Lester et al, 1990). Native postsynaptic NMDA receptor mediated currents can be directly observed using whole cell patch clamp if all other receptors are blocked and magnesium blockade is relieved by use of a magnesium free solution or, more commonly, by holding the cell at a depolarised potential.

Experimentation using pharmacological tools has indicated that postNMDAr are likely to be GluN2A containing, whilst extrasynaptic NMDA receptors are likely to be GluN2B containing which has led to a pervasive schematic of postsynaptic

GluN2A heterodimers and extrasynaptic GluN2B heterodimers. However, whilst appealing in its neatness much evidence indicates that this schematic is likely to be an oversimplification (Wyllie et al, 2013). In particular at layer V synapses in the EC, postsynaptic NMDAr currents have been shown to be highly susceptible to both GluN2A and GluN2B antagonism indicating the presence of triheteromeric receptors (Chamberlain et al, 2008). Further to this, two recent studies compared the hippocampal synapses of wildtype and GluN2A/GluN2B knockout mice in acute slices (Rauner and Kohr, 2011) and neuronal cultures (Tovar et al, 2013). In both of these studies it was seen that only a population with a GluN2A-GluN2B triheteromer majority could account for the properties of postsynaptic receptor responses in the wild type (Rauner and Kohr, 2011, Tovar et al, 2013).

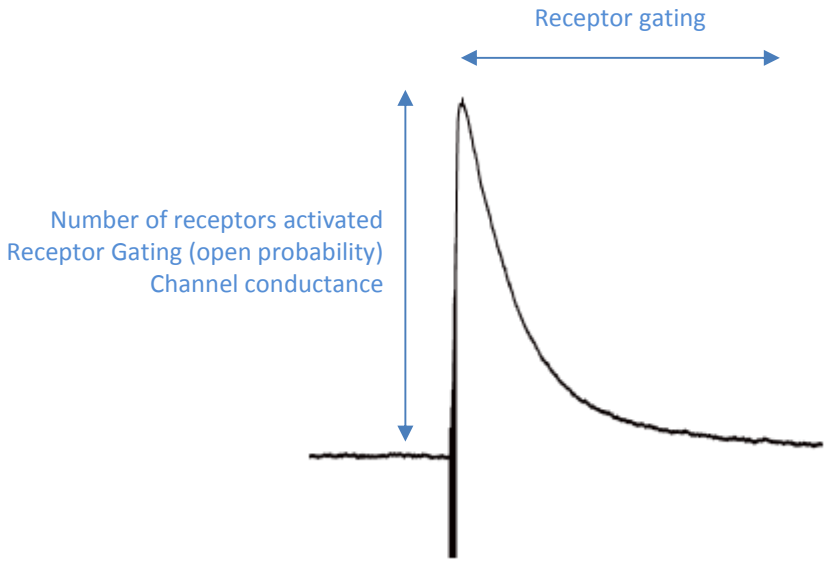

Fig. 1.7. A summary of the elements underlying the amplitude and time course of macroscopic postNMDAr evoked currents.

Methodology for reliably expressing the GluN2A-GluN2B triheteromer for direct study has recently been developed by Hansen et al, (2014) who observed the properties of this receptor using whole cell patch clamp of HEK cells and Xenopus Oocytes. In this study it was seen that the kinetics and pharmacological properties of this receptor appear to lie between those of the GluN2A and GluN2B diheteromers, but closer to the GluN2A diheteromer. Interestingly, the authors of this study suggest that this may have influenced previous indications of predominantly GluN2A diheteromeric postsynaptic NMDAr populations.

1.6 Presynaptic NMDA receptors

Whilst the effects of a neurotransmitter can be altered through mechanisms affecting the recipient postsynaptic receptors, neurotransmitter release is regulated by the activity of auto or heteroreceptors on the presynaptic nerve terminal. Presynaptic GABA receptors were the first such receptors to be identified (Dudel and Kuffler, 1961; Eccles 1964), with many types of presynaptic metabotropic and ionotropic receptors following. The possibility of NMDAr located on presynaptic terminals was first implicated in studies examining the release of noradrenaline (Fink et al, 1990; Pittaluga et al, 1992) and dopamine (Johnson and Jeng, 1991; Krebs et al, 1991; Wang, 1991) from synaptosomes which indicated that a presynaptic NMDA receptor (preNMDAr) might be a heteroreceptor for these transmitters. Early electron microscopy studies then allowed NMDAr located on presynaptic terminals to be visualised in, for example, the spinal cord (Liu et al,

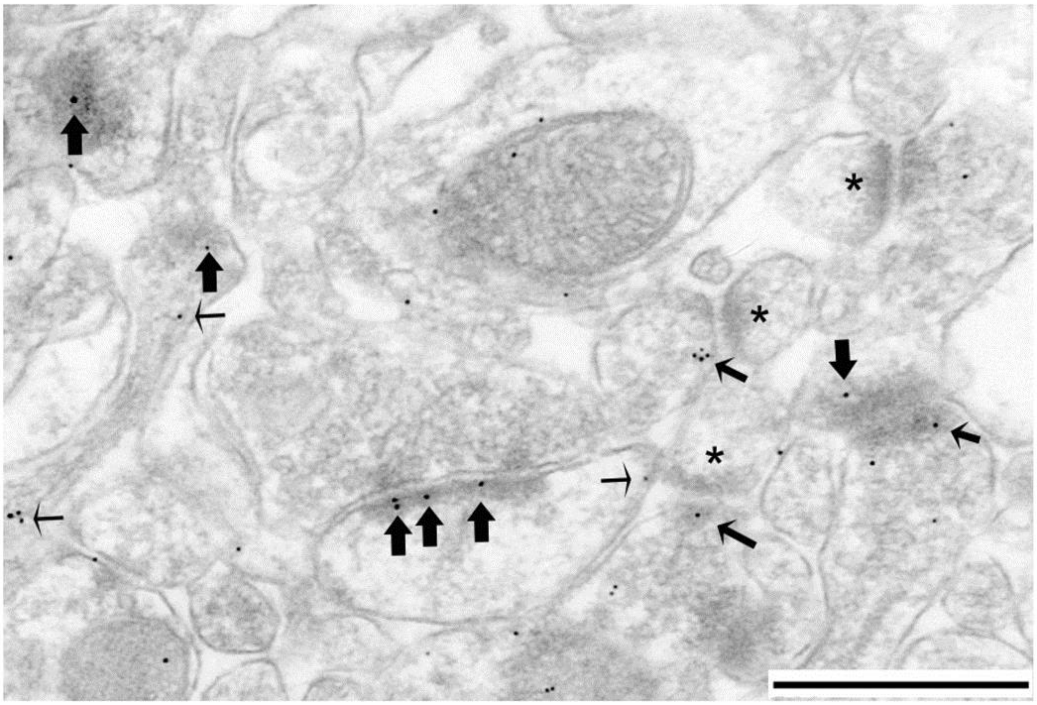

Fig. 1.8. An electron micrograph of synapses in the hippocampal CA1 region with immunogold labelling for GluN2B subunits from Aoki et al (2009**).** Large arrows indicate postsynaptic labelling, medium arrows indicate presynaptic labelling and small arrows indicate labelling inside spines. Asterisks denote unlabelled post synaptic densities. Scale bar = 500nm.

1994) and hippocampus (Siegel et al, 1994). In particular, Aoki et al (1994) directly examined different neuronal locations of NR1 subunits in the visual cortex and observed a large degree of NR1 immunoreactivity in axon terminals, explicitly linking this to the suggested preNMDAr. A more recent, high quality electron micrograph produced by Aoki et al (2009) which indicates the different subcellular locations of NMDAr in the hippocampus is shown in Fig. 1.8.

1.6.1 Regulation of glutamate release by preNMDAr

As NMDAr are present at both sides of the synapse, targeting the presynaptic receptor selectively for functional study is inherently problematic. The development of the technique of using MK801, an NMDAr blocker, dialysed into cells by inclusion in intracellular patch clamp solution to block postNMDAr by Berreta and Jones (1996) allowed the first functional demonstration of preNMDAr to be made. Here it was seen that at glutamatergic synapses in layer II of the EC preNMDAr act as autoreceptors to facilitate glutamate release. These receptors were tonically active producing an increased baseline of glutamate release. In a subsequent paper by Woodhall et al (2001) this effect was also observed in layer V of the EC and it was seen that the preNMDAr are not fully active as application of the NMDAr agonist homoquinolic acid produces a large increase in the frequency of spontaneous activity. preNMDAr were also seen to mediate frequency dependent facilitation of evoked currents at 3Hz demonstrating a role in a very short term form of plasticity (Woodhall et al, 2001).

In Woodhall et al, (2001) it was observed that the activity of preNMDAr was inhibited by cobalt ions indicating that these actions are mediated by calcium influx through the receptor pore supporting the findings of a previous calcium imaging study of the reticulospinal axons in the lamprey spinal cord (Cochilla and Alford, 1999). More recent calcium imaging has also indicated this to be the case (McGuinness et al, 2010), although a recent study by Kunz et al (2013) found that lowering the concentration of sodium ions decreases preNMDAr activity indicating that the influx of sodium ions, which would act to depolarise the terminal, may also be important. Further investigation of the tonic and activity

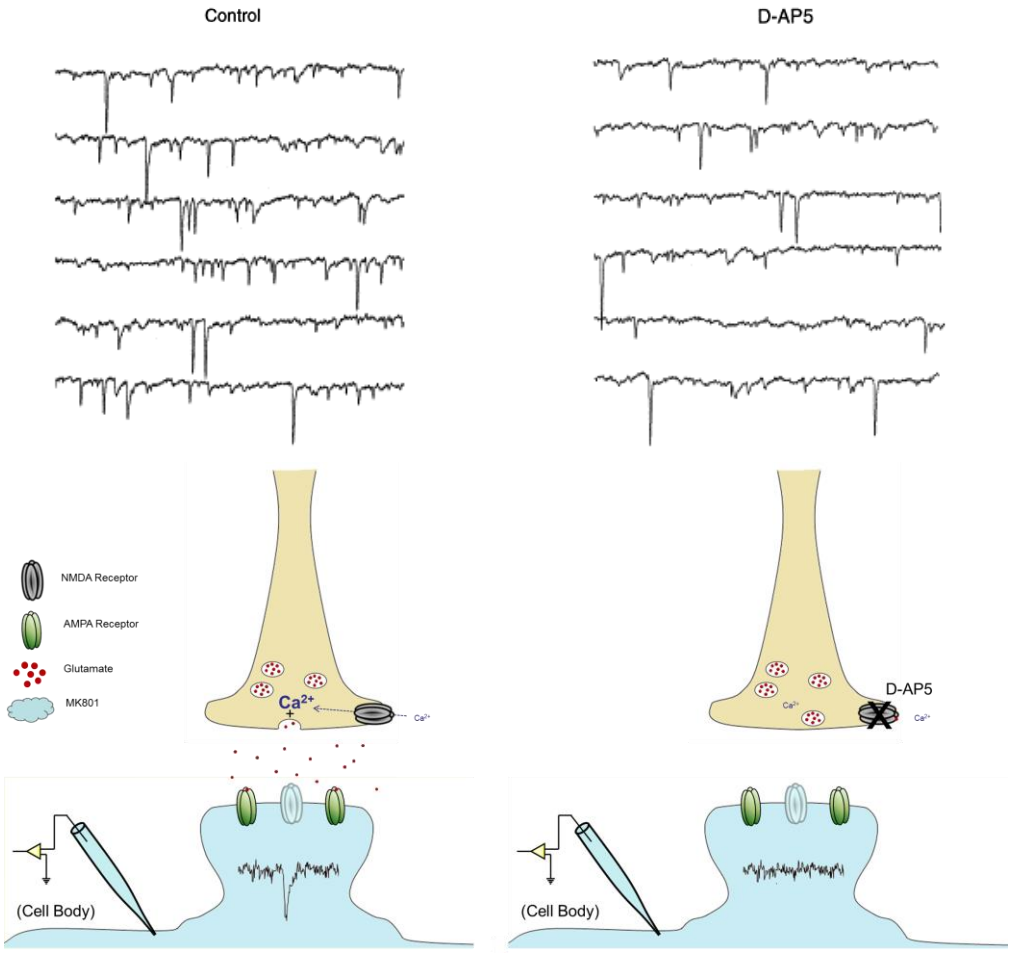

Fig. 1.9. Functional observation of preNMDAr by whole cell patch clamp. A – Example traces taken from Berretta and Jones (1996), the first functional demonstration of preNMDAr activity. B – Illustration of the experimental paradigm developed by Berretta and Jones. In this study postNMDAr were blocked by the NMDAr channel blocker MK801 which was added to intracellular patch solution. Addition of the glutamate antagonist to the bath was seen to produce a decrease in the frequency of spontaneous excitatory events with no change in amplitude. This indicated that NMDAr on glutamatergic nerve terminals were acting to promote quantal transmitter release.

dependent facilitations produced by the preNMDAr indicated that these receptors were fully sensitive to GluN2B antagonism suggesting a GluN2B diheteromeric composition (Woodhall et al, 2001). This is a common finding for preNMDAr (Jourdain et al, 2007, Brasier and Feldman, 2008 and Sjöström et al, 2003, DeBiasi et al, 1996, Li et al, 2009 and McGuinness et al, 2010) although GluN2A and

GluN3 subunit containing preNMDAr have also been reported (Suárez and Solís, 2006, Larsen et al, 2011).

Duguid and Smart (2004) have shown that preNMDAr also facilitate release at inhibitory synapses in the cerebellum and can again mediate a long-term potentiation which is elicited by retrograde glutamate. Duguid and Smart found that this form of plasticity requires CICR (calcium induced calcium release) indicating that it is mediated by interaction with presynaptic calcium stores, although Glitsch (2008) has shown that CICR is not required for the immediate facilitation of GABA release by preNMDAr. Fiszman et al (2005) also observed a similar effect on GABA release by preNMDAr at inhibitory terminals in primary neuronal cultures from the cerebellum. In this study the presence of NMDAr heteroreceptors on terminals was explicitly demonstrated by outside-out single channel patch clamp experiments from interneurone variscosities. Using this technique, preNMDAr currents were observed in 61% of the patches excised suggesting that preNMDAr expression is not ubiquitous but targeted.

1.6.2 preNMDAr and synaptic plasticity

In 2003, Sjostrom et al identified a mechanism of long-term depression (LTD) at excitatory synapses in layer 5 of the visual cortex which was mediated by preNMDAr indicating that these receptors, alongside their postsynaptic counterpart, are important as detectors/mechanisms for synaptic plasticity of the brain. Here, dual patch clamp was used to give control over presynaptic and postsynaptic cells and it was observed that timing dependent LTD (tLTD) generated by 0.1 Hz was conferred by the presynaptic cell and was dependent on preNMDAr. Although expressed presynaptically, tLTD requires postsynaptic (although not postNMDAr) activity and was also seen to require cannabinoid receptor activation indicating that endocannabinoids may act as a retrograde signalling molecule, which induce tLTD if tonic activation of preNMDAr is present. Subsequent studies have made similar observations at excitatory synapses in the somatosensory cortex (Bender et al. 2006; Nevian and Sakmann 2006; Rodriguez-Moreno and Paulsen 2008) whilst in the lateral amygdala cortical

afferents exhibit a presynaptic LTP at 30 Hz stimulation which is independent of postsynapc activity and mediated by preNMDAr (Humeau et al, 2003; Fourcaudot et al, 2008; Fourcaudot et al, 2009).

Recently the function and locus of preNMDAr have been supported by studies using 'caged' NMDAr ligands which only become active following uncaging by photolysis and this can be done in a compartment-specific manner. Rodriguez-Moreno et al (2011) synthesised a caged form of MK801 which could be internally dialysed and used this compound to investigate further tLTD in the somatosensory cortex observing that only uncaging in the axonal department abolished this effect. Additionally, by combining precise photolysis of a caged form of NMDA with calcium imaging, agonist-induced calcium influx has been observed both at interneurone and layer V pyramidal cell terminals in the cerebellum (Rossi et al, 2012) and visual cortex (Buchanan et al, 2012), respectively. Interestingly, in the study by Buchanan et al (2012) it was seen that preNMDAr were present on synapses between pyramidal cells but not on those from pyramidal cells onto basket cell interneurones. Additionally, in the experiments of Rossi et al (2012), NMDA-induced calcium transients were observed in 30% of locations along individual axons. These results further indicate that preNMDAr expression is synapse-specific. Buchanan et al (2012) used a computational model to show that such targeted expression could serve as a mechanism to reroute signals in neuronal networks during high-frequency firing.

1.6.3 preNMDAr mobility

NMDAr are now known to exhibit mobility within the neuronal membrane and the high concentration of NMDAr at the postsynaptic density (PSD) appears to be related to transient interactions with scaffolding proteins present at this location (Choquet and Triller, 2003; Lau and Zukin, 2007). In their study of NMDAr in P0-P1 mouse hippocampal cultures, Tovar and Westbrook (2002) set out a novel, pharmacological method of studying NMDAr using the irreversible, activity dependent NMDAr channel blocker MK801. Later, Yang et al (2008) adapted the methodology of Tovar and Westbrook to also examine preNMDAr mobility in

acute brain slices of the rat EC. Using recovery from MK801 blockade and preNMDAr mediated frequency-dependent facilitation of AMPA receptor currents, here preNMDAr were seen to be highly mobile compared to the postNMDAr. This could be related to predominance of NR2B over NR2A in preNMDAr which has been shown to confer higher mobility of NMDAr (Groc et al, 2006) in addition to a potentially decreased prevalence of anchoring proteins at the terminal compared to the PSD.

The experiments of Yang et al (2008) indicated that short term regulation of preNMDAr is mediated by lateral diffusion within the neuronal membrane over exocytosis/internalisation and it appears likely that preNMDAr diffuse/are trafficked into the terminal following insertion (Aoki et al, 2003) similar to postNMDAr (Lau and Zukin, 2007). PreNMDAr mobility also appears to be activity dependent with brief activation leading to down-regulation of activity and vice versa (Yang et al, 2008). Although the mechanism of this effect is yet to be determined, it could be that Ca^{2+} influx through preNMDAr leads to activation of protein kinase C, which increases NMDA mobility (Groc et al, 2004 and Fong et al, 2002), causing dispersion of preNMDAr from active sites in the terminal membrane. Given the role of preNMDAr as a mediator of plasticity, phenomena which alter preNMDAr activity, such as regulated mobility, could act as mechanisms of metaplasticity.

1.6.4 Regulation of preNMDAr

Therefore preNMDAr appear to mediate elevated levels of activity and plasticity and so may act to 'tune' neuronal networks in the developing brain. A role for preNMDAr in the adult brain has not been shown and preNMDAr appear to undergo a decline in activity during development (Corlew et al, 2007, Mameli et al, 2005, Yang et al, 2008). Using electron microscopy, Corlew et al (2007) observed that the developmental decline in preNMDAr activity was correlated to a (70-80%) decrease in the presence of GluN1 at presynaptic terminals suggesting that a redistribution of NMDAr or change in surface expression may contribute to developmental changes in preNMDAr activity. Using the methodology of Beretta

and Jones (1996), Yang et al (2006) found that the developmental decline in preNMDAr at excitatory synapses in the EC was not present in chronically epileptic rats indicating that this system may re-emerge in epileptic pathology, contributing to heightened excitability. Furthermore preNMDAr antagonism has been shown to be an action of the anticonvulsant felbamate (Yang et al, 2007) supporting a causal role for preNMDAr in seizure generation.

Whilst it appears that ambient glutamate levels are sufficient for tonic activity of preNMDAr, it is less clear how the receptor is continually free from blockade by Mg^{2+}, though it may be that local excitatory currents are sufficient to maintain frequent depolarisation of the nerve terminals due to the small size/high input resistance of this structure (Jourdain et al, 2007). Alternatively results from Larsen et al (2011) indicated that in the visual cortex, incorporation of GluN3 subunits may contribute in conferring insensitivity to voltage-dependent block by Mg^{2+} and that change in GluN3 expression may also contribute to developmental changes in preNMDAr. The co-agonist site of preNMDAr represents a potential area for selective targeting of these receptors. It has been shown that the co-agonist site of preNMDAr in the visual cortex is also tonically bound, contributing to the active state of preNMDAr although the endogenous ligand was not identified (Li and Han, 2007). A study by Papouin et al (2012) suggested that postNMDAr and extrasynaptic NMDAr were bound by D-serine and glycine, respectively and that this was due to their different subunit compositions and subsequent affinities for the two endogenous co-agonists. Furthermore it was suggested that the segregation of these receptors was due to differential inhibition of mobility by the two co-agonists. Investigation of the co-agonist regulation of preNMDAr may therefore be important to both furthering the understanding of the physiological importance and regulation of these receptors and in pharmacologically targeting these receptors for therapeutic ends.

1.7 Astrocytes and the Tripartite Synapse

Neurones and their connections are the most important elements of the brain, acting to encode changes in the environment, communicate with each other and to ultimately control the body's response, though it is often noted that neurones only represent 10% of the cells in the brain. The remainder are the non-excitable cells termed 'glia' from the Greek for 'glue' which refers to their most noticeable function; sustaining the physical structure of the brain. The function of some glia is clear such as oligodendrocytes and Schwann cells which act to insulate neuronal axons with myelin, and microglia which are phagocytic immune cells. The most abundant glia are astrocytes, these cells reside between neurones and control homeostasis of the extracellular space and envelop synapses. The homeostatic functions of astrocytes include regulating the pH and potassium content of the extracellular fluid and producing and exporting numerous molecules for neuronal function and viability such as antioxidants, neurotrophic factors and sources of energy (Allaman et al, 2011). However, whilst the importance of these actions is patent, at synapses astrocytes have been shown to have the capacity to both detect and influence neuronal activity. This has led to the view of many synapses as being 'tripartite' in the flow of information and has prompted the idea that astrocytes may have a direct involvement in biological computation and brain function (Perea et al, 2014).

Whilst astrocytes lack the machinery necessary for electrical excitability, they still have the mechanics for intracellular calcium signalling. Cytosolic calcium concentration in astrocytes is generally observed to be oscillatory, alternating between periods of accumulation, from intracellular and extracellular sources, and clearance (Zorec et al, 2012). These oscillations can occur spontaneously indicating that it is an intrinsic property of these cells (Parri and Crunelli, 2003) but are also controlled by metabotropic and ionotropic receptors in the cell membrane (Zorec et al, 2012). Activation of these receptors by neurotransmitters provides the basis by which neuronal synaptic activity can trigger calcium waves (Perea and Araque, 2005; Araque et al, 2014). Calcium waves can also propagate between astrocytes, with several possible mechanisms such as the passage of

calcium and IP3 through gap junctions or glutamatergic/purinergic paracrine signalling, though the extent to which this occurs in vivo is currently unclear (De Bock et al, 2014).

Interestingly, one of the receptors present on astrocytes is none other than the NMDAr. Functional demonstration of NMDAr on astrocytes was carried out in 2006 by Lalo et al, who utilised somatosensory cortex brain slices from mice with GFP-labelled astrocytes and observed that these receptors were indeed active at the resting membrane potential of astrocytes (-80 mV). A subsequent study by Palygin et al (2010) indicated that the pharmacological properties of these NMDAr imply the presence of GluN2C or GluN2D subunits, but also reasoned that the lack of sensitivity to Mg^{2+} indicates the presence of GluN3 subunits and a triheteromeric structure was suggested. In the study by Lalo et al (2006) it was also observed that astrocytes exhibit glutamatergic miniature spontaneous events akin to those seen in neurones, further highlighting the close association of astrocytes with the synaptic terminal. Metabotropic glutamate receptors are another, key, receptor in astrocyte regulation, as well as AMPA glutamate receptors (Parpura and Verkhratsky, 2013).

1.7.1 Gliotransmission

Importantly, however, intracellular calcium signalling also provides a mechanism by which astrocytes can respond to neuronal synaptic activity. Transmitters released by astrocytes are termed gliotransmitters and include GABA, glutamate and prostaglandins, though the best studied are glutamate and ATP both of which are released by Ca^{2+} dependent exocytosis (Zorec et al, 2012). Glial ATP can act at presynaptic P2Y receptors to suppress glutamate release (Zhang et al, 2003) and can be rapidly converted to adenosine by ectonucleotidases in the extracellular space. This adenosine can act at presynaptic adenosine receptors to depress glutamate or GABA release via A_1 receptors (Pascual et al., 2005; Serrano et al., 2006) or facilitate glutamate release via A_{2A} receptors (Panatier et al, 2011). Also, astrocytic activation of postsynaptic adenosine receptors has been shown to modulate the trafficking of postNMDAr (Deng et al, 2011). It is already clear then

that the effects of gliotransmission are highly complex and variable depending on the gliotransmitter(s) released and the properties of the synapse.

1.7.2 Astrocytes and glutamate

Astrocytes are the main source of reuptake in the removal of glutamate from the synaptic cleft, which occurs via excitatory amino acid transporters, a family of five sodium dependent glutamate transporters (Shigeri, 2004). Once inside, glutamate is converted back to the precursor glutamine by the glial enzyme glutamine synthase, and this is then transported out of the astrocyte for reuptake into terminals (Hertz et al, 1999). Though, as previously mentioned, astrocytes can also release glutamate. Multiple studies have demonstrated that astrocytic glutamate can activate extraNMDAr (Angulo et al, 2004; Shigetomi et al, 2008; Fellin et al, 2004) though one study has focussed on activation of preNMDAr (Jourdain et al, 2007).

In this study dual recordings of astrocytes and principal cells were made in the dentate gyrus and stimulation of astrocytes was seen to elicit an increase in the frequency of spontaneous excitatory currents in roughly one third of the pairs, with no effect on the amplitude of events. This effect was abolished by inhibition of exocytosis in the astrocytes and by bath application of an NMDAr antagonist but not by blockade of postNMDAr by dialysed MK801. This effect was also sensitive to GluN2B selective antagonism and electron microscopy with immunogold labelling for this protein yielded an interesting observation – that this subunit had a prevailing presynaptic distribution at sites of interaction between astrocytic and neuronal membranes (Fig. 1.10). These experiments indicate that astrocytes can activate preNMDAr by release of glutamate and may have an intimate association with these receptors. Further experiments implicated activation of purinergic P2Y receptors and metabotropic glutamate receptors as the mechanism for activation of the astrocytes in this system whilst a follow up study indicated that the cytokine tumour necrosis factor alpha was necessary for the glutamate release stage (Santello et al, 2011).

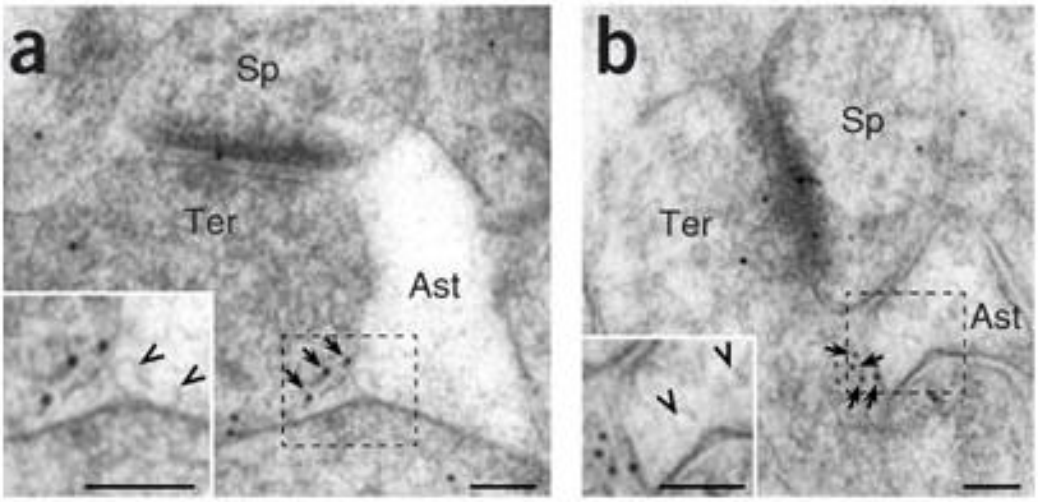

Fig. 1.10. Electron micrographs depicting hippocampal synapses with immungold labelling for the GluN2B subunit (from Jourdain et al, 2007). Arrows highlight GluN2B labelling, 'Ter' denotes terminal, 'Sp' denotes spine, 'Ast' denotes astrocyte and scale bars are 100nm. Here GluN2B containing NMDAr are seen to be located opposite astrocytic processes containing vesicles suggesting a functional coupling between these elements.

Other studies have indicated that astrocytic glutamate can also activate presynaptic metabotropic and kainate receptors (see Santello et al, 2012 and Perea et al, 2014). Furthermore, Nadkarni et al (2008) considered bidirectional astrocyte signalling at synapses by combining computational modelling of vesicular release from terminals with astrocyte calcium dynamics. Here it was demonstrated that mechanisms by which astrocytes influence presynaptic calcium may function to allow astrocytes to set an optimum probability of release in response to postsynaptic activity, sustaining effective synaptic transmission whilst avoiding neurotransmitter depletion.

1.7.3 Astrocytes in disease

The advancement in understanding of the role that astrocytes play in the maintenance and function of the brain has led to an increased focus on these cells in disease, particularly in neurodegenerative disorders but also in epilepsy. Tian et al (2005) studied in vitro epileptiform activity in rat hippocampal and

somatosensory cortical slices and utilised an acetoxymethyl ester calcium indicator which is preferentially loaded into astrocytes. Here it was observed that epleptiform-inducing agents increase calcium signalling in astrocytes independent of synaptic activity and that 70-80% of interictal paroxysmal depolarisation shifts (PDSs) are non-synaptic. These PDSs could also be induced by stimulation of astrocytes by photolysis of caged calcium and blocked by AMPAr and NMDAr antagonism indicating that glutamate release from astrocytes contributes to epileptiform discharges. Following this Gomez Gonzalo et al (2010) examined epileptiform activity in the EC and observed that Ca^{2+} elevations were present in astrocytes during ictal but not interictal events. Also, perturbation of astrocyte activity by intracellular application of a calcium chelator could reduce the area of ictal events triggered by focal application of NMDA suggesting that recurrent neurone-astrocyte signalling may support the recruitment of neurones into hypersynchonous activity in epilespy.

Reactive gliosis is a neuroinflammatory response in which glia undergo metabolic and structural changes and new glial cells are generated. Gliosis can be induced by insults to the brain making it an interesting candidate mechanism for the initiation and mediation of epileptogenesis and gliosis is indeed a common feature of human temporal lobe epilepsy (Cohen-Gadol et al, 2004; Thom et al, 2010), including in the EC (Yilmazer-Hanke et al, 2000), and in pilocarpine-induced epilepsy in rodents (Borges et al, 2003; Borges et al, 2006; Shapiro et al, 2008). As well as the control over synaptic transmission, the roles of glia in regulating extracellular ion concentrations and neuronal growth may be highly relevant (Scharfman, 2007). However, it has not been established whether gliosis may represent an aberrant, causative mechanism or if it may represent a compensatory, beneficial process or indeed neither. Also, computational analyses have demonstrated that astrocytes could influence the ability of a network to transition between synchronous and asynchronous activity (Amiri et al, 2013).

1.8 Endogenous Co-agonist Regulation of NMDA Receptors

Recently several studies have focussed on the endogenous regulation of the postNMDAr co-agonist binding site. Although the co-agonist site is a full agonist site it appears to be tonically bound, meaning that glutamate binding effectively determines the activity of postNMDAr. Glycine is a part of multiple metabolic pathways and therefore has a complex synthesis and metabolism, following release it is removed from the synapse by well-characterised reuptake mechanisms (Bear et al, 2007). D-serine is formed from L-serine by serine racemase and is degraded by D-amino acid oxidase, though the details of these processes is currently highly controversial (see section 3.4.2 for a discussion). Glycine was previously assumed to be the endogenous co-agonist at all NMDAr as it is present at high concentration in cerebrospinal fluid, although recently multiple studies have provided in depth analysis of the endogenous co-agonist regulation of postNMDAr.

Fossat et al (2012) used both recombinant yeast D-amino acid oxidase (DAAO) and bacterial glycine oxidase (GO) to remove D-serine and glycine in acute brain slices of the rat prefrontal cortex. In whole cell patch clamp recordings, removal of D-serine was seen to produce a partial decrease in the amplitude of postNMDAr mediated currents (in agreement with Panatier et al, 2006)) and this was reversed by application of exogenous D-serine. Inhibition of glial metabolism by fluoroacetate produced similar effects and was seen to reduce the concentration of D-serine in slices as measured by laser induced fluorescence. Despite glycine levels in the slices being higher than those of D-serine, GO was not seen to have an effect on postNMDAr currents but it did preclude a potentiating effect of the glycine transporter inhibitor, sarcosine. These results indicated that D-serine, produced by glia, was the main co-agonist binding these postNMDAr in part due to suppression of glycine at the synapse by transporters.

The same group subsequently made similar findings at CA3-CA1 synapses in the hippocampus (Papouin et al, 2012). Here it was also observed that GluN2A antagonism by free zinc produced a partial decrease in the amplitude of postNMDAr responses but no effect was seen by the GluN2B antagonist Ro25-

6981. Conversely, extraNMDAr responses (detected by 'puff' application of NMDA, or as tonic currents) were seen to be sensitive to glycine removal and Ro25-6981 but not zinc. Then using the 'quantum dot' approach to monitor receptor diffusion in the neuronal membrane. As previously observed (Groc et al, 2007) GluN2A were seen to be less mobile but furthermore it was seen that glycine selectively slowed down GluN2A receptors whereas D-serine selectively slowed down GluN2B receptors. Glycine has an approximately 10-fold higher affinity for GluN2B-containing NMDAr, whereas D-serine has only a slight preference for GluN2A. Based on this and their results the authors make the suggestion "that D-serine on GluN2B-NMDARs and glycine on GluN2A-NMDARs could prevent their diffusion in and out of synapses, respectively", though intuitively the observations on inhibition of diffusion would indicate the opposite.

This scheme was recently extended again (Le Bail et al, 2015). Here it was observed that at SC-CA1 synapses removal of D-serine reduced NMDAr-mediated field potentials by 84% and removal of glycine reduced these by 36% indicating that D-serine was the main co-agonist at postNMDAr here. Whereas at mPP-DG synapses removal of D-serine and glycine caused 26% and 60% reductions, respectively indicating that glycine was the dominant co-agonist at these synapses. This was not seen to be due to any difference in the availability of D-serine or glycine, though differences were seen in the effects of zinc and Ro25-6981. The effects of Ro-25-6981 were equal at both synapses (~15% inhibition) but zinc reduced the amplitude of SC-CA1 responses by 34% and mPP-DG responses by 23%, which is interpreted as indicating that GluN2B have a larger role at mPP-DG synapses, which the authors link to the higher affinity of glycine for GluN2B subunits.

This study then examines the developmental change from GluN2B to GluN2A, observing that the effects of zinc were constant but the effects of Ro25-6981 decreased from 30-35% to 15% over the P9/10 and P90 in both areas. At SC-CA1 this was paralleled by a proportional change in the co-agonist contribution from glycine to D-serine, though this was not seen at mPP-DG synapses. In SC-CA1 levels of D-serine increased 96% over this period (changing the D-serine/glycine

ratio from 0.22 to 0.47) and this was linked to changes in DAAO. Also at these synapses it was observed that the gliotoxin fluroacetate reduced responses at mature but not immature synapses and that the glycine transporter inhibitor ALX5407 potentiated responses also only at mature synapses. Based on these results and their previous observations on trafficking, the authors suggest the ambitious schematic that developmental formation of tripartite synapses at SC-CA1 promotes D-serine release and uptake of glycine and this then reduces retention of GluN2B containing NMDAr in the synapse leading to a greater GluN2A component.

Thus there have recently been many insights given into the endogenous regulation of the NMDAr co-agonist site. However, such research has typically focussed on the postNMDAr and co-agonist binding of the preNMDAr is relatively unexplored. Li et al (2007) examined preNMDAr in the visual cortex by monitoring spontaneous glutamate release and observed that a co-agonist site antagonist was able to reduce the frequency of these events indicating that the preNMDAr co-agonist site was also tonically bound. Whilst this is a useful observation it is now possible to use novel tools to further understand the endogenous regulation of the preNMDAr co-agonist site. In light of the findings at postNMDAr, we are interested in the possibility that such investigation may lead to a basis for selective targeting of these receptors.

1.9 D-Cycloserine

There has been a very large amount of interest in the therapeutic potential of the NMDAr co-agonist site partial agonist (‘partial co-agonist’) D-cycloserine (DCS) for a range of CNS disorders. Whilst there have been many exciting results, the truth is that DCS has not been widely adopted as a treatment for any CNS disorder, despite having been in use as an antibiotic (DCS is also inhibits bacterial cell wall synthesis) for over 50 years. On the one hand it is possible that the focus on DCS may merely have been driven by its unique practicality, as DCS is licensed for use in humans and has a good pharmacokinetic profile including efficient CNS penetration. However, on the other hand it is possible that DCS has not progressed

as a treatment because it is already licensed and so there is no financial incentive to develop its use. On this note it is interesting that the pharmaceutical company Naurex has developed an antibody which mimics the effects of DCS and use this as a basis for justifying its therapeutic potential (Moskal et al, 2005; Burgdorf et al, 2011). Alternatively it may that a lack of understanding over its mechanism may have contributed to confusion over how DCS should be best used.

1.9.1 Anticonvulsant properties of DCS

A handful of studies have observed an anticonvulsant action of DCS. Wlaz et al (1994) tested the effects of DCS at 5, 80 and 320 mg/kg s.c. and found that the higher doses produced an elevated current threshold for maximal electrovulsions in mice. A time course indicated that this effect was maximum at 60 minutes corresponding to peak concentration (860 µM brain tissue) in a pharmacokinetic analysis. Loscher et al (1994) examined the effects of 20-320 mg/kg (i.v.) and observed an anticonvulsant effect at higher doses in the amgydala-kindled rat model. Similar pharmacokinetic findings to the Wlaz study were observed although an anticonvulsant effect was seen to persist long after the drug had been cleared, suggesting that DCS may produce adaptive changes. Wlaz (1998) again observed an anticonvulsant effect of DCS on electroconvulsions in mice with an ED50 of 443 mg/kg (i.p.). De Sarro et al (2000) then observed that DCS (1-100 mg/kg i.p.) did not produce an anticonvulsant effect on audiogenic seizures in mice but a low dose (2.5 mg/kg) potentiated the effects of several antiepileptic drugs. Finally, Wlaz and Poleszak (2011) again observed an anticonvulsant effect DCS on electroconvulsions in mice and interestingly reported that it was potentiated by pre-treatment with glycine. However, in contrast to this, seizures are the second most commonly reported adverse event for the treatment of tuberculosis with D-cycloserine (Hwang et al, 2013) where it is typically given orally at 250 mg/day corresponding to a peak cerebrospinal fluid concentration of 128 mM (Baron et al, 1955).

1.9.2 Pro-cognitive properties of DCS

In 1989, Monahan et al, reported that low doses of DCS (0.3-10 mg/kg i.p.) increased learning in rats using passive avoidance and place learning tasks presenting the first demonstration of a cognitive enhancing effect by DCS. Later, Flood et al (1992) examined the effects of DCS on learning in mice over a large dose range using a passive avoidance task. Here it was observed that DCS enhanced learning with a biphasic or 'u-shaped' dose response curve, with a maximal effect at 10-30 mg/kg (i.p.). Flood et al (1992) observed that DCS was effective when given immediately after training indicating that these effects were necessarily on memory. Quartermain et al (1994) presented similar observations of a biphasic enhancing effect on mice in a maze learning task. Subsequently many studies have found positive effects on learning using DCS at these established cognitive enhancing doses, particularly in extinction paradigms pertaining to drug addiction (see Tomek et al, 2013) and anxiety disorders (see Hofmann et al, 2013). These findings have also been reflected in humans with several clinical studies reporting beneficial effects in enhancing cue exposure psychotherapies for anxiety disorders (Rodrigues et al, 2014) and the treatment of addiction (Myers and Carlezon, 2012). Typically a low dose of around 50 mg is used for DCS in such human studies and there is evidence that higher doses are ineffective, again indicating a u-shaped dose response (Norberg et al, 2008; Rothbaum, 2008; Hofmann et al, 2006). However, unfortunately it is currently unclear what the cognitive enhancing doses of DCS represent in terms of cerebrospinal fluid concentration.

Sheinin et al (2001) and Dravid et al (2010) have studied the pharmacology of DCS at recombinant NMDAr observing that although DCS acts at the GluN1 subunit, the respective GluN2 subunit determines its efficacy. GluN2A, GluN2B and GluN2D containing NMDA receptors all have high sub-maximal DCS efficacies (90%, 65% and 94% respectively) whilst at GluN2C containing NMDA receptors, DCS has an efficacy 200% that of endogenous agonists. Also, DCS affinity varies somewhat between these receptor subtypes with EC50s of 19, 8.2, 3.3 and 2.9 μM at GluN2A, GluN2B, GluN2C and GluN2D containing NMDA

receptors respectively. This has led to the suggestion that, in studies of DCS induced cognitive enhancement, efficacious doses represent concentrations which elicit a preferential, GluN2C mediated, cognitive enhancing effect and that at higher, non-efficacious doses effects at other receptor subtypes may interfere, removing the enhancement (Goff, 2012). Recent support for this idea comes from the ability of a GluN2C/GluN2D selective potentiator to produce DCS-like cognitive effects (Ogden et al, 2014).

1.10 Aims of the project

The overarching hypothesis of the current project was that the co-agonist sites of NMDAr are a key functional element in the physiology of the EC.

The aims of the current project were:

1. To investigate the endogenous regulation of the preNMDAr co-agonist site at glutamatergic synapses in the EC in a way comparable to studies on the endogenous regulation of the postNMDAr co-agonist site.

2. To establish whether the properties and regulation of the preNMDAr co-agonist site may provide a basis for selective targeting of preNMDAr in the EC.

3. Examine the actions of different co-agonist site partial agonists at preNMDAr and postNMDAr to investigate the functional role of the co-agonist site in the activity of these two receptor populations.

4. To examine the mechanism of DCS action at NMDAr at excitatory synapses in the EC and establish whether these receptors could be important to the therapeutic effects of DCS.

5. To explore the functional role of the co-agonist sites of pre- and post-NMDAr on emergent activity at the neuronal network level, with reference to epilepsy and cognition.

Chapter 2

Materials and Methods

2.1 General Methods

2.1.1 Ethics Statement

The use of animals in medical research requires careful ethical consideration. At The University of Bath experiments are performed in accordance with the U.K Animals (Scientific Procedures) Act 1986, European Communities Council Directive 1986 (86/609/EEC) and are subject to conformity with the University ethical review document. The normative basis of animal research is that the sacrifice of a low-salience animal has the potential to alleviate or remove suffering for humans produced by disease. During these experiments, this ethical basis was kept under consideration and informed the progression of the research towards being of clinical relevance.

2.1.2 Electrophysiology

Whole cell patch clamp is the ideal technique for the study of both preNMDAr and postNMDAr. A patch pipette is touched against the neuron soma and suction is applied, sealing the pipette and cell membrane. This seal is then ruptured by further suction producing a circuit with the whole cell membrane and allowing changes in conductance of the membrane produced by ion channels to be monitored. After gaining whole-cell access the intracellular contents of the cell are exchanged with the patch solution. In voltage clamp, the neuron is held at constant voltage and changes in conductance are monitored as changes in the current applied to maintain this voltage. Ion flow through a channel will then be determined by its permeability, the composition of the patch solution and the holding voltage.

The methodology of Berretta and Jones (1996) is a highly suitable and practical means for studying the regulation of preNMDAr in the EC. Here a high concentration of the NMDAr channel blocker MK801 is included in the patch solution and this dialyses into the cell to produce a blockade of postNMDAr. The activity of preNMDAr at synapses onto the patched cell is then inferred by monitoring the frequency and characteristics of spontaneous events. Tetrodotoxin

(TTX) can also be used to block action potentials in the brain slice, removing the possibility that network activity and postNMDAr on other cells may influence the spontaneous activity. The activity of postNMDAr was examined by electrically evoking synaptic currents and isolating the NMDAr component of the response by inhibition of all other activated receptors. The influence of magnesium blockade is removed by holding neurons at a depolarised voltage. Later in this program we studied epileptiform activity in our EC slices and to achieve this extracellular recordings were made with slices in an 'interface', non-submerged recording chamber.

2.2 Slice Preparation

Acute brain slices represent a best-compromise between physiological relevance and pharmacological control. The preparation of combined EC-hippocampal slices was carried out according to the original description by Jones and Heinemann (1988). Male Wistar rats were used and with one exception in the fourth chapter, were of juvenile age (45-55g, approximately 15-25 days old) as this age is appropriate for the study of preNMDAr and suitable for the preparation of high quality brain slices for patch clamp recording.

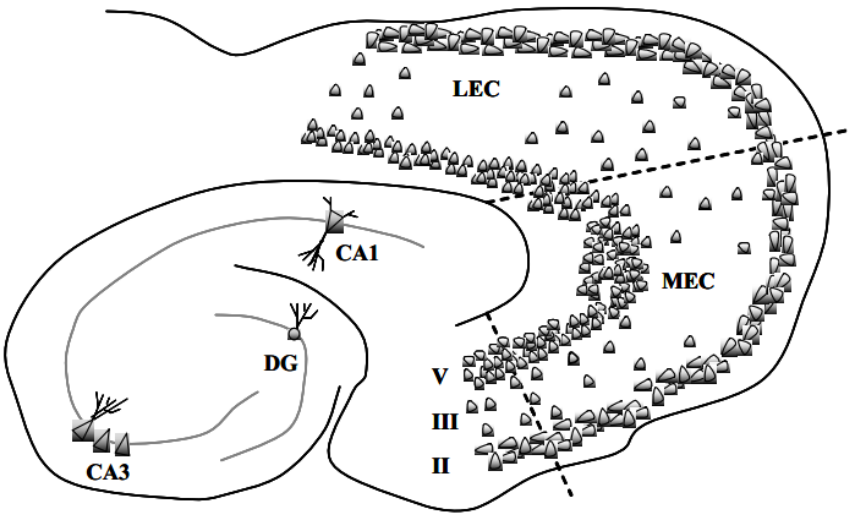

Fig. 2.1. Schematic of the combined EC-hippocampal slice. The CA1, CA3, dentate gyrus of the hippocampus and the lateral and medial areas of the EC are labelled.

Following cervical dislocation, rats were decapitated and the brain was removed and immersed in ice-chilled, oxygenated aCSF (artificial cerebrospinal fluid). The brain was then prepared by removing the cerebellum, bisecting through the midline and removing a small end portion from the dorsal surface of the two brain sections. Using the now flat dorsal surface, the brain was attached to a Teflon block ventral side up using cyano-acrylate glue. The slicing block was then loaded into a slicing chamber filled with ice-chilled, oxygenated aCSF and this was in turn loaded onto a Campden Vibroslice (Campden Instruments).

The Vibroslice utilises a vibrating blade horizontally aligned to the block and this is then moved slowly through the brain tissue. Vibration and movement speeds were adapted based on quality of slices and structural preservation of the brain. After each slice is made, the blade is lowered by 350/400uM resulting in slices with this thickness. When the ventral hippocampus and rhinal fissure are reached, the ventral half of the slices is cut away yielding the combined EC-hippocampus slice (Fig. 2.1). Up to twelve of these slices were transferred from the slicing chamber to a pre-chamber (BSC-PC, Warner Instruments) containing aCSF at room temperature. aCSF in the chamber is bubbled with carbogen producing a circular flow of oxygenated aCSF which sustains viability of the acute slices for several hours. Slices are stored at room temperature in the pre-chamber for at least one hour before use.

2.3 aCSF

The artificial cerebrospinal fluid (aCSF) used here contained as standard (in mM) NaCl (126), KCl (4), $MgSO_4$ (1.25), NaH_2PO_4 (1.4), $NaHCO_3$ (24), $CaCl_2$ (2), D-glucose (10), ascorbic acid (0.57), sodium pyruvate (5) and creatinine monohydrate (5). aCSF used for dissection and cutting additionally contained the NMDAr channel blocker ketamine (150µM), the nonsteroidal anti-inflammatory drug indomethacin (45µM), the anti-oxidant n-acetyl-cysteine (6µM), aminoguanidine (25 µM) and Coomassie Brilliant Blue (250 nM). In unpublished studies these additives have been shown to enhance slice viability. aCSF was

pH7.3 at recording temperature. The different combinations of additivies are summarised in table 2.1

	Standard aCSF	**Dissection aCSF**	**Storage aCSF**
NaCl	126mM	126mM	126mM
KCl	4mM	4mM	4mM
MgSO4	1.25mM	1.25mM	1.25mM
NaH2PO4	1.4mM	1.4mM	1.4mM
NaHCO3	24mM	24mM	24mM
CaCl2	2mM	2mM	2mM
D-glucose	10mM	10mM	10mM
Ascorbic acid	570µM	570µM	570µM
Sodium Pyruvate	5mM	5mM	5mM
Creatinine monohydrate	5mM	5mM	5mM
Indomethacin	-	45µM	45µM
N-acetyl-cysteine	-	6µM	6µM
Aminoguanidine	-	25µM	25µM
Coomaise brilliant blue	-	250nM	-
Ketamine	-	150µM	-

Table 2.1. Compositions of aCSF solutions used. Three different aCSF compositions were used, a standard composition and dissection and storage compositions which included additional compounds for slice preservation.

2.4 Patch Clamp Recordings

For patch clamp recording individual slices were transferred from storage to the recording chamber of an upright BX50WI Olympus microscope. The slices were

held in place using a slice anchor and were submerged in aCSF which was continuously circulated with a reservoir at a rate of 2ml/min. aCSF was oxygenated in the reservoir and heated to 31 ± 1 ºC using an inline heater (SH-27B, Warner Instruments) and feedback power supply (TC-324, Warner Instruments). Neurones were visualised using a CCD infrared video camera (KP-M1E/K, Hitachi Kokusai Electric Inc.) and were selected for whole cell patch clamp based on healthy appearance and observable pyramidal morphology. The entire circulating aCSF volume (including reservoir) was 10ml and the recording chamber volume was 0.5-1.0ml.

Whole cell patch-clamp pipettes with a 1–4 MΩ open tip resistance were pulled from borosilicate glass pipettes (PG120T, 1.2 mm O.D. x 0.93 mm I.D., Harvard Apparatus) using a Flaming/Brown microelectrode puller. Patch pipettes were filled with EPSC intracellular recording solution containing (in mM) D-gluconate (100), HEPES (40), QX-314 (1), ethylene glycol tetraacetic acid (0.6), NaCl (2), Mg-gluconate (5), tetraethylammonium-Cl (5), phosphocreatinine (10), ATP-Na (4), GTP-Na (0.3) which was adjusted to pH 7.3 with 1 mM CsOH solution and adjusted to 275-295 mOsm by dilution before use. Filled pipettes were then loaded onto a microelectrode holder and the two were connected electrically by a chlorinated silver wire. The microelectrode holder was then loaded onto the head stage of a 200B Axopatch amplifier in the voltage clamp configuration. A silver chloride pellet embedded on silver wire is placed in the aCSF of the recording chamber to ground the signal.

Signals were filtered at 2 kHz and digitised at 50kHz using a 1200B Digidata (Axon Instruments). Data were recorded online to computer hard disk using AxoScope software. Access resistance was measured at 5-minute intervals throughout experimentation and recordings were not used if this was seem to vary by more than 15%. Access resistance was generally of the order of 10-30 MΩ and Input resistances for the neurones recorded in these studies were of the order 500-700 MΩ. Series resistance compensation was not used and liquid junction potentials were not routinely compensated for.

Following patching, neurones were allowed to stabilise for 15-20 minutes before recording commenced and treatment conditions generally lasted 15 minutes. Drugs were applied by addition to the perfusion aCSF reservoir. For comparison of pooled data under different treatment conditions the mean was calculated for each parameter in each cell. These were used to calculate the grand mean for the data set and for significance testing with a two-tailed, paired Student's t-test. Between-slice changes were assessed using an unpaired, two-tailed Student's t-test. Normalised values were also calculated as percentage change from control and these were used to calculate average percentage changes for concentration curves. Throughout this thesis error values refer to the standard error of the grand mean.

2.5 Monitoring preNMDAr Activity

Using this intracellular solution and when neurones are held at -60 mV, small random excitatory currents are observed due to spontaneous release of synaptic glutamate. These events are mediated by glutamatergic receptors present on the recording cell. To remove the influence of postNMDAr, MK801 (5mM) is added to the intracellular solution and this blocks the postNMDAr in the recording cell (Berretta and Jones, 1996; Woodhall et al., 2001; Yang et al., 2006, 2008). In this configuration only spontaneous AMPAr events are observed and the activity of preNMDAr can be monitored by examining changes in the frequency of quantal events. Spontaneous excitatory postsynaptic currents consist of a mixture of quantal and multi-quantal events. By blocking voltage gated sodium channels, and therefore action potentials, action potential-independent quantal events can be isolated, and these are termed miniature excitatory postsynaptic currents (mEPSCs). As action potentials may be influenced by NMDAr present on other neurones in the network, or on non-terminal regions of the recording cell, throughout our studies on preNMDAr we have exclusively examined mEPSCs.

All spontaneous activity was analysed offline using Minianalysis software (Synaptosoft, Decatur). Events are detected automatically using a threshold algorithm and a checked visually. For each condition the last five minutes was analysed and the number of events and their amplitudes, rise (10-90%) and decay

(0.37 fraction) times were calculated. The number of events was used as a measure of frequency and was generally converted to frequency in Hertz.

2.6 Evoked postNMDAr potentials.

To assess postNMDAr, large postsynaptic responses were evoked by electrical stimulation of the slice using a bipolar tungsten electrode, placed laterally to the recording site. Biploar stimulations of 10-30 mA and 100 ms were applied every 20 seconds. These stimulations were generated by a Digitimer DS3 Isolated Current Stimulator and triggered using an A.M.P.I Master-8 Pulse Stimulator. Intracellular MK801 was not used and TTX was not circulated. Neurones were held at +40 mV to relieve voltage dependent blockade by Mg^{2+} and the postNMDAr component was isolated by blocking GABA receptors with Bicuculline (20 µM) and picrotoxin (50 µM) and blocking AMPA receptors with NBQX (10µM). Under these conditions evoked potentials were mediated by postNMDAr and are referred to as evoked NMDAr post synaptic currents (eNEPSC). For analysis of eNEPSC, the last five events in each treatment condition were analysed using Minianalysis and the amplitude, rise and decay times were determined. Bi-exponential fitting was carried out on the averaged event of these five, again using Minianalysis.

2.7 Extracellular Recordings

For extracellular field recordings slices were transferred to an interface-type recording chamber. Slices are unsubmergerd and the upper face of the slice is open to warm, humidified carbogen. Slices are perfused by heated (31 ± 1 ºC), oxygenated aCSF from a reservoir at a rate of 1.5 ml/min. Patch pipettes were filled with aCSF and were arranged with microelectrode holders and grounding as previously described for patch clamp. The EC was visualised using a Leica Wild MZ8 microscope and pipettes were lightly pushed into the upper brain slice surface. Field potentials were recorded using an EXT-02 extracellular amplifier (NPI Electronic). Signals were low-pass filtered at 0.5 kHz and digitised with a sample frequency of 10 kHz using a Minidigi 1B digitizer (Molecular Devices).

Data was recorded continuously to hard drive using Axoscope software. Drugs were applied by addition to perfusion aCSF reservoirs and treatment epochs were 30 minutes.

Epileptiform activity was induced by addition of strychnine (1µM), bicuculline (20µM) and picrotoxin (50µM) to the perfusion aCSF. Epileptiform activity generally began within 30 minutes of this treatment and was left to stabilise for at least 30 minutes after initiation before recording began. Novel methodology was adopted for the analysis of the epileptiform activity and this is given later.

2.8 Drugs

Drugs were generally made up as stock solutions (indicated below) and stored in aliquots at -20 ºC. Drugs were then defrosted on the day of use and added to aCSF reservoirs at such a quantity to produce the desired final concentration. For Picrotoxin (Sigma), a stock solution was made up in DMSO (Dimethyl sulfoxide) each day. MK801 (abcam) was dissolved directly into patch solution using sonication. Salts contained in aCSF were purchased from Fisher Scientific or Merck/BDH. Indomethacin, n-acetyl-L-cysteine, aminoguanidine, uric acid, Coomassie Brilliant Blue, and all items used for preparation of intracellular patch solution, aside from QX-314 (Tocris), were supplied by Sigma. Ketamine was purchased from Fort Dodge Animal Health Ltd.

Recombinant Rhodotorula gracilis D-amino acid oxidase and Bacillus subtilis glycine oxidase were provided by Professor Loredano Pollegioni, University of Insubria. These enzymes are expressed in Escherichia coli and purified as described in Fantinato et al., 2001 and Job et al., 2002. Use of these enzymes differed to that of pharmacological drugs and were applied to slices by inclusion in the perfusion aCSF for 45 minutes prior to and then throughout recordings. The drugs used were:

- 2-AP5 (D-2-Amino-5-phosphonopentanoic acid), Tocris. H_2O stock solution.

- ACBC (1-Aminocyclobutane-1-carboxylic acid) (Tocris). H_2O stock solution.
- Bicuculline methiodide, Tocris. H_2O stock solution.
- CGS15943 (9-Chloro-2-(2-furanyl)-[1,2,4]triazolo[1,5-c]quinazolin-5-amine) (Tocris). DMSO stock solution.
- CPPG ((RS)-α-Cyclopropyl-4-phosphonophenylglycine) (Tocris). DMSO stock solution.
- DCKA (5,7-Dichloro-4-hydroxyquinoline-2-carboxylic acid) sodium salt (Tocris). DMSO stock solution.
- D-cycloserine (Sigma). H_2O Stock solution.
- D-serine (Tocris). H_2O stock solution.
- Fluoroacetate sodium salt (Sigma). DMSO stock solution.
- Glycine (Tocris). H_2O stock solution.
- MCPG ((RS)-α-Methyl-4-carboxyphenylglycine) sodium salt (Tocris). DMSO stock solution.
- NBQX (2,3-dihydroxy-6-nitro-7-sulfamoyl-benzo[f]quinoxaline-2,3-dione), Tocris. DMSO stock solution
- NMDA (N-Methyl-D-aspartic acid) (Tocris). H_2O stock solution.
- Suramin hexamethodium salt (Tocris). DMSO stock solution. Strychnine hydrochloride (Tocris). H_2O stock solution.
- Tetrodotoxin citrate, Alomone Labs. H_2O stock solution.
- UBP 141 ((2R*,3S*)-1-(Phenanthrenyl-3-carbonyl)piperazine-2,3-dicarboxylic acid) (a gift from Professor David Jane, University of Bristol). DMSO stock solution.

Chapter 3

Co-agonist Regulation of Presynaptic NMDA Receptors

3.1 Introduction

As discussed in section 1.6, preNMDAr are now known to have a widespread expression in the CNS and are an important mechanism for controlling synaptic transmission and tuning neuronal networks. Several studies have indicated a role of preNMDAr in mediating synaptic plasticity changes whilst additionally work in this laboratory has shown that preNMDAr appear to have an enhanced activity in epilepsy and may contribute to seizure activity. Unlike postNMDAr, preNMDAr appear to have a diminished importance in the adult brain and so targeting the elevated activity of these receptors in epilepsy is a therapeutically practical approach for anticonvulsant development. However, clearly the greatest problem for both the wider study and therapeutic relevance of preNMDAr is that currently there is no basis for selectively targeting these receptors.

We are particularly interested in the EC due to its role in both cognitive information processing and seizure pathology in TLE. Also many previous studies have examined preNMDAr in this area and these receptors are arguably most well defined at excitatory synapses in the EC. Although sporadic reports have made more direct observations of preNMDAr function, the methodology developed by Berreta and Jones (1996) remains the most practical for the study of these receptors. As with many other regions, preNMDAr in the EC exert a tonic facilitation of glutamate release and we use the facilitation of spontaneous glutamate release as an indirect reporter for preNMDAr function. By blocking postNMDAr in the recording cell with a high concentration of MK801 added to patch clamp solutions we can isolate AMPA receptor mediated mEPSCs. We monitor the frequency of these glutamatergic events in the recording cell and can add NMDAr ligands to the brain slice to selectively monitor the effect on glutamate release at synapses onto the recorded cell.

The tonic activation of preNMDAr at excitatory synapses in the medial EC was demonstrated by a decrease in the frequency of AMPA receptor mediated events, without any change in event amplitude, upon addition of the glutamate site antagonist AP5 (Berretta and Jones, 1996). This indicated that the glutamate site

of the preNMDAr is tonically bound by ambient glutamate, in contrast to postNMDAr. Later, work by Woodhall et al (2001) demonstrated that the preNMDAr glutamate binding site was not fully bound and large increases in frequency were produced by the NMDAr agonist homoquinolic acid (HQA). This study also demonstrated that the preNMDAr in the medial EC were likely to have a GluN2B/GluN1 diheteromeric composition and that calcium entry mediated the facilitatory effects of preNMDAr in this region.

Novel tools have contributed greatly to an increase in understanding of co-agonist regulation of NMDAr (see section 1.8). In particular, the co-agonist scavenging enzymes glycine oxidase (GO) and D-amino acid oxidase (DAAO). Purified DAAO from the yeast Rhodotorula gracilis (RgDAAO) and GO from the bacterium Bacillus subtilis (BsGO) can be produced by recombinant expression in Escherichia coli cells (Fantinato et al, 2001; Job et al, 2002) and then used to selectively metabolise the substrate co-agonist in brain slices during a period of incubation (Fossat et al, 2011; le Bail et al, 2014). Secondly is the astrocyte poison fluoroacetate which is selectively uptaken into glial cells by an unknown transport mechanism (Waniewski and Martin, 1998). Within cells, fluoroacetate is incorporated into the mitochondrial Krebs cycle (aka citric acid cycle or tricarboxylic acid cycle) which is central to the production of the cellular currency of energy, adenosine triphosphate. In the Krebs cycle fluoroacetate is converted to fluorocitrate which inhibits the enzyme aconitase arresting the cycle and causing metabolic inhibition and toxicity (Hassel et al, 1997; Paulsen et al, 1987). In this chapter we have utilised these novel tools to further examine the preNMDAr in the EC. The aim of this work was to establish the nature of co-agonist regulation of the preNMDAr to ascertain whether this may be utilised for the selective targeting of different NMDAr populations.

3.2 Methods

All experiments in this chapter were performed using brain slices from juvenile rats as outlined in the methods section. mEPSCs were recorded in layer V neurones of the medial EC. In all experiments MK801 was added to intracellular patch

solutions at a concentration of 5 mM to block postNMDAr in the recorded cell and mEPSCs were isolated by application of TTX at a concentration of 1 µM. All cells had pyramidal morphology. In these cells EPSCs occur as spontaneously occurring inward currents when held at a potential of -60 mV. Although the frequency of events in layers II and V are low, clear preNMDAr mediated changes in frequency can be observed here (Jones and Woodhall, 2005). Data analysis and significance testing was carried out as outlined previously.

RgDAAO and BsGO were supplied by Professor Loredano Pollegioni of the University of Insubria, Italy. These enzymes were overexpressed in Escherichia coli cells and purified with final activities of 100 ± 15 U/mg (RgDAAO) and 0.9 ± 0.2 U/mg protein (BsGO) and high specificity for the respective co-agonist. In these experiments slices were incubated with enzymes (at 0.2 U/ml) at room temperature for at least 45 minutes before recording started and incubation continued during recording (recordings are made at 32 ^{o}C). Matched slices from the same animal were used for control and were treated in the same manner but using the appropriate buffer without enzyme. Experiments using fluoroacetate were conducted in the same manner.

3.3 Results

3.3.1 Effects of exogenously applied co-agonists on mEPSCs

To investigate the binding of the preNMDAr we first examined the effects of the endogenous NMDAr co-agonists glycine and D-serine on spontaneous AMPA receptor mediated events as a reporter for presynaptic glutamate release. mEPSCs were chosen over sEPSCs to avoid any potential complications of network derived effects from postNMDAr at other neurones. mEPSCs were recorded in three cells and glycine was applied at a concentration of 100 µM. Results are summarised in Fig. 3.1.A. No significant effects were detected in this data set. Mean frequency was 0.75 ± 0.13 Hz under control conditions and 0.73 ± 0.12 Hz in the presence of exogenous glycine. Mean event amplitude was 6.36 ± 0.13 pA in control and 6.00 ± 0.18 pA in the glycine treated condition. Mean mEPSC rise times were 4.7 ±

0.67 ms in control and 5.34 ± 0.30 ms after treatment. Mean decay time were 6.3 ± 1.24 ms and 6.3 ± 0.31.3 ms respectively.

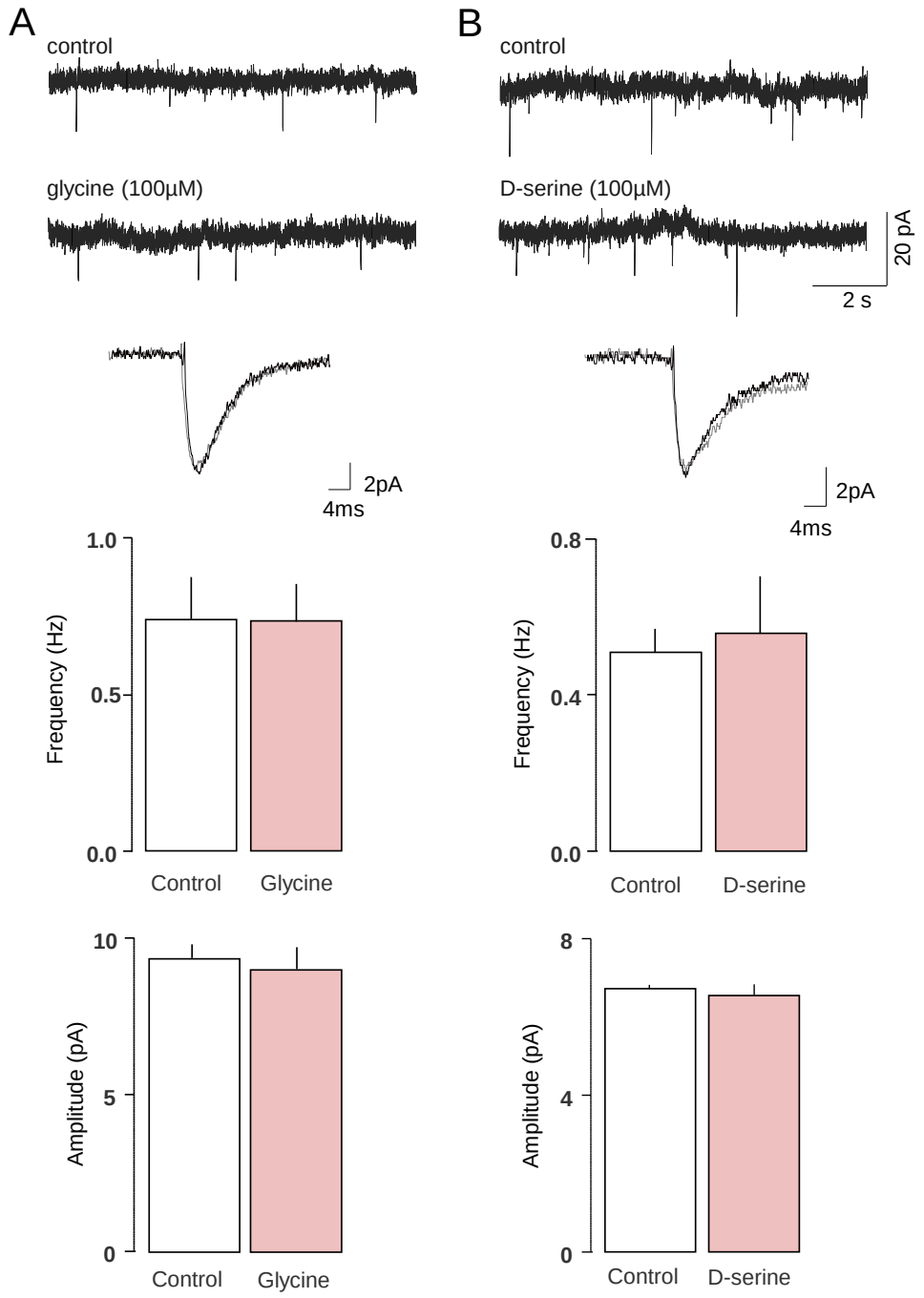

Fig. 3.1. The effects of glycine (A) and D-serine (B) on mEPSCs in EC neurones. A. Upper traces show sample voltage clamp recordings of sEPSCs in layer V neurones in the medial EC in control and treatment conditions. Lower traces depict overlaid averaged events from control (black) and treatment conditions (grey). Bar graphs represent average frequency and amplitude data from 3 neurones in the case of glycine and 4 in the D-serine experiment. The addition of glycine had little effect on the frequency or amplitude of mEPSCs. Exogenous D-serine was similarly seen to have no observable effects.

The effects of exogenous D-serine (100 µM) on mEPSCs were tested in four neurones. These results are summarised in Fig. 3.1.B. Again no significant effects were observed here. Mean frequency was 0.51 ± 0.03 Hz in the control condition and 0.56 ± 0.15 Hz during perfusion of D-serine. Mean event amplitude was 6.7 ± 0.1 pA in control and 6.52 ± 0.3 pA following treatment. Mean rise times were 4.3 ± 0.3 ms v 4.5 ± 0.3 ms and mean decay times were 5.5 ± 3.3 ms v 6.5 ± 0.3 ms in the control and D-serine treatment conditions respectively.

The lack of any significant effect for either of glycine or D-serine on mEPSC frequency indicated that these co-agonists were not affecting preNMDAr function. The most likely explanation for this was that the co-agonist site of the preNMDAr was already highly bound by an endogenous co-agonist and this situation has already been demonstrated in the visual cortex (Li et al, 2007).

3.3.2 Effects of the co-agonist site antagonist DCKA on mEPSCs

To test whether tonic binding of preNMDAr by an endogenous co-agonist contributes to the tonic activation of these receptors the effects of the NMDAr co-agonist site antagonist DCKA (10µM) on AMPA receptor dependent mEPSCs was tested in four neurones. These results are summarised in Fig. 3.2. DCKA was seen to produce a significant decrease in the frequency of events ($p<0.01$), no other significant effects were observed. mEPSC frequency was 0.80 ± 0.05 Hz under control conditions and 0.59 ± 0.01 Hz in the presence of DCKA, a decrease of ~27%**.** Mean amplitude was 8.37 ± 0.5 pA under control conditions and 7.8 ± 0.4 pA in the presence of DCKA. Mean event rise time was 4.8 ± 0.3 ms in control and 4.8 ± 0.4 ms following treatment. Mean event decay times were 5.8 ± 0.5 ms and 6.0 ± 0.7 ms respectively. The significant reduction of spontaneous excitatory events following application of DCKA, without any change in event amplitude, is a typical of a presynaptic inhibition of quantal vesicular transmitter release. This result is indicative of an antagonist effect at the preNMDAr which act to tonically facilitate glutamate release at excitatory synapses in this region (Berretta and Jones, 1996) and implied that the co-agonist binding site of the preNMDAr is indeed endogenously bound here.

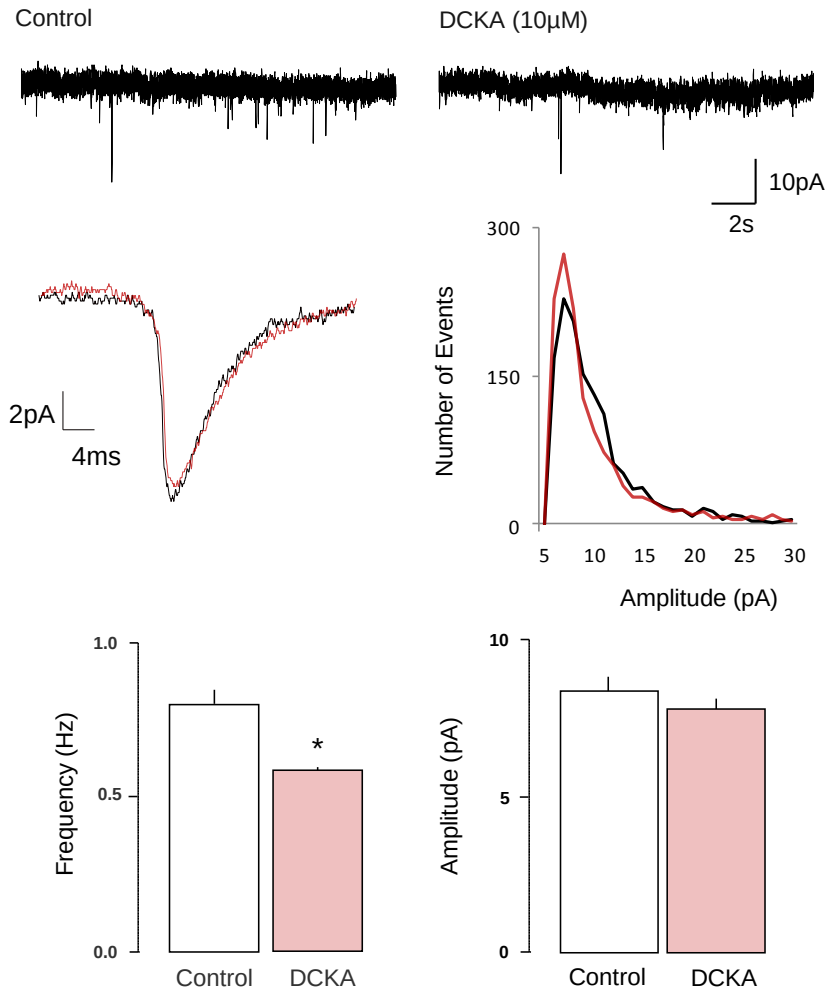

Fig. 3.2. The co-agonist site antagonist DCKA elicits a reduction in spontaneous glutamate release. Upper traces show sample voltage clamp recordings of sEPSCs in layer V neurones in the medial EC in control and treatment conditions. Averaged traces are presented from control (black) and DCKA (red) conditions, overlaid. Amplitude histogram depicts the frequency distribution of event amplitudes in control (black) and DCKA (red) conditions for four cells. In both cases a single peak, normal type distribution with a slight skew towards larger events is observed, typical of such data. The distribution of event amplitudes is qualitatively the same between conditions, indicating that changes in frequency were not due to a shift in amplitude distribution. Bar charts depict the average frequency and amplitude data. mEPSC frequency was significantly lower in the DCKA condition indicating a presynaptic inhibition of spontaneous glutamate release. * denotes $p<0.05$ significance level.

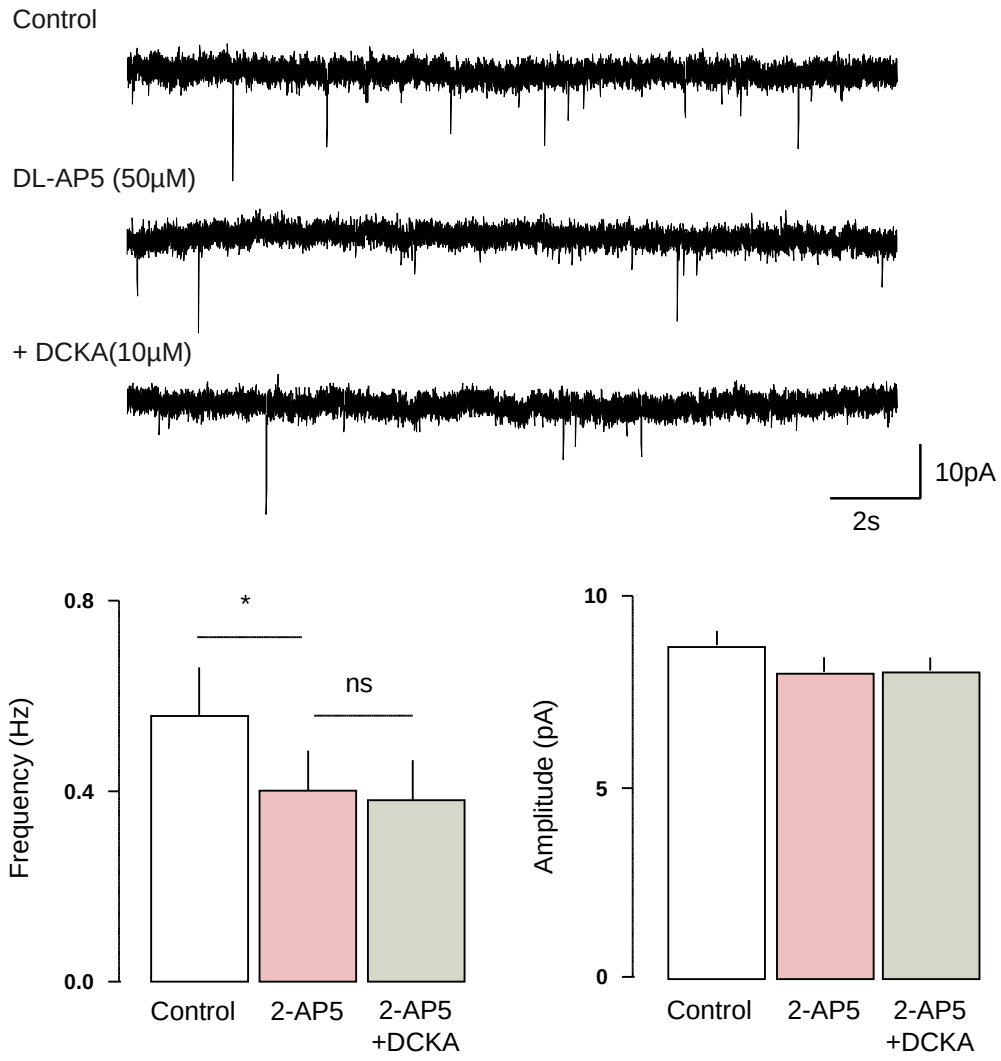

Fig. 3.3. The glutamate site antagonist 2-AP5 reduces mEPSC frequency and precludes the effects of DCKA. Sample traces are shown of recorded mEPSCs in layer V EC neurones in each condition. Bar charts depict average values from five neurones. 2-AP5 significantly and selectively reduced mEPSC frequency but further addition of DCKA elicited no further change. * denotes $p<0.05$, 'ns' denotes not significant.

To ascertain whether this effect was truly mediated by preNMDAr we examined whether the response to DCKA was affected by treatment with the prototypic NMDAr antagonist AP5. In five cells the competitive glutamate site antagonist AP5 was applied followed by DCKA, without washing out AP5. The frequency of mEPSCs was significantly decreased in the presence of AP5 ($p<0.01$) and was subsequently unchanged by addition of DCKA ($p<0.01$). No other significant changes were observed in any parameter in this data set. Mean frequency was 0.56

± 0.1 Hz under control conditions, 0.40 ± 0.1 Hz in the presence of AP5 alone, and 0.38 ± 0.1 Hz in the presence of AP5 and DCKA.

Thus AP5 precluded the inhibitory effect of DCKA confirming that this response was mediated by preNMDAr. Collectively these results indicate the following: preNMDAr at excitatory synapses in the EC are tonically bound by an endogenous co-agonist. The lack of effect by application of glycine or D-serine indicates that the endogenous binding is likely to be close to saturation. The response of mEPSCs to DCKA treatment is a suitable basis for the study of the tonic binding of preNMDAr by endogenous co-agonists. Rise times were 4.6 2.3 ms 4.7 ± 2.4 and 4.8 ± 2.4 in the control, AP5 and AP5 and DCKA treatment conditions respectively. Accordingly, mean decay times were 6.6 ± 3.5 ms 6.3 ± 3.6 ms and 6.3 ± 3.3 ms.

3.3.3 Effects of enzymatic degradation of glycine on mEPSCs

To attempt to identify the endogenous co-agonist at preNMDAr in the medial EC we now utilised co-agonist scavenging enzymes to selectively breakdown candidate ligands, an approach which has been useful for the investigation of co-agonists of postNMDAr (Fossat et al., 2011; Papouin et al., 2012).

We first investigated the possibility that the endogenous co-agonist was glycine and incubated six brain slices with BsGO. For comparison, six slices from the same preparation were subject to a sham incubation with empty buffer. In cells from each set of slices, AMPA receptor dependent mEPSCs were recorded and DCKA (10 μM) was applied. These results are displayed in shown in Fig. 3.4. In both BsGO and matched slices, mEPSC frequently was significantly lower than control in the presence of DCKA ($p<0.05$ and $p<0.01$ respectively). There were no other significant differences. The frequency of mEPSCs in untreated slices was 0.33 ± 0.04 Hz in the control period and 0.24 ± 0.026 Hz with DCKA ($p<0.01$) whilst in BsGO treated slices these values were 0.41 ± 0.1 Hz and 0.32 ± 0.1 Hz ($p<0.05$) respectively. Mean amplitudes were 8.4 ± 1.4 pA for control v 8.4 ± 1.6 pA for DCKA in untreated slices and 7.7 ± 4.1 pA for control v 7.95 ± 0.9 pA for DCKA

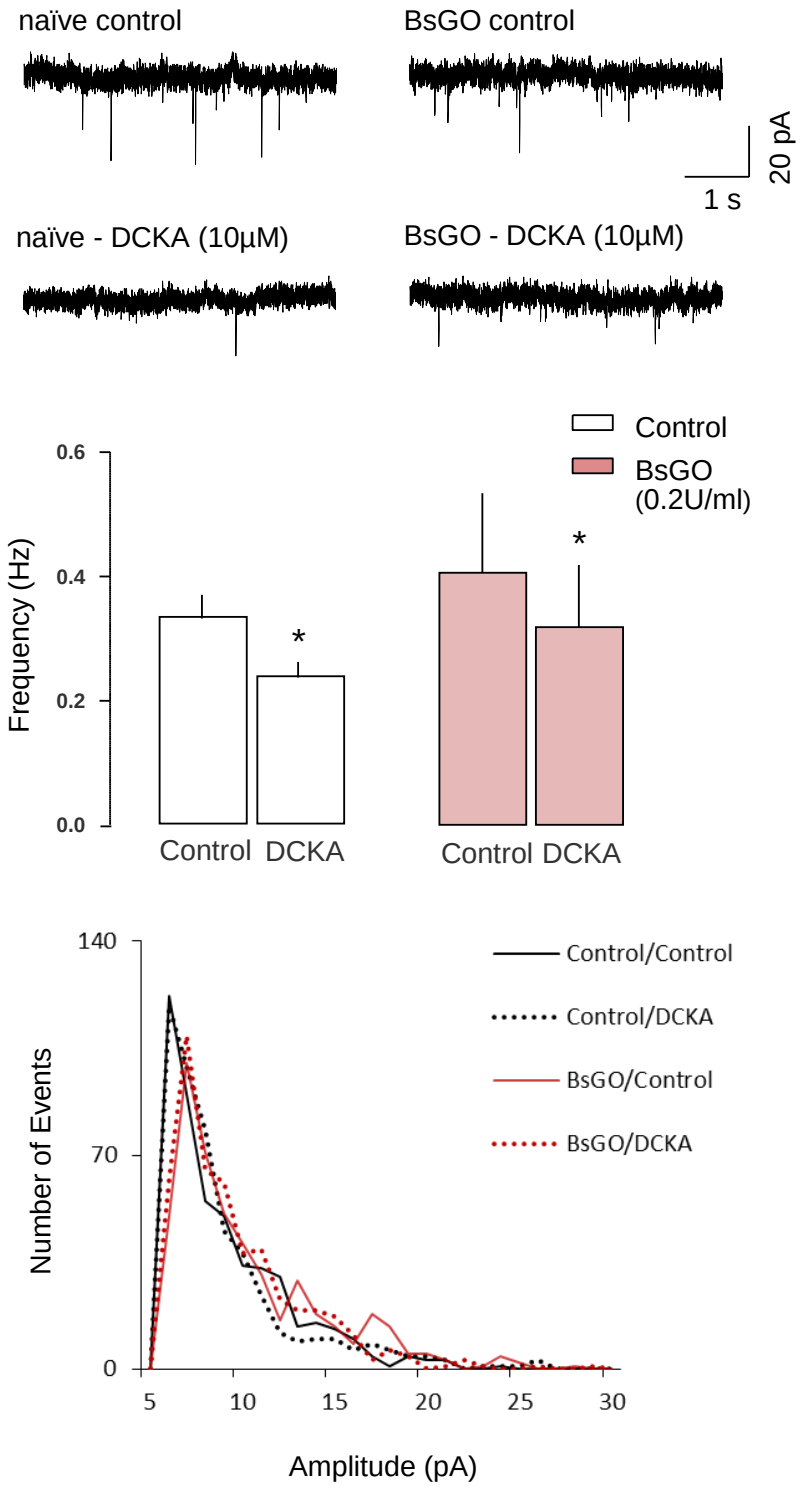

Fig. 3.4. Enzymatic removal of endogenous glycine does not affect spontaneous release of glutamate in the EC. Above, sample traces from mEPSC recordings, middle, bar chart of average frequency data from six neurones each, below, amplitude distribution histograms. Slices incubated with BsGO to remove endogenous glycine exhibited no difference to untreated, matched slices. Control mEPSC frequency was similar between groups and the previously observed frequency lowering effect of DCKA was present in both groups. * denotes $p<0.05$ significance level.

in BsGO treated slices. Control v DCKA rise times were 4.7 ± 0.9 ms v 4.7 ± 0.9 ms in untreated slices and 4.4 ± 0.4 ms v 4.3 ± 0.4 ms in BsGO treated slices. According decay time values were 7.3 ± 1.2 ms v 7.5 ± 1.3 ms in untreated slices and 7.1 ± 0.8 ms v 7.2 ± 0.75 ms in BsGO treated brain slices. Overall there was little difference between untreated and BsGO treated brain slices and the frequency of events was lowered in the presence of a co-agonist site antagonist in each. This indicated that the presence of glycine was unimportant to the function of preNMDAr suggesting that glycine was not regulating these receptors.

3.3.4 Effects of enzymatic degradation of D-serine on mEPSCs

Next we conducted the same format of experimentation but replacing BsGO with the enzyme RgDAAO which degrades the co-agonist D-serine. Again the effects of DCKA (10 μM) on AMPA receptor dependent mEPSCs were examined in six enzyme treated slices and six matched, untreated slices. These results are shown in Fig. 3.5. The frequency of mEPSCs was significantly reduced in the presence of DCKA in the untreated brain slices and no other significant differences were seen. The frequency of mEPSCs in untreated slices was 0.65 ± 0.13 Hz in the control period and 0.42 ± 0.10 Hz ($p<0.05$) in the presence of DCKA. Whereas the frequency of mEPSCs in RgDAAO treated slices was 0.38 ± 0.03 Hz in the control period and 0.36 ± 0.05 Hz in the presence of DCKA. Event amplitudes in control v DCKA conditions were 8.2 ± 0.5 pA v 8.1 ± 0.5 pA in untreated slices and 7.3 ± 0.3 pA v 7.5 ± 0.3 pA in RgDAAO treated slices. Rise times in control v DCKA were 4.8 ± 0.9 ms v 4.7 ± 0.9 ms in untreated slices and 4.8 ± 0.9 ms v 5.1 ± 1.0 ms in RgDAAO treated slices. Finally, decay times were 6.4 ± 1.2 ms v 6.7 ± 1.3 ms in untreated slices and 6.5 ± 1.5 ms v 7.1 ± 2.0 ms in RgDAAO treated slices. The frequency lowering effect of DCKA was thus not present in slices treated in RgDAAO to remove endogenous D-serine and these slices also had a noticeably lower control frequency. These results thereby indicated that the presence of D-serine was necessary for the facilitatory effects of preNMDAr in the EC and was likely to be the endogenous co-agonist at these receptors.

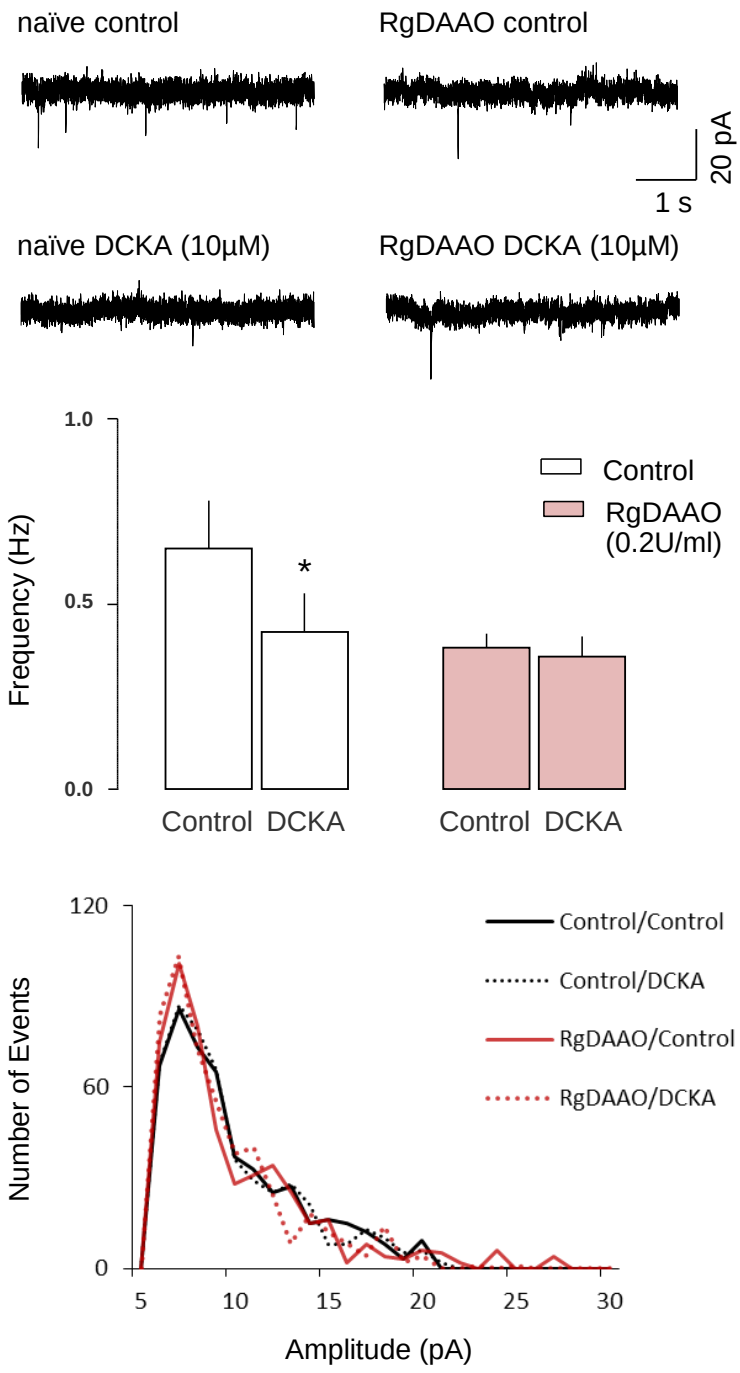

Fig. 3.5. Enzymatic removal of endogenous D-serine precludes the effects of DCKA on AMPA receptor mediated mEPSCs in the EC. Above, sample traces from mEPSC recordings, middle, bar chart of average frequency data from six neurones each, below, amplitude distribution histograms. Slices incubated with RgDAAO to remove endogenous D-serine exhibited a lower control frequency than untreated, matched slices. Again DCKA was seen to lower mEPSC frequency in naïve slices, though this was not present in slices treated with RgDAAO. Importantly, there were no substantive changes in the amplitude of events between the groups, indicating that the changes in frequency were due to changes in the probability of release. * denotes $p<0.05$ significance level.

3.3.5 Effects of glial cell inhibition by fluoroacetate on mEPSCs

As previous studies have indicated that astrocytes are a source of D-serine at NMDAr we now investigated the possibility that these cells may provide D-serine for the tonic facilitation of glutamate release by preNMDAr in the EC. We used the metabolic inhibitor fluoroacetate which is selectively uptaken by glial cells, to investigate this possibility.

Six EC-hippocampal slices were treated with fluoroacetate as outlined in 3.2 and six untreated, matched slices were used for comparison. Again AMPA receptor mediated mEPSCs were recorded in treated and untreated slices during control conditions and following perfusion of the co-agonist site antagonist DCKA (10 μM). In untreated slices the frequency of mEPSCs was significantly lowered from control during perfusion of DCKA and no other significant differences were seen. In untreated slices mEPSC frequency was 0.66 ± 0.13 Hz under control conditions and 0.45 ± 0.09 Hz ($p<0.05$) in the presence of DCKA whilst in fluoroacetate treated slices mEPSC frequency was 0.35 ± 0.03 Hz in the control period and 0.34 ± 0.04 Hz in the presence of DCKA. Mean amplitudes for control v DCKA were 7.6 ± 1.5 pA v 7.9 ± 1.9 pA in matched untreated slices and 7.0 ± 0.7 pA v 7.1 ± 0.5 pA in fluoroacetate treated slices. Mean mEPSC rise times for control v DCKA were 5.0 ± 0.9 ms v 5.1 ± 1.0 ms in untreated and 5.0 ± 0.5 ms v 5.25 ± 0.5 ms in fluoroacetate treated slices. Respective decay times were 8.9 ± 2.4 ms v 8.4 ± 2.2 ms in untreated and 7.5 ± 0.96 ms v 8.9 ± 1.3 ms in slices treated with fluoroacetate. Again the decrease in frequency independent of a change in amplitude with the co-agonist site antagonist DCKA indicated that the preNMDAr co-agonist site was tonically bound in untreated brain slices but not in slices which were treated with fluoroacetate to inhibit glial cell metabolism. Also the control frequency was noticeably lower in matched, untreated slices compared to fluoroacetate slices, mirroring the effects of RgDAAO. These findings suggested that glial cell function is necessary for the action of preNMDAr and that these cells may be important for the regulation of the preNMDAr co-agonist site by D-serine.

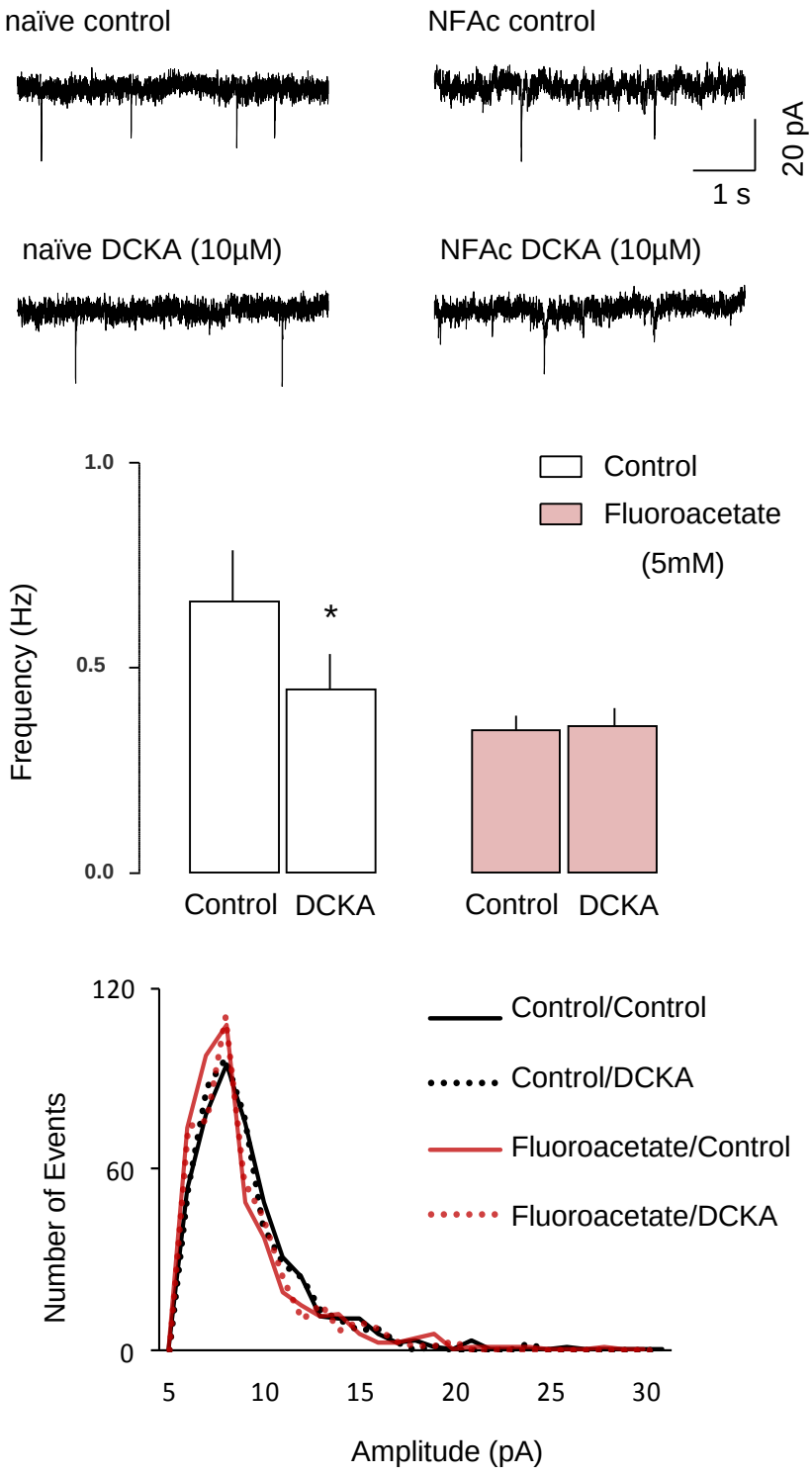

Fig. 3.6. Compromising glial cell function reduces the frequency of mEPSCs in the EC. Above, sample traces from mEPSC recordings, middle, bar chart of average frequency data from six neurones each, below, amplitude distribution histograms. Incubation with the glial cell metabolic inhibitor sodium fluoroacetate was seen to produce a lower mEPSC control frequency and an abolished DCKA response, compared to matched slices. Again there were no changes in the distribution of event amplitudes between the groups. * denotes $p<0.05$ significance level.

3.3.6 Effects of D-serine on mEPSCs in fluoroacetate treated slices

However, as glial cells have many roles and in particular are also involved in the recycling of glutamate further experimentation was needed to link this result to the co-agonist site of the preNMDAr. To achieve this we recorded mEPSCs in five brain slices treated with fluoroacetate and applied exogenous D-serine (100 µM). Results from this experiment are shown in Fig. 3.7. Here D-serine was seen to elicit a significant increase in mEPSC frequency, with no changes in any other event parameter. Under control conditions the frequency of mEPSCs was 0.23 ± 0.04 Hz and this increased to 0.3 ± 0.04 Hz in the presence of exogenous D-serine ($p<0.05$). Mean amplitude was 6.3 ± 0.13 pA in control and 6.2 ± 0.07 pA following perfusion of D-serine. Rise times for control v D-serine were 5.1 ± 0.17

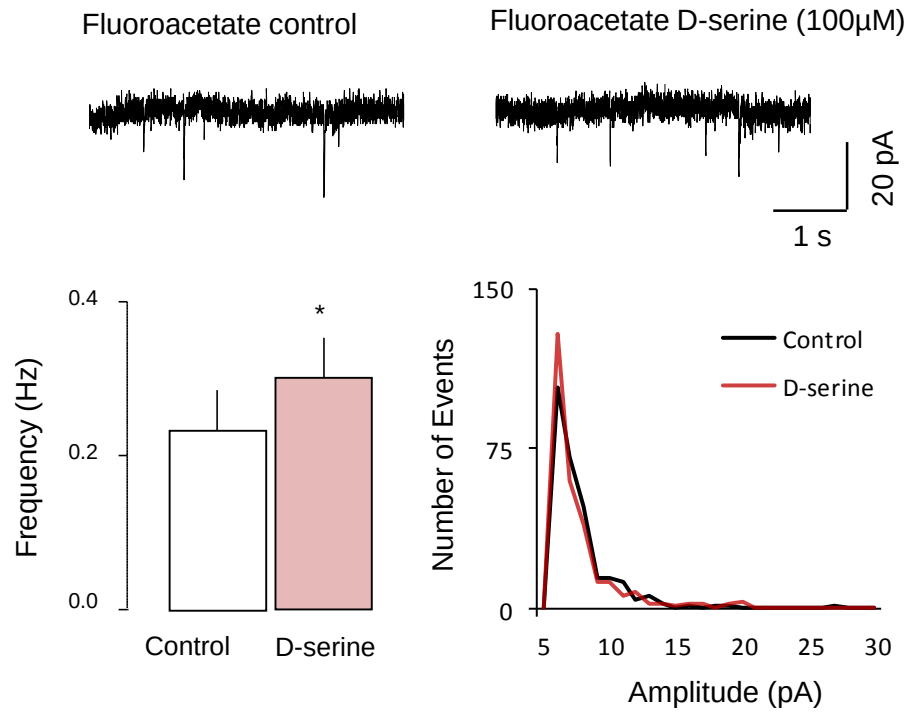

Fig. 3.7. D-serine increases mEPSC frequency in slices with compromised glial function. Above, sample traces from mEPSC recordings, lower left, bar chart of average frequency data from six neurones, lower right, amplitude distribution histograms. In slices treated with the glial cell metabolic inhibitor sodium fluoroacetate mEPSC frequency was significantly increased in the presence of exogenous D-serine, compared to control. There were no changes in the distribution of event amplitudes between the two conditions. * denotes $p<0.05$ significance level.

ms v 5.1 ± 0.16 ms and decay times were 8.1 ± 0.37 ms v 6.9 ± 0.48 ms. Thus in contrast to naïve slices, in fluoroacetate treated slices D-serine selectively increased the frequency of AMPA receptor dependent mEPSCs, indicative of a facilitatory action at preNMDAr. This indicated that a decreased supply of co-agonist was a mechanism for the decrease in preNMDAr activity produced by disrupting glial cells with fluoroacetate. Therefore it is likely that astrocytes are acting as a source of D-serine at the preNMDAr observed here.

Although the frequency of mEPSCs was significantly increased by D-serine in fluoroacetate treated slices, it remained noticeably low. As we have previously mentioned, astroglial cells are also involved in the production of glutamate and so we now investigated whether this role is important in the anti-preNMDAr effect produced by fluoroacetate treatment. To this end the effects of the glutamate site agonist NMDA (100µM) on mEPSCs were examined in five untreated brain slices and five slices treated with fluoroacetate. In both untreated and fluoroacetate treated slices, NMDA produced significant increases in mEPSC frequency, no other significant changes were observed. mEPSC frequency in untreated cells was 0.56 ± 0.17 Hz in control and 1.03 ± 0.25 Hz ($p<0.05$) in the presence of NMDA whilst in fluoroacetate treated slices, mEPSC frequency changed from 0.32 ± 0.075 Hz in control to 0.49 ± 0.13 Hz ($p<0.05$) in the presence of NMDA. Mean mEPSC amplitudes for control v NMDA perfusion were 7.4 ± 0.48 pA v 7.4 ± 0.30 pA in untreated slices and 7.5 ± 1.3 pA v 7.2 ± 0.59 pA in fluoroacetate treated slices. Likewise, rise times were 5.0 ± 0.71 ms v 6.2 ± 0.37 ms and 5.2 ± 0.66 ms v 6.4 ± 0.51 ms and decay times were 7.6 ± 0.93 ms v 7.2 ± 1.01 ms and 7.4 ± 0.93 ms v 7.6 ± 1.03 ms for untreated and fluoroacetate treated slices respectively.

Thus in both naïve slices and slices in which glial cell function has been compromised by fluoroacetate, NMDA is able to elicit increases in mEPSC event frequency indicating that the glutamate binding site of preNMDAr is not fully bound in both conditions. It is interesting that in naïve slices the increase in frequency with NMDA was ~131% whist in fluoroacetate treated slices this was noticeable less (58%). This suggests that compromising glial cells does was not compromising glutamate production, as this would logically be expected to

produce an increase in response to a glutamate site agonist. Instead it is possible that a decreased D-serine at preNMDAr is limiting the activation of these receptors in response to activation of the glutamate site.

It is possible that glial cells regulate both the glutamate and co-agonist sites of the preNMDAr. This then may explain why the facilitatory effect of the glutamate site agonist NMDA was reduced in slices with compromised glial cell function, as NMDAr are thought to require the presence of both agonist and co-agonist to open and the activation of these receptors may then be limited by reduced binding of the co-agonist site. Likewise the only partial rescue of mEPSC frequency by D-serine in fluoroacetate treated slices may be due to a reciprocal effect.

On the basis of these results then, we can conclude that astroglia are crucial to the tonic facilitatory action of preNMDAr at excitatory synapses in the EC. This regulation is mediated by D-serine and astrocytes are likely to be the source of this co-agonist at preNMDAr. However, it is noted that the reduction in control mEPSC frequency by fluoroacetate was somewhat less than that produced by RgDAAO and therefore we have not ruled out non-astrocytic sources of D-serine at preNMDAr. Though it is interesting to speculate on possible explanations for the complicated observations we have made here a more in depth study of these issues is limited by a lack of tools for direct investigation into preNMDAr pharmacology. However we have made some potentially useful observations regarding the regulation of these receptors (see 3.4.3).

3.3.7 Effects of other gliotransmitter receptor ligands on mEPSCs

The rescue of mEPSC frequency with D-serine in fluoroacetate treated slices strongly implies that glial production of this co-agonist at preNMDAr was impaired in this situation. However, it is noted that D-serine did not restore mEPSC frequency to a full extent compared to the reduction produced by fluoroacetate incubation suggesting that other mechanisms may also be important. Indeed as discussed in section 1.7, glial cells regulate synaptic transmission through multiple mechanisms. In particular, purinergic transmission is a well-known mechanism for

astrocyte-neuron signaling and we were interested in the possibility that release of adenosine or ATP may be important in the response observed here. To investigate what other mechanisms could mediate the reduced mEPSC frequency in fluoroacetate treated slices we examined the effects of several gliotransmitter receptor ligands on mEPSCs in untreated slices. Results from these experiments are shown in table. 3.1.

	Frequency (Hz)	**Amplitude (pA)**	**Rise Time (ms)**	**Decay Time (ms)**
Control	0.49 ± 0.07	9.6 ± 1.1	5.3 ± 0.9	9.0 ± 1.5
Suramin	0.45 ± 0.04	9.3 ± 1.0	5.3 ± 0.9	9.7 ± 0.7
+DCKA	0.27 ± 0.01*	8.2 ± 0.7	6.2 ± 0.6	9.3 ± 1.9
Control	0.46 ± 0.12	8.4 ± 1.1	4.8 ± 0.6	6.5 ± 1.0
CGS15943	0.48 ± 0.12	8.8 ± 1.4	5.2 ± 0.5	7.5 ± 1.0
+DCKA	0.34 ± 0.11*	8.9 ± 1.1	5.0 ± 0.6	8.0 ± 0.9
Control	0.43 ± 0.09	9.5 ± 2.1	4.5 ± 1.2	6.6 ± 1.0
UBP141	0.45 ± 0.08	9.7 ± 1.5	5.2 ± 1.4	6.0 ± 2.6

Table 3.1. The effects of the purinergic antagonists Suramin and CGS15943, and the GluN2C/D specific antagonist UBP141 on the frequency, amplitude and kinetics of mEPSCs. * denotes significantly different compared to control ($p<0.05$). n=3 for each experiment.

The broad spectrum P2X purinergic receptor antagonist suramin (100 µM) was added followed by DCKA (without washout; 10 µM) to three slices. The frequency of mEPSCs was significantly lowered following addition of DCKA, no other significant effects were seen. Then CGS15943 (1 µM), which is an antagonist of A_1, A_2A, A_2B and A_3 adenosine receptor, was added to three slices followed by DCKA (without washout; 10 µM). Again the only significant effect observed was a decrease in mEPSC frequency following perfusion of DCKA. These results

indicated that purinergic signaling is does not contribute to spontaneous glutamate release in the EC, at least not in a tonic manner, and is therefore unlikely to be involved in the effects of fluoroacetate.

Whilst an effect at preNMDAr is the most parsimonious explanation for the changes in mEPSC frequency observed here it is also interesting to consider the possibility that NMDAr on astrocytes themselves could also be involved. Recently functional NMDAr have been observed on astrocytes and have been shown to contain GluN2C/D subunits (Palygin et al, 2011). Previous work has indicated that NMDAr dependent tonic facilitation of mEPSCs in the EC is mediated by GluN2B heterodimeric receptors. Given this discrepancy in subunit dependence, it is unlikely that astrocyte NMDAr could be responsible for changes in mEPSC frequency though we decided to further examine this possibility using the NMDAr antagonist UBP141 which has a relative specificity for the GluN2C/D subunit (Morley et al., 2005). In three untreated slices we examined the effects of UBP141 (2.5 μM) on AMPA receptor mediated mEPSCs (table 3.1). However, no changes were observed from control during perfusion of UBP141. This indicated that GluN2C/D receptors were not involved in NMDAr-dependent tonic facilitation of glutamate release. Therefore it is unlikely that astrocyte NMDAr were involved in the effects on mEPSC frequency previously observed.

An additional consideration are presynaptic mGluRs which also regulate glutamate release in the EC and presynaptic mGluRs have prevsiouly been observed to be an astrocyte target (e.g. see Fiacco and McCarthy, 2004; Clasadonte and Haydon, 2012). However, it has previously been shown that such receptors here are also not tonically active (Evans et al, 2000) and are therefore not a candidate for a reduction in control frequency in treated slices.

In summary then, it appears as though purinergic signaling is not involved in tonic glial-dependent facilitation of mEPSCs. Additionally it is unlikely that NMDAr present on astrocytes themselves are involved in mediating the changes in mEPSC frequency we have observed with the co-agonist site antagonist DCKA.

3.4 Discussion

3.4.1 Overview

In this chapter I have utilized AMPA receptor mediated mEPSC frequency as a reporter of preNMDAr activity and have presented experimental data which sheds further light on the properties of preNMDAr in the EC (see Fig. 3.8). Exogenously applying the co-agonists glycine and D-serine did not affect mEPSCs, though application of the co-agonist site antagonist DCKA selectively reduced the frequency of these events. This implied that the preNMDAr co-agonist site was endogenously bound in our slices and this contributed to the tonic facilitation of glutamate release by these receptors. Enzymatic degradation of glycine and D-serine was then employed and it was seen that whilst removal of glycine produced little effect, removal of endogenous D-serine reduced control mEPSC frequency

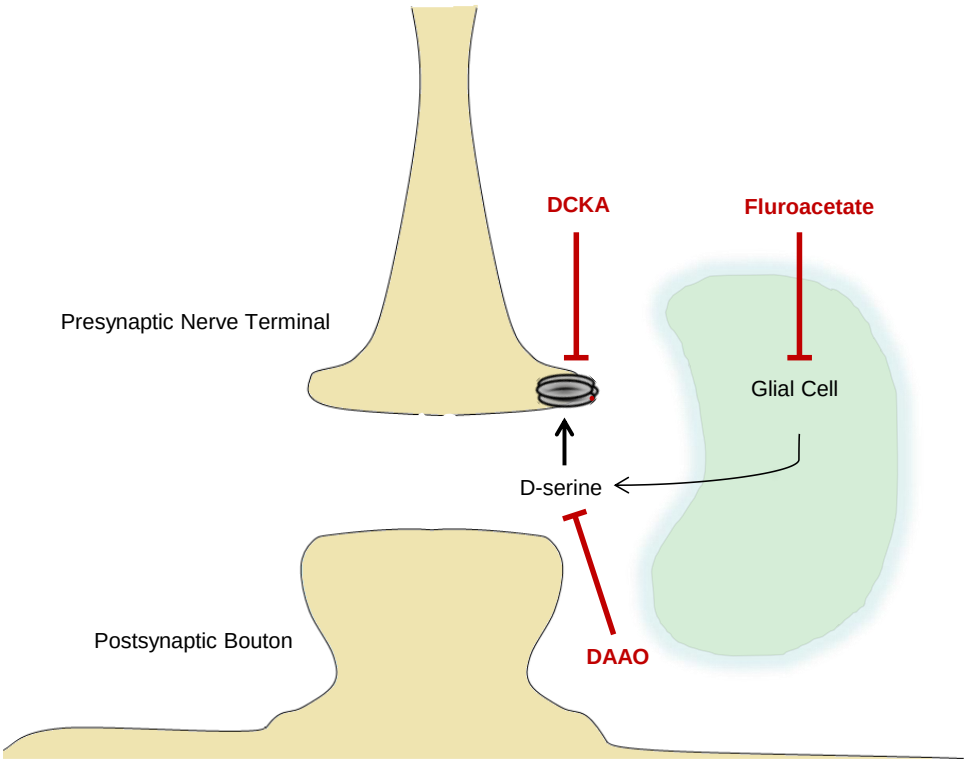

Fig. 3.8. Sites of action for compounds used to investigate co-agonist regulation of preNMDAr. DCKA, DAAO and fluroacetate were all seen to compromise the activity of these receptors. DCKA acts as an antagonist of the co-agonist site on the receptors themselves whilst DAAO breaks down the endogenous ligand D-serine, and fluroacetate inhibits its production by glial cells.

and completely precluded the effects of DCKA. This strongly implied that D-serine is the endogenous co-agonist at these receptors. Both of the effects of D-serine removal were mimicked by inhibition of glial cell metabolism by fluoroacetate and exogenous D-serine was able to partially rescue the mEPSC frequency which indicated that glial cells were likely to be a source of this endogenous D-serine at the preNMDAr. We were unable to detect any involvement of purinergic transmission or astrocyte NMDAr in the tonic regulation of mEPSC frequency.

3.4.2 Sources of D-serine

In this work we have provided some evidence that glial cells are a source of D-serine at preNMDAr. However, the production of D-serine by glial cells is highly controversial and so a fair overview of the conflicting evidence to date is necessary.

In 1999, Wolosker et al first cloned serine racemase and performed immunohistochemical experiments to detect the expression of this enzyme and D-serine itself in the hippocampus and unspecified regions of the cortex of juvenile rats. Here it was observed that both of these elements were selectively enriched in glial cells including astrocytes. In 2005, Mothet et al investigated D-serine release from astrocytes cultures, using a novel bioassay for D-serine detection. Here it was observed that kainate, AMPA and metabotropic glutamate receptor agonists prompt D-serine release and this occurs through an exocytotic mechanism which is dependent on both intracellular and extracellular calcium.

From here several subsequent studies have made similar observations. In 2006, Panatier et al examined the rat hypothalamic supraoptic nucleus which only contains oxytocinergic and vasopressinergic neurons. Immunohistochemistry here indicated that serine racemase was located exclusively in astrocytes. D-serine was shown to be the co-agonist at postNMDAr due to partial reduction of postNMDAr mediated current amplitudes upon D-serine breakdown by RgDAAO. Also in 2006, Williams et al utilized immunogold labelling, observing that D-serine was

largely localised to astrocytes throughout many regions of the adult rat brain, though is present in glutamatergic neurons in some areas such as the inferior colliculus, superior olivary complex and motor trigeminal nucleus. Later, Bergensen et al (2012) again using immunogold labelling, examined the rat hippocampus and observed that D-serine accumulated in vesicles in astrocytes and that glutamate and D-serine appeared to be localised to different vesicle pools. D-serine labelling in nerve terminals was largely ignored and was described as 'rather weak' though D-serine density in neuron terminals was 9.2 ± 1.8 particles/μm^2 (supplementary result 4), which is of the same order as for the astrocytic processes (~22 particles/μm^2, from figure 2). Then, in 2013, Martineau et al (Mothet group) used both immunohistochemical and immunogold labelling in non-specified regions of the rat cortex and observed that D-serine was "mainly" located in astrocytes but that there was a "moderate" presence in neurons, although quantification was not provided. This study then focused on mechanistic aspects of vesicular D-serine release from cultured astrocytes.

However, conflicting results have been found. Kartvelishvily, working with Wolosker and others (2006) observed that that neurons in primary culture do contain D-serine and serine racemase and suggested that previous, differing observations were due to experimental shortcomings in the immunohistochemistry. Interestingly, production of D-serine was seen to be dependent on exogenous L-serine and it was also observed that cultured neurons can release D-serine in response to NMDA and AMPA receptor activation. Miya et al (2008) examined serine racemase expression in the mouse cortex and hippocampus, utilising a serine racemase knockout mouse as a control for the first time, observing that serine racemase was present in neurons. Also, powerful evidence was provided by Benneyworth et al (2012) who utilised the Cre-loxP method to create neuronal and astrocytic conditional serine racemase knockout mice, thereby overcoming the limitations of immunohistochemistry and cell cultures. Here it was observed that knocking out serine racemase in neurons reduced overall serine racemase expression by ~60% in cortical regions compared to 15% in the astrocytic knock out, indicating a proportionally larger contribution of neuronal serine racemase. D-serine itself was only reduced in the neuronal

knockout although interesting this was to a lesser extent than serine racemase (33%) indicating a non-linear relationship, perhaps due to regulation of DAAO or the involvement of peripheral D-serine/D-serine breakdown.

The Wolosker group have now suggested the existence of a 'serine shuttle' whereby L-serine is exclusively synthesised in astrocytes and is then exported for uptake into neurons where it is converted to D-serine (Wolosker and Radzishevsky, 2013). Whilst useful for reconciling some differences in findings, there are many unclear elements in such a schematic. Therefore ultimately it is unclear what the true nature of co-agonist regulation of the NMDAr is and it would seem wise to be sceptical in the face of any simplistic scheme.

3.4.3 Implications for targeting preNMDAr

The observations here implying that preNMDAr in the EC are regulated by glial D-serine is highly interesting given the evidence for the involvement of glial cells and gliosis in epileptic pathology. It now appears that glial cells and preNMDAr are interconnected, providing a plausible basis for the mechanism by which preNMDAr activity is enhanced in epilepsy. However, the findings here may also provide an extended basis for targeting preNMDAr to allow the pathological role of these receptors to be further investigation and for potential therapeutic benefit.

In this work we have observed that endogenous co-agonist binding contributes to the tonic increase in excitatory transmission produced by preNMDAr. Given the involvement of preNMDAr in epilepsy, this then gives added support to the negative targeting of the NMDAr co-agonist site for treatment of this condition (Chiamulera et al., 1990; Singh et al, 1990; Peeters and Vanderheyden, 1992; Wu et al., 2002). In particular NMDAr are one target of the anticonvulsant felbamate and whilst this interaction is complex and currently unclear it appears to involve a negative modulation of the co-agonist site (White et al, 1995; Chang and Kuo, 2007). Interestingly work from this laboratory has indicated that felbamate inhibits preNMDAr in the EC (Yang et al, 2007), lending support to the notion that targeting the NMDAr co-agonist site in epilepsy would involve a beneficial,

presynaptic component. An interesting candidate for such an anticonvulsant on this basis is the pro-drug 4-chlorokynurenine, which is converted to the co-agonist site antagonist, 7-chlorokynuerenic acid (highly similar to DCKA) within astrocytes (Zhang et al, 2005).

Secondly, it is interesting to consider the findings of Le Bail et al (2014) where it was observed that postNMDAr in the hippocampus are bound both by D-serine and glycine. Also in prior studies by Fossat et al (2011) and Papouin et al (2013), D-serine degradation was only seen to produce partial decreases in postNMDAr currents. Although degradation of glycine did not produce any decrease in these studies, in contrast to Le Bail et al (2014), this could due to the less potent enzyme used here. We have also used a less potent form of BsGO than Le Bail et al (2014) however, importantly, we found that treatment with RgDAAO precluded the effects of the co-agonist site antagonist DCKA at preNMDAr *entirely*, which indicates that D-serine is the sole co-agonist at these receptors. Therefore it appears that preNMDAr may be unique in that the endogenous co-agonist at these receptors is solely D-serine. In light of our results implying that this D-serine is produced by glial cells it is possible that the sole co-agonist of preNMDAr binding by D-serine may be due to the intimate interaction astrocytes and these receptors as illustrated by Jourdain et al (2007). It is possible then that targeting D-serine production or removal may have a biased effect at preNMDAr and may be useful for manipulating these receptors, and it may be that postNMDAr function could be preserved by augmenting glycine. Such relevant strategies include the inhibition of serince racemase or enzymatic metabolism of D-serine both of which have previously been proposed as potentially useful approaches for the development of anticonvulsant treatments (Panizzutti et al, 2001; Sacchi et al, 2012).

Further to this it is interesting that from the extensive studies of Fossat et al (2011), Papouin et al (2013) and Le Bail et al (2014), it follows that the postNMDAr bound by D-serine are likely to be a GluN2A/GluN2B triheteromer. Previous work on preNMDAr in the EC from this laboratory has indicated that these receptors are likely to be GluN2B diheteromers. Therefore it is possible that preNMDAr

represent a pharmacologically distinct population of NMDAr which are sensitive to the removal of D-serine but only sensitive to GluN2B subtype selective antagonism.

Finally, in this work we observed that the activity of preNMDAr could not be augmented by exogenously applied co-agonists indicating that the preNMDAr co-agonist binding site was highly bound likely to the point of saturation. This again is in contrast to the postNMDAr which are commonly observed to be unsaturated (Fossat et al, 2011; Papouin et al, 2013) and this also could be utilized as a basis for selective targeting. A difference in the degree of co-agonist binding site activation would mean that theoretically, preNMDAr and postNMDAr could be distinguished between using partial agonists of the co-agonist site. This idea is particularly interesting as the co-agonist site partial agonist D-cycloserine (DCS) has been purported to have anticonvulsant properties (see 1.9.1). An NMDAr mediated anticonvulsant effect would be presumed to be an inhibitory/negative action, as NMDAr mediate excitation and anticonvulsant activity is highly typical of NMDAr antagonists (see Ghasemi and Schacter 2011). Interestingly, the efficacy of DCS varies with GluN2 subunit identity although in each case it is high (see 1.9.2). Therefore it follows that an anticonvulsant effect by DCS would be expected to occur at NMDAr which have a very high degree of endogenous co-agonist activation, which we now know applies to the preNMDAr. For both of these reasons we were highly interested to explore the action of co-agonist site partial agonists, DCS in particular, and I chose this line of enquiry for further investigation.

Chapter 4

The Effects of Partial Co-agonists at Pre- and Postsynaptic NMDA Receptors

4.1 Introduction

For two reasons we were now interested to investigate the action of NMDAr co-agonist site partial agonists at NMDAr in the EC. The first reason follows from the previous chapter where we observed that the preNMDAr co-agonist site is likely to be saturated which is in contrast to previous observations of the postNMDAr co-agonist site (Fossatt et al, 2011; Papouin et al, 2013). If there is such a difference in binding then examining the effects of different efficacy partial agonists should confirm this and may allow for selectivity to be achieved. The second reason is that the co-agonist site partial agonist D-cycloserine (DCS) has been demonstrated to be able to act as both a cognitive enhancer and an anticonvulsant drug (see 1.9), and so we were highly interested to examine the action of DCS and other partial agonists at NMDAr, particularly preNMDAr, in the EC to increase our understanding of the molecular basis of these therapeutic effects.

In brain slices, postNMDAr are commonly studied by electrically evoking NMDAr mediated synaptic responses, referred to as evoked NMDAr excitatory postsynaptic currents (eNEPSCs). As discussed in the section 1.5, it is established that the amplitude of such events represents the number of receptors which transition from glutamate bound/closed to glutamate bound/open states whilst the decay is mediated by the gating of receptors between glutamate bound/open and glutamate bound/closed states and from glutamate bound/closed to unbound/closed states. The effects of partial agonists of the co-agonist site on eNEPSCs in neuronal cultures were well studied by Priestly and Kemp (1994). Here it was observed that the efficacy of the partial agonists activating the receptor not only determined the peak amplitude of the eNEPSC but also its decay. Recent kinetic schemes of NMDAr gating have indicated why this may be the case. Compared to a NMDAr bound by a full agonist, an NMDAr bound by a partial agonist has a broadly reduced gating efficiency which results in receptors spending more time in bound/closed states (Kussius and Popescu et al, 2009). Therefore the reason why both eNEPSC peak amplitude and decay time are both determined by

agonist efficacy is likely to simply be that both are subject to the efficiency of gating transitions.

As discussed in section 1.9, there has been a large amount of research conducted into the neuropharmacological and psychopharmacological properties of DCS and the pharmacology of DCS at NMDAr in expression systems and neuronal cultures is also well elucidated. However, there has been little mechanistic study of how one links to the other. The varying efficacy of DCS means that it is unclear what effect it has in the endogenous situation and clearly the effect of a partial agonist is also dependent on the level of endogenous activation of its target. In this chapter I present novel findings exploring the action of DCS at NMDAr in the EC, an area central to both memory and epileptic pathology, using acute brain slices as a physiologically relevant preparation. We have also examined the effects of another co-agonist site partial agonist Aminocyclobutane carboxylic acid (ACBC). ACBC has not been well studied in vivo as with DCS and was chosen largely on the basis of its medium-low efficacy of 42% (Inanobe et al, 2005) to contrast DCS.

4.2 Methods

In one experiment in this chapter brain slices were from adult rats (50-60 days) and all other experiments aside one were performed using brain slices from juvenile rats. Slices were prepared as described in section 2.2 and whole cell patch voltage clamp recordings were made from neurones in layer II of the EC with pyramidal morphology. preNMDAr were again monitored using AMPA receptor mediated mEPSCs and postNMDAr function was assessed using eNEPSCs as outlined in section 2.6 (also see Fig. 4.1). Data analysis and significance testing was also carried out as outlined previously.

Many of our findings in this chapter pertain to the decay phase of eNEPSCs which is often found to have two exponential components. We observed that eNEPSCs in layer II principal neurones were also somewhat better described by biexponential over monoexponential kinetics although the difference between fits was very small (see Fig. 4.2.A). In addition to this small difference, the parameters

produced by biexponential fitting were seen to be highly variable and this precluded meaningful analysis. Owing to this and the lack of any inference that such analysis provides I have described decay phases with a monoexponential time constant in keeping with the data of Priestley and Kemp (1994). This time constant (referred to as 'decay time') was simply calculated by the time taken to reach the 0.37 fraction of peak amplitude, eliminating any variability introduced by fitting procedures. The correct basis of eNEPSCs was confirmed by blockade with 2-AP5 (50µM) in three neurones (Fig.4.2.B). In eNEPSC experiments baseline holding current was also monitored as changes in this parameter can be indicative of effects at extraNMDAr. However, no changes in holding current were observed throughout these experiments.

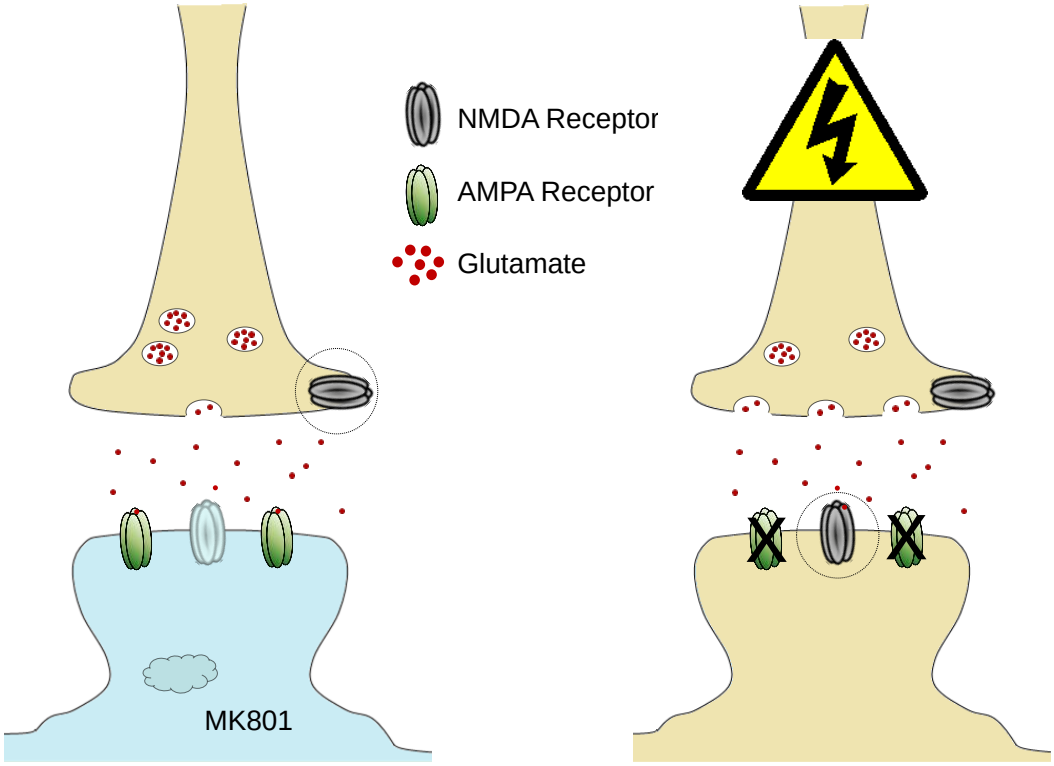

Fig. 4.1. Experimental paradigms used for the study of pre and post synaptic NMDAr. Left, to study preNMDAr, the frequency of AMPA receptor mediated mEPSCs were used as a reporter for the activity of these receptors whilst postNMDAr were blocked by intracellular MK801 (see also Fig. 1.9). Right, to study postNMDAr, all other synaptic receptors were blocked and postNMDAr mediated currents (eNEPSCs) were evoked via bipolar electrical stimulation.

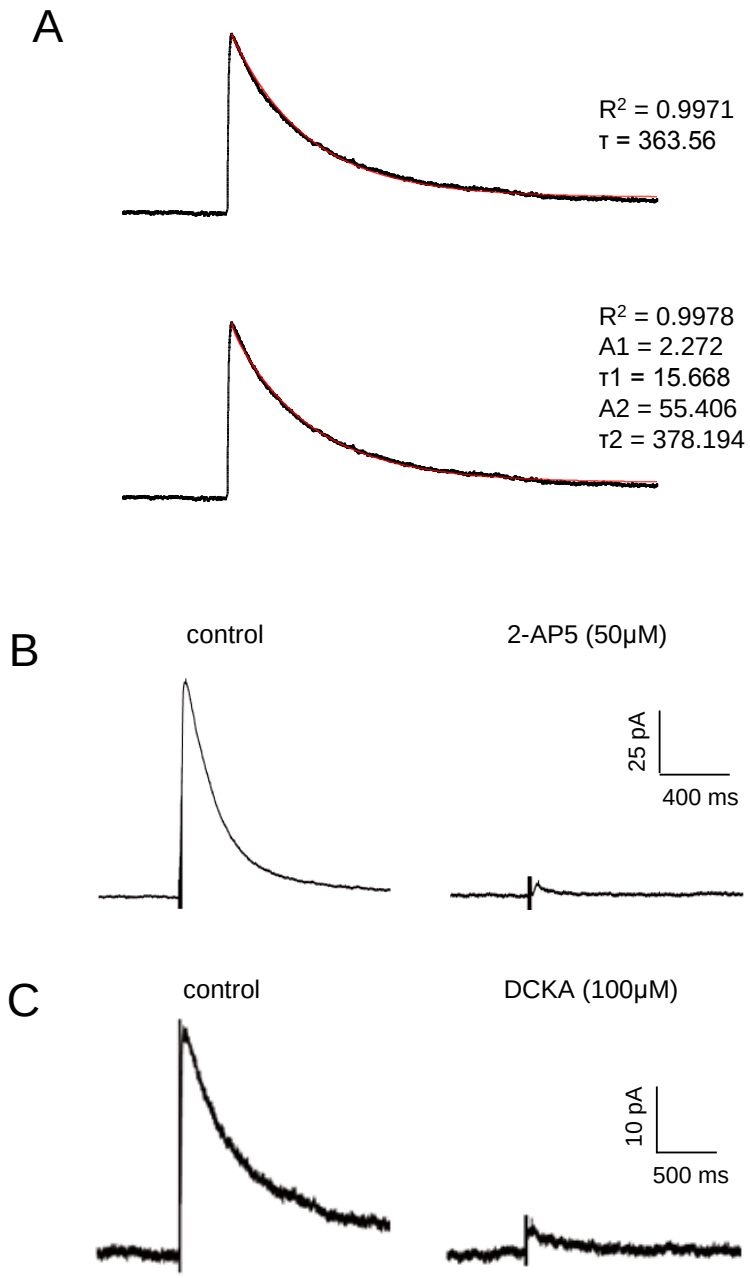

Fig. 4.2 The eNEPSC response. A – Monoexponential and biexponential fitting of the eNEPSC decay phase. eNEPSCs are sometimes described as having two exponential components, a fast (τ1, A1) and a slow (τ2, A2) exponential. T is the exponential time constant and A is the factor of multiplication. Here, we observed that eNEPSCs were well described by biexponential kinetics, with a high coefficient of determination (R2) but were also very well described by a monoexponential decay. B – An example trace showing removal of the eNEPSC response by the prototypic NMDAr antagonist 2-AP5. This confirmed that the responses here were mediated by NMDAr. C – An example trace showing abolishment of the eNEPSC by the coagonist site antagonist, DCS. This indicated that activation of the NMDAr coagonist site, as well as the agonist site, mediated this response**.**

4.3 Results

4.3.1 Effects of DCS and ACBC at preNMDAr

To begin our study of the effects of co-agonist site partial agonists at NMDAr in the EC I examined the effects of the high efficacy co-agonist site partial agonist, DCS at preNMDAr. The activity of these receptors was again monitored using AMPA receptor mediated mEPSCs as a reporter for the release of glutamate. In six layer II neurones these events were recorded and the effects of DCS at a concentration of 300 µM was tested followed by the addition of 2-AP5 (50 µM) without washout of DCS. The results from this experiment are summarised in Fig. 4.3. The frequency of mEPSCs was significantly lowered following addition of 2-AP5 (50 µM), compared to control, and no other significant changes were seen. The mean frequency of mEPSCs was 0.65 ± 0.29 Hz in control, 0.62 ± 0.32 Hz in the presence of DCS and 0.47 ± 0.23 Hz ($p<0.05$) following addition of 2-AP5. Mean amplitudes were 7.0 ± 0.4 pA, 6.9 ± 0.4 pA and 6.9 ± 0.36 pA in the control, DCS and DCS + 2-AP5 conditions respectively. Mean rise times were 2.2 ± 0.4 ms, 2.4 ± 0.4 ms and 2.1 ± 0.3 ms and mean decay times were 2.2 ± 0.3 ms, 2.0 ± 0.3 ms and 2.0 ± 0.3 ms for these three conditions. Therefore in this experiment we did not observe any effect of DCS at preNMDAr dependent glutamate release. However, further addition of the antagonist 2-AP5 again, selectively decreased mEPSC frequency confirming that preNMDAr were active here.

The effect of DCS on mEPSCs was again tested in a further 6 neurones, at a lower concentration of 100 µM but no significant changes were observed. Mean mEPSC frequencies for control and DCS treatment conditions were 0.55 ± 0.1 Hz and 0.53 ± 0.2 Hz respectively and likewise mean amplitudes were 8.5 ± 1.0 pA and 8.6 ± 1.1 pA. Respective mean rise times for control v DCS were 2.6 ± 0.4 ms v 2.5 ± 0.4 ms and decay times were 3.8 ± 1.2 ms v 4.1 ± 1.2 ms. The lack of any effect of DCS repeated here confirmed that DCS was not eliciting any effect on spontaneous glutamatergic release. From these experiments then it appeared that DCS did not affect the function of preNMDAr on tonic glutamate release in the EC. On this basis it seemed unlikely that preNMDAr would be relevant to the

neuro- and psychopharmacological properties of DCS and that other receptor populations were more likely to give an insight into the molecular basis of DCS action. These results also indicated that DCS may be a useful tool to study the possible differences in co-agonist binding between NMDAr populations.

We next tested the effects of the low efficacy co-agonist site partial agonist, ACBC (1mM) on mEPSCs in 5 layer II neurones. These experiments were carried out by Emma Robson. Data from these experiments is summarised in Fig. 4.4. The frequency of mEPSCs was significantly reduced following perfusion of ACBC and no other significant changes were observed. Mean mEPSC frequencies for control v ACBC were 1.7 ± 0.3 Hz v 1.2 ± 0.2 Hz ($p<0.05$) and mean amplitudes were 6.9 ± 0.3 pA v 6.5 ± 0.3 pA) or in frequency distribution of event amplitudes. Likewise, average mEPSC rise times were 2.18 ± 0.14 ms v 2.38 ± 0.06 ms and decay times were 2.85 ± 0.26 ms v 3.27 ± 0.23 ms. This selective decrease in AMPA receptor mediated mEPSCs indicated that ACBC was reducing the tonic activity of preNMDAr.

Therefore, whilst a high efficacy partial agonist of the co-agonist site did not affect preNMDAr, a lower efficacy co-agonist produced an inhibitory effect. In the previous chapter it was established that the co-agonist site of preNMDAr has a high level of tonic activity due to endogenous binding by D-serine. Therefore the most parsimonious explanation for the observations at hand is that DCS had no effect because its efficacy is closely matched to the endogenous activation of the preNMDAr co-agonist site and so there will be no change in the overall activity of this receptor population when it is added. However, when ACBC is added and displaces the full agonist D-serine, although it may bind the entire preNMDAr population, as its efficacy is less that the overall endogenous activation of these sites, it produces a reduction in the function of this receptor population.

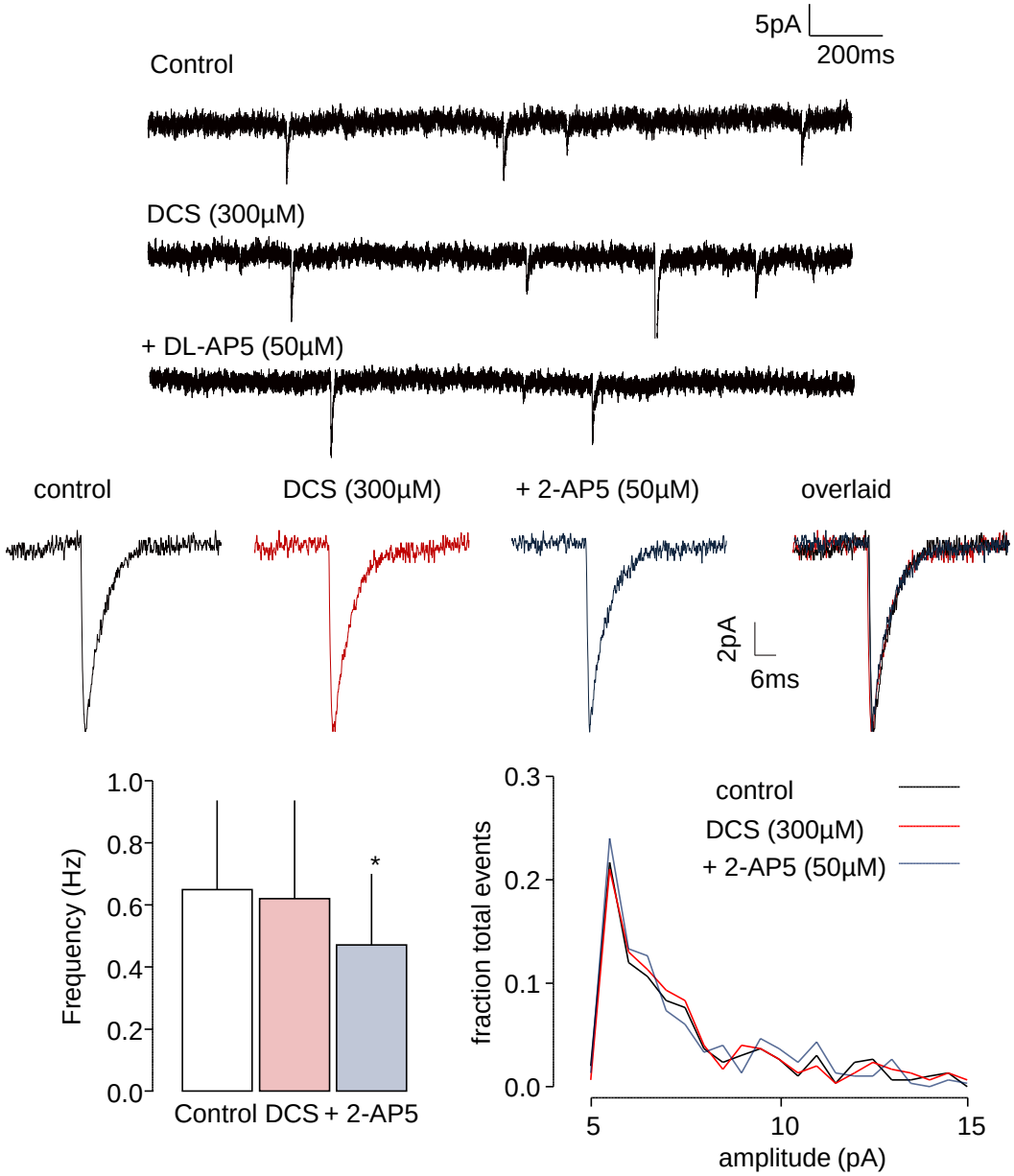

Fig. 4.3. The effects of DCS on mEPSCs in layer II neurones of the medial EC. The high efficacy co-agonist site partial agonist, DCS was added at 300 µM followed by the glutamate site antagonist 2-AP5 (50 µM), without washout of DCS. Upper traces show sample voltage clamp recordings in control, DCS and 2-AP5 treatment conditions. Lower traces are averaged events from control (black) and DCS (red) and 2-AP5 (Blue). An overlaid trace on the right clearly shows no differences in kinetics or amplitude. Bottom left, a bar graph representing average frequency data. mEPSC frequency unchanged in the presence of DCS but is significantly lowered following treatment with 2-AP5. Bottom right, a histogram representing the amplitude distributions of events in the three conditions. There was no effects on amplitude in this data set, indicating that the change in frequency by 2-AP5 reflected a decreased glutamate release probability. * denotes $p<0.05$ significance level, n=6.

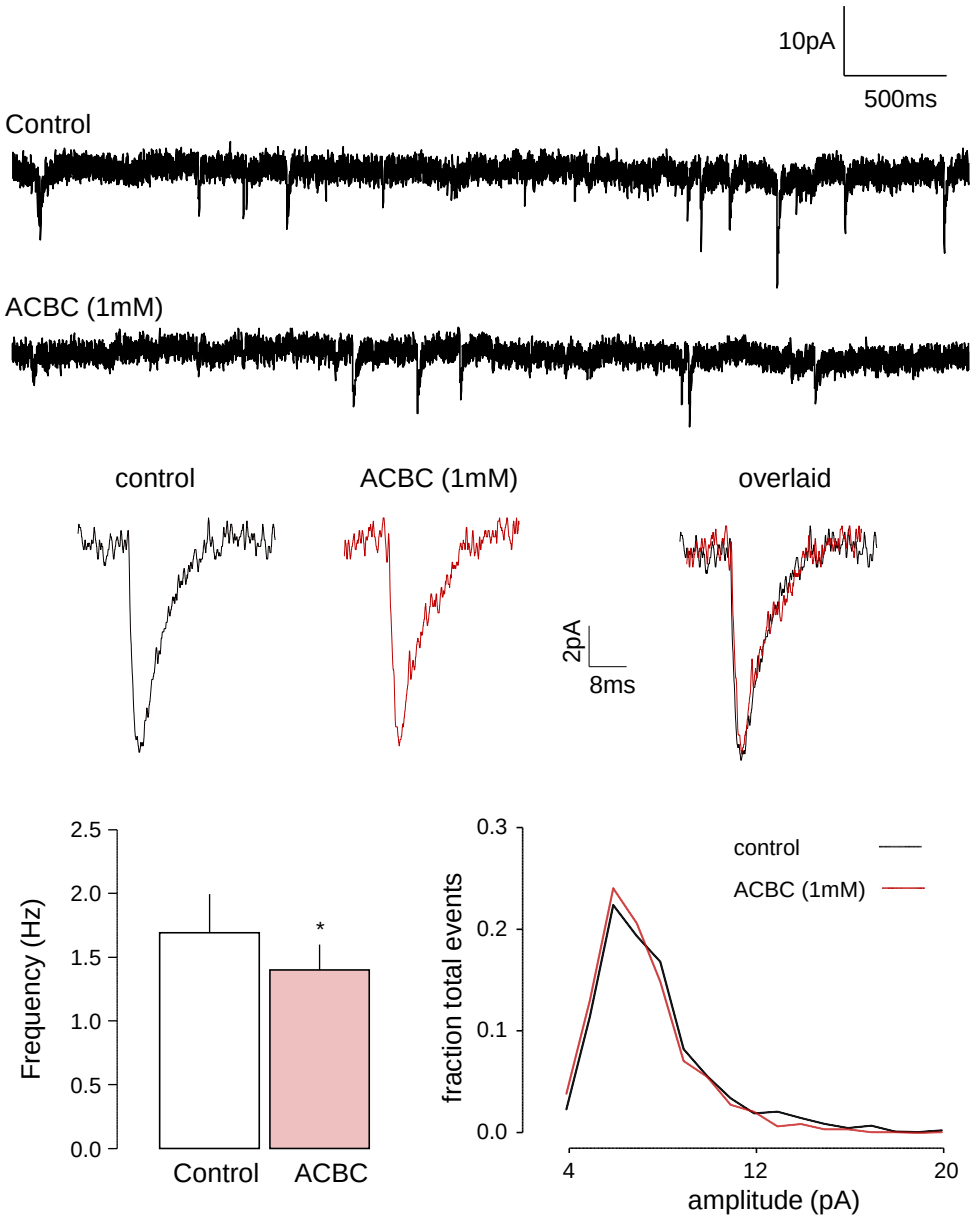

Fig. 4.4. The effects of ACBC on mEPSCs in layer II EC neurones. The low efficacy partial coagonist ACBC was tested at 1 mM in five neurones. Upper traces illustrate mEPSC frequency in the control condition and in the presence of ACBC, averaged traces for control (black) and ACBC (red) are shown below. In the bottom left, a bar graph of average frequency for the data set. In the bottom right, a histogram of mEPSC amplitudes in the two conditions. ACBC produced a significant decrease in mEPSC frequency without affecting the amplitude of these events, characteristic of a inhibitory presynaptic action. * denotes $p<0.05$ significance level.

Although this schematic largely fits with our observations in the previous chapter we previously observed a lack of effect of exogenous D-serine on preNMDAr which suggested that the co-agonist site was not only highly bound but saturated.

To this then there are two possible explanations. The preNMDAr co-agonist site is saturated by endogenous D-serine and DCS does reduce the activity of this site but it is below the threshold of detection. Alternatively the preNMDAr co-agonist may be matched to the high efficacy of DCS and the effects of D-serine are limited by the activation of the preNMDAr agonist (glutamate) site, or are themselves too small to detect. However, a third explanation is offered in section 4.4.3.

4.3.2 Effects of DCS at postNMDAr

To examine the effects of DCS at principal cell postNMDAr in the EC, eNEPSCs were recorded in six neurones and DCS was applied at 1-30 µM. Results from this experiment are shown in Fig. 4.5. Interestingly there were no significant effects on the amplitude of these events, but the decay time was significantly reduced at all concentrations of DCS. Average eNEPSC amplitude at control was 190.9 ± 53.8 pA and 160.6 ± 35.3 pA in the presence of 30 µM DCS. Average rise times were 44.7 ± 9.3ms in the control period and 52.3 ± 15.1ms at 30 µM DCS. Average decay times were 593.8 ± 94.6 in control and 417.4 ± 78.7ms ($P<0.01$) in the presence of 30µM DCS. The reduction of decay time was concentration dependent and from normalised data the maximum effect was 68.1 ± 5.9% at 30 µM and the IC50 was 2.1 µM. Fascinatingly then, DCS was exerting a kinetic effect at eNEPSCs but not effecting the peak amplitude of these events and further experiments were conducted to determine the basis of this effect.

To confirm that DCS was acting at the postNMDAr co-agonist site we conducted a reversal experiment using the co-agonist site antagonist DCKA. eNEPSCs were recorded in eight neurones and 100 µM DCKA was applied followed by DCS first at 2 mM and then increased to 10 mM, without washout of DCKA. Results from this experiment are shown in Fig. 4.6. DCKA abolished the eNEPSC response. eNEPSC amplitude was significantly lower than control during perfusion of 2mM but not 10mM eNEPSC and decay time was significantly reduced at both concentrations of DCS. There were no significant effects on eNEPSC rise time. Average normalised eNEPSC amplitude was recovered to 42.4 ± 7.3% of control at 2 mM and 73.9 ± 13.6% at 10mM DCS. Average normalised eNEPSC decay

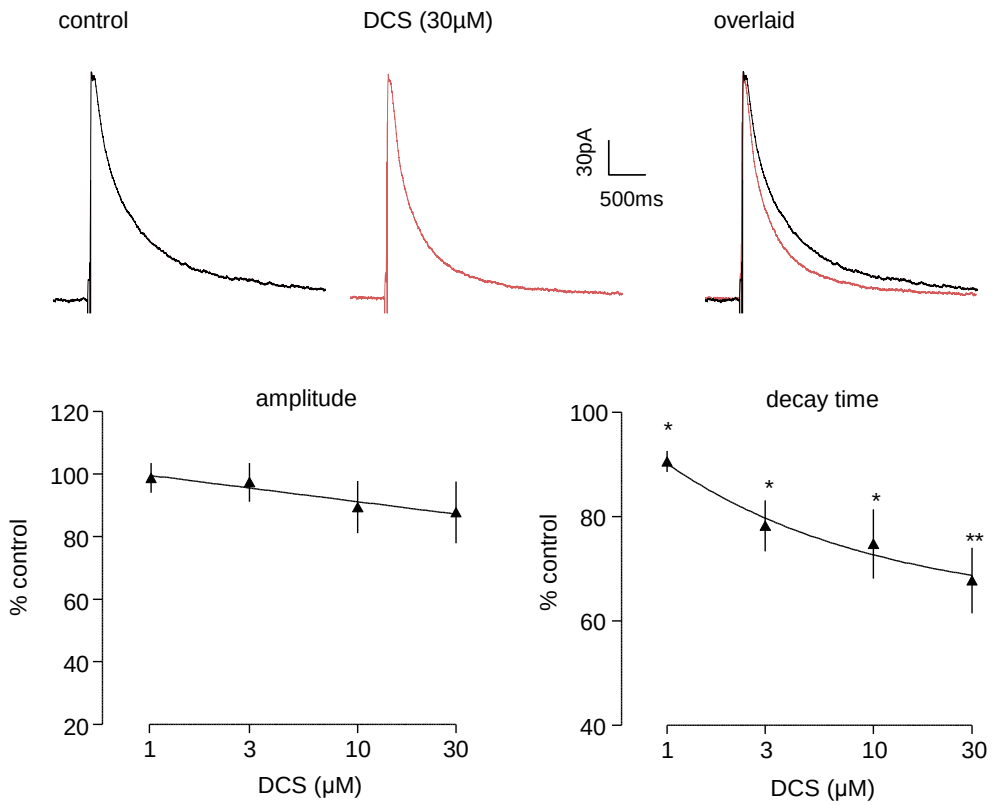

Fig. 4.5. The effects of DCS on eNEPSCs in layer II of the medial EC. DCS was added during recording of eNEPSCs over the 1-30 µM range in six neurones. Example eNEPSCs from control (black) and at 30 µM DCS (red) are above, traces are overlaid on the right. Averaged, normalised data is shown beneath for amplitude (left) and decay time (right), inhibition curves are fitted over the concentration range. DCS produced a clear, concentration dependent decrease in eNEPSC decay time, which was seen to plateau at 30 µM. DCS had no similar effect on the amplitude of the eNEPSCs. * denotes $p<0.05$ significance level, ** denotes $p<0.01$ significance level.

time was recovered to 26.1 ± 2.3% at 2 mM DCS and 34.4 ± 1.8% at 10 mM DCS. The removal of eNEPSC response by DCKA indicated that the postNMDAr was indeed active, contributing to this response. Although not completely, the abolished amplitude of eNEPSCs by the competitive co-agonist site antagonist DCKA was largely reversed by high concentrations of DCS indicating that DCS was indeed acting as a co-agonist at postNMDAr in our eNEPSC experiments.

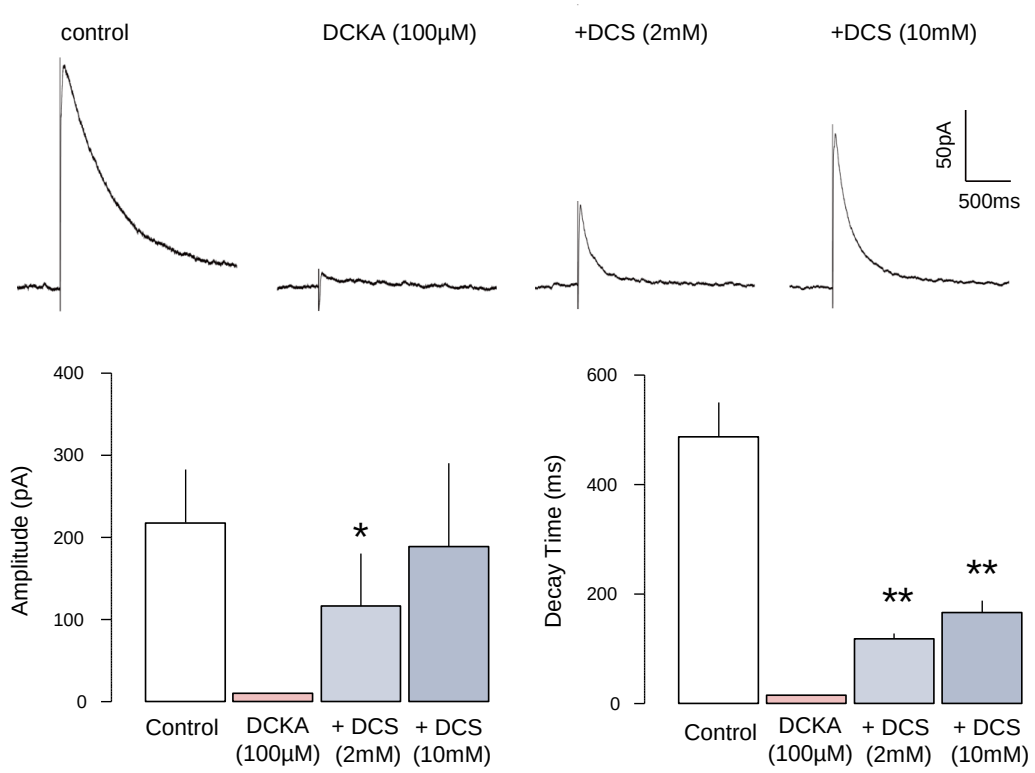

Fig. 4.6. DCS rescues the eNEPSC from abolition by DCKA. In eight neurones, the co-agonist site antagonist DCKA was added at 100 µM followed by DCS at 2 mM and then at 10 mM, without washout of DCKA. Example average eNEPSCs from each condition are shown above and averaged amplitude and decay time data from all experiments are shown below in bar chart form. eNEPSCs were completely blocked by DCKA, though high concentrations of the partial agonist DCS were able to reverse this blockade, indicating a competitive, opposing effect. Recovered eNEPSCs had significantly lower decay time than control. * denotes $p<0.05$ significance level, ** denotes $p<0.01$ significance level.

To further confirm that the kinetic effect of DCS that we had observed was due to a partial agonist action, we examined whether it was reversed by a full agonist. eNEPSCs were recorded in seven neurones and DCS was applied at a submaximal concentration (10 µM) followed by a high concentration of D-serine (1 mM), without washout. Results from these experiments are shown in Fig. 4.7. eNEPSC decay time was again significantly decreased in the presence of DCS and significantly higher than control following addition of D-serine. eNEPSC amplitude was also significantly above control after addition of D-serine and no other significant effects were detected. Normalised decay time was 84.7 ± 2.9% of control in the 10 µM DCS condition and 109.8 ± 2.1% with subsequent addition of D-serine. Normalised eNEPSC amplitude was 126 ± 4.0% following addition

of D-serine. Mean decay times for control, DCS and DCS+D-serine conditions were 391.0 ± 26.6 ms, 333.0 ± 28.7 ms ($p<0.01$) and 430.1 ± 31.5 ms ($p<0.01$), respectively and mean amplitudes were 123.5 ± 23.9 pA, 124.8 ± 26.2 pA and 160.1 ± 34.3 pA ($p<0.05$) respectively. Likewise, mean rise times were 42.3 ± 16 ms, 49.6 ± 23.8 ms and 68.0 ± 46.9 ms respectively. The decrease in eNEPSC decay time produced by DCS was therefore effectively counteracted by a full agonist. Therefore it was concluded that the selective kinetic effect of DCS at eNEPSC were indeed due to a partial agonist effect at the NMDAr co-agonist binding site. The increase in eNEPSC amplitude produced by D-serine indicated that the postNMDAr co-agonist binding site is not saturated and this limits the eNEPSC response. The increase in eNEPSC decay time beyond control produced by D-serine was highly interesting and is discussed later.

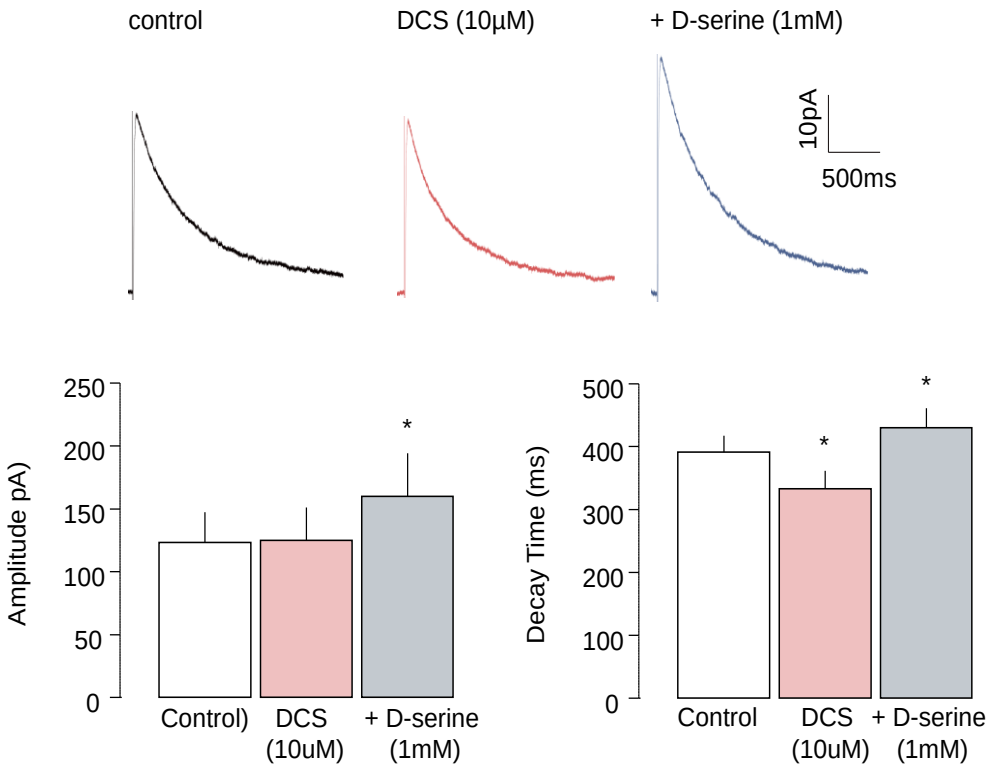

Fig. 4.7. D-serine opposes the effects of DCS on eNEPSCs. eNEPSCs were recorded in seven neurones and a submaximal concentration of DCS (10 µM) was added followed by the coagonist site full agonsit D-serine (1 mM) without washout. Sample averaged eNEPSCs from control and DCS (red) and D-serine (blue) treatment conditions are shown above. Overall average amplitude and decay time bar charts are below. Again DCS selectively decreased the decay of eNEPSCs, this effect was reversed beyond control by D-serine. D-serine also significantly increased the amplitude of eNEPSCs. * denotes $p<0.05$ significance level.

Therefore we have shown that DCS is indeed acting as a partial co-agonist at postNMDAr in the EC but that it produces a selective effect on the decay phase of macroscopic synaptic responses. The most parsimonious explanation for this is that the postNMDAr are activated by a full efficacy co-agonist but the overall concentration is matched to the efficacy of DCS. Then, when DCS is added, the maximal number of receptors opening is substantially unchanged but the macroscopic decay is reduced.

4.3.3 Effects of ACBC at postNMDAr

We now examined the effects of the low efficacy co-agonist site partial agonist ACBC at principal cell postNMDAr in the EC. eNEPSCs were recorded in seven layer II neurones and ACBC was added cumulatively at 30 µM, 100 µM, 300 µM and 1 mM. Results from this experiment are presented in Fig. 4.8. ACBC produced concentration dependent decreases in both eNEPSC amplitude and decay, which were significant at 300 µM and 1 mM for amplitude and at every concentration for decay time. There were no effects on rise time. Average eNEPSC measurements for the control and 1 mM ACBC periods were 239.4 ± 47.3 pA and 141.5 ± 21.2 pA ($p<0.05$), respectively, for amplitude, 524.8 ± 102.96 ms and 249.0 ± 26.5 ms ($p<0.05$), respectively, for decay time and 31.3 ± 4.2 ms and 30.3 ± 5.3 ms for rise time. The effects of ACBC appeared to be approaching maximum at 1mM, where the normalised eNEPSC decay was 57.5 ± 12.4% and the normalised amplitude was 62.0 ± 5.9%. In contrast to DCS then, ACBC decreased both the decay time and amplitude of eNEPSCs, which is consistent with an NMDAr partial agonist with an efficacy which is lower than the tonic level of activation. Therefore it appears that due to high levels of endogenous co-agonist binding, ACBC has negative effects on the activity of both preNMDAr and postNMDAr on principal neurones in the EC.

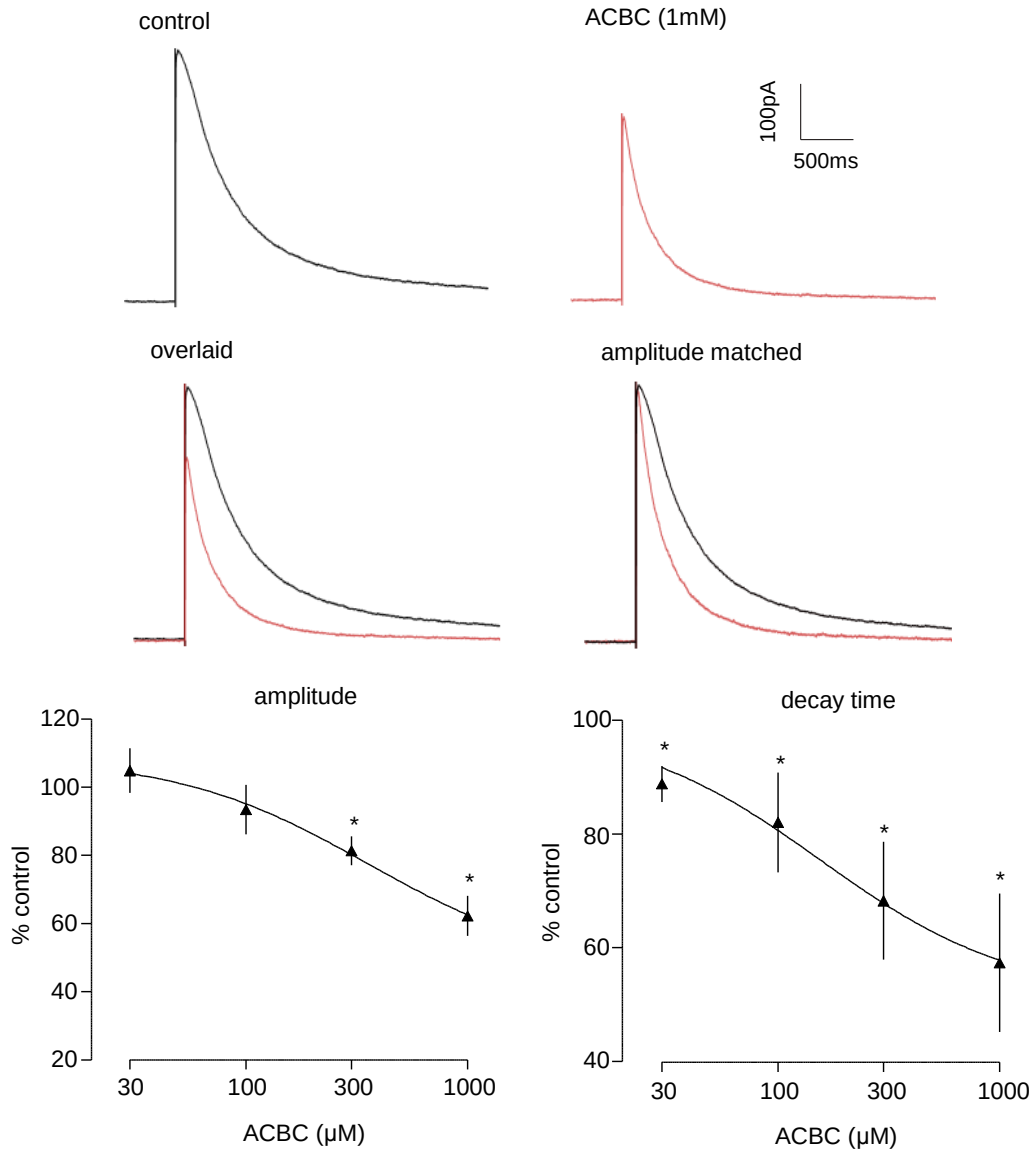

Fig. 4.8. The effects of ACBC on eNEPSCs in the EC. ACBC was added to eNEPSCs in over the 0.03-1 mM range in seven neurones. Example eNEPSCs for the control (black) and 1 mM ACBC (red) periods are shown above, left. Overlaid traces, and overlaid traces with matched amplitudes are shown on the right. Average, normalised amplitude and decay time data is shown beneath with fitted concentration response curves. ACBC was seen to elicit large concentration dependent decreases in decay time but also significantly reduced the amplitude of eNEPESCs, reflecting its lower efficacy. * denotes $p<0.05$ significance level.

4.3.4 Effects of D-serine at postNMDAr

To elucidate the tonic activation of the postNMDAr we wanted to examine the action of a full agonist at these receptors. Although we had previously applied D-serine to eNEPSCs to test the nature of DCS, we now tested the effects of D-serine (100 µM) singly at eNEPSCs in six cells. These results are summarised in Fig. 4.9. eNEPSC amplitude and decay time were significantly increased in the presence of exogenous D-serine, with no effect on rise time. Mean peak amplitude was 205.5 ± 40.7 pA in control and 240.3 ± 50.1pA ($p<0.05$) during perfusion of D-serine and mean decay times changed from 381.3 ± 105 ms to 450.5 ± 112 ms ($p<0.01$). Mean rise times were 36.2 ± 8.0 ms in the control period and 33.4 ± 6.3 ms with D-serine. The average normalised amplitude in the presence of exogenous D-serine was 115.9 ± 4.0% and the average normalised decay time was 121 ± 4.4%. This result again indicated that the postNMDAr co-agonist site is highly, but not fully activated.

4.3.5 Effects of DCS at postNMDAr in the adult EC

In the previous chapter we observed that preNMDAr are regulated by D-serine, likely with a glial source. Whilst the potential importance of glial dysregulation in epilepsy, of preNMDAr in epilepsy and the age dependence of preNMDAr function are discussed in the general introduction. Further to this, D-serine has also been implicated in ageing and changes in the developing brain (Hashimoto et al, 1993; Turpin et al, 2011). Given these ideas we were highly interested in the prospect of a unifying schematic of enhanced glial co-agonist signalling in the juvenile brain and in epilepsy. To this end we prepared slices using adult rats (50-60 days) and examined co-agonist binding at postNMDAr, as the most directly observable NMDAr population. As DCS appeared to be matched to the endogenous co-agonist activation of postNMDAr in juvenile brain slices it was now an excellent tool to test whether binding of this site was different in adult slices. In adult brain slices eNEPSCs were recorded in 5 neurones and DCS was added at 1 mM. However, the only significant effect of DCS was on decay time, which had a mean value of 372.9 ± 69.2 ms in control and 226.4 ± 34.0 ms ($p<0.05$)

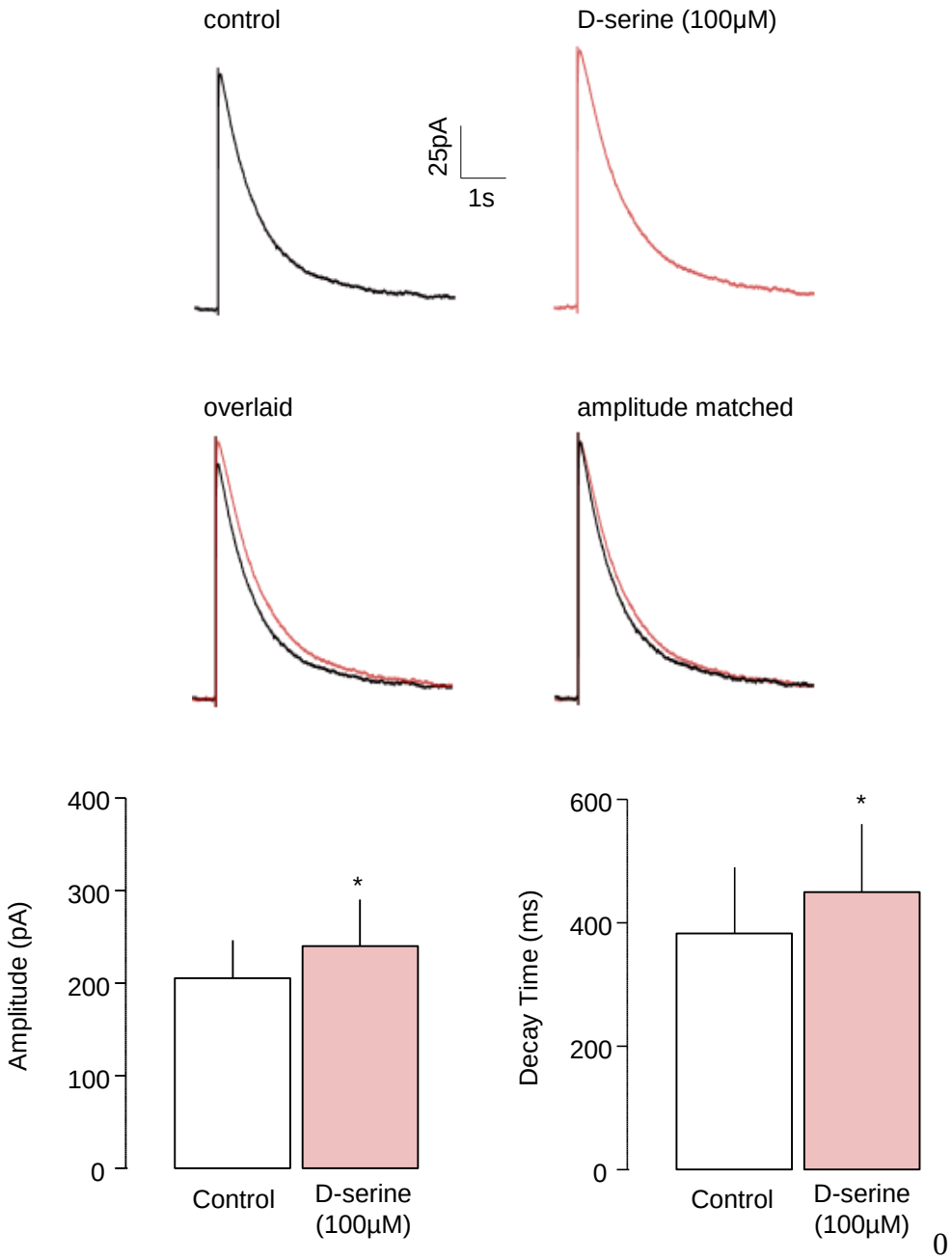

Fig. 4.9. The effects of D-serine on eNEPSCs in the mEC. eNEPSCs were recorded in six layer II neurones and the effects of D-serine (100 µM) were tested. Above, example eNEPSCs from control (black) and D-serine (red) treatment periods. Middle, traces are overlaid and overlaid with matched amplitudes for decay time comparison. Below, dataset amplitude and decay time bar charts. Interestingly the endogenous full coagonist D-serine produced small but significant increases in both the amplitude and decay time of eNEPSCs here. * denotes $p<0.05$ significance level.

following DCS perfusion. This corresponded to a normalised value of 63.7 ± 6.7% of control following DCS treatment. Mean amplitudes were 112.8 ± 34.6 pA in control and 113.3 ± 33.1 pA with DCS. Mean rise times were 37.7 ± 12.5 ms in control and 27.9 ± 6.4 ms with DCS. So in adult slices DCS again only affected the decay of eNEPSCs. Again the amplitude of these events was not affected and so it appears that the level of endogenous postNMDAr co-agonist binding is constant between the adult and juvenile rat EC.

4.4 Discussion

4.4.1 Overview

In this chapter I have used mEPSCs and eNEPSCs to study the effects of co-agonist site partial agonists at pre and post synaptic NMDAr, respectively, in the EC. The high efficacy partial agonist DCS had no effect on mEPSCs and had no effect on the amplitude of eNEPSCs but reduced the decay time. This effect was confirmed to be due to a partial agonist action at NMDAr co-agonist sites. The low efficacy partial agonist selectively reduced the frequency of mEPSCs and also reduced the amplitude, as well as the decay time, of eNEPSCs. The full agonist D-serine increased the amplitude of eNEPSCs by 15-26% and also increased the decay time of eNEPSCs. The effects of DCS on eNEPSC were unchanged in brain slices from adult rats.

4.4.2 Endogenous activation and pharmacology of postNMDAr

A parsimonious explanation for the lack of effect of DCS on eNEPSC amplitude was that the postNMDAr co-agonist sites are endogenously activated at a level which is matched to the efficacy of DCS. However, if this endogenous activation was provided by a higher/full efficacy agonist then DCS would still be expected to alter the macroscopic decay. As previously discussed, endogenous activation of these sites is thought to be provided by a full agonist, probably D-serine (Papouin et al, 2012). High exogenous concentrations of the full agonist D-serine increased the amplitude of eNEPSC responses by 15-26% indicating that the postNMDAr

co-agonist sites were originally 79-87% tonically active. This is indeed in agreement with the efficacy of DCS on eNEPSCs which was calculated to be 86 ± 5% by Priestley and Kemp (1994) in neuronal cultures. Also consistent with this simple explanation is that the lower efficacy partial agonist ACBC did decrease eNEPSC amplitude, in addition to decay time.

Interestingly, in their investigation of the subtype dependence of DCS efficacy, Dravid et al (2010) calculated that at GluN2A and GluN2B heterodimers, DCS had 90% and 65% efficacy, respectively. Previous work from this laboratory as indicated that the postNMDAr at hand are likely to be a triheteromer (Chamberlain et al, 2008). Although the efficacy of DCS at these receptors has not been established, as the pharmacological properties of triheteromers have generally been observed as lying between the two respective diheteromers, an efficacy of 86 ± 5% is consistent with such a triheteromeric structure.

The observed increase in NMDAr decay time following application of exogenous D-serine is also highly interesting, particularly as currently endogenous binding of the NMDAr co-agonist site is thought to be by full agonists only. One possible explanation is that in the control condition there are partially liganded NMDAr openings, which contribute to a submaximal macroscopic decay, but these are not present when the co-agonist site is saturated with an exogenous agonist. On this note it is interesting that DCS recovered eNEPSC amplitude from DCKA blockade but the decay times were disproportionately low, which may again implicate partially liganded openings. However, partially liganded openings are not thought to occur with the NMDAr (see Schorge and Colquhoun, 2003).

Perhaps the most likely explanation however is that in the control condition postNMDAr co-agonist sites are bound by a mix of glycine and D-serine as observed by Le Bail et al (2014). These receptors may produce a submaximal decay compared to receptors bound by D-serine alone, which occurs when the high concentration of exogenous D-serine is added. However, to my knowledge there is no data comparing macroscopic decay kinetics with glycine bound and D-serine bound NMDAr. In their extensive kinetic study, Priestley and Kemp (1994) tested

glycine but not D-serine, although it is interesting to note that L-Alanine was almost a full agonist (96%) but had a greatly different effect on macroscopic decay compared to glycine (375ms for L-Alanine vs 502ms for glycine). Thus it is conceivable that D-serine could produce higher macroscopic decay times than a D-serine/glycine mix.

4.4.3 Endogenous Activation of preNMDAr and selective targeting of postNMDAr

In this chapter we observed that DCS had no observable effect at preNMDAr whilst the lower efficacy ACBC appeared to reduce the tonic activity of these receptors on glutamate release. In the previous chapter however, we observed that the preNMDAr co-agonist site may be saturated, as D-serine also had no effect on these receptors. Again as the only method available for studying the activity of preNMDAr was indirect it is difficult to establish exactly why DCS and D-serine did not affect preNMDAr activity. Due to this we are unable to make clear deductions on the binding of the preNMDAr co-agonist site. It is highly plausible that the lack of effect on of DCS on glutamate release was a function of the preNMDAr tonic activity. A kinetic effect on postNMDAr is clearly impactful as glutamate binding to postNMDAr is rapidly removed following unbinding from these receptors concluding the synaptic signal via these receptors. However, at the preNMDAr, glutamate is readily available and so a faster rate of closing may not be of large significance to these receptors as activation of these receptors is continuous.

Some inference may be achievable by observing the pattern of effects of D-serine, DCS and ACBC at preNMDAr and postNMDAr. D-serine enhanced postNMDAr but had no observable effect at preNMDAr, DCS did not affect eNEPSC amplitude (but did affect kinetics) and did not affect preNMDAr and ACBC reduced both preNMDAr and postNMDAr activity. Perhaps it is more likely then, that preNMDAr and postNMDAr have a similar level of co-agonist binding, which is arguably a sensible schematic, given the shared synaptic location of these two populations. It may be that the kinetic effects of DCS are not noticeably disruptive

to the role of preNMDAr in regulating transmitter release. The lack of effect of D-serine at preNMDAr may then be due to activity of this receptor population being limited by the activity of glutamate sites (Woodhall et al, 2001)., which are not saturated in contrast to postNMDAr during synaptic firing.

Although it may seem to be the most likely explanation for the results so far, as mentioned it was not possible to explicitly probe this idea. If true, it would indicate that, unfortunately, the co-agonist site may not be a suitable basis for distinguishing between preNMDAr and postNMDAr. However, functionally we have achieved selectivity for postNMDAr, as DCS produced a functional effect at postNMDAr but not preNMDAr and this may be useful in selectively examining postNMDAr over preNMDAr.

4.4.4 Molecular basis of DCS action

The kinetic role of co-agonist site partial agonists has been well studied previously (Priestley and Kemp, 1994). However, here we have presented the novel observation that in a physiologically relevant situation, DCS selectively reduces the decay of NMDAr synaptic currents in principal neurones, in the EC at least, and that this is due to the level and nature of the endogenous co-agonist site activation.

On a simple level DCS has reduced the extent of NMDAr signalling in these cells and this effect is an anti-NMDAr effect. This is clearly highly interesting given the observations that DCS can act as an anticonvulsant and a cognitive enhancer. As previously mentioned anticonvulsant activity is highly typical of NMDAr antagonists (see Ghasemi and Schacter, 2011, Table 4) and as NMDAr are excitatory receptors it is highly plausible that this reduction in NMDAr signalling on principal cells represents an antiepileptic property. As discussed in section 1.9 the cognitive enhancing properties of DCS are typically seen at lower doses and a currently popular theory of cognitive enhancement by DCS is that it is mediated by a biased effect at GluN2C containing NMDAr, which are present on other types of neurone and glial cell but not typically on principal cells. The findings in this

chapter do not conflict with this theory and indeed if the effect at principal cell postNMDAr did indeed underlie an anticonvulsant property at higher concentrations, it could also underlie the abolished cognitive effect at higher concentrations. However, it is interesting to consider that the NMDAr blocker memantine is an approved cognitive enhancer in the treatment of Alzheimer's disease, where it may act to redress 'noisy' NMDAr signalling. Therefore it is possible that DCS act similarly and the anti-NMDAr effects observed here may underlie cognitive enhancement by DCS.

Whilst such a simplistic discussion is interesting, both cognition and epileptic activity clearly involve highly complicated processes that extend beyond the level of single neurones. A selective kinetic effect at postNMDAr in principal cells is highly interesting in this regard given the role that such kinetics may play in activity on the network level. Whilst it is possible to speculate, the complex, emergent nature of network activity makes prediction problematic and necessitates empirical investigation. Thus we were now highly interested to study the effects of DCS on the level of the neuronal network to try to establish how the novel findings here might be linked to the neuropharmacological and psychopharmacological properties of DCS. We were also highly interested that our results here indicated that DCS now represented a unique tool for selectively investigating the role of kinetics of the NMDAr in emergent network activity. Furthermore by contrasting the effects of DCS with other ligands, we may gain an insight into the roles of the different receptor populations.

Chapter 5

The Effects of Partial Co-agonists on Epileptiform Activity in the Entorhinal Cortex

5.1 Introduction

For two reasons it was of interest to now examine the effects of the co-agonist site partial agonists on epileptiform activity in the EC. Firstly, previous reports have indicated both an anticonvulsant and a pro-convulsant potential of DCS. Moreover, there has been a great deal of interest in DCS as a cognitive enhancer. By examining the effects of partial agonists on epileptiform activity we may shed light on these findings and the therapeutic possibilities offered by such compounds. Secondly, as we have now examined the actions of these compounds in brain slices we can use them as tools to produce insights into the mechanics of epileptiform bursts. Furthermore, we consider that epileptiform activity induced by $GABA_A$ is of interest more generally for the study of the neuronal synchronisation as, though artificial, it represents a simplified form of emergent network activity.

Hypersynchronous epileptiform activity can be induced in brain slices through various means which act to shift the balance of activity in favour of excitation; here we have examined epileptiform activity induced by blockade of $GABA_A$ receptors by bicuculline. In the hippocampal-EC structure, such epileptiform activity has been shown to originate in the medial EC (Jones and Lambert, 1990). Extracellular epileptiform activity consists largely of bursts of high amplitude spikes and sometimes with single spikes between these bursts. Going beyond this highly general description is problematic as such activity is highly variable between and within slices. This variability and the complicated form of epileptiform activity make analysis highly problematic with most studies resorting to descriptions of visual interpretation without providing any quantification. Therefore to examine the effects of partial agonists on epileptiform activity meaningfully it was necessary to develop new methods of analysis to allow changes to be objectively quantified and significance testing to be performed.

The $GABA_A$ receptor is the major source of inhibition in the CNS and epileptiform activity induced by $GABA_A$ blockade is necessarily majorly constituted by principal cell interactions. Therefore this form of network synchronisation is

relatable to the previous work examining principal cell NMDAr populations. In layer II of the EC glycine receptors and/or bicuculline insensitive $GABA_A$ receptors may also contribute to inhibition (Greenhill et al, 2014) and for this reason the non-competitive $GABA_A$ receptor inhibitor picrotoxin, and the glycine receptor antagonist strychnine were used alongside bicuculline here. Furthermore, in the previous chapter we observed that when this combination of drugs is applied (in addition to an AMPA receptor antagonist) only an NMDAr response remains when the synapses are stimulated. This indicates that in the presence of the current cocktail of drugs, only NMDA and AMPA receptors are likely to be active post-synaptically. The aims of this chapter are then to examine the effects of the ligands of interest on epileptiform activity in the EC.

5.2 Methods

In combined EC-hippocampal rat brain slices, extracellular recordings were made from layer II of the medial EC as described in the general methods section. Epileptiform activity was provoked by continuous perfusion of strychnine (1 µM), bicuculline (20 µM) and picrotoxin (50 µM) and left to stabilise for at least 40 minutes after initiation before the addition of drugs. Drugs were perfused for 25 minutes and washout periods were 45 minutes.

Novel methodology for the gross analysis of epileptiform activity was devised with Dr. Peter Massey. Using the program DataView (Dr. W. J. Heitler, University of St Andrews), extracellular recordings are rectified and then smoothed by calculating a 50 ms moving average (mean) which is iterated ten times. In processed traces, events over the last five minutes of each treatment condition were then detected using a threshold crossing algorithm. The times between events (‘gaps’), and the durations, amplitudes and areas of the events were then automatically calculated. The number of events in this period were also counted and used to calculate the overall frequency of events. The processing of traces and the gross analysis is shown in Fig. 5.1. This methodology allowed large numbers of events to be analysed, countering the large variability of this data.

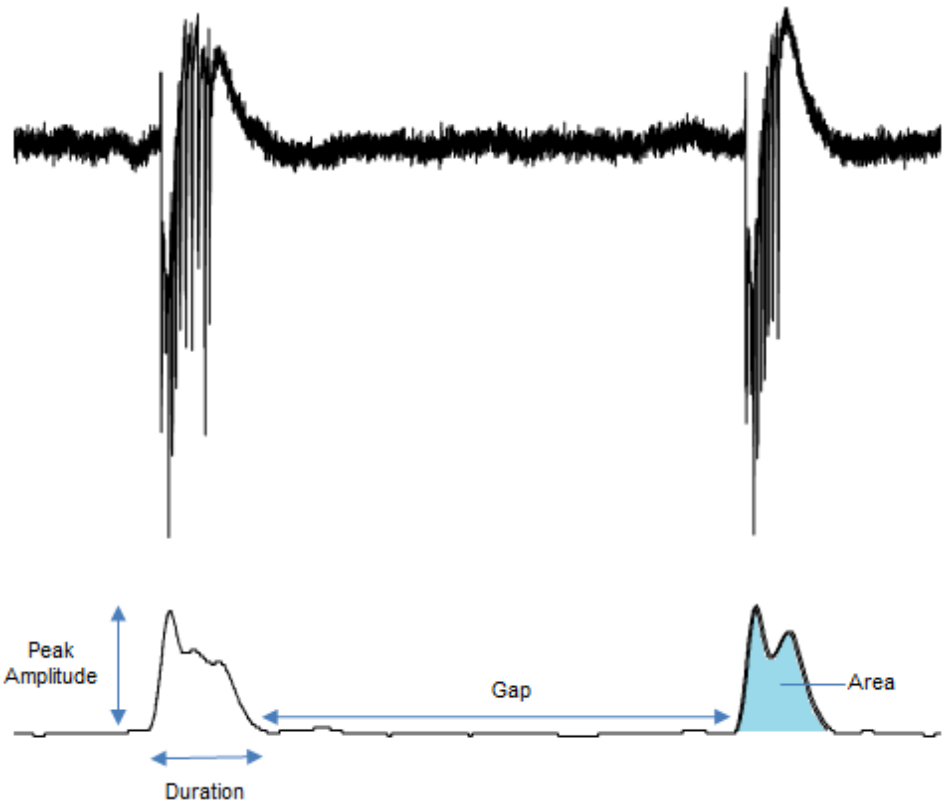

Fig. 5.1. Example trace of typical epileptiform activity in raw and processed forms and analysis parameters of processed traces. Raw traces of epileptiform recordings (above) were rectified and smoothed to produce easily quantifiable events (below). For the last five minutes in each treatment condition, these processed events were analysed and peak amplitudes (mV), durations (ms), gaps (ms) and areas (μVs) were calculated as indicated. The frequency at which epileptiform bursts occurred was calculated through counting the number of events in the 5 minute analysis period. The inter-event intervals for the spikes within (unprocessed) events was also calculated for the last 5 events in each condition.

The form of epileptiform events was also examined. Typical epileptiform activity contains within event spikes and these were analysed using Minianalysis software (Synaptosoft, Decatur). Spikes were detected visually and the inter-event-intervals (IEI), rise (10-90%) and decay (0.37 fraction) times were calculated. analysis was carried out on the last five epileptiform events in each treatment condition and pooled together producing one set of data per condition, per cell. Amplitudes from this analysis were not considered as this was examined in the more powerful gross analysis.

For every parameter of analysis in each cell and condition a mean and standard deviation is calculated. From these the coefficient of variation (standard deviation divided by the mean; CoV) was calculated as a measure of consistency. The differences between the mean and CoV in the drug conditions and the control condition were tested for significance using a paired, two tailed Student's t-test. For each treatment condition the grand mean was then calculated as well as a mean CoV, termed 'variability', and the standard errors of each.

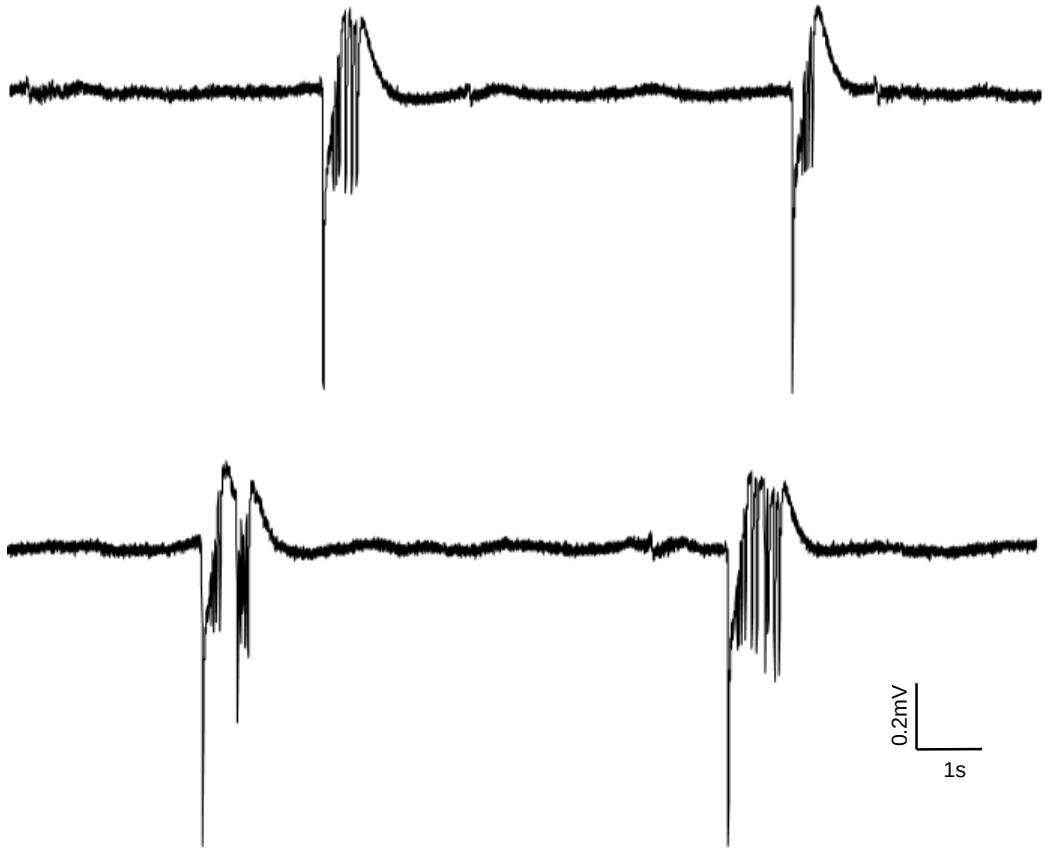

Fig. 5.2. Variability of epileptiform burst activity. Four consecutive epileptiform bursts from one slice in the control condition are shown to illustrate the highly variable nature of this activity. As is the case here, epilepfiform bursts in layer II of the EC were often seen to occur at fairly regular intervals and also the amplitude of such activity is generally consistent in scale. However, the intraburst characteristics and duration of these bursts is highly variable making meaningful analysis problematic. Here we have introduced methodology which allows large numbers of bursts to be analysed easily, countering somewhat the large within slice variability.

Due to the highly variable nature of this activity (see Fig. 5.2), we have chosen to additionally point to results which were below the $p<0.1$ level i.e. results which would be significant with a one-tailed test. These results which tended towards significance are denoted by the letter 'T'. However, it is important to note the increased possibility of false positive results due to the large amount of comparisons made here. Owing to the large number of parameters analysed, in figures we have focussed on results which were indicated to be relevant by changing during one of these experiments. CoV is referred to as 'variability' in figures. Example traces in results figures are selected as being representative of the changes detected.

5.3 Results

5.3.1 Effects of DCS on epileptiform activity in the EC

We were now highly interested to investigate the effects of DCS on epileptiform bursts as a form of emergent network activity related to epilepsy and to contrast these with our previous findings. In combined EC-hippocampal brain slices from juvenile rats epileptiform activity was induced by continual perfusion of the $GABA_A$ receptor antagonists bicuculline and picrotoxin and the glycine receptor antagonist strychnine, which remove inhibitory synaptic activity onto principal cells in the EC. In seven slices treated this way, DCS was then perfused at three concentrations, 3, 30 and 300 µM, followed by a washout period. Results from these experiments are shown in Fig. 5.3a and Fig. 5.3b.

Fig. 3a summarises the analysis of the effects of DCS on burst inter-event-interval (IEI), that is, the time between spikes within the epileptiform bursts. DCS across the concentrations tested, had no discernible effect on the IEI of epileptiform bursts which remained at an average of 74-76 ms, the reciprocal within frequency for this being 13.2 - 13.5 Hz. However, one significant effect was observed during the washout period. Here IEI was still unchanged but the variability of the IEI within slices was reduced. In other words, although the average IEI was unchanged, it had become more consistent during the washout period. Such a result during washout

of a drug indicates that DCS may have elicited an adaptive response resulting in a reflective change following its removal.

Whilst having no detectable effect on the within burst IEI, the gross analysis of this data indicated that DCS produced substantial changes in the magnitude of epileptiform bursts (Fig. 5.3b). The mean duration of epileptiform bursts in these slices was 1.18 ± 0.12 s in the control condition and was then elevated to 1.26 ± 0.13 s during perfusion of 3 µM DCS ($p<0.1$), 1.42 ± 0.14 s during perfusion of 30 µM DCS ($p<0.05$) and 1.39 ± 0.13 s during perfusion of 300 µM DCS ($p<0.05$) and returned nominally to baseline (1.22 ± 0.11 s) following washout of DCS. Interestingly the peak amplitude of bursts followed a similar pattern with a mean value of 0.18 ± 0.05 mV for control and values of 0.21 ± 0.05 mV for 3 µM DCS, 0.25 ± 0.05 mV for 30 µM DCS ($p<0.05$), 0.23 ± 0.05 mV for 300 µM DCS and 0.16 ± 0.04 mV for the washout period. Also, the average area of epileptiform events, which is clearly related to the duration and peak amplitude, followed this pattern with a value of 190 ± 47 µVs in control and values of 232 ± 49 µVs for 3 µM DCS ($p<0.01$), 302 ± 63 µVs for 30 µM DCS ($p<0.01$), 272 ± 54 µVs for 300 µM ($p<0.01$) and 199 ± 50 µVs for the washout period. The frequency at which bursts occurred was 0.15 ± 0.03 Hz during control and was unchanged during this experiment.

Clearly we were highly interested to observe that DCS increased the magnitude of these epileptiform bursts in terms of duration, peak amplitude and area. Furthermore we were highly interested to observe that these effects were maximal at the intermediate concentration, 30µM, which corresponds to the Emax of DCS at postNMDAr calculated in the previous chapter (4.3.2). Also, as each of these parameters was seen to return to control levels following washout of DCS, these effects were unlikely to be merely due to progressive changes in the epileptiform activity with time.

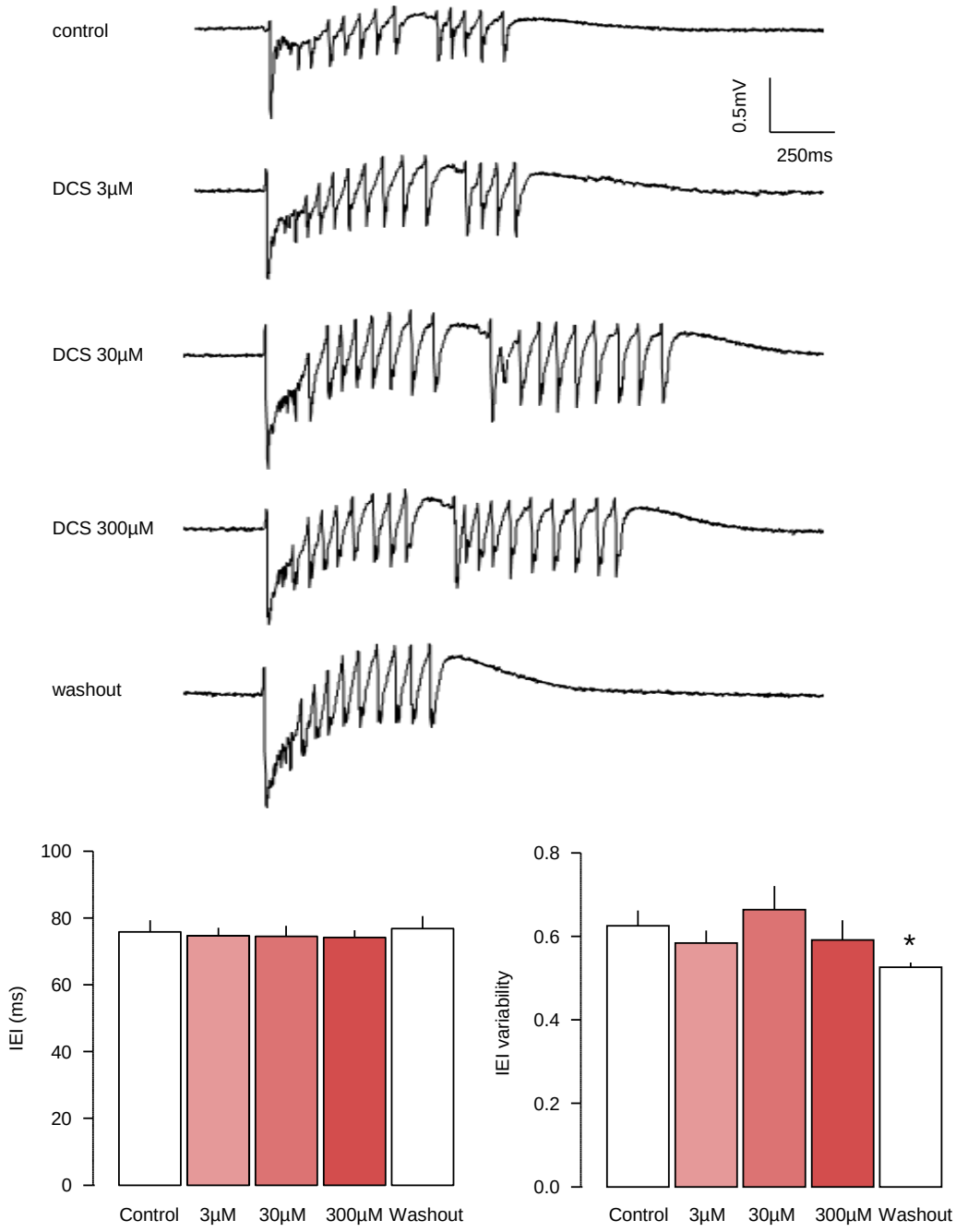

Fig. 5.3a. The effects of DCS on epileptiform activity in the medial EC, within burst analysis. During disinhibition-induced epileptiform activity, DCS was added at 3, 30 and then 300 µM, followed by a washout period. Above are example traces showing a characteristic epileptiform burst from each condition. Below are bar charts of the grand mean inter-event interval (IEI) across samples (left) and the mean IEI CoV (right), termed 'variability'. Whilst there were no changes in these parameters with DCS, interestingly during the washout period, IEI variability was significantly lower than control. * denotes $p<0.5$, $n=7$.

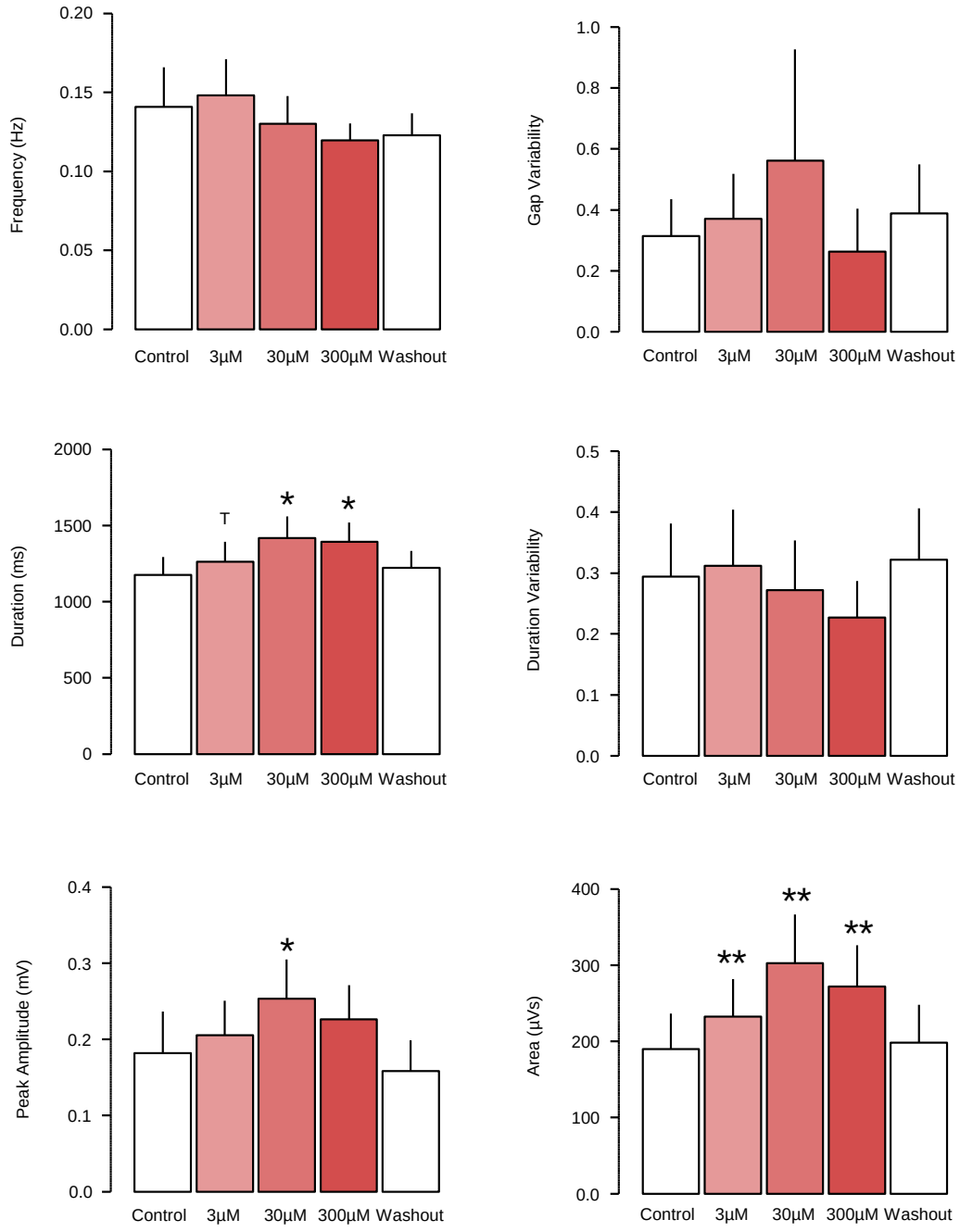

Fig. 5.3b. The effects of DCS on epileptiform activity in the medial EC, gross analysis. For the same data set as Fig .5.3a, a large scale gross analysis of epileptiform events is presented. Bar charts are shown for the grand mean of the frequencies at which bursts occurred during the 5 minute analysis period ('frequency'), mean CoV of times between the events ('gap variability'), grand mean of event durations ('duration'), mean CoV of durations ('duration variability'), grand mean of event amplitudes ('peak amplitude') and grand mean of event areas ('area'). This powerful analysis indicated several significant changes in epileptiform bursts with DCS from control. Interestingly, the durations, peak amplitudes and areas of events were significantly increased by DCS and followed a U-shaped dose response, with maximal changes at 30µM. T denotes $p<0.1$, * denotes $p<0.5$, ** denotes $p<0.01$, n=7.

5.3.2 Effects of ACBC on epileptiform activity in the EC

Having established the effects of DCS on epileptiform activity, we were now interested to examine the effects of the other NMDAr co-agonist site partial agonist which we have characterised, ACBC. To achieve this, in five brain slices with induced epilptiform activity, ACBC was added cumulatively at 100 µM, 300 µM and 1 mM, followed by D-serine at 100 µM (with washout of ACBC). The within burst analysis of these experiments is shown in Fig. 5.4a. The IEI within the epileptiform bursts was seen to be significantly elevated by perfusion of ACBC, progressing with the concentration applied, and was then further increased by D-serine. The average value in control was 92.2 ± 12.4 ms and values were then 101.6 ± 13.9 ms for 100 µM ACBC ($p<0.05$), 141.5 ± 29.6 ms for 300 µM ACBC, 148.5 ± 25.1 ms for 1 mM ACBC ($p<0.05$) and 182.6 ± 26.5 ms for D-serine ($p<0.01$). No changes in within slice IEI variability were observed.

Results from the gross analysis of this data is shown in Fig.5.4b. The frequency at which epileptiform bursts occurred over the analysis period was lowered at the higher concentrations of ACBC, although it was only approaching significance at the higher concentration it did appear to be reversed during perfusion of D-serine. Average values for this parameter were 0.15 ± 0.02 Hz for control, then 0.17 ± 0.03 Hz for 100 µM ACBC, 0.13 ± 0.01 Hz for 300 µM ACBC, 0.10 ± 0.01 Hz for 1 mM ACBC ($p<0.1$) and 0.15 ± 0.02 Hz for D-serine. The average peak amplitude of bursts followed a similar pattern with a control value of 0.17 ± 0.06 mV and values of 0.17 ± 0.06 mV for 100 µM ACBC, 0.14 ± 0.05 mV for 300 µM ACBC, 0.12 ± 0.04 mV for 1 mM ACBC ($p<0.1$) and 0.15 ± 0.04 mV for D-serine. The duration and area of bursts and was essentially unchanged during the experiments, with average control values of 1.11 ± 0.18 s and 152 ± 48 µVs, respectively. Finally the within slice variability (average CoV) of the gaps between bursts was unaltered by application of ACBC but was significantly reduced during the perfusion of D-serine. In other words, the time between events became more consistent following the application of D-serine.

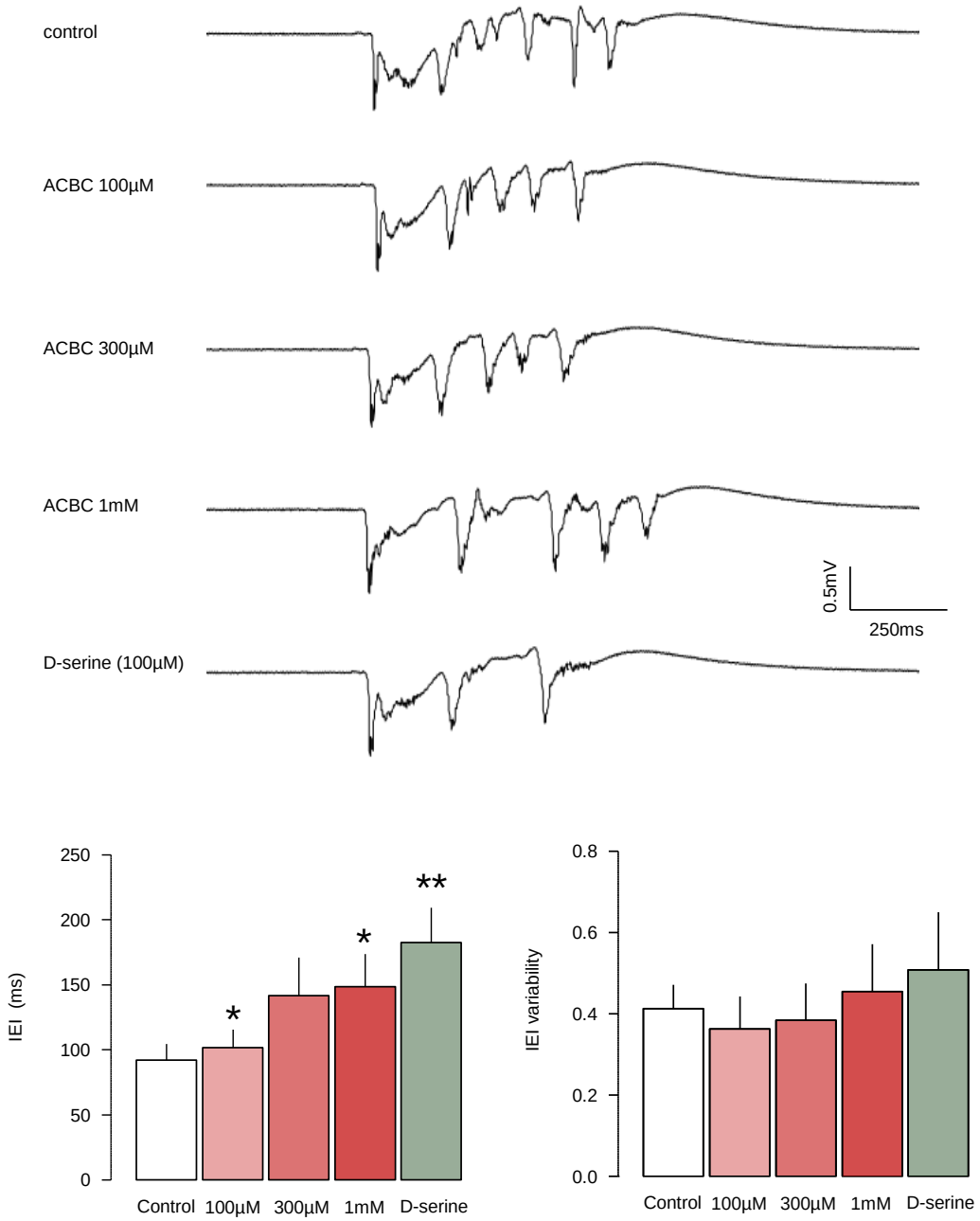

Fig. 5.4a. The effects of ACBC on epileptiform activity in the medial EC, within burst analysis. During field recording of epileptiform burst activity, ACBC was added at 100 µM, 300 µM and then 1 mM, followed by D-serine at 100 µM with washout of ACBC. Above are example recording traces of epileptiform bursts during each condition in one experiment. Below are bar charts of the mean inter-event interval (IEI) and IEI variability. Interestingly, ACBC progressively and significantly increased the interval between events within epileptiform bursts (i.e. a decrease in their frequency). However, this was further increased during perfusion of D-serine. * denotes $p<0.5$, ** denotes $p<0.01$, n=5.

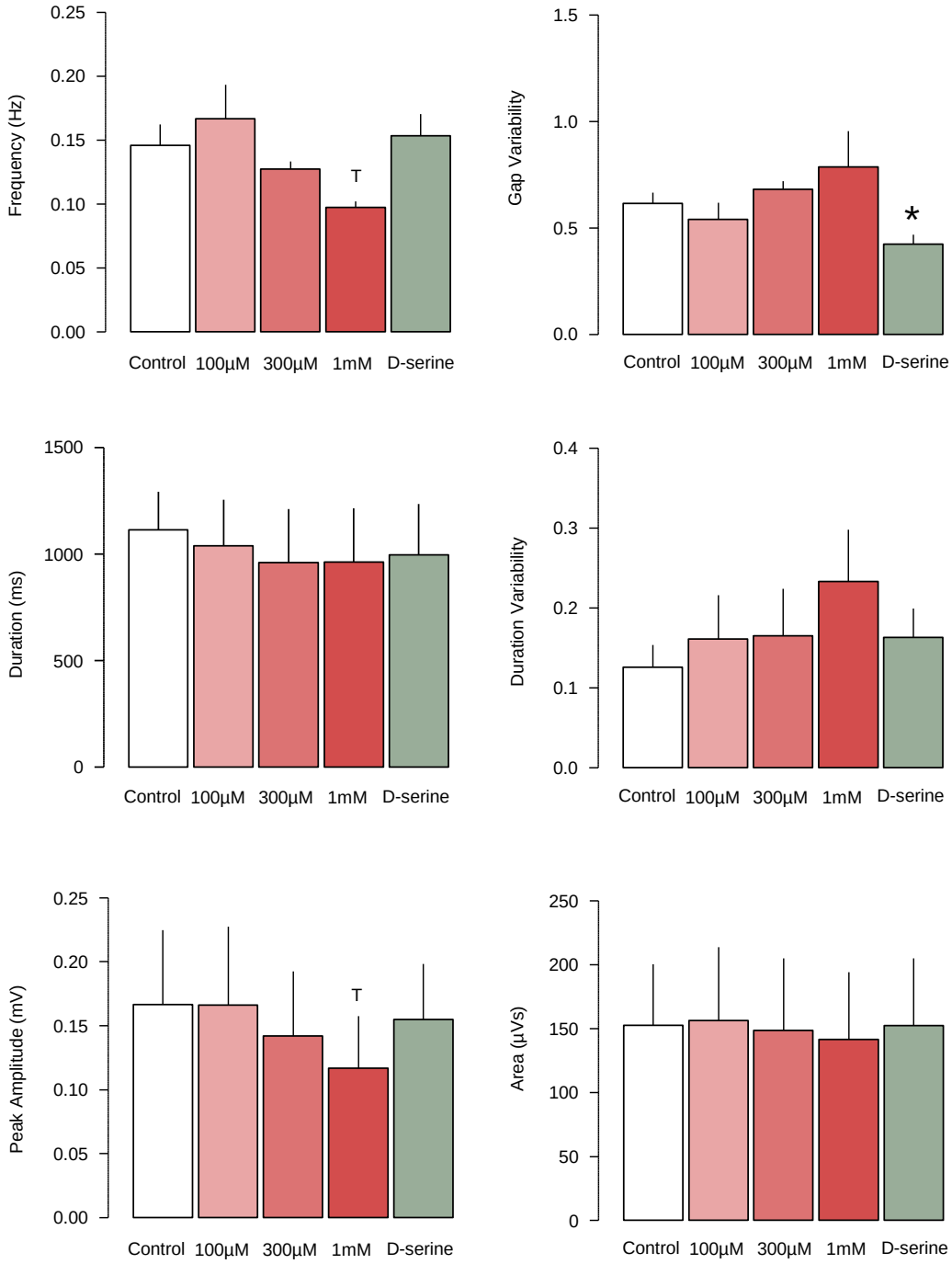

Fig. 5.4b. The effects of ACBC on epileptiform activity in layer II of the EC, gross analysis. In the same experiment as Fig. 5.4a, a gross analysis of epileptiform events was conducted. Bar charts are presented showing mean data across samples for the parameters of interest. Both the frequency at which epileptiform bursts occurred, and their peak amplitudes appeared to undergo a concentration dependent decrease with ACBC, which was tending towards significance at 1 mM. Also, the variability of the time between events (gap variability) was significantly decreased following perfusion of D-serine. T denotes $p<0.1$, * denotes $p<0.5$, $n=5$.

In summary then, the low efficacy partial agonist ACBC was here seen to increase the time between spikes (IEI) within the epileptiform bursts. However, this parameter was further increased by the full agonist D-serine. ACBC also appeared to produce a concentration dependent decrease in the peak amplitude of epileptiform bursts as well as the frequency at which they occur, and these effects reversed when ACBC was replaced with exogenous D-serine. Interestingly, the variability in gaps between events was unaffected by ACBC but was decreased in the D-serine condition.

5.3.3 Effects of D-serine followed by DCS on epileptiform bursts

Finally we were interested in whether the effects of DCS on epileptiform activity were likely to be due to the anti-NMDAr effect, such as that which we had observed at postNMDAr. To this end we tested the effects of the full agonist D-serine (100 µM) and then DCS (300 µM), applied separately, on epileptiform activity in seven slices. The within burst analysis of this data is shown in Fig. 5.5a, IEI was 70.6 ± 9.5 ms in control and was unaffected by either treatment. Fig. 5.5b shows results from the gross analysis, though interestingly again here there were no notable effects throughout. The frequency at which bursts occurred was 0.11 ± 0.03 Hz in the control period, 0.10 ± 0.02 Hz in the presence of D-serine and 0.11 ± 0.01 Hz in the presence of DCS. Average burst duration was 1.34 ± 0.34 s in control, 1.48 ± 0.35 s with D-serine and 1.53 ± 0.31 s with DCS. Average peak amplitude was 0.24 ± 0.06 mV in control, 0.24 ± 0.06 mV in D-serine and 0.23 ± 0.05 Hz with DCS.

Fascinatingly, then D-serine appeared to have no discernible effect on epileptiform activity, despite having a positive effect at postNMDAr when examined with eNEPSCs (4.3.4). However, here we also did not see that any of the effects of DCS observed in 5.3.1 were replicated when DCS was applied following D-serine. These results may suggest that adaptive changes have taken place with D-serine treatment which then alter the network's response to DCS. Our previous experimentation in 5.3.1 indicated that the washout conditions used were effective

at removing drug, although here the previously established effects of DCS were precluded following treatment with D-serine, despite being washed out.

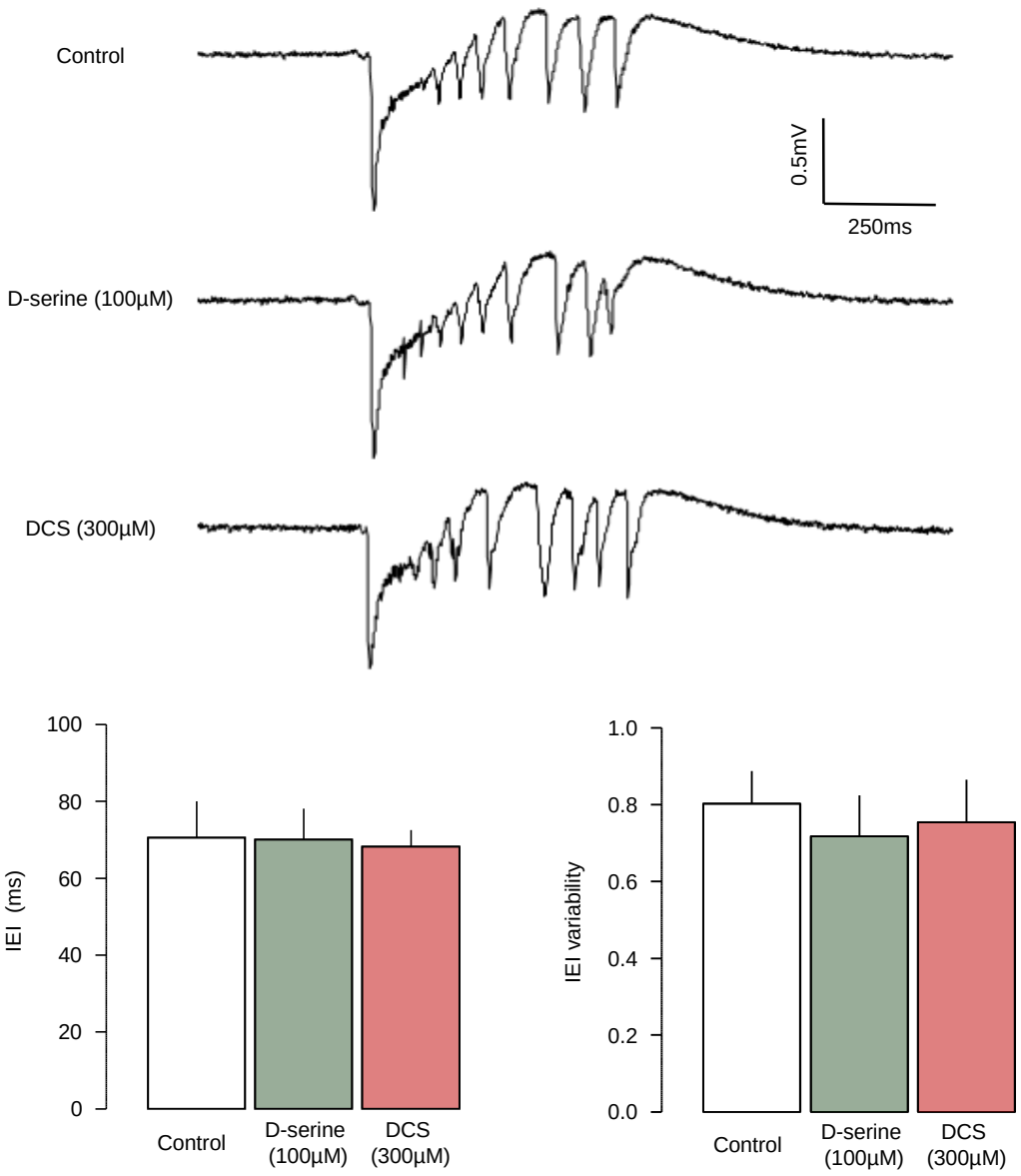

Fig. 5.5a. The effects of D-serine and DCS on epileptiform activity, within burst analysis. In 7 slices, epileptiform activity was induced and the effects of 100 µM D-serine followed by 300 µM DCS (with washout of D-serine), were examined. Above are representative traces from one slice for each treatment condition, below are bar charts of data across slices of average IEI and the IEI variability of events within bursts. In this experiment neither D-serine or DCS elicited any significant change in the characteristics of the within burst spikes.

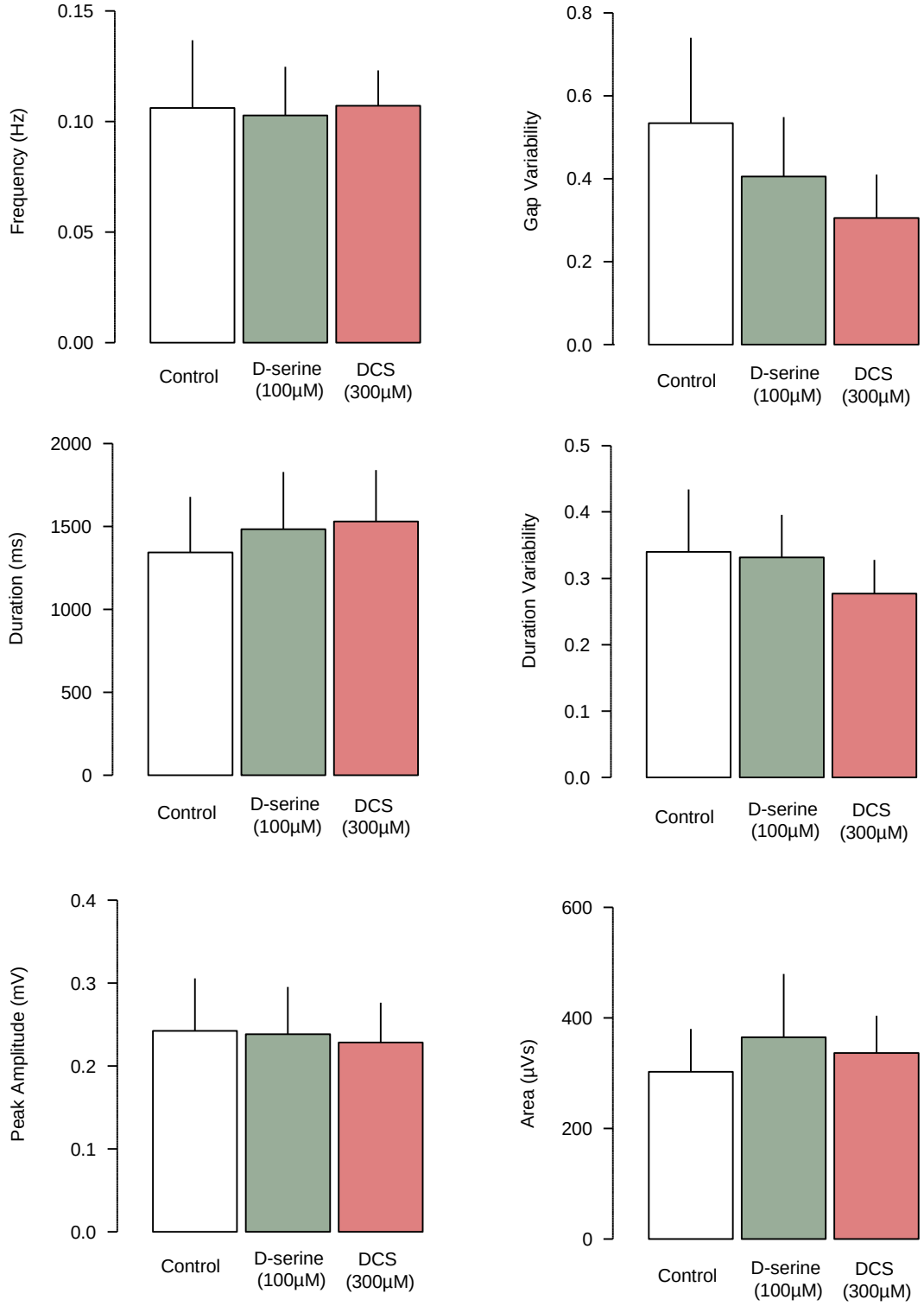

Fig. 5.5b. The effects of D-serine and DCS on epileptiform activity in the EC, gross analysis. Bar charts are given for the parameters of interest resulting from large scale gross analysis of recordings from the experiments of Fig. 5.5a. Again no consistent effects were observed in this data set with the gross analysis. n=7.

5.4 Discussion

Without inhibition, spontaneous action potentials in principal cells can spread rapidly through the excitatory network and when these action potentials reach a frequency threshold, the entire network is activated producing a population response. This threshold is thought to represent the average requirement of excitation for a neurone to fire, summed across the network (De la Prida et al, 2006, Cohen et al, 2006). The population response consists of every neurone firing in synchronisation. Principal cell firing drives this response, but the recurrent excitation also drives principal cell firing. This is emergence, the self-organisation of a complex system giving rise to a distinct form of activity.

During the population response, on the single cell level a prolonged depolarisation with superimposed bursts of spikes is seen. (It is important to note the potential for confusion here, as generally the word 'burst' has been used here to describe the episodes of spiking on the extracellular level). These spikes are action potentials and the burst form in which they occur is due to the intrinsic bursting characteristics of pyramidal neurones. These bursting characteristics are thought to result due to the coupling between dendrites and soma portions of the neurones, either electrically and/or via intracellular calcium dynamics. This initial depolarisation with superimposed bursts of spikes corresponds to the initial singular spike seen at on the extracellular field level, which represents this activity coordinated across neurones and is commonly termed the paroxysmal depolarising shift. After this several similar but smaller groups of events termed 'after discharges' can occur in the intracellular recording, corresponding to the secondary spikes in the field recording burst (Traub et al, 1993).

The AMPA receptor is the most crucial receptor in disinhibition induced epileptiform activity as blockade of this receptor is commonly seen to virtually abolish all population events, whilst blockade of NMDA receptors can reduce the amplitude and duration of epileptiform activity (Lee and Hablitz, 1991; Thompson and West, 1986; Dingledine et al, 1986; Jones and Lambert, 1990). As mentioned previously, the form of the population response is thought to be determined by the

intrinsic bursting characteristics of the principal cells. This neuronal bursting is highly dynamic and in computational models of epileptiform activity a fast AMPA receptor synaptic conductance provides the timely recurrent excitation required to produce a synchronised population response (Traub et al, 1993).

5.4.1 DCS action on epileptiform activity

In the experiments here, the effects of DCS were pro-synchronous. DCS increased both the peak amplitude and the duration of the epileptiform bursts. As the effects of duration closely mirrored those on amplitude this indicates that the two effects may share a common basis. It is possible that the effects of DCS at NMDAr during epileptiform bursting differs to those seen in quiescent slices. Or it may be possible that the effects seen here arise from areas within the brain slice where the NMDAr regulation is different. However, if DCS was now increasing amplitude/decay time we would expect similar effects with D-serine. Likewise if it was now decreasing amplitude we would expect the effects to be similar to ACBC, both of which were not the case. So it is likely that the effects of DCS here were unchanged from those observed at the NMDAr in the previous chapter (see section 4.3, 4.4).

We were somewhat surprised then that DCS, which decreases the decay time of postNMDAr conductance, had pro-synchronous effects. One possible way to reconcile these findings may be to consider the AMPA receptor. As mentioned previously, the AMPA receptor is the most crucial receptor to epileptiform activity but the AMPA receptor also has very fast kinetics. So in terms of kinetic behaviour at least, by selectively reducing the decay of the postNMDAr with DCS we have effectively made them more AMPA receptor–like, without sacrificing the extent of the conductance which they provide. In other words the fact that AMPA receptors are the principal receptor in the production of epileptiform activity supports the notion that faster kinetics are pro-synchronous. As mentioned previously, computational models require a fast excitatory synaptic conductance to convey the quickly dynamic form of neuronal activity for synchronisation across the network. In the presence of DCS, the average postNMDAr is now closing faster and are therefore able to re-open sooner and respond to glutamate release

more frequently. Given insights from the AMPA receptors, this is a highly plausible basis for a pro-synchronous effect.

A different way to think about this may be to consider the reduced Traub computational model of disinhibition induced epileptiform activity produced by Pinksky and Rinzel (1993). This model indicates that during AMPA receptor blockade, the postNMDAr is sufficient for neurones to excite each other and fire, in line with intracellular observations (Traub et al, 1993), although the firing is muted in length as activity in the network does not persist for as long. However, in the extracellular field the signal is abolished, as the firing is no longer synchronised between neurones. The modelling indicates that this occurs due to the properties of the postNMDAr conductance, which introduce an element of unpredictability or 'chaos' into the network, causing rapid desynchronisation when AMPA receptors are not active. Perhaps then, by reducing the atypical kinetics of the postNMDAr conductance we have reduced this element of desynchronising chaos. The amplitude of the extracellular signal was then enhanced by DCS because the firing of neurones was more coordinated, and the length of the events was extended because the network was less prone to desynchronise.

An alternative explanation could be based on the idea that in the presence of exogenous DCS, all postNMDAr would now be decaying at the same rate. Prior to the addition of DCS, postNMDAr responses could be decaying at varying rates, possibly due to the difference in glycine and D-serine bound. This change to a unified postNMDAr decay time would then be a highly plausible basis for increasing the synchrony of the neuronal network. However, if this was the case a similar response would be expected when exogenous D-serine was applied as this would also act to unify the decay of postNMDAr, but D-serine lacked any such effect (5.3.3).

Clearly in light of the well-established biphasic dose relationship of DCS in cognitive enhancement (see section 5.1) we were extremely interested to observe that the prosynchronous effects of DCS followed a biphasic pattern. Furthermore the maximal effect was seen at 30 μM which was chosen as the central

concentration as it was observed to be the Emax at postNMDAr in principal cells. This, alongside the fact that these slices were disinhibited, indicates that the prosynchronous effects were indeed mediated by postNMDAr on principal cells. Unfortunately it is not currently known what CNS concentration is produced by a pro-cognitive dose of DCS as this would now be useful in ascertaining the possible relationship between these effects and cognitive enhancement by DCS.

But why should a higher concentration produce a non-maximal effect here? One possible explanation is that interneurons were still able to have an inhibitory action via non-postsynaptic $GABA_B$ receptors. If this were the case then at 300 µM DCS, a pro-postNMDAr effect at interneurons may be enlarged relative to the effect at principal cells in comparison to when at 30 µM. There is evidence that inhibition of $GABA_B$ does have a small influence on picrotoxin induced epileptiform activity (De la Prida et al, 2006; Cohen et al, 2006). The prosynchronous effects observed here are clearly unlikely to underlie an anticonvulsant effect. However, if the schematic suggested here is correct it is possible then that an effect at interneurons may predominate at higher doses, producing an anticonvulsant effect. As previously mentioned (section 4.1) Wlaz et al (1994) found that an anticonvulsant dose of DCS represented a concentration of 860 µM in brain tissue, which would fit with this schematic.

DCS was not seen to have any effect on the IEI within bursts although after washout, IEI variability was seen to decrease. As discussed earlier, these spikes represent coordinated periods of action potential bursts in the contributing neurones. It is unclear why washout of DCS should provoke a change in the variability of IEI but a change from control with the washout of a drug suggests that an adaptive response has taken place. Although it is only a single result, the possibility of adaptive plasticity changes taking place following DCS treatment is again clearly of interest when considering the pro-cognitive properties of DCS. However these properties are typically highly acute suggesting that immediate effects of DCS are responsible.

5.4.2 ACBC action on epileptiform activity

The mechanism of the effects of ACBC on epileptiform activity is more difficult to dissect as we have observed that ACBC has less specific effects at NMDAr. Indeed, unlike DCS, we observed that ACBC not only reduces the decay time of postNMDAr responses but also reduces the amplitude of these responses. Furthermore we have observed that ACBC can reduce glutamate release and as epileptiform activity entirely dependent on effective glutamatergic transmission, a presynaptic inhibition of glutamate release would very much be expected to generally antagonise this form of activity. It is interesting to contrast the effects of ACBC with those of DCS although ACBC still had two actions at principal cell NMDAr that DCS did not and so it problematic to comment on whether such differences are due to the reduction in the amplitude of postNMDAr responses or in glutamate release, by ACBC.

In contrast to DCS the effects of ACBC were generally anti-synchronous. Although not strictly significant, ACBC appeared to both reduce the peak amplitude of epileptiform bursts and reduced the frequency at which bursts occurred. Neither of these effects occurred with DCS, indicating that they would not be directly due to a decrease in decay time of postNMDAr responses. As previously discussed, the peak amplitude of the epileptiform burst likely indicates the degree of coordination of cell firing which could foreseeably occur due to reduction in excitation via a postNMDAr inhibition or a preNMDAr inhibition. However, the latency between bursts is likely to represent the threshold of excitation required for neurones to fire, summed across the network (De la Prida et al, 2006). As postNMDAr are thought to be only weakly active in non-depolarised cells due to the voltage dependent Mg^{2+} blockade, this may be more likely to be due to a presynaptic inhibition of glutamate release. An inhibition of glutamate release may reduce the effectiveness of excitation via AMPA receptors prolonging the time taken to reach the threshold of excitation whereby mutual depolarisation occurs.

The most pronounced effect of ACBC on epileptiform activity however, was on the intraburst IEI, where ACBC reduced the number of spikes within epileptiform events. This again was not seen with DCS. Such an effect indicates that less synchronised groups of action potential bursts are occurring and could again foreseeably be due to a direct reduction in postNMDAr conductance or an indirect reduction of AMPA receptor activity through preNMDAr. However, this result is confused by the even more pronounced increase following replacement of ACBC with D-serine. As D-serine has opposing effects at NMDAr it is puzzling that it would extend the response of ACBC. When D-serine was applied as the initial drug in section 5.3.3, no effect on intraburst IEI was seen at all. Again then there appears to be complex adaptive changes taking place during this activity and thus all inferences reliant on theory which is influenced by purely mechanical computational models should be made with caution.

It is interesting that ACBC did not replicate any of the responses to DCS. Whilst the effects of DCS were all positive, 'pro-synchronous' effects, the effects of ACBC were all negative 'anti-synchronous effects'. It is interesting then that whilst, as discussed, the (selective) reduction in postNMDAr decay time by DCS resulted in pro-synchronous changes, the multitude of effects of ACBC which included a reduction in postNMDAr decay time were anti-synchronous. It is therefore likely that the extent of excitatory transmission provided by the amplitude of postNMDAr responses and the effective release of glutamate are more important to epileptiform synchrony than the kinetics of the postNMDAr response. As previously discussed, this activity represents a severe over-excitation of a neuronal network and is thereby a model for epileptic seizures. Therefore these results can be taken to indicate that ACBC is a potential candidate for anticonvulsant drug therapy.

5.4.3 Treatment of epileptiform activity with D-serine followed by DCS

When D-serine was applied as the initial drug it was not seen to have any effects on epileptiform activity. Furthermore, when D-serine was subsequently replaced by DCS again no effects were observed. It is unclear why the full agonist D-serine

should have no effect on this activity. In the previous chapter it was observed that D-serine increased the amplitude and decay time of eNEPSCs, though only to a small extent. It is possible that then that this small change is simply not mechanically important to the epileptiform activity, though it is not possible to speculate further on why this would be the case.

It is again unclear why none of the previously observed effects of DCS should be replicated when it was applied following treatment by D-serine. It is highly plausible that this may have been influenced by the post-maximal concentration of 300 μM used here. Therefore these results are somewhat inconclusive. However, again this may indicate the importance of adaptive effects in epileptiform activity in the EC-hippocampal slices. The activity we have examined here likely involves the entire EC-hippocampal circuit and given the large capacity of this system for synaptic plasticity there is a clear basis for such adaptive changes to take place.

Chapter 6

General Discussion

6.1 Co-agonist Regulation of PreNMDAr

6.1.1 Glial D-serine as an endogenous ligand at preNMDAr

Initial work utilised mEPSC frequency as an indirect measure of preNMDAr activity to extend the characterisation of this receptor in the medial EC. Experiments with co-agonists and co-agonist site antagonists indicated that endogenous binding of the preNMDAr co-agonist site contributes to the tonic facilitatory action of these receptors. Experiments with scavenging enzymes indicated that the endogenous co-agonist was D-serine and further experiments with fluoroacetate suggested that this D-serine came from glial cells. Glial cells are increasingly being recognised as being important for computation in the brain and may exhibit a direct association with preNMDAr. This finding extends such ideas and adds an additional layer of complexity to the interactions at tripartite synapses. As preNMDAr are a target for the treatment of epilepsy, these results support existing initiatives to target the NMDAr co-agonist site for anticonvulsant therapy.

6.1.2 Selective targeting of NMDAr

A principle aim of this line of experimentation was to examine whether the co-agonist site could be useful as a basis for establishing a selective pharmacological profile of preNMDAr. From these results and others it appears that preNMDAr may be unique in that D-serine appears to be the sole endogenous co-agonist at these receptors. It is possible then that targeting D-serine production would affect preNMDAr activity more greatly than other NMDAr populations, which could also then possibly be compensated for by increasing glycine. The complete inhibition of preNMDAr by GluN2B antagonists may further aid discrimination of these receptors. However, most simply we observed that unlike postNMDAr, the preNMDAr co-agonist site appears to be saturated. This difference in degree of activation indicated the possibility of selectively targeting one receptor population over the other using a co-agonist site partial agonist.

6.2 The Actions of Co-agonist Site Partial Agonists at NMDAr in the EC

6.2.1 Co-agonist regulation and pharmacology of the postNMDAr

We examined the effects of the full co-agonist D-serine, the high efficacy partial co-agonist DCS and the low efficacy partial co-agonist ACBC on eNEPSC responses in principle cells of the medial EC. By examining the effects of these co-agonists of varying efficacy on the macroscopic response we were able to establish that the postNMDAr here exhibits an endogenous co-agonist activation of 79-87%. This matched with the efficacy of DCS as reported by Priestley and Kemp (1994), around 85%. Interestingly more recent studies have examined DCS efficacy at recombinant NMDAr, and this value lies between those for GluN2A and GluN2B diheteromers, supporting previous evidence that the postNMDAr has a GluN1(x2)/GluN2A/GluN2B triheteromic structure. Examining the effects of exogenous D-serine on the decay of the eNEPSC indicated that the endogenous binding of the postNMDAr sites was by a full or very high efficacy co-agonist but probrably not by pure D-serine, possibly by a mixture of D-serine and glycine as recently demonstrated for the hippocampus. This would then be in contrast to the endogenous co-agonist regulation of preNMDAr in the EC which we have shown to be mediated exclusively by D-serine.

6.2.2 DCS is a tool for investigating the role of postNMDAr kinetics

Examining the effects eNEPSCs at principal cells, we observed that DCS effected only the kinetics of these events, acting to decrease the decay time. This appeared to occur due to the level of endogenous postNMDAr co-agonist site activation and the identity of the endogenous co-agonist. The level of activation appeared to be matched to the efficacy of DCS meaning DCS did not change the amplitude of the events. However, the endogenous co-agonist had a higher efficacy, producing the larger control decay time. Moreover, DCS did not appear to have any effect at preNMDAr in the EC, though the exact reason for this is less clear (see section 4.4.3)**.** So with DCS, at principal cells in the EC at least, we see a selective effect at postNMDAr over preNMDAr. Furthermore, this is a selective effect to reduce

the decay of the postNMDAr response. Therefore we have shown that DCS is a highly intriguing tool for investigating the role of the uniquely long kinetics of the postNMDAr, at principal cells in brain slices. In contrast the lower efficacy ACBC decreased the amplitude, as well as the decay, of eNEPSCs and also had an inhibitory action at preNMDAr.

6.3 The Actions of Co-agonist Site Agonists on Epileptiform Synchrony in the EC

6.3.1 The long decay of PostNMDAr on principal cells is anti-synchronous

With disinhibition induced epileptiform activity in the EC, DCS was tested at three concentrations, with a middle concentration corresponding to the Emax for the reduction of eNEPSC decay time (30 µM) at principal cells. The results were highly interesting. We observed that DCS across these concentrations, increased the amplitude and duration of population extracellular activity indicating a greater and more sustained synchrony of the network (sections 5.3.1 and 5.4.1). Fascinatingly the concentration dependence of this effect was biphasic, peaking at 30 µM. Owing to the nature of disinhibition induced epileptiform activity, which is an emergent form of activity arising from the recurrent excitatory network, and that this response peaked at the eNEPSC Emax, we believe that this was mediated by an effect at postNMDAr on principal cells. Also, as this effect was not replicated at all with a lower efficacy co-agonist or a full co-agonist, we believe that it was indeed produced by the action at postNMDAr which we had observed with eNEPSCs, that is, a selective reduction in decay time.

This leads to what may be the most fascinating implication of this work: that the long decay of postNMDAr on principal cells is anti-synchronous and this finding has potentially profound implications for the study of diseases which are suggested to be disorders of network dynamics, such as epilepsy and psychosis. This result raises the question of why the long decay of the postNMDAr would be anti-synchronous, and why the brain would work at sub-maximal level of synchrony. An interesting explanation for this would be that the brain has evolved based on a

compromise between the benefits of good neuronal synchrony and the risk of epilepsy resulting from excessive synchrony. This idea would imply an evolutionary balance between the synchronous properties of the varying neuronal receptors.

6.3.2 Cognitive enhancement by DCS could be mediated by a negative kinetic effect at GluN2A/B containing NMDAr at principal cells

Owing largely to the high efficacy of DCS, the cognitive enhancement produced by DCS has been commonly thought to occur through a pro-NMDA effect. This also fits with the simple view of NMDAr as being a broadly pro-cognitive receptor. More recently, the pharmacology of DCS has been well established and it has been observed that at GluN2C containing receptors, DCS has an efficacy 200% that of glycine, compared to sub-maximal efficacies at the other NMDAr subtypes (see section 4.11). This has led to the idea that the pro-cognitive effects of DCS are mediated by GluN2C containing receptors, which are commonly located on non-principal cells such as interneurons (see Dravid et al, 2010; Goff et al, 2012; Ogden et al, 2014). Crucially this schematic accounts for the biphasic dose response curve of DCS in cognitive enhancement.

Initially, our observations with DCS at eNEPSCs seemed to fit such a schematic as we had observed essentially an anti-NMDAr effect at principal cells. However, subsequently we observed a pro-synchronous response of DCS which was mediated by this action at principal cell postNMDAr, and these have been shown to be a GluN2A/B triheteromeric subtype. Moreover, this effect was biphasic itself and so can also account for the u-shaped dose response. Although this is an artificial form of synchrony in slices of rat brain, such an effect could plausibly underlie a cognitive enhancement in vivo. We therefore propose an alternative theory of DCS action: that the cognitive enhancement occurs by a negative kinetic effect at GluN2A/GluN2B containing postNMDAr on principal cells which counterintuitively causes an enhanced neuronal network synchrony. On this idea it is interesting to note that the clinically utilised cognitive enhancer memantine has been shown to enhance gamma and theta oscillations in cortical brain regions

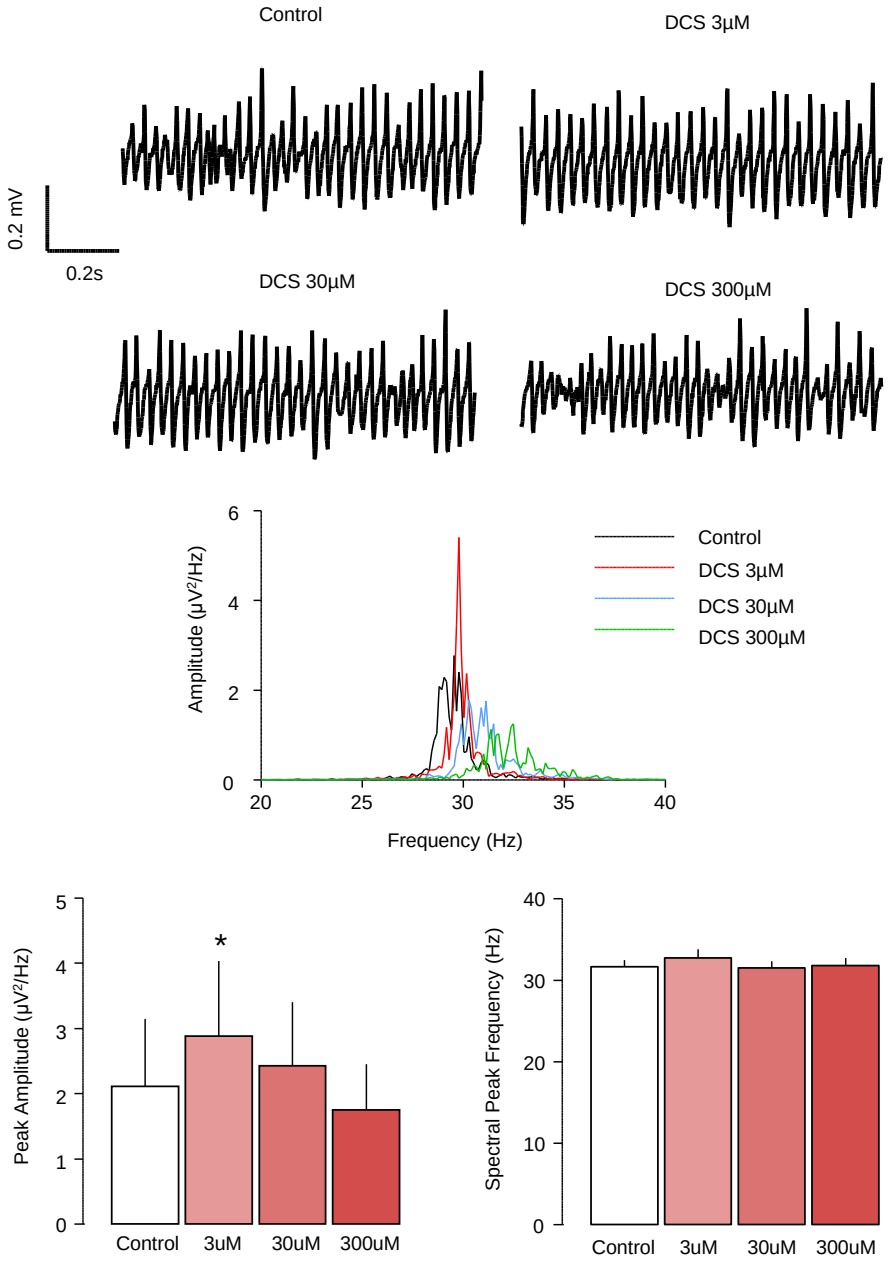

Fig. 6.1. The effects of DCS on gamma frequency oscillations. These experiments were carried out by Nadine Aboutara and Emma Robson. Above; sample traces, mid; a sample power spectrum produced by analysis of a one minute period of the continuous oscillation using a fast fourier transform, below; average data for 9 brain slices. Continuous gamma oscillations were induced in brain slices using kainic acid, and measured in the hippocampus as this activity was too weak in the EC for reliable study. At 3µM DCS significantly ($p<0.05$) increased the peak spectral amplitude of these oscillations, but this effect progressively diminished at 30µM and 300µM. Again then there appears to be a U-shaped pro-synchronous response, but peaking at a lower concentration than as was observed for the effects on epileptiform activity. Within our theory this could be explained by the fact that these slices are not disinhibited, meaning a larger anti-synchronous effect from interneurons and thus a lower concentration at which the pro-synchronous effect by pyramidal cells is overcome

of conscious rats (Ahnaou et al., 2014). Memantine is an NMDAr channel blocker and thus as we have observed for DCS, has essentially an anti-NMDAr action.

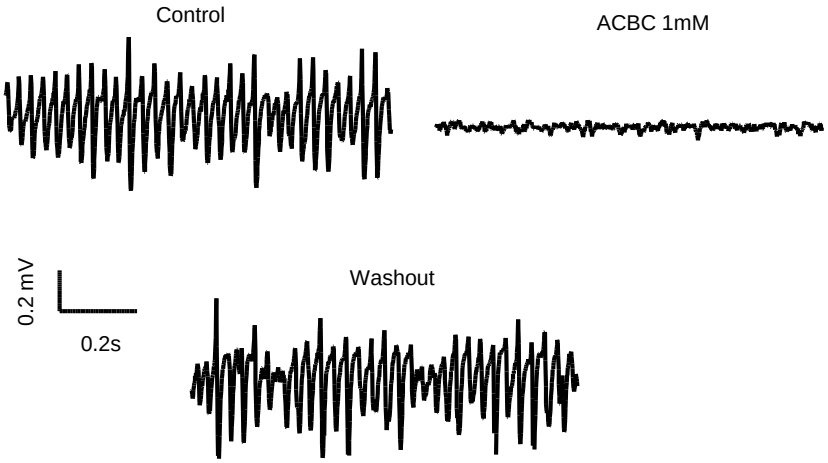

Fig. 6.2. The effects of ACBC on gamma frequency oscillations. This experiment was carried out by Nadine Aboutara and Emma Robson. ACBC abolished gamma synchrony and the response then recovered following washout. This is in agreement with the antisynchronous effects of ACBC observed on epileptiform activity in section 5.3.2.

Recently, further experiments from this laboratory have extended this study to the effects of DCS and ACBC on gamma oscillations, a more physiologically relevant form of synchronised behaviour which is thought to be highly important in cognition (see Wang, 2010). Interestingly this work has largely been seen to match well with the observations made in the study of epileptiform activity (Fig. 6.1 & 6.2), adding support to the observations on the synchronous properties of NMDAr and novel theory of cognitive enhancement by DCS presented here.

6.3.3 Other implications

The effects of the lower efficacy co-agonist ACBC on epileptiform activity were unrelated to those of DCS and were anti-synchronous. This is interesting as, like DCS, we observed that ACBC also reduced eNEPSC decay but unlike DCS, ACBC also decreased eNEPSC amplitude. Additionally, we also observed that unlike DCS, ACBC can reduce the tonic facilitation of glutamate release by preNMDAr. As such it is not possible to attribute which effect underlies this switch

from pro-synchrony to anti-synchrony. However, as a reduction of efficiency of glutamate release would alter transmission by the crucially important AMPA receptor, the inhibitory effect at preNMDAr is a highly plausible candidate for this stalk change in effect between the two co-agonists. Whatever the mechanism, these results indicate the possibility that ACBC or a similar compound may be a potential lead for anticonvulsant therapy. Interestingly D-serine was not seen to have any effect on epileptiform activity, when applied as the principal drug, and the reason for this is unclear. Other results with each drug indicated the capacity of this activity to undergo adaptive changes in response to treatment and indicating that more complex inferences, which are beyond the scope of the current work, may be important.

References

Ahnaou A, Huysmans H, Jacobs T, Drinkenburg WHIM (2014) Cortical EEG oscillations and network connectivity as efficacy indices for assessing drugs with cognition enhancing potential. Neuropharmacology 86:362-377.

Allaman I, Bélanger M, Magistretti PJ (2011) Astrocyte-neuron metabolic relationships: for better and for worse. Trends in Neurosciences 34:76-87.

Amiri M, Hosseinmardi N, Bahrami F, Janahmadi M (2013) Astrocyte-neuron interaction as a mechanism responsible for generation of neural synchrony: a study based on modeling and experiments. J Comput Neurosci 34:489-504.

Angulo MC, Kozlov AS, Charpak S, Audinat E (2004) Glutamate released from glial cells synchronizes neuronal activity in the hippocampus. The Journal of Neuroscience 24:6920-6927.

Aoki C, Fujisawa S, Mahadomrongkul V, Shah PJ, Nader K, Erisir A (2003) NMDA receptor blockade in intact adult cortex increases trafficking of NR2A subunits into spines, postsynaptic densities, and axon terminals. Brain Research 963:139-149.

Aoki C, Lee J, Nedelescu H, Ahmed T, Ho A, Shen J (2009) Increased levels of NMDA receptor NR2A subunits at pre- and postsynaptic sites of the hippocampal CA1: An early response to conditional double knockout of presenilin 1 and 2. The Journal of Comparative Neurology 517:512-523.

Aoki C, Venkatesan C, Go CG, Mong JA, Dawson TM (1994) Cellular and subcellular-localization of NMDA-R1 subunit immunoreactivity in the visual-cortex of adult and neonatal rats. Journal of Neuroscience 14:5202-5222.

Araque A, Carmignoto G, Haydon Philip G, Oliet Stéphane HR, Robitaille R, Volterra A (2014) Gliotransmitters travel in time and space. Neuron 81:728-739.

Avoli M, D'Antuono M, Louvel J, Köhling R, Biagini G, Pumain R, D'Arcangelo G, Tancredi V (2002) Network and pharmacological mechanisms leading to epileptiform synchronization in the limbic system in vitro. Progress in Neurobiology 68:167-207.

Banke TG, Traynelis SF (2003) Activation of NR1/NR2B NMDA receptors. Nat Neurosci 6:144-152.

Barbara Olasov Rothbaum PD (2008) Critical parameters for D-cycloserine enhancement of cognitive-behaviorial therapy for obsessive-compulsive disorder. Am J Psychiat 165:293-296.

Baron H, Epstein IG, Mulinos MG, Nair KG (1955) Absorption, distribution, and excretion of cycloserine in man. Antibiotics annual 3:136-140.

Bear MF, Connors BW, Paradiso MA (2007) Neuroscience: exploring the brain. Philadelphia, PA: Lippincott Williams & Wilkins.

Benari Y, Tremblay E, Riche D, Ghilini G, Naquet R (1981) Electrographic, clinical and pathological alterations following systemic administration of kainic acid, bicuculline or pentetrazole - metabolic mapping using the deoxyglucose method with special reference to the pathology of epilepsy. Neuroscience 6:1361-1391.

Bender VA, Bender KJ, Brasier DJ, Feldman DE (2006) Two coincidence detectors for spike timing-dependent plasticity in somatosensory cortex. The Journal of Neuroscience 26:4166-4177.

Benneyworth M, Li Y, Basu A, Bolshakov V, Coyle J (2012) Cell selective conditional null mutations of serine racemase demonstrate a predominate localization in cortical glutamatergic neurons. Cell Mol Neurobiol 32:613-624.

Bergersen LH, Morland C, Ormel L, Rinholm JE, Larsson M, Wold JFH, Røe ÅT, Stranna A, Santello M, Bouvier D, Ottersen OP, Volterra A, Gundersen V (2012) Immunogold detection of L-glutamate and D-serine in small synaptic-like microvesicles in adult hippocampal astrocytes. Cerebral Cortex 22:1690-1697.

Berretta N, Jones RSG (1996) Tonic facilitation of glutamate release by presynaptic N-methyl-d-aspartate autoreceptors in the entorhinal cortex. Neuroscience 75:339-344.

Borges K, Gearing M, McDermott DL, Smith AB, Almonte AG, Wainer BH, Dingledine R (2003) Neuronal and glial pathological changes during epileptogenesis in the mouse pilocarpine model. Experimental Neurology 182:21-34.

Borges K, McDermott D, Irier H, Smith Y, Dingledine R (2006) Degeneration and proliferation of astrocytes in the mouse dentate gyrus after pilocarpine-induced status epilepticus. Experimental Neurology 201:416-427.

Brasier DJ, Feldman DE (2008) Synapse-specific expression of functional presynaptic NMDA receptors in rat somatosensory cortex. The Journal of Neuroscience 28:2199-2211.

Buchanan Katherine A, Blackman Arne V, Moreau Alexandre W, Elgar D, Costa Rui P, Lalanne T, Tudor Jones Adam A, Oyrer J, Sjöström PJ (2012) Target-specific expression of presynaptic NMDA receptors in neocortical microcircuits. Neuron 75:451-466.

Burgdorf J, Zhang X-l, Weiss C, Matthews E, Disterhoft JF, Stanton PK, Moskal JR (2011) The N-methyl-d-aspartate receptor modulator GLYX-13 enhances learning and memory, in young adult and learning impaired aging rats. Neurobiology of Aging 32:698-706.

Buzsáki G (2006) Rhythms of the brain. Oxford; New York: Oxford University Press.

Buzsaki G, Moser EI (2013) Memory, navigation and theta rhythm in the hippocampal-entorhinal system. Nature Neuroscience 16:130-138.

Chamberlain SEL, Yang J, Jones RSG (2008) The role of NMDA receptor subtypes in short-term plasticity in the rat entorhinal cortex. Neural plasticity 2008:13.

Chang H-R, Kuo C-C (2007) characterization of the gating conformational changes in the felbamate binding site in NMDA channels. Biophysical Journal 93:456-466.

Chiamulera C, Costa S, Reggiani A (1990) Effect of NMDA-insensitive and strynchnine-insensitive glycine site antagonists on NMDA-mediated convulsions and learning. Psychopharmacology 102:551-552.

Cho YH, Jaffard R (1995) Spatial location learning in mice with ibotenate lesions of entorhinal cortex or subiculum. Neurobiology of Learning and Memory 64:285-290.

Choquet D, Triller A (2003) The role of receptor diffusion in the organization of the postsynaptic membrane. Nat Rev Neurosci 4:251-265.

Clasadonte J, Haydon PG (2010) Astrocytes and epilepsy. Epilepsia 51:53-53.

Clements JD, Lester RAJ, Tong G, Jahr CE, Westbrook GL (1992) The time course of glutamate in the synaptic cleft. Science 258:1498-1501.

Cochilla AJ, Alford S (1999) NMDA receptor-mediated control of presynaptic calcium and neurotransmitter release. The Journal of Neuroscience 19:193-205.

Cohen-Gadol AA, Pan JW, Kim JH, Spencer DD, Hetherington HH (2004) Mesial temporal lobe epilepsy: a proton magnetic resonance spectroscopy study and a histopathological analysis. J Neurosurg 101:613-620.

Cohen I, Huberfeld G, Miles R (2006) Emergence of disinhibition-induced synchrony in the CA3 region of the guinea pig hippocampus in vitro. The Journal of Physiology 570:583-594.

Cohen I, Navarro V, Le Duigou C, Miles R (2003) Mesial temporal lobe epilepsy: A pathological replay of developmental mechanisms? Biol Cell 95:329-333.

Collingridge GL, Volianskis A, Bannister N, France G, Hanna L, Mercier M, Tidball P, Fang G, Irvine MW, Costa BM, Monaghan DT, Bortolotto ZA, Molnár E, Lodge D, Jane DE (2013) The NMDA receptor as a target for cognitive enhancement. Neuropharmacology 64:13-26.

Collins RC, Tearse RG, Lothman EW (1983) Functional-anatomy of limbic seizures - focal discharges from medial entorhinal cortex in rat. Brain Research 280:25-40.

Colquhoun D, Hatton CJ, Hawkes AG (2003) The quality of maximum likelihood estimates of ion channel rate constants. Journal of Physiology-London 547:699-728.

Colquhoun D, Lape R (2012) Allosteric coupling in ligand-gated ion channels. The Journal of General Physiology 140:599-612.

Corlew R, Wang Y, Ghermazien H, Erisir A, Philpot BD (2007) Developmental switch in the contribution of presynaptic and postsynaptic NMDA receptors to long-term depression. The Journal of Neuroscience 27:9835-9845.

De Bock M, Decrock E, Wang N, Bol M, Vinken M, Bultynck G, Leybaert L (2014) The dual face of connexin-based astroglial Ca^{2+} communication:

A key player in brain physiology and a prime target in pathology. Biochimica et Biophysica Acta (BBA) - Molecular Cell Research 1843:2211-2232.

De Sarro G, Gratteri S, Naccari F, Pasculli MP, De Sarro A (2000) Influence of d-cycloserine on the anticonvulsant activity of some antiepileptic drugs against audiogenic seizures in DBA/2 mice. Epilepsy Research 40:109-121.

DeBiasi S, Minelli A, Melone M, Conti F (1996) Presynaptic NMDA receptors in the neocortex are both auto- and heteroreceptors. Neuroreport 7:2773-2776.

Del Castillo J, Katz B (1954) Quantal components of the end-plate potential. The Journal of Physiology 124:560-573.

Del Castillo J, Katz B (1957) Interaction at end-plate receptors between different choline derivatives. Proceedings of the Royal Society Series B-Biological Sciences 146:369-380.

Deng Q, Terunuma M, Fellin T, Moss SJ, Haydon PG (2011) Astrocytic activation of A1 receptors regulates the surface expression of NMDA receptors through a Src kinase dependent pathway. Glia 59:1084-1093.

Dickerson BC, Eichenbaum H (2010) The episodic memory system: neurocircuitry and disorders. Neuropsychopharmacology 35:86-104.

Dravid SM, Burger PB, Prakash A, Geballe MT, Yadav R, Le P, Vellano K, Snyder JP, Traynelis SF (2010) Structural determinants of D-cycloserine dfficacy at the NR1/NR2C NMDA receptors. The Journal of Neuroscience 30:2741-2754.

Du F, Eid T, Lothman EW, Kohler C, Schwarcz R (1995) Preferential neuronal loss in layer-III of the medial entorhinal cortex in rat models of temporal-lobe epilepsy. Journal of Neuroscience 15:6301-6313.

Dudel J, Kuffler SW (1961) Presynaptic inhibition at the crayfish neuromuscular junction. The Journal of Physiology 155:543-562.

Duguid IC, Smart TG (2004) Retrograde activation of presynaptic NMDA receptors enhances GABA release at cerebellar interneuron-Purkinje cell synapses. Nat Neurosci 7:525-533.

Eccles JC (1964) Presynaptic inhibition in the spinal cord. Progr Brain Res 12:65-91.

Eichenbaum H (2001) The hippocampus and declarative memory: cognitive mechanisms and neural codes. Behavioural Brain Research 127:199-207.

Eichenbaum H, Cohen NJ (2014) Can we reconcile the declarative memory and spatial navigation views on hippocampal function? Neuron 83:764-770.

Evans DI, Jones RSG, Woodhall G (2000) Activation of presynaptic group III metabotropic receptors enhances glutamate release in rat entorhinal cortex.

Fantinato S, Pollegioni L, Pilone PS (2001) Engineering, expression and purification of a His-tagged chimeric D-amino acid oxidase from Rhodotorula gracilis. Enzyme Microb Technol 29:407-412.

Fellin T, Pascual O, Gobbo S, Pozzan T, Haydon PG, Carmignoto G (2004) Neuronal synchrony mediated by astrocytic glutamate through activation of extrasynaptic NMDA receptors. Neuron 43:729-743.

Fink K, Bönisch H, Göthert M (1990) Presynaptic NMDA receptors stimulate noradrenaline release in the cerebral cortex. European Journal of Pharmacology 185:115-117.

Fiszman ML, Barberis A, Lu C, Fu Z, Erdélyi F, Szabó G, Vicini S (2005) NMDA receptors increase the size of GABAergic terminals and enhance GABA release. The Journal of Neuroscience 25:2024-2031.

Flood JF, Morley JE, Lanthorn TH (1992) Effect of memory processing by D-cycloserine, an agonist of the NMDA glycine receptor. European Journal of Pharmacology 221:249-254.

Fong DK, Rao A, Crump FT, Craig AM (2002) Rapid synaptic remodeling by protein kinase C: reciprocal translocation of NMDA receptors and calcium/calmodulin-dependent kinase II. The Journal of Neuroscience 22:2153-2164.

Fossat P, Turpin FR, Sacchi S, Dulong J, Shi T, Rivet J-M, Sweedler JV, Pollegioni L, Millan MJ, Oliet SHR, Mothet J-P (2012) Glial D-serine gates NMDA receptors at excitatory synapses in prefrontal cortex. Cerebral Cortex 22:595-606.

Fourcaudot E, Gambino F, Casassus G, Poulain B, Humeau Y, Luthi A (2009) L-type voltage-dependent Ca2+ channels mediate expression of presynaptic LTP in amygdala. Nat Neurosci 12:1093-1095.

Fourcaudot E, Gambino F, Humeau Y, Casassus G, Shaban H, Poulain B, Lüthi A (2008) cAMP/PKA signaling and RIM1α mediate presynaptic LTP in the lateral amygdala. Proceedings of the National Academy of Sciences 105:15130-15135.

Fried I (1993) Anatomic temporal lobe resections for temporal lobe epilepsy. Neurosurgery clinics of North America 4:233-242.

Gazzaniga MS, Ivry RB, Mangun GR (2009) Cognitive neuroscience : the biology of the mind. New York: W.W. Norton.

Ghasemi M, Schachter SC (2011) The NMDA receptor complex as a therapeutic target in epilepsy: a review. Epilepsy & Behavior 22:617-640.

Gielen M, Retchless BS, Mony L, Johnson JW, Paoletti P (2009) Mechanism of differential control of NMDA receptor activity by NR2 subunits. Nature 459:703-707.

Glasier MM, Sutton RL, Stein DG (1995) Effects of unilateral entorhinal cortex lesion and ganglioside GM1 treatment on performance in a novel water maze task. Neurobiology of Learning and Memory 64:203-214.

Glitsch MD (2008) Calcium influx through N-methyl-d-aspartate receptors triggers GABA release at interneuron–Purkinje cell synapse in rat cerebellum. Neuroscience 151:403-409.

Goff DC (2012) D-cycloserine: an evolving role in learning and neuroplasticity in schizophrenia. Schizophrenia Bulletin 38:936-941.

Goldring S, Edwards I, Harding GW, Bernardo KL (1992) Results of anterior temporal lobectomy that spares the amygdala in patients with complex partial seizures. J Neurosurg 77:185-193.

Goldring S, Edwards I, Harding GW, Bernardo KL (1993) Temporal lobectomy that spares the amygdala for temporal lobe epilepsy. Neurosurgery clinics of North America 4:263-272.

Gomez-Gonzalo M, Losi G, Chiavegato A, Zonta M, Cammarota M, Brondi M, Vetri F, Uva L, Pozzan T, de Curtis M, Ratto GM, Carmignoto G (2010)

An excitatory loop with astrocytes contributes to drive neurons to seizure threshold. PLoS Biol 8.

Greenhill SD, Chamberlain SEL, Lench A, Massey PV, Yuill KH, Woodhall GL, Jones RSG (2014) Background synaptic activity in rat entorhinal cortex shows a progressively greater dominance of inhibition over excitation from deep to superficial layers. Plos One 9.

Groc L, Choquet D, Stephenson FA, Verrier D, Manzoni OJ, Chavis P (2007) NMDA receptor surface trafficking and synaptic subunit composition are developmentally regulated by the extracellular matrix protein reelin. The Journal of Neuroscience 27:10165-10175.

Groc L, Heine M, Cognet L, Brickley K, Stephenson FA, Lounis B, Choquet D (2004) Differential activity-dependent regulation of the lateral mobilities of AMPA and NMDA receptors. Nat Neurosci 7:695-696.

Groc L, Heine M, Cousins SL, Stephenson FA, Lounis B, Cognet L, Choquet D (2006) NMDA receptor surface mobility depends on NR2A-2B subunits. Proceedings of the National Academy of Sciences 103:18769-18774.

Hafting T, Fyhn M, Molden S, Moser MB, Moser EI (2005) Microstructure of a spatial map in the entorhinal cortex. Nature 436:801-806.

Hansen Kasper B, Ogden Kevin K, Yuan H, Traynelis Stephen F (2014) Distinct functional and pharmacological properties of triheteromeric GluN1/GluN2A/GluN2B NMDA receptors. Neuron 81:1084-1096.

Hashimoto A, Nishikawa T, Oka T, Takahashi K (1993) Endogenous D-serine in the rat brain: N-methyl-D-aspartate receptor-related distribution and aging. Journal of Neurochemistry 60:783-786.

Hassel B, Bachelard H, Jones P, Fonnum F, Sonnewald U (1997) Trafficking of amino acids between neurons and glia in vivo: Effects of inhibition of glial metabolism by fluoroacetate. J Cereb Blood Flow Metab 17:1230-1238.

Hertz L, Dringen R, Schousboe A, Robinson SR (1999) Astrocytes: Glutamate producers for neurons. Journal of Neuroscience Research 57:417-428.

Heuser JE, Reese TS, Dennis MJ, Jan Y, Jan L, Evans L (1979) Synaptic vesicle exocytosis captured by quick freezing and correlated with quantal transmitter release. Journal of Cell Biology 81:275-300.

Hofmann SG, Meuret AE, Smits JJ, et al. (2006) Augmentation of exposure therapy with d-cycloserine for social anxiety disorder. Archives of General Psychiatry 63:298-304.

Hofmann SG, Smits JAJ, Rosenfield D, Simon N, Otto MW, Meuret AE, Marques L, Fang A, Tart C, Pollack MH (2013) D-cycloserine as an augmentation strategy with cognitive-behavioral therapy for social anxiety disorder. Am J Psychiat 170:751-758.

Humeau Y, Shaban H, Bissiere S, Luthi A (2003) Presynaptic induction of heterosynaptic associative plasticity in the mammalian brain. Nature 426:841-845.

Hwang TJ, Wares DF, Jafarov A, Jakubowiak W, Nunn P, Keshavjee S (2013) Safety of cycloserine and terizidone for the treatment of drug-resistant tuberculosis: a meta-analysis [Review article]. The International Journal of Tuberculosis and Lung Disease 17:1257-1266.

Inanobe A, Furukawa H, Gouaux E (2005) Mechanism of partial sgonist sction at the NR1 subunit of NMDA receptors. Neuron 47:71-84.

Job V, Molla G, Pilone MS, Pollegioni L (2002) Overexpression of a recombinant wild-type and His-tagged Bacillus subtilis glycine oxidase in Escherichia coli. European Journal of Biochemistry 269:1456-1463.

Johnson KM, Jeng YJ (1991) Pharmacological evidence for N-methyl-D-aspartate receptors on nigrostriatal dopaminergic nerve-terminals. Canadian Journal of Physiology and Pharmacology 69:1416-1421.

Jones RS, Heinemann U (1988) Synaptic and intrinsic responses of medical entorhinal cortical cells in normal and magnesium-free medium in vitro.

Jones RSG, Lambert JDC (1990) The role of excitatory amino-acid receptors in the propagation of epileptiform discharges from the entorhinal cortex to the dentate gyrus in vitro. Exp Brain Res 80:310-322.

Jones RSG, Woodhall GL (2005) Background synaptic activity in rat entorhinal cortical neurones: differential control of transmitter release by presynaptic receptors. The Journal of Physiology 562:107-120.

Jourdain P, Bergersen LH, Bhaukaurally K, Bezzi P, Santello M, Domercq M, Matute C, Tonello F, Gundersen V, Volterra A (2007) Glutamate

exocytosis from astrocytes controls synaptic strength. Nat Neurosci 10:331-339.

Karakas E, Simorowski N, Furukawa H (2011) Subunit arrangement and phenylethanolamine binding in GluN1/GluN2B NMDA receptors. Nature 475:249-253.

Kartvelishvily E, Shleper M, Balan L, Dumin E, Wolosker H (2006) Neuron-derived D-serine release provides a novel means to activate N-Methyl-D-aspartate receptors. Journal of Biological Chemistry 281:14151-14162.

Kopniczky Z, Dochnal R, Macsai M, Pal A, Kiss G, Mihaly A, Szabo G (2006) Alterations of behavior and spatial learning after unilateral entorhinal ablation of rats. Life Sciences 78:2683-2688.

Krebs MO, Desce JM, Kemel ML, Gauchy C, Godeheu G, Cheramy A, Glowinski J (1991) Glutamatergic control of dopamine release in the rat striatum - evidence for presynaptic N-methyl-D-aspartate receptors on dopaminergic nerve terminals. Journal of Neurochemistry 56:81-85.

Kunz PA, Roberts AC, Philpot BD (2013) Presynaptic NMDA receptor mechanisms for enhancing spontaneous neurotransmitter release. The Journal of Neuroscience 33:7762-7769.

Kussius CL, Popescu GK (2009) Kinetic basis of partial agonism at NMDA receptors. Nat Neurosci 12:1114-1120.

Lalo U, Pankratov Y, Kirchhoff F, North RA, Verkhratsky A (2006) NMDA receptors mediate neuron-to-glia signaling in mouse cortical astrocytes. The Journal of Neuroscience 26:2673-2683.

Lape R, Colquhoun D, Sivilotti LG (2008) On the nature of partial agonism in the nicotinic receptor superfamily. Nature 454:722-727.

Larsen RS, Corlew RJ, Henson MA, Roberts AC, Mishina M, Watanabe M, Lipton SA, Nakanishi N, Perez-Otano I, Weinberg RJ, Philpot BD (2011) NR3A-containing NMDARs promote neurotransmitter release and spike timing-dependent plasticity. Nat Neurosci 14:338-344.

Lau CG, Zukin RS (2007) NMDA receptor trafficking in synaptic plasticity and neuropsychiatric disorders. Nat Rev Neurosci 8:413-426.

Le Bail M, Martineau M, Sacchi S, Yatsenko N, Radzishevsky I, Conrod S, Ait Ouares K, Wolosker H, Pollegioni L, Billard J-M, Mothet J-P (2015)

Identity of the NMDA receptor coagonist is synapse specific and developmentally regulated in the hippocampus. Proceedings of the National Academy of Sciences 112:E204-E213.

Lee C-H, Gouaux E (2011) Amino terminal domains of the NMDA receptor are organized as local heterodimers. Plos One 6.

Lester RAJ, Clements JD, Westbrook GL, Jahr CE (1990) Channel kinetics determine the time course of NMDA receptor-mediated synaptic currents. Nature 346:565-567.

Li Y-H, Han T-Z (2007) Glycine binding sites of presynaptic NMDA receptors may tonically regulate glutamate release in the rat visual cortex.

Li Y-H, Wang J, Zhang G (2009) Presynaptic NR2B-containing NMDA autoreceptors mediate glutamatergic synaptic transmission in the rat visual cortex. Current Neurovascular Research 6:104-109.

Liu H, Wang H, Sheng M, Jan LY, Jan YN, Basbaum AI (1994) Evidence for presynaptic N-methyl-D-aspartate autoreceptors in the spinal-cord dorsal horn. Proceedings of the National Academy of Sciences of the United States of America 91:8383-8387.

Loescher W, Wlaz P, Rundfeldt C, Baran H, Honack D (1994) Anticonvulsant effects of the glycine/NMDA receptor ligands D-cycloserine and D-serine but not R-(+)-HA-966 in amygdala-kindled rats. British Journal of Pharmacology 112:97-106.

Lopantsev V, Avoli M (1998) Laminar organization of epileptiform discharges in the rat entorhinal cortex in vitro. The Journal of Physiology 509:785-796.

Maass A, Schuetze H, Speck O, Yonelinas A, Tempelmann C, Heinze H-J, Berron D, Cardenas-Blanco A, Brodersen KH, Stephan KE, Duezel E (2014) Laminar activity in the hippocampus and entorhinal cortex related to novelty and episodic encoding. Nature Communications 5.

Mameli M, Carta M, Partridge LD, Valenzuela CF (2005) Neurosteroid-induced plasticity of immature synapses via retrograde modulation of presynaptic NMDA receptors. The Journal of Neuroscience 25:2285-2294.

Martineau M, Shi T, Puyal J, Knolhoff AM, Dulong J, Gasnier B, Klingauf J, Sweedler JV, Jahn R, Mothet J-P (2013) Storage and uptake of D-serine

into astrocytic synaptic-like vesicles specify gliotransmission. The Journal of Neuroscience 33:3413-3423.

Mayer ML, Westbrook GL (1987) Permeation and block of N-methyl-D-aspartic acid receptor channels by divalent cations in mouse cultured central neurones. The Journal of Physiology 394:501-527.

McGuinness L, Taylor C, Taylor RDT, Yau C, Langenhan T, Hart ML, Christian H, Tynan PW, Donnelly P, Emptage NJ (2010) Presynaptic NMDARs in the hippocampus facilitate transmitter release at theta frequency. Neuron 68:1109-1127.

Menendez de la Prida L, Huberfeld G, Cohen I, Miles R (2006) Threshold behavior in the initiation of hippocampal population bursts. Neuron 49:131-142.

Milivojevic B, Doeller CF (2013) Mnemonic networks in the hippocampal formation: from spatial maps to temporal and conceptual codes. Journal of Experimental Psychology-General 142:1231-1241.

Miya K, Inoue R, Takata Y, Abe M, Natsume R, Sakimura K, Hongou K, Miyawaki T, Mori H (2008) Serine racemase is predominantly localized in neurons in mouse brain. The Journal of Comparative Neurology 510:641-654.

Monahan JB, Handelmann GE, Hood WF, Cordi AA (1989) D-cycloserine, a positive modulator of the N-methyl-D-aspartate receptor, enhances performance of learning tasks in rats. Pharmacology Biochemistry and Behavior 34:649-653.

Mony L, Zhu SJ, Carvalho S, Paoletti P (2011) Molecular basis of positive allosteric modulation of GluN2B NMDA receptors by polyamines. Embo J 30:3134-3146.

Morley RM, Tse H-W, Feng B, Miller JC, Monaghan DT, Jane DE (2005) Synthesis and pharmacology of N1-substituted piperazine-2,3-dicarboxylic acid derivatives acting as NMDA receptor antagonists. Journal of Medicinal Chemistry 48:2627-2637.

Moskal JR, Kuo AG, Weiss C, Wood PL, O'Connor Hanson A, Kelso S, Harris RB, Disterhoft JF (2005) GLYX-13: A monoclonal antibody-derived

peptide that acts as an N-methyl-d-aspartate receptor modulator. Neuropharmacology 49:1077-1087.

Mothet J-P, Pollegioni L, Ouanounou G, Martineau M, Fossier P, Baux G (2005) Glutamate receptor activation triggers a calcium-dependent and SNARE protein-dependent release of the gliotransmitter D-serine. Proceedings of the National Academy of Sciences of the United States of America 102:5606-5611.

Myers KM, Carlezon Jr WA (2012) D-Cycloserine effects on extinction of conditioned responses to drug-related cues. Biological Psychiatry 71:947-955.

Nadkarni S, Jung P, Levine H (2008) Astrocytes optimize the synaptic transmission of information. PLoS Comput Biol 4.

Nevian T, Sakmann B (2006) Spine Ca2+ signaling in spike-timing-dependent plasticity. The Journal of Neuroscience 26:11001-11013.

Norberg MM, Krystal JH, Tolin DF (2008) A meta-analysis of D-cycloserine and the facilitation of fear extinction and exposure therapy. Biological Psychiatry 63:1118-1126.

Ogden KK, Khatri A, Traynelis SF, Heldt SA (2014) Potentiation of GluN2C/D NMDA receptor subtypes in the amygdala facilitates the retention of fear and extinction learning in mice. Neuropsychopharmacology 39:625-637.

Okeefe J (1976) Place units in hippocampus of freely moving rat. Experimental Neurology 51:78-109.

Paganelli MA, Kussius CL, Popescu GK (2013) Role of cross-cleft contacts in NMDA receptor gating. Plos One 8.

Palygin O, Lalo U, Verkhratsky A, Pankratov Y (2010) Ionotropic NMDA and P2X1/5 receptors mediate synaptically induced Ca2+ signalling in cortical astrocytes. Cell Calcium 48:225-231.

Panatier A, Theodosis DT, Mothet J-P, Touquet B, Pollegioni L, Poulain DA, Oliet SHR (2006) Glia-derived D-serine controls NMDA receptor activity and synaptic memory. Cell 125:775-784.

Panatier A, Vallée J, Haber M, Murai Keith K, Lacaille J-C, Robitaille R (2011) Astrocytes are endogenous regulators of basal transmission at central synapses. Cell 146:785-798.

Panizzutti R, De Miranda J, Ribeiro CS, Engelender S, Wolosker H (2001) A new strategy to decrease N-methyl-d-aspartate (NMDA) receptor coactivation: Inhibition of d-serine synthesis by converting serine racemase into an eliminase. Proceedings of the National Academy of Sciences 98:5294-5299.

Paoletti P (2011) Molecular basis of NMDA receptor functional diversity. European Journal of Neuroscience 33:1351-1365.

Papouin T, Ladépêche L, Ruel J, Sacchi S, Labasque M, Hanini M, Groc L, Pollegioni L, Mothet J-P, Oliet Stéphane HR (2012) Synaptic and extrasynaptic NMDA receptors are gated by different endogenous coagonists. Cell 150:633-646.

Parpura V, Verkhratsky A (2013) Astroglial amino acid-based transmitter receptors. Amino Acids 44:1151-1158.

Parri HR, Crunelli V (2003) The role of Ca2+ in the generation of spontaneous astrocytic Ca2+ oscillations. Neuroscience 120:979-992.

Parsons C, Danysz W, Dekundy A, Pulte I (2013) Memantine and cholinesterase inhibitors: complementary mechanisms in the treatment of Alzheimer's disease. Neurotox Res 24:358-369.

Pascual O, Casper KB, Kubera C, Zhang J, Revilla-Sanchez R, Sul J-Y, Takano H, Moss SJ, McCarthy K, Haydon PG (2005) Astrocytic purinergic signaling coordinates synaptic networks. Science 310:113-116.

Paulsen RE, Contestabile A, Villani L, Fonnum F (1987) An in vivo model for studying function of brain-tissue temporarily devoid of glial-cell metabolism - the use of fluorocitrate. Journal of Neurochemistry 48:1377-1385.

Peeters B, Vanderheyden PML (1992) In vitro and in vivo characterization of the NMDA receptor-linked strychnine-insensitive glycine site. Epilepsy Research 12:157-162.

Perea G, Araque A (2005) Glial calcium signaling and neuron–glia communication. Cell Calcium 38:375-382.

Perea G, Sur M, Araque A (2014) Neuron-glia networks: Integral gear of brain function. Frontiers in Cellular Neuroscience 8.

Pinsky PF, Rinzel J (1994) Intrinsic and network rhythmogenesis in a reduced Traub model for CA3 neurons. J Comput Neurosci 1:39-60.

Pittaluga A, Raiteri M (1992) N-methyl-D-aspartic acid (NMDA) and non-NMDA receptors regulating hippocampal norepinephrine release. I. Location on axon terminals and pharmacological characterization. Journal of Pharmacology and Experimental Therapeutics 260:232-237.

Popescu G, Auerbach A (2003) Modal gating of NMDA receptors and the shape of their synaptic response. Nat Neurosci 6:476-483.

Prasad KMR, Patel AR, Muddasani S, Sweeney J, Keshavan MS (2004) The entorhinal cortex in first-episode psychotic disorders: A structural magnetic resonance imaging study. Am J Psychiat 161:1612-1619.

Priestley T, Kemp JA (1994) Kinetic study of the interactions between the glutamate and glycine recognition sites on the N-methyl-D-aspartic acid receptor complex. Molecular Pharmacology 46:1191-1196.

Quartermain D, Mower J, Rafferty MF, Herting RL, Lanthorn TH (1994) Acute but not chronic activation of the NMDA-coupled glycine receptor with D-cycloserine facilitates learning and retention. European Journal of Pharmacology 257:7-12.

Ranganath C, Yonelinas AP, Cohen MX, Dy CJ, Tom SM, D'Esposito M (2004) Dissociable correlates of recollection and familiarity within the medial temporal lobes. Neuropsychologia 42:2-13.

Rauner C, Köhr G (2011) Triheteromeric NR1/NR2A/NR2B receptors constitute the major N-Methyl-d-aspartate receptor population in adult hippocampal synapses. Journal of Biological Chemistry 286:7558-7566.

Retchless BS, Gao W, Johnson JW (2012) A single GluN2 subunit residue controls NMDA receptor channel properties via intersubunit interaction. Nat Neurosci 15:406-413.

Riou M, Stroebel D, Edwardson JM, Paoletti P (2012) An alternating GluN1-2-1-2 subunit arrangement in mature NMDA receptors. Plos One 7.

Rodrigues H, Figueira I, Lopes A, Goncalves R, Mendlowicz MV, Coutinho ESF, Ventura P (2014) Does D-cycloserine enhance exposure therapy for anxiety disorders in humans? A meta-analysis. Plos One 9.

Rodríguez-Moreno A, Kohl MM, Reeve JE, Eaton TR, Collins HA, Anderson HL, Paulsen O (2011) Presynaptic induction and expression of timing-dependent long-term depression demonstrated by compartment-specific photorelease of a use-dependent NMDA receptor antagonist. The Journal of Neuroscience 31:8564-8569.

Rodriguez-Moreno A, Paulsen O (2008) Spike timing-dependent long-term depression requires presynaptic NMDA receptors. Nat Neurosci 11:744-745.

Roof RL, Zhang Q, Glasier MM, Stein DG (1993) Gender-specific impairment on morris water maze task after entorhinal cortex lesion. Behavioural Brain Research 57:47-51.

Rossi B, Ogden D, Llano I, Tan YP, Marty A, Collin T (2012) Current and calcium responses to local activation of axonal NMDA receptors in developing cerebellar molecular layer interneurons. Plos One 7.

Sacchi S, Caldinelli L, Cappelletti P, Pollegioni L, Molla G (2012) Structure-function relationships in human d-amino acid oxidase. Amino Acids 43:1833-1850.

Salussolia Catherine L, Wollmuth Lonnie P (2012) Flip-flopping to the membrane. Neuron 76:463-465.

Santello M, Bezzi P, Volterra A (2011) TNFα controls glutamatergic gliotransmission in the hippocampal dentate gyrus. Neuron 69:988-1001.

Santello M, Calì C, Bezzi P (2012) Gliotransmission and the tripartite synapse. In: Synaptic Plasticity, vol. 970 (Kreutz, M. R. and Sala, C., eds), pp 307-331: Springer Vienna.

Sanz-Clemente A, Nicoll RA, Roche KW (2013) Diversity in NMDA receptor composition: many regulators, many consequences. The Neuroscientist 19:62-75.

Scharfman HE (2007) The neurobiology of epilepsy. Curr Neurol Neurosci Rep 7:348-354.

Schorge S, Colquhoun D (2003) Studies of NMDA receptor function and stoichiometry with truncated and tandem subunits. Journal of Neuroscience 23:1151-1158.

Serrano A, Haddjeri N, Lacaille J-C, Robitaille R (2006) GABAergic network activation of glial cells underlies hippocampal heterosynaptic depression. The Journal of Neuroscience 26:5370-5382.

Shapiro LA, Wang L, Ribak CE (2008) Rapid astrocyte and microglial activation following pilocarpine-induced seizures in rats. Epilepsia 49:33-41.

Sheinin A, Shavit S, Benveniste M (2001) Subunit specificity and mechanism of action of NMDA partial agonist d-cycloserine. Neuropharmacology 41:151-158.

Shigeri Y, Seal RP, Shimamoto K (2004) Molecular pharmacology of glutamate transporters, EAATs and VGLUTs. Brain Research Reviews 45:250-265.

Shigetomi E, Bowser DN, Sofroniew MV, Khakh BS (2008) Two forms of astrocyte calcium excitability have distinct effects on NMDA receptor-mediated slow inward currents in pyramidal neurons. The Journal of Neuroscience 28:6659-6663.

Siegel AM, Wieser HG, Wichmann W, Yasargil GM (1990) Relationships between MR-imaged total amount of tissue removed, resection scores of specific mediobasal limbic subcompartments and clinical outcome following selective amygdalohippocampectomy. Epilepsy Research 6:56-65.

Siegel SJ, Brose N, Janssen WG, Gasic GP, Jahn R, Heinemann SF, Morrison JH (1994) Regional, cellular, and ultrastructural distribution of N-methyl-D-aspartate receptor subunit-1 in monkey hippocampus. Proceedings of the National Academy of Sciences of the United States of America 91:564-568.

Singh L, Oles RJ, Tricklebank MD (1990) Modulation of seizure susceptibility in the mouse by the strychnine-insensitive glycine recognition site of the NMDA receptor ion channel complex. British Journal of Pharmacology 99:285-288.

Sjöström PJ, Turrigiano GG, Nelson SB (2003) Neocortical LTD via coincident activation of presynaptic NMDA and cannabinoid receptors. Neuron 39:641-654.

Sloviter RS, Zappone CA, Harvey BD, Frotscher M (2006) Kainic acid-induced recurrent mossy fiber innervation of dentate gyrus inhibitory

interneurons: Possible anatomical substrate of granule cell hyperinhibition in chronically epileptic rats. The Journal of Comparative Neurology 494:944-960.

Sobolevsky AI, Rosconi MP, Gouaux E (2009) X-ray structure, symmetry and mechanism of an AMPA-subtype glutamate receptor. Nature 462:745-756.

Sperling MR, Oconnor MJ, Saykin AJ, Plummer C (1996) Temporal lobectomy for refractory epilepsy. JAMA-J Am Med Assoc 276:470-475.

Squire LR, Stark CEL, Clark RE (2004) The medial temporal lobe. Annu Rev Neurosci 27:279-306.

Stranahan AM, Mattson MP (2010) Selective vulnerability of neurons in layer II of the entorhinal cortex during aging and Alzheimer's disease. Neural plasticity 2010:108190.

Stringer JL (1994) Pentylenetetrazol elicits epileptiform activity in the dentate gyrus of the urethane-anesthetized rat by activation of the entorhinal cortex. Brain Research 636:221-226.

Suárez LM, Solís JM (2006) Taurine potentiates presynaptic NMDA receptors in hippocampal Schaffer collateral axons. European Journal of Neuroscience 24:405-418.

Subramaniam S, Rho JM, Penix L, Donevan SD, Fielding RP, Rogawski MA (1995) Felbamate block of the N-methyl-D-aspartate receptor. Journal of Pharmacology and Experimental Therapeutics 273:878-886.

Thom M, Liagkouras I, Elliot KJ, Martinian L, Harkness W, McEvoy A, Caboclo LO, Sisodiya SM (2010) Reliability of patterns of hippocampal sclerosis as predictors of postsurgical outcome. Epilepsia 51:1801-1808.

Tian G-F, Azmi H, Takano T, Xu Q, Peng W, Lin J, Oberheim N, Lou N, Wang X, Zielke HR, Kang J, Nedergaard M (2005) An astrocytic basis of epilepsy. Nat Med 11:973-981.

Tomek S, Lacrosse A, Nemirovsky N, Olive M (2013) NMDA receptor modulators in the treatment of drug addiction. Pharmaceuticals 6:251-268.

Tovar KR, McGinley MJ, Westbrook GL (2013) Triheteromeric NMDA receptors at hippocampal synapses. The Journal of Neuroscience 33:9150-9160.

Tovar KR, Westbrook GL (2002) Mobile NMDA receptors at hippocampal synapses. Neuron 34:255-264.

Traub RD, Miles R, Jefferys JG (1993) Synaptic and intrinsic conductances shape picrotoxin-induced synchronized after-discharges in the guinea-pig hippocampal slice. The Journal of Physiology 461:525-547.

Turpin FR, Potier B, Dulong JR, Sinet PM, Alliot J, Oliet SHR, Dutar P, Epelbaum J, Mothet JP, Billard JM (2011) Reduced serine racemase expression contributes to age-related deficits in hippocampal cognitive function. Neurobiology of Aging 32:1495-1504.

van Haeften T, Baks-te-Bulte LN, Goede PH, Wouterlood FG, Witter MP (2003) Morphological and numerical analysis of synaptic interactions between neurons in deep and superficial layers of the entorhinal cortex of the rat. Hippocampus 13:943-952.

van Strien NM, Cappaert NLM, Witter MP (2009) The anatomy of memory: an interactive overview of the parahippocampal-hippocampal network. Nature Reviews Neuroscience 10:272-282.

Vicini S, Wang JF, Li JH, Zhu WJ, Wang YH, Luo JH, Wolfe BB, Grayson DR (1998) Functional and pharmacological differences between recombinant N-Methyl-d-Aspartate receptors.

Wang JKT (1991) Presynaptic glutamate receptors modulate dopamine release from striatal synaptosomes. Journal of Neurochemistry 57:819-822.

Wang XJ (2010) Neurophysiological and Computational Principles of Cortical Rhythms in Cognition. Physiol Rev 90:1195-1268.

Waniewski RA, Martin DL (1998) Preferential utilization of acetate by astrocytes is attributable to transport. The Journal of Neuroscience 18:5225-5233.

White SH, Harmsworth WL, Sofia DR, Wolf HH (1995) Felbamate modulates the strychnine-insensitive glycine receptor. Epilepsy Research 20:41-48.

Williams SM, Diaz CM, Macnab LT, Sullivan RKP, Pow DV (2006) Immunocytochemical analysis of D-serine distribution in the mammalian

brain reveals novel anatomical compartmentalizations in glia and neurons. Glia 53:401-411.

Wlaź P (1998) Anti-convulsant and adverse effects of the glycineB receptor ligands, D-cycloserine and L-701,324: comparison with competitive and non-competitive N-methyl-D-aspartate receptor antagonists. Brain Research Bulletin 46:535-540.

Wlaz P, Baran H, Loscher W (1994) Effect of the glycine/NMDA receptor partial agonist, D-cycloserine, on seizure threshold and some pharmacodynamic effects of MK-801 in mice. European Journal of Pharmacology 257:217-225.

Wlaz P, Poleszak E (2011) Differential effects of glycine on the anticonvulsant activity of D-cycloserine and L-701,324 in mice. Pharmacol Rep 63:1231-1234.

Wolosker H, Radzishevsky I (2013) The serine shuttle between glia and neurons: implications for neurotransmission and neurodegeneration. Biochemical Society Transactions 41:1546-1550.

Wolosker H, Sheth KN, Takahashi M, Mothet J-P, Brady RO, Ferris CD, Snyder SH (1999) Purification of serine racemase: Biosynthesis of the neuromodulator d-serine. Proceedings of the National Academy of Sciences 96:721-725.

Woodhall G, Evans DI, Cunningham MO, Jones RSG (2001) NR2B-containing NMDA autoreceptors at synapses on entorhinal cortical neurons.

Wu H-Q, Lee S-C, Scharfman HE, Schwarcz R (2002) l-4-Chlorokynurenine attenuates kainate-induced seizures and lesions in the rat. Experimental Neurology 177:222-232.

Wyllie DJA, Livesey MR, Hardingham GE (2013) Influence of GluN2 subunit identity on NMDA receptor function. Neuropharmacology 74:4-17.

Yang J, Chamberlain SEL, Woodhall GL, Jones RSG (2008) Mobility of NMDA autoreceptors but not postsynaptic receptors at glutamate synapses in the rat entorhinal cortex. The Journal of Physiology 586:4905-4924.

Yang J, Wetterstrand C, Jones RSG (2007) Felbamate but not phenytoin or gabapentin reduces glutamate release by blocking presynaptic NMDA receptors in the entorhinal cortex. Epilepsy Research 77:157-164.

Yang J, Woodhall GL, Jones RSG (2006) Tonic facilitation of glutamate release by presynaptic NR2B-containing NMDA receptors is increased in the entorhinal cortex of chronically epileptic rats. The Journal of Neuroscience 26:406-410.

Yilmazer-Hanke DM, Wolf HK, Schramm J, Elger CE, Wiestler OD, Blumcke I (2000) Subregional pathology of the amygdala complex and entorhinal region in surgical specimens from patients with pharmacoresistant temporal lobe epilepsy. Journal of Neuropathology and Experimental Neurology 59:907-920.

Yuan H, Hansen KB, Vance KM, Ogden KK, Traynelis SF (2009) Control of NMDA receptor function by the NR2 subunit amino-terminal domain. The Journal of Neuroscience 29:12045-12058.

Zhang DX, Williamson JM, Wu H-Q, Schwarcz R, Bertram EH (2005) In situ–produced 7-chlorokynurenate has different effects on evoked responses in rats with limbic epilepsy in comparison to naive controls. Epilepsia 46:1708-1715.

Zhang J-m, Wang H-k, Ye C-q, Ge W, Chen Y, Jiang Z-l, Wu C-p, Poo M-m, Duan S (2003) ATP released by astrocytes mediates glutamatergic activity-dependent heterosynaptic suppression. Neuron 40:971-982.

Zhang W, Howe JR, Popescu GK (2008) Distinct gating modes determine the biphasic relaxation of NMDA receptor currents. Nat Neurosci 11:1373-1375.

Zhou X, Chen Z, Yun W, Ren J, Li C, Wang H (2014) Extrasynaptic NMDA receptor in excitotoxicity: function revisited. The Neuroscientist.

Zolamorgan S, Squire LR, Clower RP, Rempel NL (1993) Damage to the perirhinal cortex exacerbates memory impairment following lesions to the hippocampal-formation. Journal of Neuroscience 13:251-265.

Zorec R, Araque A, Carmignoto G, Haydon PG, Verkhratsky A, Parpura V (2012) Astroglial excitability and gliotransmission: an appraisal of Ca2+ as a signalling route. ASN Neuro 4.

Publications

Conference abstracts

Robson, E., Lench, AM, Jones RSG. (2015) Functional presynaptic kainate receptors in layer II and V of the rat entorhinal cortex. To be presented at BNA 2015, Edinburgh, April 2015

Lench AM, Massey PV, Jones RSG. (2014) D-Cycloserine acts to selectively affect kinetics of evoked NMDA responses in the rat entorhinal cortex. Presented at SfN, Washington, November 2014

Lench AM, Massey PV, Jones RSG. (2014). Effects of partial agonists of the coagonist binding site on postsynaptic NMDAr in rat entorhinal cortex. Presented at FENS, Milan July 2014.

Lench AM, Massey PV, Jones RSG. (2013) D-serine is an endogenous coagonist at presynaptic NMDA receptors in the rat entorhinal cortex. Proc. BNA meeting, London, April 2013

Massey PV, Lench AM, Jones RSG. (2013). GluK1 kainate receptors play a key role in seizure-like activity in the entorhinal cortex of organotypic brain slices Proc BNA, London, April 2013.

Massey PV, Carpenter J, Lench AM, Jones RSG. (2013) AED sensitivity in a novel model of acquired epilepsy in organotypic entorhinal-hippocampal slices. Proc BPS http://www.pa2online.org/abstract/abstract.jsp?abid=31231&author=lench&cat=-1&period=55

Lench AM, Massey PV, Jones RSG. (2013) Astrocytic D-serine is the co-agonist for presynaptic NMDA receptors in the rat entorhinal cortex. Proc BPS. http://www.pa2online.org/abstract/abstract.jsp?abid=31186&author=lench&cat=-1&period=55

Massey PV, Lench AM, Jones RSG. (2012) An in vitro chronic model of epilepsy in organotypic brain slice cultures of the rat entorhinal cortex. Proc. BPS. http://www.pa2online.org/abstract/abstract.jsp?abid=30815&author=lench&cat=-1&period=52

Massey PV, Lench AM, Jones RSG. (2012) Seizure-like activity in the entorhinal cortex of organotypic brain slices requires NMDA and GluK1 kainate receptors. Proc. BPS. http://www.pa2online.org/abstract/abstract.jsp?abid=30867&author=lench&cat=-1&period=52

Grandjean T, Lench AM, JWT, Chappell MJ, O'Donnell CJ. (2010). Experimental and Mathematical Analysis of Hepatic Uptake. Presented at the 8th CESPT Satellite Symposium: 4th International Graz Congress on Pharmaceutical Engineering, Graz August 2010.

Lench AM, Chamberlain SEL, Wonnacott, S, Jones RSG. (2008) α7-nicotinic acetylcholine receptors facilitate spontaneous glutamate release in the rat prefrontal cortex. Proc. BPS http://www.pa2online.org/abstract/abstract.jsp?abid=29149&author=lench&cat=-1&period=-1

OPEN ACCESS Freely available online

PLOS ONE

Background Synaptic Activity in Rat Entorhinal Cortex Shows a Progressively Greater Dominance of Inhibition over Excitation from Deep to Superficial Layers

Stuart David Greenhill[1¤a], Sophie Elizabeth Lyn Chamberlain[1¤b], Alex Lench[1], Peter Vernon Massey[1], Kathryn Heather Yuill[3], Gavin Lawrence Woodhall[2], Roland Spencer Gwynne Jones[1]*

1 Department of Pharmacy and Pharmacology, University of Bath, Claverton Down, Bath, United Kingdom, **2** Aston Brain Centre, School of Life and Health Sciences, Aston University, Birmingham, United Kingdom, **3** School of Biomedical & Healthcare Sciences, Plymouth University Peninsula Schools of Medicine and Dentistry, Plymouth, United Kingdom

Abstract

The entorhinal cortex (EC) controls hippocampal input and output, playing major roles in memory and spatial navigation. Different layers of the EC subserve different functions and a number of studies have compared properties of neurones across layers. We have studied synaptic inhibition and excitation in EC neurones, and we have previously compared spontaneous synaptic release of glutamate and GABA using patch clamp recordings of synaptic currents in principal neurones of layers II (L2) and V (L5). Here, we add comparative studies in layer III (L3). Such studies essentially look at neuronal activity from a presynaptic viewpoint. To correlate this with the postsynaptic consequences of spontaneous transmitter release, we have determined global postsynaptic conductances mediated by the two transmitters, using a method to estimate conductances from membrane potential fluctuations. We have previously presented some of this data for L3 and now extend to L2 and L5. Inhibition dominates excitation in all layers but the ratio follows a clear rank order (highest to lowest) of L2>L3>L5. The variance of the background conductances was markedly higher for excitation and inhibition in L2 compared to L3 or L5. We also show that induction of synchronized network epileptiform activity by blockade of GABA inhibition reveals a relative reluctance of L2 to participate in such activity. This was associated with maintenance of a dominant background inhibition in L2, whereas in L3 and L5 the absolute level of inhibition fell below that of excitation, coincident with the appearance of synchronized discharges. Further experiments identified potential roles for competition for bicuculline by ambient GABA at the $GABA_A$ receptor, and strychnine-sensitive glycine receptors in residual inhibition in L2. We discuss our results in terms of control of excitability in neuronal subpopulations of EC neurones and what these may suggest for their functional roles.

Citation: Greenhill SD, Chamberlain SEL, Lench A, Massey PV, Yuill KH, et al. (2014) Background Synaptic Activity in Rat Entorhinal Cortex Shows a Progressively Greater Dominance of Inhibition over Excitation from Deep to Superficial Layers. PLoS ONE 9(1): e85125. doi:10.1371/journal.pone.0085125

Editor: Clayton T. Dickson, University of Alberta, Canada

Received April 11, 2013; **Accepted** November 22, 2013; **Published** January 15, 2014

Funding: Peter Massey is supported by the NC3Rs (Grant Number G1000059; http://www.nc3rs.org.uk/). Alex Lench is an MRC student. Stuart Greenhill received a studentship from the University of Bath. Sophie Chamberlain received a studentship from the BBSRC. The funders had no role in study design, data collection and analysis, decision to publish, or preparation of the manuscript.

Competing Interests: The authors have declared that no competing interests exist.

* E-mail: r.s.g.jones@bath.ac.uk

¤a Current address: School of Biosciences, Cardiff University, United Kingdom
¤b Current address: MRC Centre for Synaptic Plasticity, Department of Physiology and Pharmacology, School of Medical Sciences, University of Bristol, United Kingdom

Introduction

The entorhinal cortex (EC) acts as a dynamic processor of information entering and leaving the hippocampus. The lamina and columnar structure of the EC provides a means of internal integration of information processing, and organization of its inputs and outputs determines its associative interactions with the rest of the neuraxis. The perforant path provides the major source of hippocampal input, projecting from layer II (L2; principally to the dentate gyrus and CA3) and layer III neurones (L3; principally to CA1 and the subiculum). These neurones receive convergent input from higher order cortices directly, and via adjacent cortices (presubiculum, perirhinal, parahippocampal). Hippocampal output is directed back to the neocortex via projections from CA1 and subiculum to neurones in layer V (L5) of the EC. In addition, the deeper neurones have associative connections with neurones in the superficial layers, and these provide a substrate for reverberant activity, which may be involved in reinforcement of stored information. The intimate association of the EC and the hippocampus probably indicates a complementary role of these areas in memory processes [1–2].

Increasing attention is being paid to the crucial role of the EC in spatial memory, in particular, in spatial representation and navigation [3]. To navigate, most animals derive spatial cues from external landmarks, combining this with computation of position from motional self-location cues. Principal neurones in the hippocampus may function as place cells to fulfill the former function, whilst grid cells, head-direction cells, and conjunctive cells (both grid and head-direction properties) in other areas, including the EC, may contribute to the latter [3]. Within the EC

there appears to be a lamina-based gradation of function, with L2 cells biased towards grid function, those in L3 towards head-direction, and L5 towards conjunctive function.

Other studies point to a lamina-specific delineation of functional responsiveness within the EC. For example, slow-wave oscillations (akin to cortical up-down states) in the EC are prominent in L3, but similar activity is weaker in L2, and L5 is reluctant or unable to participate in such activity [4]. Pharmacologically-induced gamma-frequency oscillation are also more pronounced in L3 compared to deeper and more superficial layers [5], whereas theta oscillatory activity is more prominent in L2, than in L3 or L5 [6].

EC dysfunction has often been implicated in neurological disorders particularly temporal lobe epilepsy (TLE) [7–15]. *In vitro* experiments in rat brain slices have demonstrated a pronounced susceptibility of the EC to acutely provoked epileptogenesis [16–23]. Pharmacologically induced seizures arise predominantly in the EC and propagate to adjacent cortical and hippocampal areas [16,20,24–27], but within the EC, acute epileptiform activity appears to be initiated in deep layers of the EC [16,20,21,27,28] leading to the suggesting that deep layers may be more susceptible to pathological synchronization [20,21,29].

The functional roles played by subpopulations of neurones in integrative processing and pathological activity will be dependent on many factors, including their intrinsic properties and connectivity within internal and external networks. Increasing attention has been paid to the role of background synaptic activity in modulating the properties of cortical neurones and determining input and output responsiveness. Individual cortical neurones are synaptically targeted by thousands of inputs derived from both excitatory (glutamate) and inhibitory (GABA) neurones in a dense and complex network. Both transmitters are continuously released by action potentials within network interconnections and by activity-independent release (miniature events). This background synaptic activity is a reflection of the moment-to-moment state of the network and is suggested to be instrumental in determining the excitability of any given neurone. It provides a source of stochastic resonance enhancing gain and signal detection [30–34]. Such activity may play a major role in shaping the processing of entrant, reentrant and afferent information in the EC.

One way of studying background synaptic activity is to monitor spontaneous excitatory and inhibitory currents using whole cell patch clamp recording, and we have adopted this approach in the EC to make qualitative comparisons of background inhibition and excitation in L5 and L2 neurones [35–38]. In the present investigation we have extended these observations to include L3 pyramidal neurones. However, there are a number of technical limitations with this approach (see methods), and, more recently, we have employed an analytical method to estimate global background synaptic conductances from measurement of fluctuations in membrane potential (termed VmD) derived from sharp electrode, intracellular recordings [39–44]. In the current investigation we have used both whole cell patch clamp recording, and VmD estimations to compare fast background inhibition mediated via $GABA_A$-receptors ($GABA_A$r) and excitation mediated by AMPA-receptors (AMPAr) in L2, L3 and L5 neurones in the EC. We have investigated how these background synaptic conductances are altered during progressive synchronization of network activity.

Materials and Methods

Ethics statement

All experiments were performed in accordance with the U.K. Animals (Scientific Procedures) Act 1986, European Communities Council Directive 1986 (86/609/EEC) and the University of Bath ethical review document, which requires that the number of animals used is kept to a minimum and every precaution was taken to reduce suffering and stress. At this institution, all research work involving use of animal tissue requires submission of a consideration of ethical implications form by the principal investigator. This is reviewed by a second investigator, external to the research group, and by the Head of Department, and requires signatory approval from both before being submitted to and reviewed by the Departmental Research Ethics Officer (DREO). The DREO will discuss any issues raised with the investigator. The DREO submits report to the University Ethics Committee detailing the ethical implications of all research within the Department on an annual basis. This ensures that the ethical implications of the research have been considered and that there is be a process in place for managing any ethical issues. All these processes have been adhered to in the current experimental work.

Slice preparation

EC slices were prepared [45] from male Wistar rats (60–100 g; P28–40) anaesthetised with ketamine (120 mg/kg) plus xylazine (8 mg/kg). Rats were decapitated and the brain removed and immersed in artificial cerebrospinal fluid (aCSF; see below for composition) at 4°C. Slices (400 μM) were cut using a Campden Vibroslice and stored in aCSF bubbled with carbogen (95% O_2/5% CO_2) at room temperature. Because of the orientation of the cutting [45], ours slices were largely restricted to more ventral locations, so dorso-ventral variation in intrinsic properties of neurones was minimized. To increase neuronal survival and viability, ketamine (4 μM) and indomethacin (45 μM) were included in the cutting solution and the antioxidants, n-acetyl-l-cysteine (6 μM) and uric acid (100 μM), added to both cutting and storage solutions. We have established (Woodhall, G.L. and Jones, R.S.G., unpublished observations) that the use of additives during cutting and storage produces robust and long-lasting slices, but does not have any apparent effect on the pharmacology of glutamate or GABA transmission. Nevertheless, in both recording situations slices were allowed to equilibrate in the recording chambers for at least 1 hour prior to recording to allow for washout of these agents. For patch clamp recordings slices were transferred to a recording chamber perfused (2 ml/min) with oxygenated aCSF at 31–32°C on an Olympus BX50WI microscope. Neurones were visualized using DIC optics and an infrared video camera. In VmD experiments slices were transferred to a recording chamber where they were held at the interface between a continuous perfusion of oxygenated aCSF (1.5 ml/min) maintained at 32±0.5°C and warm, moist carbogen gas. Intracellular recordings were made "blind" from slices visualised with a binocular microscope (Wild M8). The perfusion and storage aCSF contained (in mM): NaCl (126), KCl (3.25), NaH_2PO_4 (1.4), $NaHCO_3$ (19), $MgSO_4$ (2), $CaCl_2$ (2), and D-glucose (10). For cutting the slices at 3–4°C, $NaHCO_3$ was increased to 25 mM to maintain pH at acceptable levels (7.3).

Experimental approaches

As noted, we have used two experimental approaches to examine background synaptic activity in these studies. The more traditional approach involves whole cell voltage clamp recording of spontaneous synaptic currents. This is essentially looking at background activity from a presynaptic viewpoint, comparing the probabilistic release of glutamate and GABA, and making the assumption that a higher rate of release will result in greater postsynaptic excitation or inhibition, respectively, and vice versa. There are several technical issues with this approach. Experimen-

tal conditions are tailored towards recording of either excitatory or inhibitory currents in isolation, and therefore do not take into account how alterations in network activity and the postsynaptic responses to either transmitter may be altered by changes in the other. Recordings are conducted at somatic sites and these will not adequately detect events at distal dendritic sites. This means that frequencies of IPSCs and EPSCs will not reflect a true contribution of inhibition or excitation to overall cellular activity. The differential location of excitatory and inhibitory synapses also means that synaptic excitation (distal location) may be underestimated compared to inhibition (more proximal) by this approach. Patch solutions for recording of synaptic currents generally include Na^+ and K^+-channel blockers to improve postsynaptic space-clamp and partially obviate some of the issues with recording resolution. However, this means that a realistic estimation of cellular excitability is impossible.

We have developed a complementary approach based on what is referred to as the VmD method. This was developed by Alain Destexhe and colleagues [42–44], using the presumptive synaptic activity of model neurones to attempt to recreate the biological activity of real neurones under conditions of intense synaptic activity (referred to as a "high-conductance state" [42–44]). We have adapted this mathematical approach as a means of quantifying the background synaptic activity based on the ongoing biological fluctuations in real neurones. The approach essentially looks at background synaptic activity from a postsynaptic perspective. The VmD method relies on the premise that momentary fluctuation in somatic membrane potential largely reflects the combined effects of on-going global inhibitory and excitatory postsynaptic conductances, which result from the presynaptic transmitter release occurring in response to network activity. Although this method was developed and tested using theoretical and experimental approaches applicable to high conductance *in vivo* network states, we have experimentally and pharmacologically validated its use to estimate background conductances in the relatively quiescent conditions extant in EC slices, and, subsequently, employed it to determine the effects of diverse anticonvulsants on these conductances [39–41]. There are potential errors and limitations that have to be considered in terms of establishing absolute levels of background conductances, particularly membrane potential fluctuations arising from intrinsic membrane ion channels [42]. However, since we are looking principally at relative differences within and between neurones, these are not prohibitive issues, and it provides an excellent way to complement studies of presynaptic release with overall postsynaptic activity.

Whole-cell patch clamp recordings of transmitter release

Patch pipettes pulled from borosilicate glass were used for recording spontaneous or miniature excitatory postsynaptic currents (sEPSCs and mEPSCs, respectively). They were filled with a Cs-gluconate based solution containing (in mM) D-gluconate (100), HEPES (40), QX-314 (1), EGTA (0.6), $MgCl_2$ (5), TEA-Cl (10), phosphocreatinine (5); ATP-Na (4) and GTP-Na (0.3). To record spontaneous or miniature inhibitory PSCs (sIPSCs and mIPSCs), the patch solution contained CsCl (100), HEPES (40), QX-314 (1), EGTA (0.6), TEA-Cl (10), $MgCl_2$ (5), ATP-Na (4) and GTP-Na (0.3). Solutions were adjusted to 275 mOsmol and pH 7.3 with CsOH. Whole-cell voltage clamp recordings (holding potential −60 mV) were made from pyramidal neurones in L3 of the medial division of the EC, using an Axopatch 200B amplifier. Signals were filtered at 2 kHz and digitized at 20 kHz. Series resistance compensation was not employed, but access resistance (10–30 MΩ) was monitored at regular intervals and cells were discarded if it changed by more than ±10%. Liquid junction potentials (EPSC +12.0 mV; IPSC +10.2 mV) were estimated using pClamp-8 software, and compensated for in the holding potentials. When recording IPSCs, AMPA-receptors and NMDA-receptors were blocked with bath applied NBQX and 2-AP5, respectively.

Data were recorded using Axoscope software, and Minianalysis (Synaptosoft, Decatur) was used for analysis of PSCs off-line. Spontaneous events were detected using a threshold-crossing algorithm. Cumulative probability distributions of interevent interval (IEI) were compared using the Kolmogorov-Smirnoff test (KS). When data were pooled for this analysis, a minimum of 200 events was sampled during a continuous recording period for each neurone under each condition. Mean amplitudes, rise times (10–90%) and total decay times were compared using a t-test.

VmD estimations of postsynaptic background conductances

Sharp electrodes pulled from borosilicate glass and filled with potassium acetate (3M, pH adjusted to 7.3); tip resistances of 80–120 MΩ) were used to make intracellular voltage recordings using an Axoprobe 1A amplifier (Molecular Devices). When membrane potential had stabilised after impalement, estimates of global background excitation (E_{bg}) and inhibition (I_{bg}) were derived from membrane potential fluctuations at regular intervals throughout the recordings using the VmD method. This approach was derived by Rudolph *et al.*, [42] and we have adapted it for recording in EC slices [39–41]. Precise technical details of the approach are available in these papers [39,42], and are not repeated here. Briefly, neurones were depolarised (for 15–20 s) by injection of two levels of known positive current via the recording electrode. The values of the currents differed from neurone to neurone, but were maintained the same throughout any individual experiment. One level was chosen to elicit a depolarization to within 1–2 mV of action potential threshold, and the second was adjusted to depolarize the neurone to about half way between this and resting membrane potential. Membrane potential fluctuations at these two levels were fitted to Gaussian distributions (Prism 4 software, GraphPad, San Diego, USA) and the mean and variance of the membrane potential determined. Leak conductance in each neurone was calculated from the ohmic response produced by a small (0.1 nA 100 ms) hyperpolarizing current, injected at resting membrane potential. These parameters, together with mean reversal potentials for AMPA-receptors and $GABA_A$r mediated synaptic responses ([39] plus unpublished data), allowed us to use the VmD relationship to quantitatively estimate background inhibitory and excitatory conductances resulting from global network input onto individual neurones. Statistical analysis (paired *t*-tests or one-way ANOVA) was performed with Prism 4 software. All error values in the text refer to standard error of the mean.

Cellular excitability was determined by injecting depolarizing current pulses at resting potential. Action potential (AP) thresholds with respect to resting membrane potential were determined using brief incremental peri-threshold injections of depolarising current (0.1–1.0 nA, 50 ms) via the recording electrode. Trains of action potentials were also elicited by longer, supra-threshold current pulses (0.2–1.0 nA, 200 ms), and the number of spikes per pulse determined.

In some experiments, designed to compare the effects of blocking GABA inhibition in L2, we employed extracellular recording of spontaneous epileptiform activity. In these studies we used patch pipettes (filled with normal ACSF, and broken back to give tip resistances of around 1–5 MΩ) and an NPI EX-10C

differential amplifier for recording local field potential activity. In some cases simultaneous recordings were made in different layers.

Materials

Salts used in preparation of aCSF and electrode solutions were purchased from Merck/BDH or Fisher Scientific (UK). Indomethacin, n-acetyl-l-cysteine and uric acid were purchased from Sigma (UK). Ketamine was supplied by Fort Dodge Animal Health Ltd (Southampton, UK) and xylazine by Bayer AG (Leverkusen, Germany). Drugs were applied by bath perfusion. The following drugs were supplied by Tocris UK or Ascent Scientific UK: 2-AP5 (D-2-amino-5-phosphonopentanoic acid), NBQX (6-nitro-7-sulphamoylbenzo[f]quinoxalone-2,3-dione disodium), bicuculline methiodide, QX-314 (N-(2,6-Dimethylphenylcarbamoylmethyl) triethylammonium chloride). Picrotoxin and strychnine HCl were purchased from Sigma UK.

Results

Lamina comparison of spontaneous GABA and glutamate release

Previous work from this laboratory has detailed characteristics of s/mEPSCs and s/mIPSCs in L2 and L5 of the EC [35–38]. To complete the laminar comparison of spontaneous release of glutamate and GABA across the EC, we have made similar studies in L3 and we present representative data (from 19 neurones each for sEPSCs and sIPSCs) here. We stress that some of the data are from previously published studies [35,38] but a summary (supplemented by some additional recordings) is presented here for direct comparative purposes.

EPSCs. The properties of EPSCs in the 3 layers are summarized in Figure 1. As in L2 and L5 [35], the vast majority of sEPSCs were mediated via AMPAr (Figure 1A). Thus, spontaneous currents were essentially undetectable in the presence of AMPAr antagonists (NBQX, SYM 2206, or GYKI 53655) at a holding potential of −60 mV. However, at more positive holding potentials, occasional small slow events could be detected; these reversed at around 0 mV and were blocked by 2-AP5, indicating that in this layer, as in L2 and L5 [35], sEPSCs mediated by NMDA receptors were evident at a very low frequency.

The mean IEI of sEPSCs in L3 was 198±28 ms, corresponding to a mean frequency of 5.1±1.1 Hz, which is considerably higher than that of sEPSCs in either L5 (714±39 ms) or L2 (756±28 ms) (Figure 1B; cf. [38]). In contrast, the mean amplitude (Figure 1C) in L3 (14.1±0.7 pA) did not differ greatly from the other layers, although it was slightly greater than that in L2 (13.2±0.3 pA) and less than that in L5 (15.7±0.5 pA). Rise and decay kinetics (Figure 1D) in L3 (1.8±0.2 ms and 5.9±0.5 ms, respectively) were similar to those recorded for sEPSCs in L5 (1.9±0.1 ms and 5.7±0.3 ms; [35]), but both parameters were slower in L2 (2.5±0.1 ms and 8.0±0.4 ms; [35]). Previously, we have also shown that neurones in all layers are not particularly electronically compact, with estimated electrotonic lengths of 2.5 and 1.6 in L5 and L2, respectively [35]. The value estimated for L3 (1.6; [46]) was the same as that in L5, so it is possible that the faster kinetics of sEPSCs in L3 and L5 may be associated with the shorter electronic lengths of the neurones in these layers compared to L2.

There was a clear difference between L3 and L2 or L5 in the contribution of activity-dependent release to overall spontaneous release (Figure 1E). Thus, in L3 neurones, application of TTX (1 μM; n = 8) caused a 6-fold increase in IEI from 220±28 ms to 1284±243 ms, reflecting a decrease in frequency from 6.4±1 Hz to 1.0±0.3 Hz. The mean amplitude of events (Figure 1E) was slightly less in the presence of TTX, but not significantly so. However when we examined the cumulative probability distributions in pooled data, it was apparent that there was a loss of some of the larger amplitude events, which produced a significant ($P<0.01$; KS) shift to the left, evident at the top end of the distribution. In contrast, in both L2 and L5, TTX only caused a 15–20% reduction in sEPSC frequency [35]. Thus, L3 neurones show a much great preponderance of action potential driven release compared to the other layers where activity-independent, monoquantal release predominates.

IPSCs. IPSCs in L3 neurones were recorded at a holding potential of −60 mV, with symmetrical [Cl^-], where they were evident as fast inward currents. In agreement with our studies in L2 and L5 [37] these were largely eliminated (n = 7) by the $GABA_A$-receptor blocker, gabazine (20 μM; Figure 2A). However, the glycine receptor antagonist, strychnine, applied before gabazine (1 μM), also had a weak effect on sIPSCs reducing the frequency by around 10–20% (n = 6) without affecting amplitude (mean IEI 168±117 ms v 198±134 ms Figure 2A). KS analysis of the cumulative probability distribution of IEIs (not shown) from pooled data indicated an effect that just reached significance ($P<0.01$). We found a similar small reduction with strychnine in L2 neurones previously [37]. We have now added further studies to those in this previous sample and the summary data shown in Figure 2A confirm a small, but significant, decrease in frequency of sIPSCs in L2 with no effect in L5.

Overall, sIPSCs in L3 (n = 19) occurred at a high frequency (10–15 Hz; Figure 2B) reflected by a mean IEI of 112±21 ms, which is similar to that seen in L2 (IEI 87±2 ms; Woodhall et al, 2005) and much shorter than that in L5 (IEI 404±10 ms; Woodhall et al, 2005). Mean amplitude in L3 (30.9±2.0 pA; Figure 2C) was larger than that in either L2 or L5 (24.0±1.8 and 25.7±3.9 pA respectively; [37]). Mean decay time of sIPSCs in L3 was 15.8±1.5 ms, which is longer than those seen in the other layers (L2 10.5 ms; 10.6 in L5), but rise time (2.2±0.2 ms) was similar to those reported for L2 and L5 (2.0±0.03 ms and 1.9±0.03 ms, respectively; Figure 2D; [37])

The relative contribution of action potential driven and action potential-independent release was determined (Figure 2E). IEI of sIPSCs in the presence of TTX (1 μM) approximately doubled from 112±21 ms to 238±44 ms (n = 10) in L3. This represents a decrease in frequency from 15.5±2.8 Hz to 6.0±1.1 Hz, indicating that approximately half of the IPSCs are action potential-dependant. This effect is similar to that seen in L5 where the IEI more than doubled (from 368.2±13.1 ms to 979.9±31.5 ms; [37]), but contrasts markedly to L2 where TTX had little or no effect [37]. In terms of absolute numbers of sIPSCs, L3 neurones actually showed a much greater decrease than L5 in the presence of TTX, as a result of their higher baseline frequency of sIPSCs.

EPSC to IPSC comparison

Looking at baseline levels of spontaneous synaptic activity across the three layers, there are some general and obvious differences. The most prominent difference in sEPSCs is the higher frequency noted in L3. Amplitudes are similar, with slightly larger events in L5, and in terms of kinetics the slower decay time in L2 is prominent. In the case of inhibition, the high frequency of sIPSCs in L2 and L3 compared to L5 is the most notable difference. To gain a better comparative picture of overall spontaneous synaptic activity across the three layers, we derived arbitrary charge transfer (CT) values for spontaneous synaptic activity. These values are the product of mean frequency, amplitude and decay times.

For sEPSCs, CT was highest in L3 (340.3) and approximately the same in L2 (147.8) and L5 (125.3) (Figure 3 top). In the case of

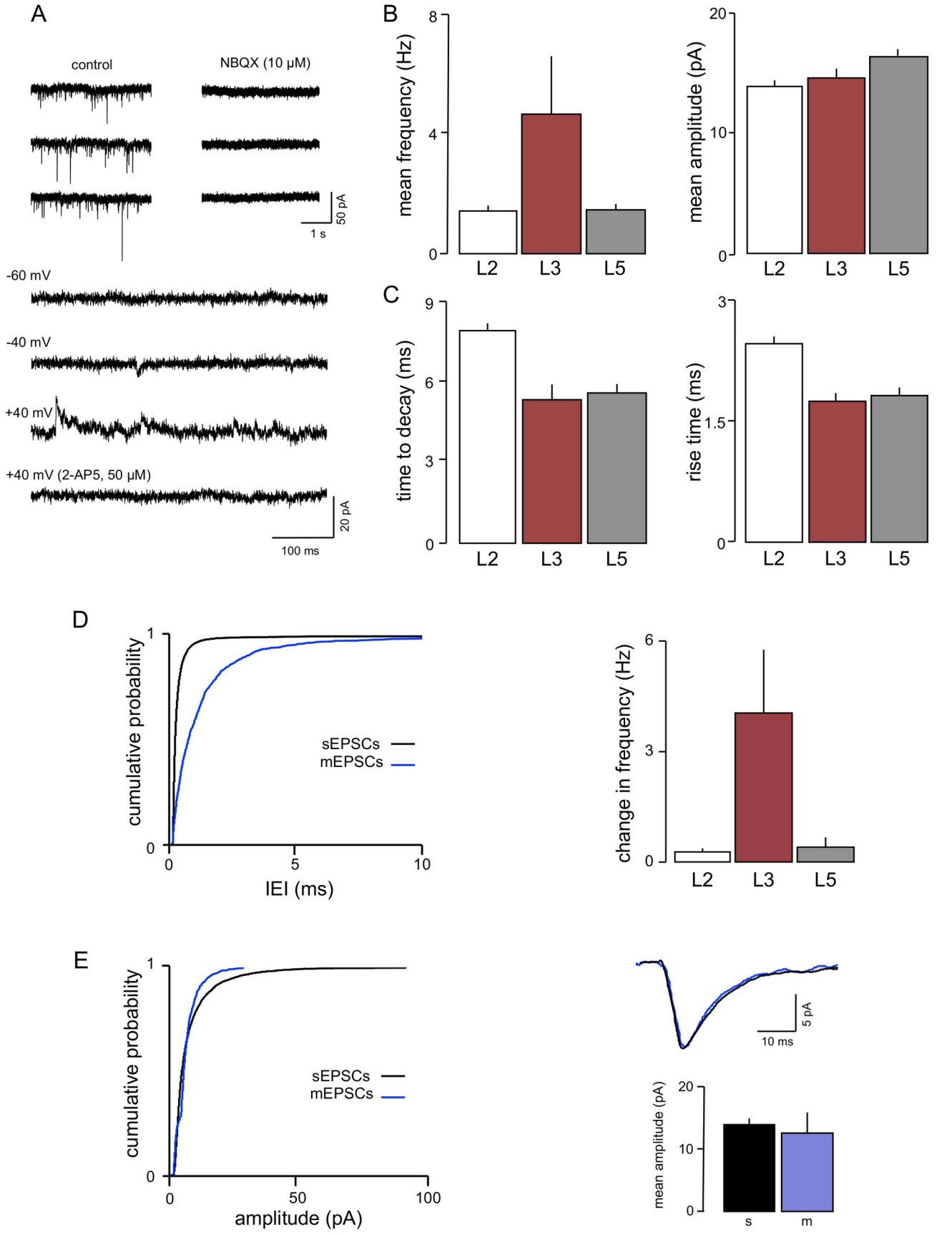
A
control
NBQX (10 μM)
50 pA
1 s
-60 mV
-40 mV
+40 mV
+40 mV (2-AP5, 50 μM)
20 pA
100 ms
B
mean frequency (Hz)
mean amplitude (pA)
L2
L3
L5
C
time to decay (ms)
rise time (ms)
D
cumulative probability
sEPSCs
mEPSCs
IEI (ms)
change in frequency (Hz)
E
cumulative probability
sEPSCs
mEPSCs
amplitude (pA)
5 pA
10 ms
mean amplitude (pA)
s
m

Figure 1. Characteristics of EPSCs in L3. A. Voltage clamp recordings from one neurone show that the AMPAr antagonist NBQX essentially abolished sEPSCs. At more positive holding potentials, occasional, slow sEPSCs were detected that were mediated by NMDAr, as they were blocked by 2-AP5. B. A comparison of sEPSC properties Showed that the mean frequency of events in L3 was greater than that in either L2 or L5. Amplitudes were similar across layers, but kinetics (C) were slower in L2 compared to the deeper layers. D. Action potential driven release accounts for a much higher proportion of spontaneous excitation in L3. Cumulative probability analysis of data pooled from 10 neurones (graph on left) showed a large increase in IEI (shift to the right) in L3 that was substantially greater than that seen in L2 or L5. This is very clearly illustrated by the bar graphs (right) showing the accompanying change in frequencies (sEPSC frequency minus mEPSC frequency). E. Neither amplitude nor kinetics of EPSCs in the same neurones were significantly different in the presence of TTX (mEPSCs shown in blue).
doi:10.1371/journal.pone.0085125.g001

sIPSCs (Figure 3 middle), again L3 gave the highest CT value at 4345.2. This was followed by L2 at 2898.0 with L5 markedly lower at 653.8. Cortical neurones are under a simultaneous and continuous bombardment from both glutamate and GABA synapses. Although we have not recorded excitatory and inhibitory currents simultaneously in individual neurones, we determined the ratio of CT values as an approximate measure of the relative influence of spontaneous excitation to inhibition across the different populations of neurones. This gave inhibition:excitation (I:E) ratios of 19.6. in L2 followed by 12.8 in L3 and 5.2 in L5 (Figure 3 bottom). These values represent, at best, a rough comparison, as sEPSCs and sIPSCs were recorded isolated from each other, and the former were recorded with inhibition intact but the latter with excitation blocked. Nevertheless, they do indicate that overall, background inhibition predominates in all three populations, but that its relative strength is more marked in a progression from deep to superficial in the EC.

Laminar comparison of global background synaptic activity

Recordings of sEPSCs and sIPSCs give an indication give us some idea of the relative level of inhibition and excitation exerted via the network, from a presynaptic view point and on a moment-to-moment basis. However, a more integrated assessment of the on-going inhibition and excitation seen by the postsynaptic cell and its effects on excitability requires a different approach. We have adopted the VmD method [39,42] to assess global synaptic conductances, estimating background GABAergic inhibition and glutamatergic excitation concurrently in the same neurone. We have used this approach to complement and extend the results of our whole cell patch clamp studies, and to examine whether background network activity may be instrumental in determining the susceptibility of different populations of EC neurones to participation in synchronous activity.

The comparative lamina data obtained using the VmD approach are illustrated in Figure 4. I_{bg}, estimated in L5 neurones ($n = 10$; Figure 4A), was 6.1 ± 1.7 nS. Concurrently, E_{bg} was about half this at 3.1 ± 0.7 nS, with a mean I:E ratio in these neurones of 2.3 ± 0.6. Similar estimations in L3 neurones ($n = 17$) gave a much higher I_{bg} of 11.2 ± 2.1 nS and a slightly greater E_{bg} of 4.1 ± 0.7 nS, but the I:E ratio based on these estimates was similar to that in L5 at 2.7 ± 0.5. I_{bg}, estimated in L2 neurones (14.3 ± 2.7; $n = 11$), exceeded that in L3 and was substantially greater than that in L5. In contrast, E_{bg} was similar (2.9 ± 0.3 nS) to L5 but again lower than L3. Consequently the I:E ratio in L2 (4.6 ± 0.4) was considerably higher than that recorded in the other layers. Comparing the data from whole cell patch clamp recordings (Figure 3), and VmD measurements (Figure 4) shows a good correlation between the levels of inhibition and excitation derived from the intracellular and whole-cell patch clamp recordings, with the standout difference between the layers being the greater preponderance of inhibition in L2.

As noted above, strychnine caused a small but significant reduction in sIPSC frequency in L2 in patch clamp recordings, so we determined its effect on I_{bg} and E_{bg} ($n = 4$). There was no significant change in E_{bg} with the glycine receptor antagonist (3.1 ± 1.1 v 2.9 ± 1.3), and although I_{bg} fell slightly (11.1 ± 3.3 v 9.9 ± 2.7) the change was not significant. The I:E ratio was unaltered (3.7 ± 0.7 v 3.3 ± 0.7).

The VmD approach also allows us to estimate of the variance of the global background conductances. Destexhe and his colleagues [42–44] have suggested that conductances reflect the overall rate of release from the afferent neurones, whereas the variance may be related to the temporal correlation of the release in the presynaptic inputs. Thus, a large variance could reflect large numbers of synaptic terminals releasing transmitter synchronously or semi-synchronously [42–44]. However, this association is based on large numbers of synapses releasing at a high rate in an in vivo-like situation [42–44] and there are obvious limitations in making similar inferences from variance measures in our slices, where we are studying reduced networks (and hence synapses numbers) with a consequent reduction in release rates. Nevertheless, we did find some marked differences in mean variances in the different layers of the EC (Figure 4B). Under resting conditions, the mean variance of I_{bg} in L2 neurones was 5215 ± 407 pS. This contrasts markedly with L3 and L5 where the mean variances were 99 ± 49 pS and 105 ± 27 pS, respectively. Likewise, the variance of E_{bg} was considerably greater in L2 neurones (2107 ± 333 pS) compared to L3 (88 ± 21 pS). The variance in E_{bg} was lowest in L5 (27 ± 24 pS).

One possible confounding factor in comparing L2 to L3 and L5, is the heterogeneity of neurones in the former. Previous studies, including from this laboratory, have suggested that neurones in L2 with a pronounced time-dependent inward rectification (TDIR) during hyperpolarization, due to a strong expression of I_h, are likely to be stellate in nature, whereas those that do not exhibit TDIR are more likely to present pyramidal-like morphology [19,47]. Based on subsequent recordings in several hundred L2 neurones (R.S.G. Jones, unpublished), we have found that there is much more of a continuum within the correlation of expression of TDIR and morphological characteristics, and a demarcation of stellate v pyramidal on this basis is less clear than originally supposed. Nevertheless, we thought it worthwhile to compare background conductances in neurones with prominent TDIR, to those in which it is less evident. We used the population of neurones from the analysis above, together with a further 10 in which we just recorded baseline conductances. In these 21 neurones we classified 15 with clear TDIR and 6 where TDIR was minimal (non-TDIR). Mean I_{Bg} was 15.1 ± 3.6 nS (variance 3829 ± 851 pS) in the former and 13.4 ± 4.0 nS (variance 4628 ± 711 pS) in the latter. In neurones with TDIR, E_{Bg} was 3.1 ± 0.9 nS (variance 1707 ± 402 pS) and in non-TDIR neurones it was 2.9 ± 0.9 nS (variance 2223 ± 512 pS). None of these values differed between the groups or from the values in the pooled neurones. I:E ratios were also very similar (5.0 ± 0.7 v 4.4 ± 0.9). Thus, it seems unlikely the differences in L2 compared to L3 and L5 are explicable in terms of heterogeneity of morphology/intrinsic properties in the L2 population.

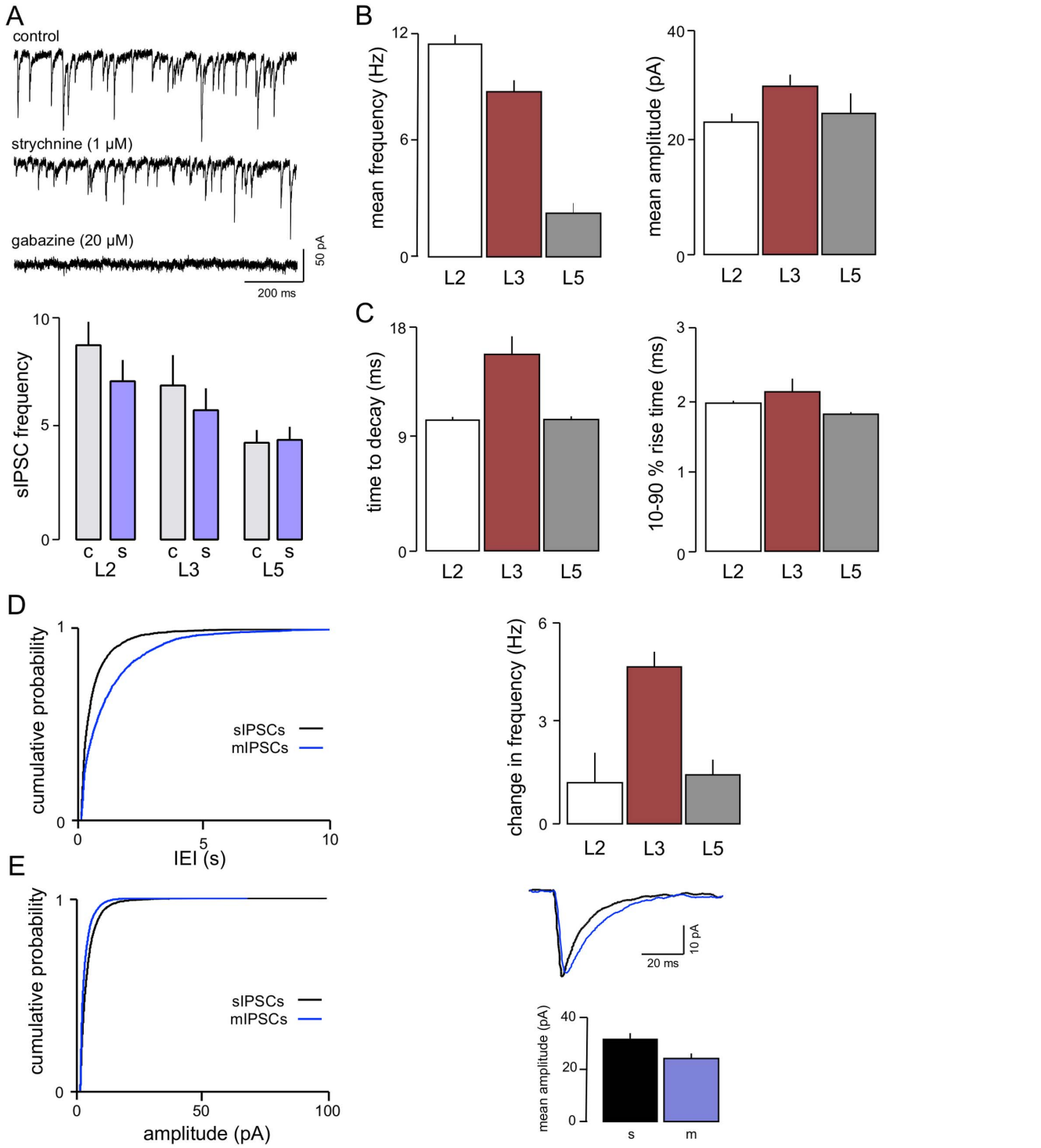

Figure 2. Characteristics of IPSCs in L3. A voltage clamp recordings from one neurone show that sIPSCs are largely mediated by $GABA_Ar$. However, there was a reduction in frequency with the glycine receptor antagonist strychnine. Although this generally only amounted to around 10–15% it was significant when assessed by a paired t-test. A similar effect was seen previously in L2 [37]. We have added a number of new recordings to this data and the reduction again just reaches significance with a paired t-test. In contrast, no effect of strychnine was seen in L5. B. sIPSC frequency was lower than in L2 but still considerably higher than in L5, whereas the both mean amplitude and decay time in L3 (C) were greater than either of the other layers (D). Action potential driven GABA release, like glutamate release (see Figure 1) was more prominent in L3 compared to L2 or L5. Thus application of TTX resulted in a marked change in frequency of events (sEPSC frequency minus mIPSC frequency). (E) In addition, the mean amplitude of events was also lower in TTX, although time to decay was slower.
doi:10.1371/journal.pone.0085125.g002

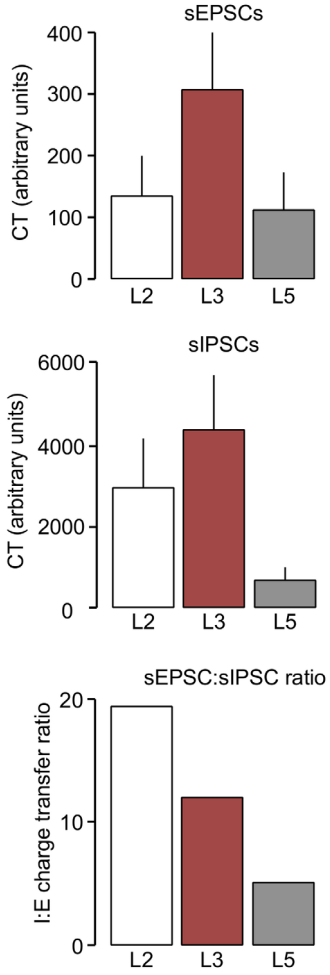

Figure 3. Comparison of inhibition to excitation in whole cell patch clamp studies. The total charge transfer (CT) associated with sEPSCs, was greatest in L3 and approximately equal in L2 and L5. Charge transfer of sIPSCs was also greatest in the middle layer, but substantially markedly less in L5 than the more superficial layers. The resultant ratio calculations suggested a substantial dominance of inhibition in all layers, with L2 showing by far the greatest bias and L5 the least.
doi:10.1371/journal.pone.0085125.g003

Another potential confounding factor in comparing background synaptic conductances across layers could be the intrinsically generated theta oscillations reported to occur in L2 stellate neurones at depolarized potentials [48,49,50]. However, similar intrinsic oscillations have also been reported in L5 neurones, although not in L3 [51,52,53]. Whilst intrinsic theta oscillations do appear to be a characteristic of L2 neurones, in over 25 years of recording EC neurones, we have not seen such oscillations consistently expressed to the same extent as reported by others [48,49,50]. It does not appear to be present in all neurones that would be tentatively identified as stellate on the basis of TDIR, and, when detectable, can be weak and intermittent. Even if present, it should not influence our VmD estimations since Vm fluctuations are estimated on a considerably higher moment-to-moment time scale (in 10 ms bins) than that pertaining to the low frequency (7–8 Hz) intrinsic theta oscillations. Nevertheless, we looked at this as a possible confounding factor in our VmD estimations in L2. We subdivided the population of neurones with TDIR into those in which we could see evidence of theta oscillatory activity (n = 8) and those where we could not (n = 7). In the former, I_{Bg} was 12.2±4.6 nS, and in the latter, non-significantly different at 13.3±5.0 nS. Likewise, E_{Bg} was also very similar in the two populations (2.9±0.7 nS v 3.5±1.2 nS).

The oscillatory activity in L2 is principally dependent on a low-threshold, persistent Na- current and can be eliminated by Na-channel blockade [48,49]. We recorded from L2 neurones with electrodes containing QX-314 (50 mM), to block the Na-currents (n = 5). We also substituted Cs-methanesulphonate (2 mM) for K-acetate in the recording solution, which eliminates TDIR [19,47] (although the underlying I_h-current does not play a prominent role in oscillatory activity [48]). We estimated conductances 4–5 minutes after impalement with these electrodes and the values obtained were well within the range of those seen with K-acetate electrodes (10.1±2.0 nS and 3.2±0.5 nS for I_{Bg} and E_{Bg}, respectively). Fifteen minutes after impalement, Na-dependent action potentials had disappeared, and there was no evidence of TDIR, or of theta oscillatory activity at depolarized potentials. Respective values for inhibition and excitation at this time were 12.2±2.7 nS and 3.6±0.3 nS. Neither conductance was significantly altered when comparing the early and late time points and ratios remained remarkably similar (3.2 v 3.5). Thus, we are confident, that intrinsically generated oscillatory activity is unlikely to influence the comparison of VmD estimations in L2.

Background activity during acute network synchronization-Blocking $GABA_A$r in cortical slices leads to progressive network synchronization culminating in emergent paroxysmal events that have often been used as a model of epileptiform activity. The EC is no exception and we have previously shown that such events are likely to originate in L5 and propagate from here to other layers of the EC and to other areas [18,20,21]. We have also shown that events in L2 are less frequent and not as pronounced as those in the L5 and we have suggested that the intrinsic properties of the superficial network may make them less susceptible to synchronization [20,29]. We have used the VmD approach to chart the time course of changes in background inhibition and excitation that occur across L2, L3 and L5 in the period leading to overt synchronization of the synaptic networks. The intracellular recordings in the different layers were not conducted simultaneously but represent distinct data sets in different slices. As far as possible, matched experiments in slices from the same animal were conducted on the same day.

Examples of intracellularly recorded, network-driven, paroxysmal depolarizing shifts in the different layers during perfusion with the $GABA_A$r antagonist, bicuculline (10 μM), are shown in Figure 5A. For illustrative purposes these were actually recorded in the same slice (although not concurrently) after synchronous network activity had developed, and the events are typical of those arising during early network synchronization. They can vary somewhat between slices and preparations, but are fairly stereotypical in morphology. They are emergent network driven events as they correspond to population events recorded extracellularly at adjacent sites (not shown). Those in L3 and L5 were similar, and different in several ways from those in L2. Due to the complex nature of events it is difficult to quantify them meaningfully, but nominal values give some indication of differences. Peak amplitudes from resting potential (ignoring spikes) were almost the same in L5 and L3 (42±8 mV and 37±9 mV, respectively) but considerably and significantly greater ($P>0.05$) than those in L2 (16±6 mV). Duration was greatest in L5 (687±88 ms) followed by L3 (489±101 ms) and L2 (242±44 ms), and the number of spikes (full or truncated) associated with events showed a similar pattern (26±11 v 14±6 v 6±2). We measured the mean latency to appearance of the first

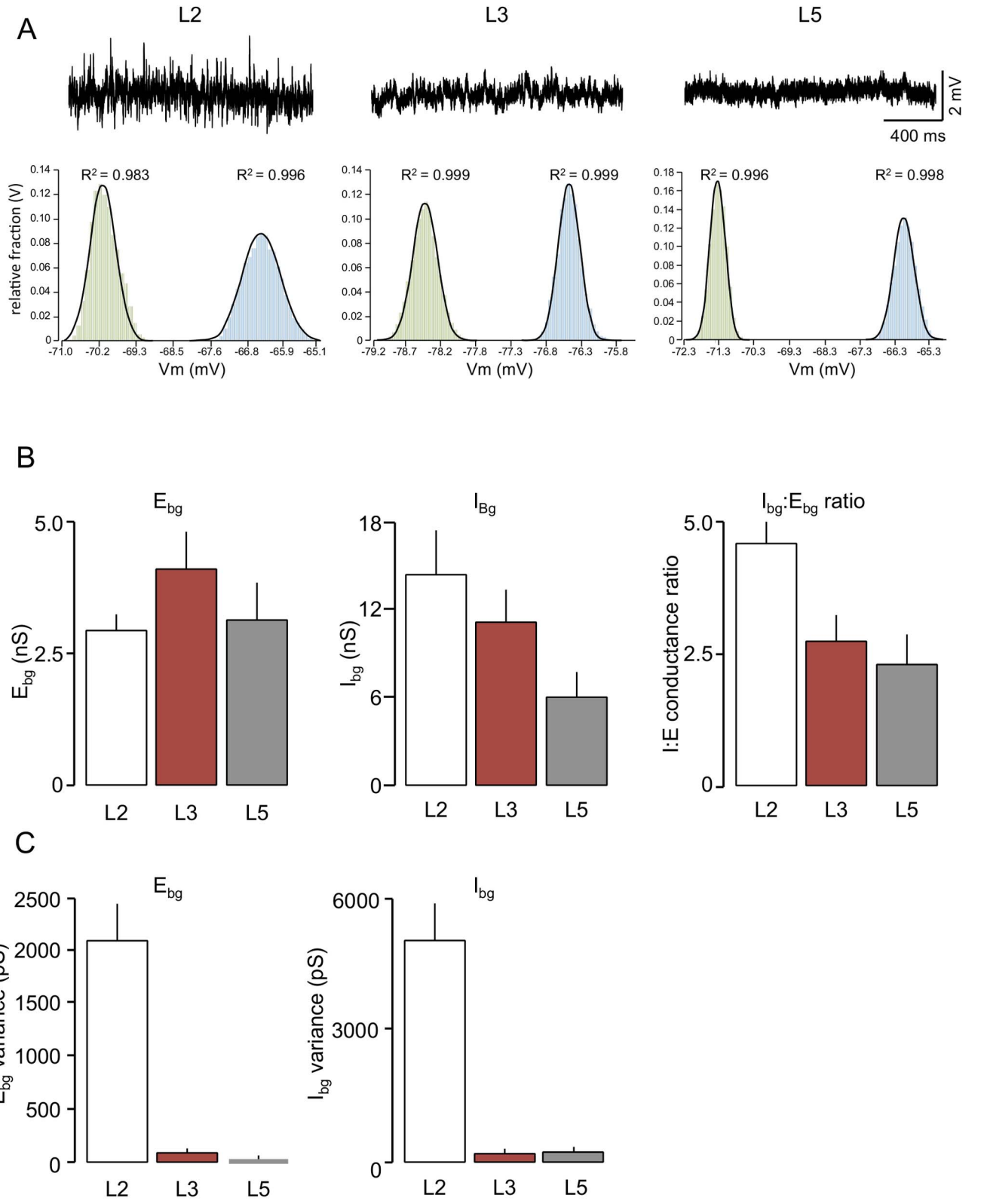

Figure 4. Simultaneous VmD estimations of excitatory and inhibitory background conductances. A. The raw traces show sample intracellular recordings from three neurones recorded in the same slice, and showing a great peak-to-peak voltage activity in L2. Estimation of background inhibition and excitation (see methods) required calculation of mean and variance of membrane potential at two levels of injected current (not shown). The histograms show the frequency distributions of membrane fluctuations at the two levels of injected current (geen being closer to resting potential and blue slightly more depolarized) in sample neurones from each layer. The solid lines on the graphs show the potential fluctuations constrained to a Gaussian function and in each case the goodness of fit (R^2) was close to unity. B. Comparison of average data for background synaptic conductances estimated in the three layers of the EC. Background excitation (E_{Bg}) was highest in L3 and approximately 40%

higher than that in L2 or L5. Inhibition (I_{Bg}) was greatest in L2 followed by L3 and L5. The resultant ratios showed a predominance of inhibition in a ll three layers, but in L2 this was this was almost double that seen in the other layers. C. The variance associated with the conductances (which is suggested to reflect the level of temporal synchrony in presynaptic inputs) was dramatically higher for both inhibition and excitation in L2 than in either of the deeper layers.
doi:10.1371/journal.pone.0085125.g004

spontaneous event after the entry of the antagonist into the bath (Figure 5B) and this showed that synchronized discharges appeared at around 450 s from initial exposure to bicuculline in both L3 and L5 but was significantly ($P>0.05$) delayed in L2 appearing around 700 s.

Thus, this comparison supports our previous studies [20] showing a greater susceptibility to disinhibition-induced synchronicity amongst L5 neurones compared to L2, and puts L3 intermediate between the two. We have now used the VmD approach to document how this may be related to changes in I:E balance and excitability during the process of disinhibition. We have previously described some of this information for L3 neurones [40], and now present a fuller description with comparison to L5 and L2.

Figure 6C illustrates the time course of changes in background conductances during perfusion with bicuculline (10 μM) in L5 neurones (n = 6). As expected, there was a rapid decrease in I_{bg} during the first 2 minutes of contact with the antagonist, concurrent with a small, but non-significant, decrease in E_{bg}. At this stage the absolute levels of the conductances were approximately equal. Thereafter, I_{bg} continued to decline whereas E_{bg} returned to its original level, with the absolute magnitude of the conductance levels reversing between 2 and 4 minutes. The net effect of these changes was a substantial switch in I:E ratio to favour excitation compared to the bias towards inhibition under control conditions. Results for L3 neurones (Figure 6B) were similar, but the decline in I_{bg} was less rapid and the reversal of conductance levels occurred a little later (around 5 min). I:E ratio in L3 neurones also reversed in favour of excitation, and, although the change was slightly less rapid, it reached the same end point as in L5 and the time of appearance of paroxysmal activity occurred when the I:E ratio reached approximate equivalence (Figure 6D).

Results for L2 neurones (n = 6) are shown in Figure 6A. Again, there was an initial rapid fall in I_{bg}. However, after 4 min, this had plateaued at around 45% of control, and thereafter there was no further substantial fall. E_{bg} showed little concurrent change, and the absolute values of the conductances did not reverse at any point. Consequently, although the I:E ratio fell by around 50%, it always remained substantially in favour of inhibition (Figure 6C,D). Thus, the delayed appearance of spontaneous synchronized events and, perhaps, the extent of synchronization in L2 could be related to the amount of residual inhibition. We have also monitored the variance of the background conductances throughout application of bicuculline (Figure 7). During bicuculline perfusion, the variance of E_{bg} initially fell quite steeply and then essentially plateaued. Perhaps not surprisingly, the variance of I_{bg} fell precipitously, but then actually increased towards control levels. In L3, the variance of I_{Bg} fell markedly but that of E_{Bg} was largely unaltered. Likewise, in L5 the variance of I_{bg} fell progressively throughout, whereas, after an initial fall, there was a delayed increase in E_{bg} variance taking it beyond control levels.

Finally, we noted small changes in intrinsic neuronal excitability in all three layers during perfusion with bicuculline. In L2, spike threshold fell slightly from 18.8±0.4 mV (positive to rest) to 17±0.7 mV, and in L3 from 20.6±18.2 mV to 18.2±0.9 mV, although neither change reached significance. In L5, threshold

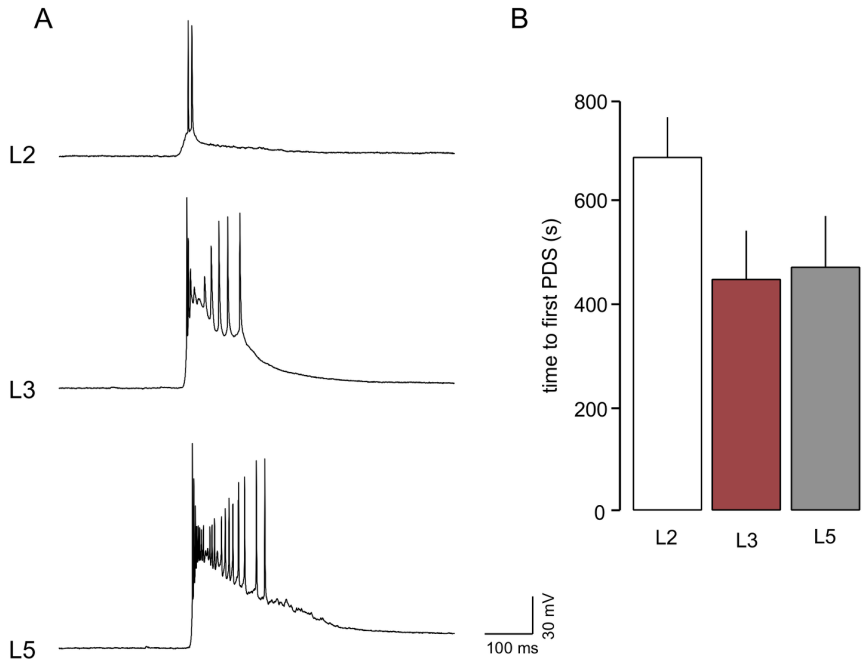

Figure 5. Bicuculline induced paroxysmal depolarizing shifts in EC neurones. A. Intracellular recordings show large depolarizing events associated with multiple spikes were recorded in both L5 and L3 during bicuculline (10 μM) perfusion. In L2 these were much smaller and often associated with just one or two spikes. B. In addition their appearance (timed from the entry of bicuculline into the bath) was delayed in L2 compared to the deeper layers.
doi:10.1371/journal.pone.0085125.g005

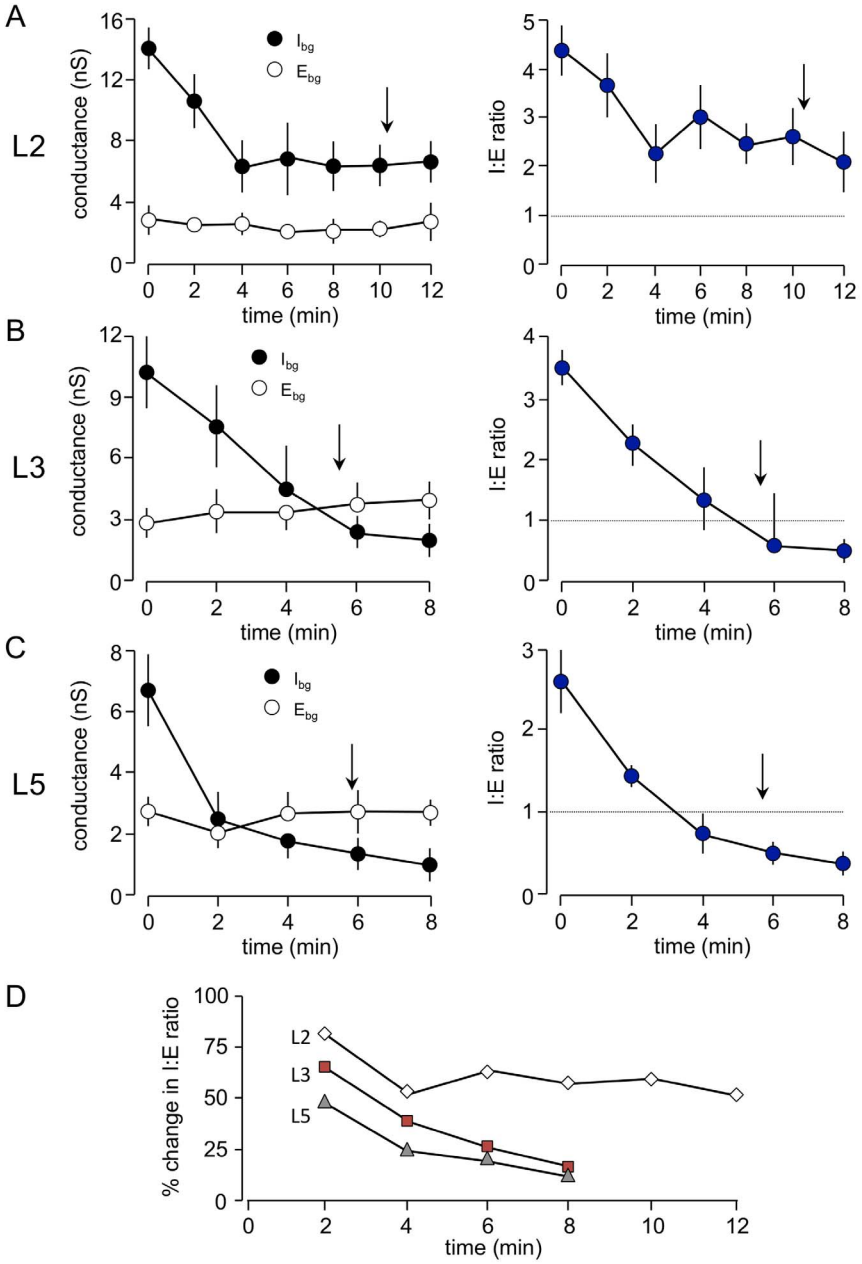

Figure 6. Time course of changes in global background synaptic conductances during perfusion with bicuculline. Bicuculline (10 μM) was appied at time 0. Arrows show the approximate time at which paroxysmal activity appeared. In all cases, once synchronized activity was established it became difficult to conduct further meaningful VmD measurements as the events increased in frequency and complexity. A. In L2 inhibition declined rapidly for the first 5–6 minutes before stabilizing at around 30–40% of control. Background excitation was largely unaffected. Despite this, the fall in estimated inhibition, the latter predominated throughout and the I:E ratio never fell below 1. B. In L3 inhibition also fell rapidly over 5 minutes and continued to decline reaching a loss of around 85–90%. Simultaneously, excitation showed a gradual increase, although this did not reach significance. The combine effect was a sustained decrease in I:E ration that reversed in favour of excitation around the time when paroxysmal activity appeared. C. Changes in background activity in L5 were similar to those in L3 except that the fall in inhibition was even more precipitous, and reached close to 100% in some cases. D. The time course of changes in I:E ratio show that this occurred more rapidly in L5 than L3 but reached a similar end-point whereas that in L2 never reached the same level as that in either of the deeper layers.
doi:10.1371/journal.pone.0085125.g006

was reduced from 24.2±0.5 mV to 20.7±0.8 mV, and this was significant ($P<0.05$). However, it should be noted that the normalized change was very similar in all three layers (around 9 to 10%). Concurrently, the number of spikes evoked by a long depolarizing pulse was slightly increased in all layers (L2: 4.0±0.8 v 5.7±0.6; L3: 4.3±0.3 v 5.5±1.0; L5: 2.7±0.2 v 3.3±0.9) but none of the changes reached significance. The normalized changes were again similar in all layers (around +13%). Thus, there were indications that the loss of background synaptic inhibition increased intrinsic excitability *per se* (cf [39]), and this could contribute to an overall increase in network excitability.

An important question concerns the origin of the residual inhibition in L2. Our patch clamp studies showed that glycine receptors were likely to make a minor contribution to spontaneous

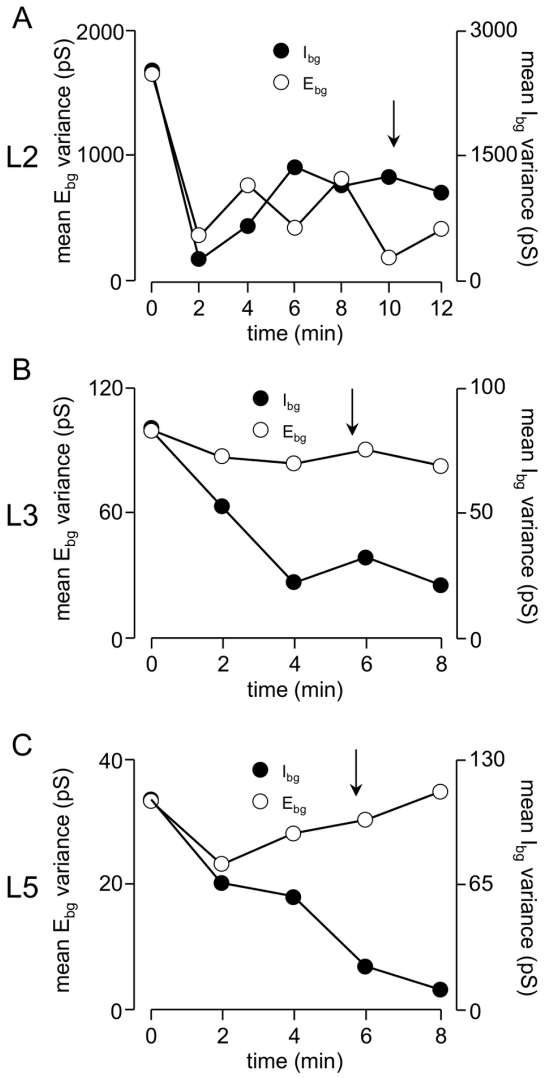

Figure 7. Changes in variance of background conductances during bicuculline perfusion. There were substantial differences in variances between and within layers, but scales have been adjusted to allow for comparison of the time course of changes. A. In L2 the variance (and thus synchronicity) of both inhibition and excitation fall rapidly over 2–3 minutes and thereafter remained reasonably stable at the lower level, although that of inhibition tended to increase again after the first fall. B. In L3 variance of inhibition fell steadily and remained stable whereas that of excitation showed little change. C. Similar to L3, inhibition variance fell throughout in L5, but an initial fall in variance of excitation was followed by a clear recovery to control levels. Again, the arrows indicate the approximate time at which paroxysmal activity appeared.
doi:10.1371/journal.pone.0085125.g007

inhibition in L2, although the VmD analysis did not show a significant fall in I_{bg} with strychnine. Nevertheless, we thought it worthwhile to examine whether strychnine could enhance the epileptogenic effects of bicuculline in L2. In 4 slices where bicuculline failed to elicit synchronous discharges in L2, subsequent addition of strychnine (up to 4 μM) failed to provoke the appearance of such activity. In a further 4 slices where brief discharges were present, these were unaffected by strychnine (1–2 μM). However, in 2 slices, brief synchronized discharges appeared to be enhanced by strychnine (1 μM; not shown), a weak effect that reversed on washing out the antagonist. To attempt to further block the residual inhibition in L2 we combined bicuculline and strychnine with the non-competitive blocker, picrotoxin (n = 4). Fifteen minutes after perfusion with bicuculline and strychnine E_{bg} was essentially unaltered compared to control (4.1±1.1 nS v 4.5±1.2 nS). I_{Bg} was concurrently reduced from 13.9±3.9 nS to 6.3±2.7 nS, similar to or slightly greater than to the fall seen with bicuculline alone (see above). Subsequent addition of picrotoxin saw a further fall in I_{Bg} to 4.9±2.3 nS ($P<0.05$). Overall, the changes reflect a fall in I:E ratio from 4.4±1.1 in control to 1.5±0.6 with all 3 antagonists present, and show that the combined blockers resulted in a greater decline in inhibition (by approximately 60%) than with bicuculline alone (40–50%), although the decrease was still less than that seen with bicuculline alone in either L3 or L5.

The combination of blockers did appear to be associated with an increased severity of epileptiform discharges in L2 (n = 6). This is illustrated Figure 8. In these slices bicuculline-induced discharges were already present, and we applied the other blockers sequentially and cumulatively, and compared the epileptiform activity induced, using extracellular recording. We found that addition of strychnine resulted in a weak enhancement of the discharges in three slices and these were then further enhanced by picrotoxin. In one slice strychnine had little detectable effect, but the discharges were enhanced by picrotoxin. In two other slices picrotoxin was applied first and enhanced the discharge; subsequently, strychnine further enhanced the discharge in one but had little effect in the other. When simultaneous recordings were made in other layers, we saw little change in the local discharges when picrotoxin and strychnine were added to bicuculline.

Discussion

Patch clamp recordings of EPSCs in L3 revealed a greater degree of spontaneous excitation compared to L2 and L5. This was mainly reflected by a substantially higher frequency of sEPSCs. Interestingly, the frequency of mEPSCs was very similar in all 3 layers, indicating that activity dependent release driven by action potentials was considerably higher in L3. Using paired intracellular recordings we have previously shown a relatively high incidence of single axon connections between principal cells in L3 [46]. It is possible that the greater frequency of sEPSCs seen in our patch clamp recordings reflects a high level of spontaneous firing in recurrent axon collaterals between L3 pyramids. What may also be significant is that spontaneous firing rates of L3 neurones *in vivo* is generally higher than those in L5 or L2, which could contribute to greater recurrent excitation in the middle layer [6]. In addition, we have provided evidence for a high degree of electrical coupling between L3 neurones [46], which could reinforce a high level of recurrent excitation. There was a similar incidence of recurrent excitatory connections in L5 and L3, although the recurrent EPSPs were considerably smaller in the deeper layer [46], but a lower neuronal firing rate could be a factor in a lower recurrent excitation and hence lower frequency of sEPSCs. Interestingly, Quilichini *et al.*, [6] found no correlation between the firing rate of neurones and intrinsic excitability suggesting that the former was dependent on the network connectivity rather than biophysical characteristics.

In previous patch clamp recordings we demonstrated that spontaneous GABA release in L2 was dramatically higher than in L5 [37]. The current experiments show strong similarity between L2 and L3 in this respect, with a high level of baseline release. However, in L3, action potential driven IPSCs (around 50%) accounted for a much higher proportion of baseline release than in

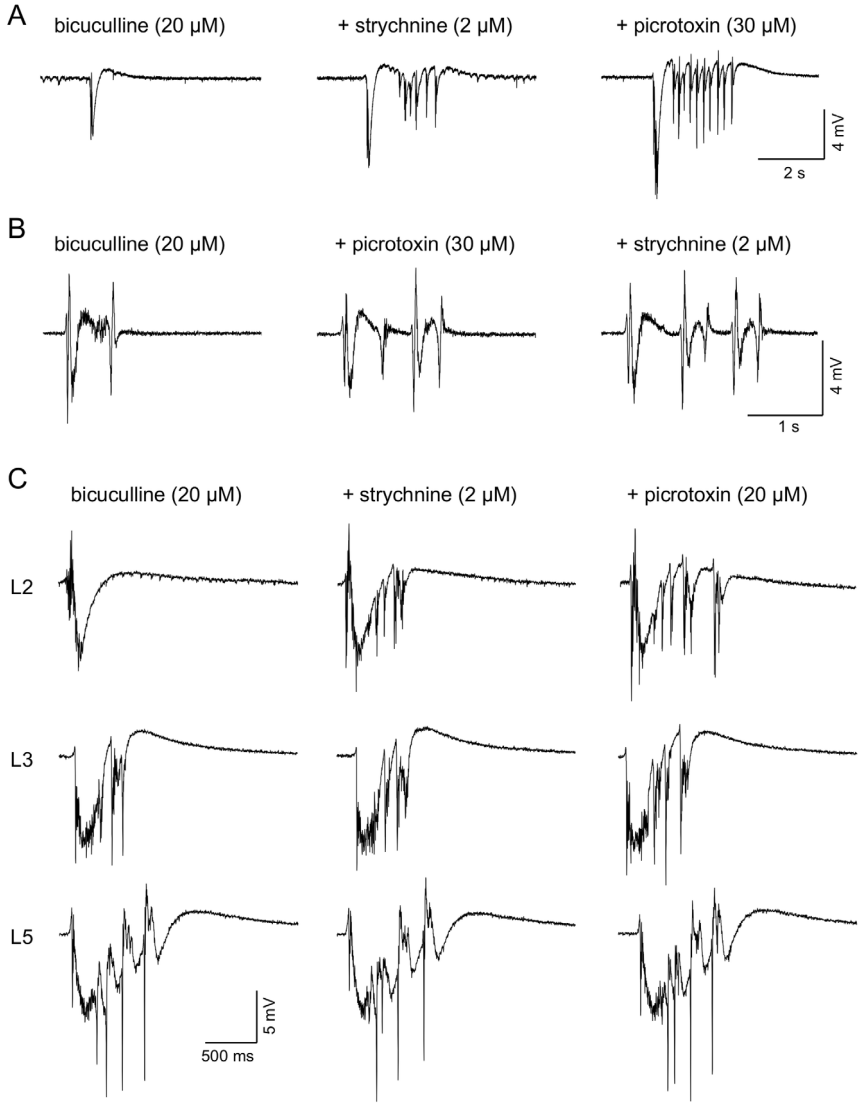

Figure 8. Additional effects of strychnine and glycine on paroxysmal activity in L2. A. In the presence of bicuculline the spontaneous activity recorded in L2 consisted of single brief negative-gong events. Following addition of strychnine this was joined by a series of brief afterdischarges. A further, and more pronounced, exacerbation of the activity was seen when the non-competitive $GABA_A$r antagonist, picrotoxin was added to the cocktail. B. A similar study in L2 of another slice shows that the same result was obtained when the order of application of strychnine and picrotoxin was reversed. C. In this slice we made simultaneous recordings at locations in L2, L3 and L5. Spontaneous events in bicuculline were briefer and less complex than those seen in the deeper layers (cf. Fig. 5). Addition of strychnine and then picrotoxin, as in the other studies increased the duration and complexity of events in L2, but left those in L3 and L5 largely unaltered.
doi:10.1371/journal.pone.0085125.g008

L2, where sIPSC and mIPSC frequencies were almost the same. Thus, a patch-clamp comparison of spontaneous glutamate release in the three layers shows that levels are highest in L3, with L5 next, and L2 lower than L5, but not dramatically so. In contrast, spontaneous GABA release is highest in L2, with L3 similar but L5 dramatically lower than either. Monitoring the frequency of spontaneous currents can be misleading and probably tells us little about the level of functional background inhibition or excitation. Estimating arbitrary charge transfer levels associated with spontaneous currents over time may give us a better picture of this, and these estimations suggested a dominance of inhibition over excitation in all three layers, with a rank order of I:E ratio L2>L3>L5. However, this comparison gives an approximate view of the situation at best because the somatic whole cell patch clamp recordings assess inhibitory and excitatory currents in isolation, and are also likely to exclude many events occurring at distal dendritic sites. Nevertheless, it does give a *relative* picture of what the neurones see from their presynaptic inputs in terms of excitatory and inhibitory network activity.

To obviate some of the limitations associated with the patch clamp recordings, and to align the presynaptic activity with what the neurone undergoes postsynaptically, we made VmD measurements [42] to estimate global background excitation and inhibition. This has a number of advantages: it specifically estimates conductances mediated via AMPAr activation and $GABA_A$r activation, which are, overwhelmingly, the source of background postsynaptic excitation and inhibition, respectively; inhibitory and excitatory conductances are estimated concurrently in the same neurone, and essentially reflect network input to all compartments (somatic, dendritic) integrated across the whole

neurone; within limitations, the variance of the conductances may partly reflect the degree of correlation between presynaptic inputs, and hence, the state of the network; sharp electrode recordings permit simultaneous measures of neuronal excitability.

VmD estimations of postsynaptic conductances generally aligned with the presynaptic activity monitored by the whole cell patch clamp experiments, although relative differences were less pronounced. Thus, E_{bg} was approximately equal in L2 and L5, and, although higher in L3, not dramatically so. I_{bg} was highest in L2, lower in L3, but considerably lower in L5 compared to the more superficial neurones. In agreement with CT estimations from the patch clamp recordings, I:E ratios from VmD estimations again showed a dominance of inhibition over excitation in all three layers, and the rank order was the same, albeit with a somewhat reduced difference between L3 and L5. This suggests that the dominant effect of on-going presynaptic network activity in all layers in our slices is inhibition. Although the brain slice, with its reduced synaptic network, reflects a generally quiescent situation, there is qualitative agreement with the situation *in vivo*. For example, VmD estimations from *in vivo* intracellular recordings in parietal cortex (layer not specified) of un-anaesthetized cats [54], show that an inhibition-dominant network situation is extant during both the awake state, and during natural sleep, although the I:E ratio in the latter was higher in the former (approx. 3.9) compared to the latter (approx. 2.6). Interestingly, the I:E ratio during wakefulness is similar to that seen in L3 and L5 neurones in our experiments, whilst that in L2 approximated the sleep state in vivo. It would be a huge leap of imagination to propose that the networks in L5/L3 are in an "awake state" whereas that in L2 is "sleeping", but the data does suggest that network excitability in L2 and, thus, afferent transfer to the hippocampus, is very tightly controlled by synaptic inhibition.

It has been suggested that the variance of postsynaptic background synaptic conductances may give an estimate of the average correlation of inhibitory or excitatory activity in the presynaptic inputs, with a high variance predicting some degree of synchronization [42–44]. It should be noted that this prediction relates to the in vivo situation where transmitter release rates are likely to be much higher than in our slices. Examination of the variances across layers in our slices reveals that the most obvious difference was the high degree of variance in both E_{bg} and I_{bg} in L2 compared to L3 and L5. If we make the assumption that conductance variance provides a measure of synaptic correlation, even under the relatively quiescent conditions in the slice, this could be taken as evidence that there is some degree of synchronization in the network of L2. This may be supported by observations that the power of theta, gamma and high-frequency oscillations, which could reflect synchronized network activity, is high in superficial layers compared to the deeper layers [5,6,55,56].

If we accept that that there may be some correlated activity in L2 synaptic inputs, it is possible to speculate that such a property could be related to the level and organization of synaptic inhibition. It is clear that number, diversity, and synaptic connectivity of inhibitory neurones is progressively greater as we move from L5 through L3 to L2 of the EC [57–69], and this is reflected by functional measures of inhibition (present study; [37,38]). Network synchrony can be driven by interneurone-interneurone interactions and/or interneurone/principal cell interconnectivity [70–73]. Thus, it is possible that the high variance of I_{bg} in L2 is at least partly due to correlated release from GABA inputs resulting from interneuronal interactions with principal neurones and other interneurones. Using paired cell recordings we demonstrated a paucity of recurrent connectivity between principal neurones in L2 [46]. This was confirmed by a recent study [74], which also showed that the high level of inhibition in L2 is congruent with extensive interconnectivity of principal neurones via interneurones. We previously demonstrated that basket-like interneurones in L2 have widespread axonal arbors restricted to the layer and have a powerful NMDAr mediated excitatory drive [75]. A reduction in the number of these neurones or blockade of the NMDAr-mediated drive onto them disrupts gamma oscillations, which may depend on synchrony within the principal neurone-interneurone connectivity [76].

It has long been accepted that synaptic inhibition is able to "balance" and control neuronal excitation. Trevelyan *et al.*, [77] provided a very clear demonstration of how emergence of network synchronization during epileptiform activity is restrained by on-going synaptic inhibition. In our studies, reducing background inhibition by blocking $GABA_AR$ resulted in a rapid synchronization in L5 and the emergence of interictal-like epileptiform activity. Despite a much higher level of background inhibition, the result was almost identical in L3, and this could be associated with the higher initial E_{bg} in this layer, suggesting that the inhibition-excitation balance is crucial in restraining network synchronization. Paradoxically, L2, which may already have a degree of correlative activity in its synaptic networks, was relatively resistant to emergent network synchronization when inhibition was pharmacologically reduced with bicuculline. Emergent synchronization was delayed, was less marked than in other layers, and was not seen in some slices that did display such activity in other layers.

Examination of the changes in I_{bg} and E_{bg} during bicuculline perfusion revealed that the former fell rapidly and network synchronization emerged around the time when its absolute value was exceeded by the latter, in both L5 and L3. However, this did not occur in L2 and normalized data showed that I_{bg} was reduced by only 50–60% compared to 80–90% in the deeper layers. Residual inhibition in L2 could have a source other than $GABA_Ar$ activation, and one possibility is that it could be mediated by glycine. There is evidence for expression of glycine receptors in the EC with the β-subunit, in particular, apparently localized to the superficial layers [78] and glycine elicits strychnine-sensitive inward currents in L2 neurones [79]. sIPSC frequency is weakly reduced by strychnine in L2 but not L5 (present study; [37]). The VmD approach will not readily distinguish between GABA and glycine as the reversal potentials for the two are essentially the same, but we did not find any overwhelming evidence that glycine receptors make a major contribution to the residual inhibition in L2. I_{bg} showed a very small, but non-significant fall during blockade of receptors with strychnine. Although we occasionally found that strychnine appeared to enhance the synchronizing effects of $GABA_Ar$ blockade in L2, in the majority of cases it had no such effect. Interestingly, glycine receptors in L2 can be desensitized by GABA but the reverse is not true [79]. Thus, it is possible that glycine inhibition may actually become more effective as GABA-inhibition is reduced by bicuculline, but this was not really supported by the failure of strychnine to consistently enhance the effects of bicuculline. Finally, strychnine also slightly reduced sIPSCs in L3 as well as L2, but residual inhibition was not evident in in VmD estimations in the former.

An alternative explanation for residual inhibition is that very high levels of ambient GABA associated with spontaneous release are able to compete with the bicucullne to maintain the level of spontaneous inhibition. Addition of the non-competitive $GABA_Ar$ blocker, PTX did reduce I_{Bg} to a greater extent than bicuculline alone, although there was still around 30–35% residual inhibition in L2. Thus, the source of the residual inhibition in L2 is still a

matter for debate, but what seems clear is that the overall "inhibitory veto" [70] is much stronger in this layer than in L3 and L5.

The significance of our results for the overall functional roles of the EC in physiological processes is a matter for speculation at present. Nevertheless, it is clear that the network properties across layers support very different processing roles and capabilities. For example, as mentioned above, L2 neurones express prominent grid cell properties that contribute to a vital role in spatial navigation. Grid firing is suggested to be generated within the recurrent inhibitory microcircuitry of this layer rather than dependent on recurrent excitatory interactions [74]. Our current, and previous, observations [38,46,75] support the suggestion of predominance of recurrent inhibition in this layer and an inherent rhythmicity in this network that could help define grid cell activity. The powerful background synaptic inhibition may be crucial in this regard. Destexhe [44] has argued that spike firing and patterning in cortical networks is determined by fluctuations in background inhibitory "noise". The high level of background inhibition, coupled with a low level of background excitation could support a crucial role in determining grid cell patterning. Varying ratios could be deterministic in different firing patterns and functionalities in other layers.

Author Contributions

Conceived and designed the experiments: RSGJ GLW SDG SELC KHY. Performed the experiments: RSGJ GLW SDG SELC AL PVM KHY. Analyzed the data: RSGJ GLW SDG SELC AL PVM. Wrote the paper: RSGJ GLW SDG SELC AL PVM.

References

1. Eichenbaum H (2001) The long and winding road to memory consolidation. Nat Neurosci 4: 1057–1058.
2. Squire LR, Stark CE, Clark RE (2004) The medial temporal lobe. Ann Rev Neurosci 27: 279–306.
3. Witter MP, Moser EI (2006) Spatial representation and the architecture of the entorhinal cortex. Trends Neurosci 29: 671–678.
4. Cunningham MO, Pervouchine DD, Racca C, Kopell NJ, Davies CH, et al. (2006) Neuronal metabolism governs cortical network response state. Proc Natl Acad Sci USA 103: 5597–5601.
5. Cunningham MO, Davies CH, Buhl EH, Kopell N, Whittington MA (2003) Gamma oscillations induced by kainate receptor activation in the entorhinal cortex in vitro. J Neurosci 23: 9761–9769.
6. Quilichini P, Sirota A, Buzsáki G (2010) Intrinsic circuit organization and theta-gamma oscillation dynamics in the entorhinal cortex of the rat. J Neurosci 30: 11128–11142.
7. Rutecki PA, Grossman RG, Armstrong D, Irish-Loewen S (1989) Electrophysiological connections between the hippocampus and entorhinal cortex in patients with complex partial seizures. J Neurosurg 70: 667–675.
8. Lothman EW, Bertram EH, Kapur J, Stringer JL (1990) Recurrent spontaneous hippocampal seizures in the rat as a chronic sequalae to limbic status epilepticus. Epilepsy Res 6: 110–119.
9. Spencer SS, Spencer DD (1994) Entorhinal-hippocampal interactions in medial temporal lobe epilepsy syndrome. Epilepsia 35: 721–727.
10. Siegel AN, Wieser HG, Wichnann W, Yasargil GM (1990) Relationships between MR imaged total amount of tissue removed, resection scores of specific mediobasal limbic sub-compartments and clinical outcome following selective amygdala-hippocampectomy. Epilepsy Res 63: 56–65.
11. Goldring S, Edwards I, Harding GW, Bernardo KL (1992) Results of anterior temporal lobectomy that spares the amygdala in patients with complex partial seizures. J Neurosurg 77: 185–193.
12. Sperling MR, O'Connor MF, Saykin AJ, Plummer C (1996) Temporal lobectomy for refractory epilepsy. J Am Med Ass 276: 470–475.
13. Wennberg R, Arruda F, Quesney LF, Olivier A (2002) Pre-eminence of extra-hippocampal structures in the generation of mesial temporal seizures: evidence from human depth electrode recordings. Epilepsia 4: 716–726.
14. Du F, Whetsell WO, Abu-Khalil B, Blumenkopf B, Lothman EW, et al. (1993) Preferential neuronal loss in layer III of the entorhinal cortex in patients with temporal lobe epilepsy. Epilepsy Res 16: 223–233.
15. Bernasconi N, Natsume J, Bernasconi A (2005) Progression in temporal lobe epilepsy: differential atrophy in mesial temporal structures. Neurology 6: 223–228.
16. Avoli M, Barbarosie M, Lucke A, Nagao T, Lopantsev V, et al. (1996) Synchronous GABA-mediated potentials and epileptiform discharges in the rat limbic system in vitro. J Neurosci 16: 3912–3924.
17. Bear J, Lothman EW (1993) An in vitro study of focal epileptogenesis in combined hippocampal-parahippocampal slices. Epilepsy Res 14: 183–193.
18. Jones RSG (1988) Epileptiform events induced in entorhinal cortical cells by GABA-antagonists in vitro are partly mediated by N-methyl-D-aspartate receptors. Brain Res 457: 113–121.
19. Jones RSG (1994) Synaptic and intrinsic responses of cells of origin of the perforant path in layer II of the rat entorhinal cortex in vitro. Hippocampus 4: 335–353.
20. Jones RSG, Lambert JDC (1990) Synchronous discharges in the rat entorhinal cortex in vitro: Site of initiation and the role of excitatory amino acid receptors. Neuroscience 34, 657–670.
21. Jones RSG, Lambert JDC (1990) The role of excitatory amino acid receptors in the propagation of epileptiform discharges from entorhinal cortex to the dentate gyrus in vitro. Exp Brain Res 80: 310–322.
22. Rafiq A, DeLorenzo RJ, Coulter DA (1993) Generation and propagation of epileptiform discharges in a combined entorhinal cortex/hippocampal slice. J Neurophysiol 70: 1962–1974.
23. Walther H, Lambert JD, Jones RSG, Heinemann U, Hamon B (1986) Epileptiform activity in combined slices of the hippocampus, subiculum and entorhinal cortex during perfusion with low magnesium medium. Neurosci Lett 69: 156–161.
24. Iijima T, Witter MP, Ichikawa M, Tominaga T, Kajiwara R, et al. (1996) Entorhinal-hippocampal interactions revealed by real-time imaging. Science 272: 1176–1179.
25. Buchheim K, Weissinger F, Siegmund H, Holtkamp M, Schuchmann S, et al. (2002) Intrinsic optical imaging reveals regionally different manifestation of spreading depression in hippocampal and entorhinal structures in vitro. Exp Neurol 175: 76–86.
26. Weissinger F, Buchheim K, Siegmund H, Heinemann U, Meierkord H (2000) Optical imaging reveals characteristic seizure onsets, spread patterns, and propagation velocities in hippocampal-entorhinal cortex slices of juvenile rats. Neurobiol Dis 7: 286–298.
27. D'Arcangelo G, Tancredi V, Avoli M (2001) Intrinsic optical signals and electrographic seizures in the rat limbic system. Neurobiol Dis: 993–1005.
28. Lopantsev V, Avoli M (1996) Reverberation of chloride-dependent synaptic potentials in the rat entorhinal cortex in vitro. Neurosci Lett 210: 5–8.
29. Jones RSG (1993) Entorhinal-hippocampal connections: a speculative view of their function. Trends Neurosci 16: 58–64.
30. Pare D, Shink E, Gaudreau H, Destexhe A, Lang EJ (1998) Impact of spontaneous synaptic activity on the resting properties of cat neocortical pyramidal neurons in vivo. J Neurophysiol 79: 1450–1460.
31. Shu Y, Hasenstaub A, Badoual M, Bal T, McCormick DA (2003) Barrages of synaptic activity control the gain and sensitivity of cortical neurons. J Neurosci 23: 10388-103401.
32. Stacey WC, Durand DM (2001) Synaptic noise improves detection of subthreshold signals in hippocampal CA1 neurons. J Neurophysiol 86: 1104–1112.
33. Destexhe A, Pare D (1999) Impact of network activity on the integrative properties of neocortical pyramidal neurons in vivo. J Neurophysiol 81: 1531–1547.
34. Ho N, Destexhe A (2000) Synaptic background activity enhances the responsiveness of neocortical pyramidal neurons. J Neurophysiol 84: 1488–1496.
35. Berretta N, Jones RSG (1996) A comparison of spontaneous synaptic EPSCs in layer V and layer II neurones in the rat entorhinal cortex in vitro. J Neurophysiol 76: 1089–1100.
36. Bailey SJ, Dhillon A, Woodhall GL, Jones RSG (2004) Lamina-specific differences in $GABA_B$-autoreceptor mediated regulation of spontaneous GABA release in rat entorhinal cortex. Neuropharmacology 46: 31–42.
37. Woodhall GL, Bailey SJ, Thompson SE, Evans DI, Jones RSG (2005) Fundamental differences in spontaneous synaptic inhibition between deep and superficial layers of the rat entorhinal cortex. Hippocampus 15: 232–245.
38. Jones RSG, Woodhall GL (2005) Background synaptic activity in rat entorhinal cortical neurones: differential control of transmitter release by presynaptic receptors. J Physiol 562: 107–120.
39. Greenhill SD, Jones RSG (2007) Simultaneous estimation of global background synaptic inhibition and excitation from membrane potential fluctuations in layer III neurones of the rat entorhinal cortex in vitro. Neuroscience 147: 884–892.
40. Greenhill SD, Jones RSG (2010) Diverse antiepileptic drugs increase the ratio of background synaptic inhibition to excitation and decrease neuronal excitability in neurones of the rat entorhinal cortex in vitro. Neuroscience 167: 456–474.
41. Greenhill SD, Morgan NH, Massey PV, Woodhall GL, Jones RSG (2012) Ethosuximide modifies network excitability in the rat entorhinal cortex via an increase in GABA release. Neuropharmacology 62: 807–814.
42. Rudolph M, Piwkowska Z, Badoual M, Bal T, Destexhe A (2004) A method to estimate synaptic conductances from membrane potential fluctuations. J Neurophysiol 91: 2884–2896.
43. Rudolph M, Destexhe A (2004) Inferring network activity from synaptic noise. J Physiol Paris 98: 452–466.

44. Destexhe A (2010) Inhibitory "noise". Front Cell Neurosci 4(9): 1–7.
45. Jones RSG, Heinemann U (1988) Synaptic and intrinsic responses of medial entorhinal cortical cells in normal and magnesium-free medium in vitro. J Neurophysiol 59: 1476–1496.
46. Dhillon A, Jones RSG (2000) Laminar differences in recurrent excitatory transmission in the rat entorhinal cortex in vitro. Neuroscience 99: 413–422.
47. Alonso A, Klink R (1993) Differential electroresponsiveness of stellate and pyramidal-like cells of medial entorhinal cortex layer II. J Neurophysiol 70: 128–143.
48. Klink R, Alonso A (1993) Ionic mechanisms for the subthreshold oscillations and differential electroresponsiveness of medial entorhinal cortex layer II neurons. J Neurophysiol 70: 144–57.
49. Alonso A, Llinás RR (1989) Subthreshold Na^+-dependent theta-like rhythmicity in stellate cells of entorhinal cortex layer II. Nature 342: 175–177.
50. Erchova I, Kreck G, Heinemann U, Herz AV (2004) Dynamics of rat entorhinal cortex layer II and III cells: characteristics of membrane potential resonance at rest predict oscillation properties near threshold. J Physiol 560: 89–110.
51. Hamam BN, Kennedy TE, Alonso A, Amaral DG (2000) Morphological and electrophysiological characteristics of layer V neurons of the rat medial entorhinal cortex. J Comp Neurol 418: 457–472.
52. Dickson CT, Magistretti J, Shalinsky M, Hamam B, Alonso A (2000) Oscillatory activity in entorhinal neurons and circuits. Mechanisms and function. Ann N Y Acad Sci 911: 127–150.
53. Schmitz D, Gloveli T, Behr J, Dugladze T, Heinemann U (1998) Subthreshold membrane potential oscillations in neurons of deep layers of the entorhinal cortex. Neuroscience 85: 999–1004
54. Rudolph M, Pospischil M, Timofeev I, Destexhe A (2007) Inhibition determines membrane potential dynamics and controls action potential generation in awake and sleeping cat cortex. J Neurosci 27: 5280–5290.
55. Cunningham MO, Halliday DM, Davies CH, Traub RD, Buhl EH, et al. (2004) Coexistence of gamma and high-frequency oscillations in rat medial entorhinal cortex in vitro. J Physiol 559: 347–353.
56. Cunningham MO, Whittington MA, Bibbig A, Roopun A, LeBeau FE, et al. (2004) A role for fast rhythmic bursting neurons in cortical gamma oscillations in vitro. Proc Natl Acad Sci USA 101: 7152–7157.
57. Kohler C, Wu JY, Chan-Palay V (1985) Neurons and terminals in the retrohippocampal region in the rat's brain identified by anti-gamma-aminobutyric acid and anti-glutamic acid decarboxylase immunocytochemistry. Anat Embryol 173: 335–344.
58. Kohler C, Chan-Palay V (1982) The distribution of cholecystokinin-like immunoreactive neurons and nerve terminals in the retrohippocampal region in the rat and guinea pig. J comp Neurol 210: 136–146.
59. Kohler C, Chan-Palay V (1983) Somatostatin and vasoactive intestinal polypeptide-like immunoreactive cells and terminals in the retrohippocampal region of the rat brain. Anat Embryol 167: 151–172.
60. Lotstra F, Vanderhaeghen JJ (1987) High concentration of cholecystokinin neurons in the newborn human entorhinal cortex. Neurosci Lett 80: 191–196.
61. Rogers JH (1992) Immunohistochemical markers in rat cortex: co-localization of calretinin and calbindin-D28k with neuropeptides and GABA. Brain Res 587: 147–157.
62. Wouterlood FG, Hartig W, Bruckner G, Witter MP (1995) Parvalbumin-immunoreactive neurons in the entorhinal cortex of the rat: localization, morphology, connectivity and ultrastructure. J Neurocytol 24: 135–153.
63. Wouterlood FG, van Denderen JC, van Haeften T, Witter MP (2000) Calretinin in the entorhinal cortex of the rat: distribution, morphology, ultrastructure of neurons, and co-localization with gamma-aminobutyric acid and parvalbumin. J comp Neurol 425: 177–192.
64. Wouterlood FG, Pothuizen H (2000) Sparse colocalization of somatostatin- and GABA-immunoreactivity in the entorhinal cortex of the rat. Hippocampus 10: 77–86.
65. Fujimaru Y, Kosaka T (1996) The distribution of two calcium binding proteins, calbindin D-28K and parvalbumin, in the entorhinal cortex of the adult mouse. Neurosci Res 24: 329–343.
66. Miettinen M, Koivisto E, Riekkinen P, Miettinen R (1996) Coexistence of parvalbumin and GABA in nonpyramidal neurons of the rat entorhinal cortex. Brain Res 706: 113–122.
67. Miettinen M, Pitkanen A, Miettinen R (1997) Distribution of calretinin-immunoreactivity in the rat entorhinal cortex: coexistence with GABA. J comp Neurol 378: 363–378.
68. Mikkonen M, Soininen H, Pitkanen A (1997) Distribution of parvalbumin-, calretinin-, and calbindin-D28k-immunoreactive neurons and fibers in the human entorhinal cortex. J comp Neurol 388: 64–88.
69. Arellano JI, DeFelipe J, Munoz A (2002) PSA-NCAM immunoreactivity in chandelier cell axon terminals of the human temporal cortex. Cereb Cortex 12: 617–624.
70. Cobb SR, Buhl EH, Halasy K, Paulsen O, Somogyi P (1995) Synchronization of neuronal activity in hippocampus by individual GABAergic interneurons. Nature 378: 75–78.
71. Traub RD, Cunningham MO, Gloveli T, LeBeau FE, Bibbig A, et al. (2003) GABA-enhanced collective behavior in neuronal axons underlies persistent gamma-frequency oscillations. Proc Natl Acad Sci USA 100: 11047–11052.
72. Traub RD, Bibbig A, LeBeau FE, Cunningham MO, Whittington MA (2005) Persistent gamma oscillations in superficial layers of rat auditory neocortex: experiment and model. J Physiol 562: 3–8.
73. Traub RD, Bibbig A, LeBeau FE, Buhl EH, Whittington MA (2004) Cellular mechanisms of neuronal population oscillations in the hippocampus in vitro. Ann Rev Neurosci 27: 247–278.
74. Couey JJ, Witoelar A, Zhang SJ, Zheng K, Ye J, et al. (2013) Recurrent inhibitory circuitry as a mechanism for grid formation. Nat Neurosci 16: 318–324.
75. Jones RSG, Buhl EH (1993) Basket-like interneurones in layer II of the entorhinal cortex exhibit a powerful NMDA-mediated synaptic excitation. Neurosci Lett 149: 5–9.
76. Cunningham MO, Hunt J, Middleton S, LeBeau FE, Gillies MJ, et al. (2006) Region-specific reduction in entorhinal gamma oscillations and parvalbumin-immunoreactive neurons in animal models of psychiatric illness. J Neurosci 26: 2767–2776.
77. Trevelyan AJ, Sussillo D, Watson BO, Yuste R (2006) Modular propagation of epileptiform activity: evidence for an inhibitory veto in neocortex. J Neurosci 26: 12447–12455.
78. Malosio ML, Marquèze-Pouey B, Kuhse J, Betz H (1991) Widespread expression of glycine receptor subunit mRNAs in the adult and developing rat brain. EMBO J 10: 2401–2409.
79. Breustedt J, Schmitz D, Heinemann U, Schmieden V (2004) Characterization of the inhibitory glycine receptor on entorhinal cortex neurons. Eur J Neurosci 19: 1987–1991.

PLOS | ONE

RESEARCH ARTICLE

Differential Effects of D-Cycloserine and ACBC at NMDA Receptors in the Rat Entorhinal Cortex Are Related to Efficacy at the Co-Agonist Binding Site

Alex M. Lench, Emma Robson, Roland S. G. Jones*

Department of Pharmacy and Pharmacology, University of Bath, Bath, United Kingdom

* r.s.g.jones@bath.ac.uk

Citation: Lench AM, Robson E, Jones RSG (2015) Differential Effects of D-Cycloserine and ACBC at NMDA Receptors in the Rat Entorhinal Cortex Are Related to Efficacy at the Co-Agonist Binding Site. PLoS ONE 10(7): e0133548. doi:10.1371/journal.pone.0133548

Editor: Shashank M. Dravid, Creighton University, UNITED STATES

Received: March 9, 2015

Accepted: June 29, 2015

Published: July 20, 2015

Data Availability Statement: All relevant data are within the paper and its Supporting Information files.

Funding: The Medical Research Council provided a studentship and materials for Alex Lench. The Biotechnology and Biological Sciences Research Council Provided a studentship for Emma Robson. The funders had no role in study design, data collection and analysis, decision to publish, or preparation of the manuscript.

Competing Interests: The authors have declared that no competing interests exist.

Abstract

Partial agonists at the NMDA receptor co-agonist binding site may have potential therapeutic efficacy in a number of cognitive and neurological conditions. The entorhinal cortex is a key brain area in spatial memory and cognitive processing. At synapses in the entorhinal cortex, NMDA receptors not only mediate postsynaptic excitation but are expressed in presynaptic terminals where they tonically facilitate glutamate release. In a previous study we showed that the co-agonist binding site of the presynaptic NMDA receptor is endogenously and tonically activated by D-serine released from astrocytes. In this study we determined the effects of two co-agonist site partial agonists on both presynaptic and postsynaptic NMDA receptors in layer II of the entorhinal cortex. The high efficacy partial agonist, D-cycloserine, decreased the decay time of postsynaptic NMDA receptor mediated currents evoked by electrical stimulation, but had no effect on amplitude or other kinetic parameters. In contrast, a lower efficacy partial agonist, 1-aminocyclobutane-1-carboxylic acid, decreased decay time to a greater extent than D-cycloserine, and also reduced the peak amplitude of the evoked NMDA receptor mediated postsynaptic responses. Presynaptic NMDA receptors, (monitored indirectly by effects on the frequency of AMPA receptor mediated spontaneous excitatory currents) were unaffected by D-cycloserine, but were reduced in effectiveness by 1-aminocyclobutane-1-carboxylic acid. We discuss these results in the context of the effect of endogenous regulation of the NMDA receptor co-agonist site on receptor gating and the potential therapeutic implications for cognitive disorders.

Introduction

The entorhinal cortex (EC) acts as a crucial dynamic processer of information entering and leaving the hippocampus, controlling its interaction with the rest of the neuraxis. This intimate association means that the EC plays a pivotal role in declarative and spatial memory, particularly spatial cognition, representation and navigation, and in other cognitive processes such as

attention, and conditioning [1–5]. Dysfunction of the EC and of EC-hippocampal interactions has been implicated in many pathological conditions, particularly initiation and propagation of temporal lobe seizures and the cognitive abnormalities/decline associated with a variety of psychiatric/neurological disorders (including schizophrenia, bipolar and depressive disorders, Alzheimer's disease, Parkinson's disease, Huntington's disease, amyotrophic lateral sclerosis etc.; see refs in [6]). This laboratory has a longstanding interest in control of neuronal activity and excitability in entorhinal networks. One focus of this research has been the role and regulation of NMDA receptors (NMDArs) in both normal synaptic function and epileptic activity [6–8].

The NMDAr consists of two obligatory GluN1 subunits and two GluN2 subunits. A glutamate binding site is present on the GluN2 subunit whilst a co-agonist site that can be activated endogenously by both glycine and D-serine is located on the GluN1 subunit. There has been an interest in targeting the NMDAr co-agonist binding site for therapeutic treatment of CNS disorders (see [9]). Cognitive decline is a pronounced characteristic of Alzheimer's disease and other dementias, but is also a feature of Parkinson's disease, Huntington's disease, stroke, amyotrophic lateral sclerosis, epilepsy, and psychosis [10–15]. D-cycloserine (DCS), which is used therapeutically as an antimicrobial agent, is a partial agonist at the NMDAr co-agonist binding site, and has been demonstrated to induce cognitive enhancement at low doses in behavioural and psychological studies [16–25]. Thus, it could be useful in treatment of neurodegenerative disorders involving cognitive decline, in therapy of mood and thought disorders such as schizophrenia and depression, and for augmenting psychotherapies for the treatment of drug addiction and anxiety disorders. On the other hand, DCS has also been suggested to have direct antiepileptic actions or be a useful adjunct in the treatment of epilepsy [26–28]. In this context it is interesting that epilepsy is often associated with cognitive impairment, and this may be related to a loss of D-serine and reduced co-agonist regulation of the NMDAr [29]. Thus, DCS could have a dual effect to reduce seizures and restore cognitive activity in people with epilepsy.

We have previously shown that presynaptic NMDArs (preNMDArs) on excitatory terminals can tonically facilitate the release of glutamate at EC synapses [30–32]. These receptors are predominantly diheteromeric GluN1-N2B receptors [8,31,32] whereas those located postsynaptically at the same sites may be largely triheteromeric GluN1-N2A-N2B receptors [8]. Recently, we have investigated the co-agonist regulation of the preNMDAr and shown that endogenous D-serine, released from astrocytes, is the preferred ligand for the co-agonist-binding site, which appears to be fully saturated by the ligand under baseline conditions [33]. Given the potential therapeutic relevance of the co-agonist binding site, we have now examined the effects of partial agonists at this site. We compared effects on the presynaptic NMDAr-mediated regulation of glutamate release in the EC to actions on NMDAr-mediated responses at postsynaptic sites (postNMDAr). Our data indicate a differential modulation of the receptors by the two partial agonists, which was apparently dependent on efficacy. These effects could be relevant to putative therapeutic actions of the ligands.

Materials and Methods

Ethics Statement

Experiments conformed with the U.K. Animals (Scientific Procedures) Act 1986, European Communities Council Directive 1986 (86/609/EEC) and were subject to conformity with the University of Bath ethical review document. The research reported in this study is not directly regulated by Home Office procedures, as it was all conducted using Schedule 1 procedures. Nevertheless, all experiments were subject to internal ethical review and were specifically approved by the University's Animal Welfare and Ethical Review Body Committee. This

ensures that the minimum number of animals is used and that every precaution is taken to reduce suffering and stress. All research involving use of animal tissue at the University of Bath requires a consideration of ethical implications by the principal investigator. A second investigator, external to the research group, reviews this and signatory approval from both the external reviewer and Head of Department, is required preceding further review by the Departmental Research Ethics Officer. The Ethics Officer submits a report to the Animal Welfare and Ethical Review Body Committee discussion with the investigator. These processes ensure that ethical implications of the research have been adequately considered and that there is a process in place for managing ethical issues. The Animal Users Committee monitors all licenced and Schedule 1 procedures at quarterly meetings.

Slice preparation

Combined hippocampal-entorhinal brain slices from male or female juvenile Wistar rats (50–100g; P28–38) were prepared as described previously [34]. Following cervical dislocation, rats were decapitated and the brain rapidly removed into oxygenated artificial cerebrospinal fluid (aCSF; see below for composition) at 4°C. Slices (300 μm thick) were cut (Campden Vibroslice or Model 7000smz microtomes) at 4°C and transferred to a storage chamber containing oxygenated aCSF maintained at room temperature. They were allowed to recover for 1 hour before being used for electrophysiological recording. The aCSF contained (in mM) NaCl (126), KCl (4), $MgSO_4$ (1.25), NaH_2PO_4 (1.4), $NaHCO_3$ (24), $CaCl_2$ (2), D-glucose (10), ascorbic acid (0.57), sodium pyruvate (5) and creatinine monohydrate (5). Ketamine (4 μM), indomethacin (45 μM), aminoguanidine (25 μM) and Coomassie Brilliant Blue (250 nM) were included in the cutting solution, and both cutting and storage solutions also contained the antioxidants, n-acetyl-L-cysteine (2 μM) and uric acid (100 μM), to aid neuronal survival and viability. We have previously established that the use of these additives facilitates production of robust and viable slices, but does not affect the pharmacology of glutamate transmission. Of particular concern is the possibility that residual ketamine may compromise studies of NMDAr responses in the experiments. However, we have used ketamine as a neuroprotectant, both as an anaesthetic prior to decapitation and in cutting solutions for over 20 years, and before introducing it into routine use investigated this extensively, finding no evidence that this was an issue. In our current protocols, slices are kept in a ketamine-free storage chamber for a minimum of 1 hour (in reality most are stored for 2 hours plus) before transfer and then washed in the recording chamber for a further 30–40 minutes before recording. The storage chamber has a large-sink circulating volume of around 40 ml and the recording chamber is perfused at 2 ml/min. The very high reverse rate constant for ketamine means that its dissociation from the receptor channel is likely to be rapid and complete before actual recording commences. The ability to elicit large repeatable NMDAr responses in the tissue suggests that residual ketamine is unlikely to be an issue.

Whole-cell patch clamp recordings

After recovery, individual slices were transferred to a chamber on an Olympus BX50WI microscope and perfused (~2 ml/min) with oxygenated aCSF at 31–32°C, where they were allowed to further equilibrate before recording began. Neurones were visualised using differential interference contrast optics and an infrared video camera.

Whole cell patch clamp recordings were made with an Axopatch 200A or 200B amplifier using borosilicate glass pipettes pulled on a Flaming-Brown microelectrode puller. To record AMPA receptor (AMPAr) mediated miniature excitatory postsynaptic currents (mEPSCs) we used a Cs-gluconate based intracellular solution containing (in mM) D-gluconate (100),

HEPES (40), QX-314 (1), EGTA (0.6), NaCl (2), Mg-gluconate (5), tetraethylammonium-Cl (5), phosphocreatinine (10), ATP-Na (4), GTP-Na (0.3) and MK801 (5mM). The solution was adjusted to pH 7.3 with CsOH and to 275–290 mOsm by dilution. Recordings were conducted in the presence of TTX (1 μM) to eliminate activity-dependent glutamate release. To permit recording of AMPAr-mediated responses in isolation, postNMDArs were blocked by inclusion of MK-801 in the patch pipettes. This also allowed us to monitor activity at preNMDArs without the complication of postsynaptic receptor activation/blockade. This approach was developed and validated in this laboratory [7,30–32], and has been used successfully by others [35–40].

Miniature EPSCs were recorded at a holding potential of -60mV, filtered at 2 kHz, digitised at 50kHz, and stored using AxoScope software. Access resistance was monitored at 5-minute intervals throughout recording and if it varied by greater than 15% neurones were excluded from analysis. Series resistance compensation was not used. Input resistances for the neurones recorded in these studies were of the order 500–700 MΩ. Data recording commenced 15–20 minutes after gaining whole cell access and then continued for at least 15 minutes during control and each drug treatment condition. mEPSCs were analysed offline using a threshold-crossing algorithm in Minianalysis software (Synaptosoft, Decatur) over stable 5-minute periods of recording. Average frequency was compared before and after drug application. Amplitudes of spontaneous currents were determined as median values for each neurone as these better reflect the population distributions (normal distribution with a skew towards larger amplitude events) than arithmetical means. Median values were then averaged for comparative illustrative purposes. We have used this approach in previous studies [41]. The kinetics of mEPSCs were compared via arithmetical means. Statistical comparisons of drug effects on mean frequency and kinetics and mean median amplitudes within cells employed a two-tailed paired t-test.

Evoked postsynaptic responses were elicited by electrical stimulation using a bipolar tungsten electrode placed on the surface of the slice lateral to the recording site in the EC. Bipolar pulses (10–30 mA, 100 ms duration) were delivered at intervals of 20 seconds. Again, recordings were made using whole cell patch clamp but without intracellular MK801 and extracellular TTX. To isolate evoked NMDAr-mediated EPSCs (eNEPSCs), neurones were recorded at a holding potential of +40 mV in the presence of NBQX (10 μM), bicuculline (20 μM) and picrotoxin (50 μM). That NMDArs mediated the recorded responses was confirmed by abolition with 2-AP5. After gaining whole cell access, no stimulation was applied for at least 20 minutes to allow series resistance and cell activity to stabilise. Drugs were applied by addition to the perfusion aCSF, and each concentration was perfused for 10 minutes before increasing to the next to construct cumulative concentration-response curves. The amplitude, rise time and decay time of eNEPSCs were analysed off-line using Minianalysis software (Synaptosoft, Decatur). In analysis of various treatments on decay time, this was calculated as the time taken to reach 37% of peak amplitude.

To determine the effects of drug treatments on eNEPSCs, in each neurone the last five events in each treatment epoch were averaged and the amplitude, rise time, decay time were determined. The mean and standard error were then calculated for the group and are given for overall measurements for data sets. The statistical significance of differences between control and drug treatments was assessed using a two-tailed paired t-test. Normalised values were also calculated as percentage change from control and these were used to calculate average percentage changes.

Materials

Salts used in preparation of aCSF were purchased from Fisher Scientific (UK). Indomethacin, aminoguanidine, n-acetyl-L-cysteine, uric acid, Coomassie Brilliant Blue, and agents used in

the preparation of the patch pipette solution, apart from QX-314 (Tocris UK) and MK801, were purchased from Sigma (UK). Ketamine was supplied by Fort Dodge Animal Health Ltd (Southampton, UK). Drugs were stored as frozen, concentrated stock solutions in distilled water and applied by dilution in the aCSF perfusion immediately before use. The following drugs were supplied by Tocris UK or Ascent Scientific UK: DCS, ACBC (1-aminocyclobutane-1-carboxylic acid), DCKA (5,7-dichlorokynurenic acid), 2-AP5 (D,L-2-amino-5-phosphono-pentanoic acid), MK801, D-serine, TTX, NBQX (6-nitro-7 sulphamoylbenzo[f]quinoxalone-2,3-dione disodium), bicuculline methiodide and picrotoxin.

Results

Experiments were conducted on neurones in layer II of the medial EC. We did not attempt to specifically identify neurones by dye injection. The selected neurones had identifiable pyramidal or stellate cell morphology when viewed with DIC and are likely to be glutamatergic principal neurones.

Effects of DCS at presynaptic NMDArs

PreNMDArs tonically facilitate the spontaneous release of glutamate at excitatory synapses in the EC [30,31]. In a recent study we showed that the co-agonist site of the receptor is endogenously bound by D-serine. Thus, exogenous application of the full agonist, had little effect on spontaneous release, but co-agonist site antagonists reduced it, suggesting a saturation of the receptor/effect by endogenous D-serine [33].

In the first set of experiments we determined the effect of the partial agonist, DCS, using the frequency of mEPSCs mediated by AMPAr as a reporter for glutamate release and, hence, preNMDAr activity [30]. DCS (300 μM) had no observable effect on mEPSC frequency in 6 neurones (Fig 1A). In control conditions, mean frequency was 0.65±0.29 Hz and this was almost identical in the presence of DCS (0.62±0.32 Hz). However, subsequent addition of 2-AP5 (50 μM) reduced the frequency of mEPSCs to 0.47±0.23 Hz, a decrease to 71.1±4.3% of control (Fig 1A) confirming that preNMDArs were operative at these synapses to tonically facilitate glutamate release. DCS failed to alter either the mean amplitude of mEPSCs (7.0±0.4 pA *v* 6.9±0.4 pA), or their frequency distribution (Fig 1B and 1C), and these parameters were also unchanged with further addition of 2-AP5 (mean amplitude 6.9±0.4pA). Likewise, decay kinetics (control 2.22±0.32 ms) were unaltered, either by DCS alone (1.98±0.30 ms) or DCS plus 2-AP5 (2.00±0.28 ms). Finally, neither mEPSC rise time nor baseline holding current was altered in any situation (not shown). The lack of effect on kinetics is clearly shown by the averaged mEPSCs shown in Fig 1C. DCS was also tested, at a lower concentration (100 μM; n = 6) and again had no observable effect on mEPSC parameters (e.g. frequency 0.55±0.14 Hz in control and 0.53±0.19 Hz in DCS; other data not shown). These data confirm that glutamate release was subject to tonic facilitation by preNMDAr, but, at the concentrations tested, the partial agonist at the co-agonist binding site did not alter the effects of presynaptic receptor activation.

Postsynaptic NMDAr mediated EPSCs in the EC

In the presence of AMPAr and $GABA_A$ receptor blockers, stimulation in the EC lateral to the recording site elicited large, slowly decaying EPSCs in layer II neurones voltage clamped at +40 mV. These were abolished by 2-AP5, confirming that they were mediated by postNMDArs (Fig 2A; n = 3). In addition, we also tested the effect of a high concentration (100 μM, determined to be close to Emax) of the co-agonist site competitive antagonist, DCKA (Fig 2B; n = 3). This also rapidly (<5 minutes) abolished the eNEPSC and confirmed that the co-agonist site of the

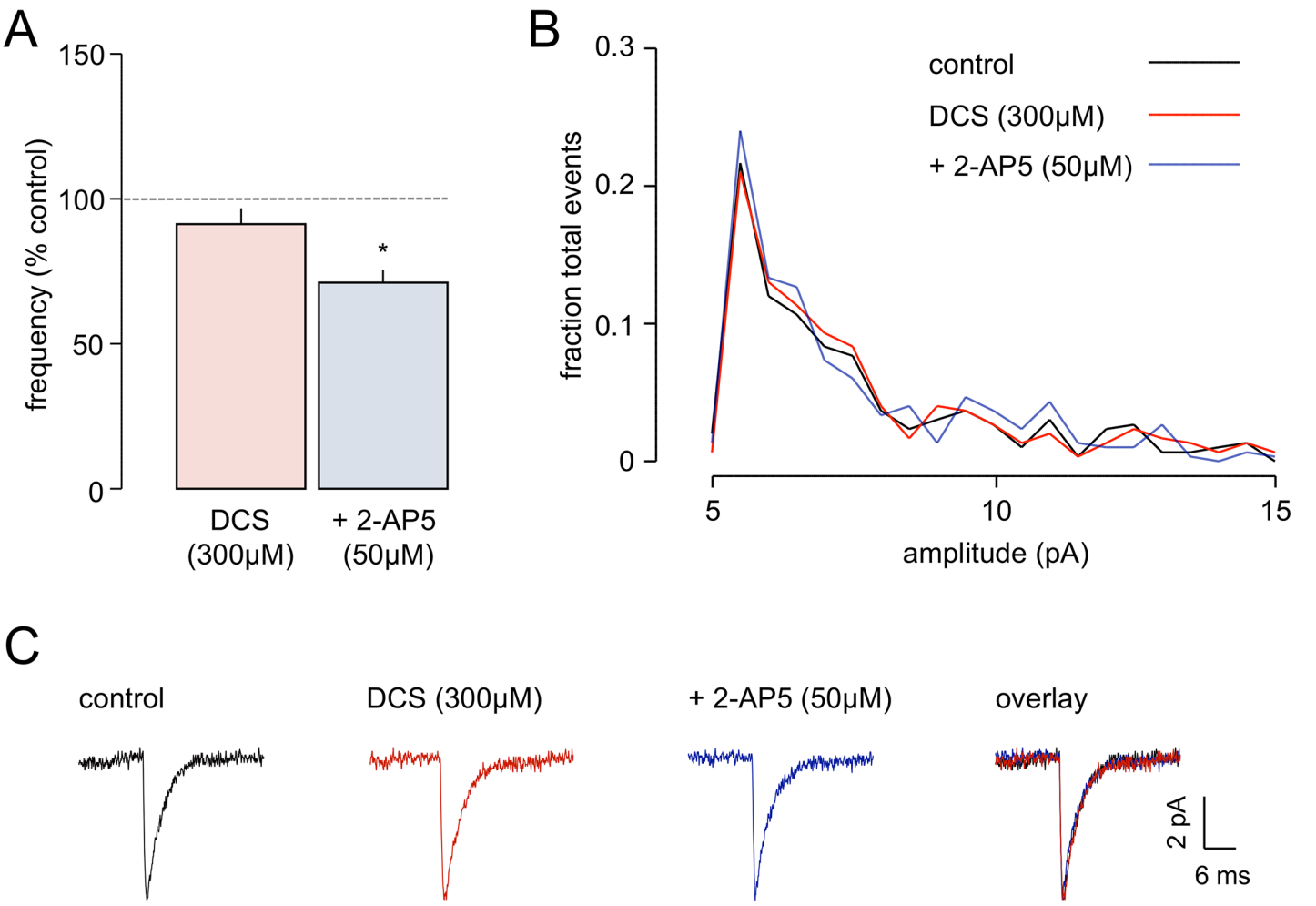

Fig 1. Effects of DCS on preNMDAr activity. A. The histograms show average normalised changes in frequency of mEPSCs with DCS and 2-AP5 in six neurones. DCS was without effect whereas subsequent, cumulative addition of 2-AP5 reduced frequency by ~30%. **B.** The graphs show that the frequency distribution of amplitudes of mEPSCs was unaltered by either antagonist. C. Average mEPSCs (n = 20) in one neurone showing the lack of change in amplitude, rise or decay time with either drug. * $P<0.05$.

doi:10.1371/journal.pone.0133548.g001

postNMDAr was endogenously activated. We have previously examined other aspects of the pharmacology of these eNEPSCs in entorhinal neurones and determined that they are likely to be mediated by triheteromeric GluN1-GluN2A-GluN2B receptors [8]. The slow decay of eNEPSC in other neurones has been shown to be bi-exponential [42] so we looked at this possibility in our neurones. We found that the decay of the eNEPSC in layer II was only marginally better described by biexponential decay kinetics, compared to monoexponential (Fig 2C). The decay time constants were variable from neurone to neurone, particularly in the case of the slow phase of decay, where the variability precluded any meaningful analysis, so in all studies we have assumed monoexponential decay, and compared the time taken to decline to 37% of peak amplitude.

Effects of D-serine at postsynaptic NMDArs

As noted above, we have previously shown that the co-agonist site of the preNMDAr is essentially saturated (or very close to it) by endogenous D-serine [33]. However this did not appear to be the case with the postNMDArs at EC synapses. Thus, exogenous application of the full

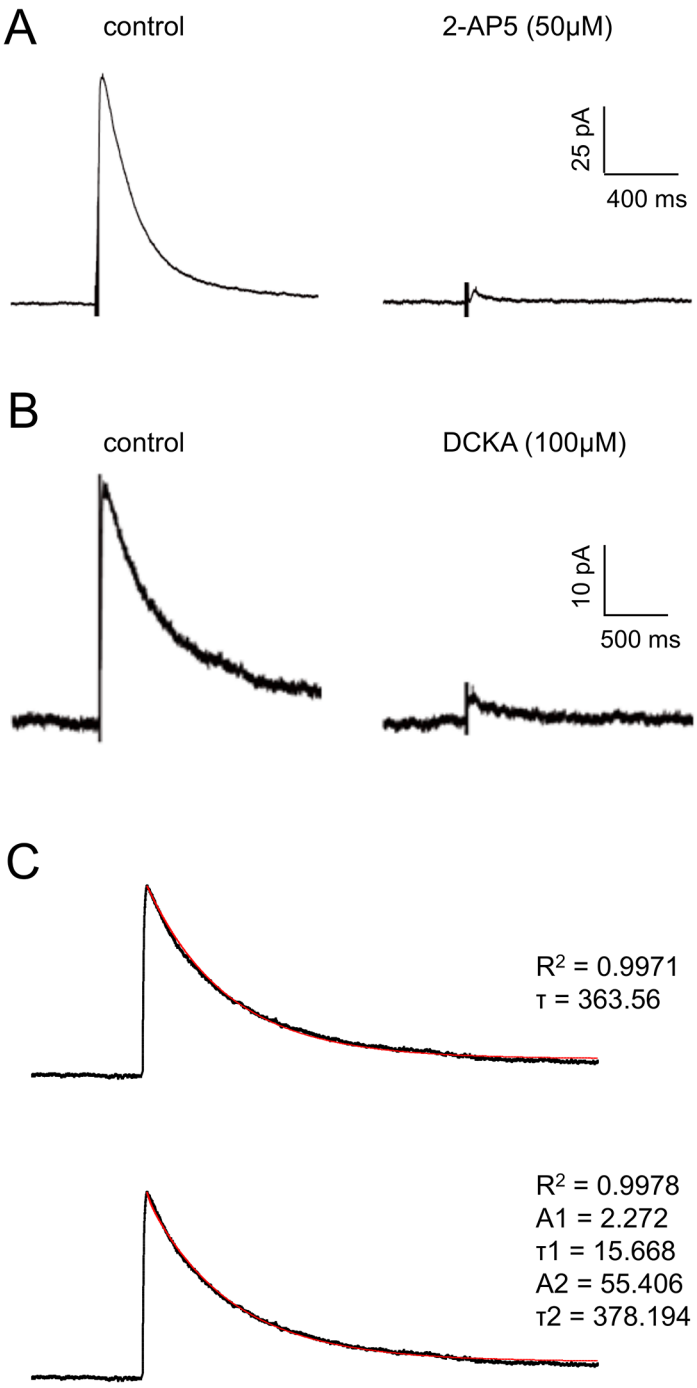

Fig 2. eNEPSCs in entorhinal neurones. The traces show voltage clamp recordings of eNEPSCs evoked in layer II neurones in the medial EC. Each response is the average of at least 5 events. **A.** The addition of the competitive antagonist, 2-AP5 abolished the eNEPSC. **B.** Likewise, application of the co-agonist site antagonist, DCKA, was also able to abolish the eNEPSC. **C**. The decay of n averaged (n = 8) eNEPSC was fitted with either a mono- (top) or bi-exponential function. Whilst R^2 values show an excellent fit to a biexponential decay, the mono-exponential fit was almost as good. The slow decay corresponding to tau-2 in the biexponential fit was extremely variable from neurone to neurone, and precluded meaningful analysis. Since the mono-exponential fit was excellent, in all further studies we assumed a mono-exponential decay.

doi:10.1371/journal.pone.0133548.g002

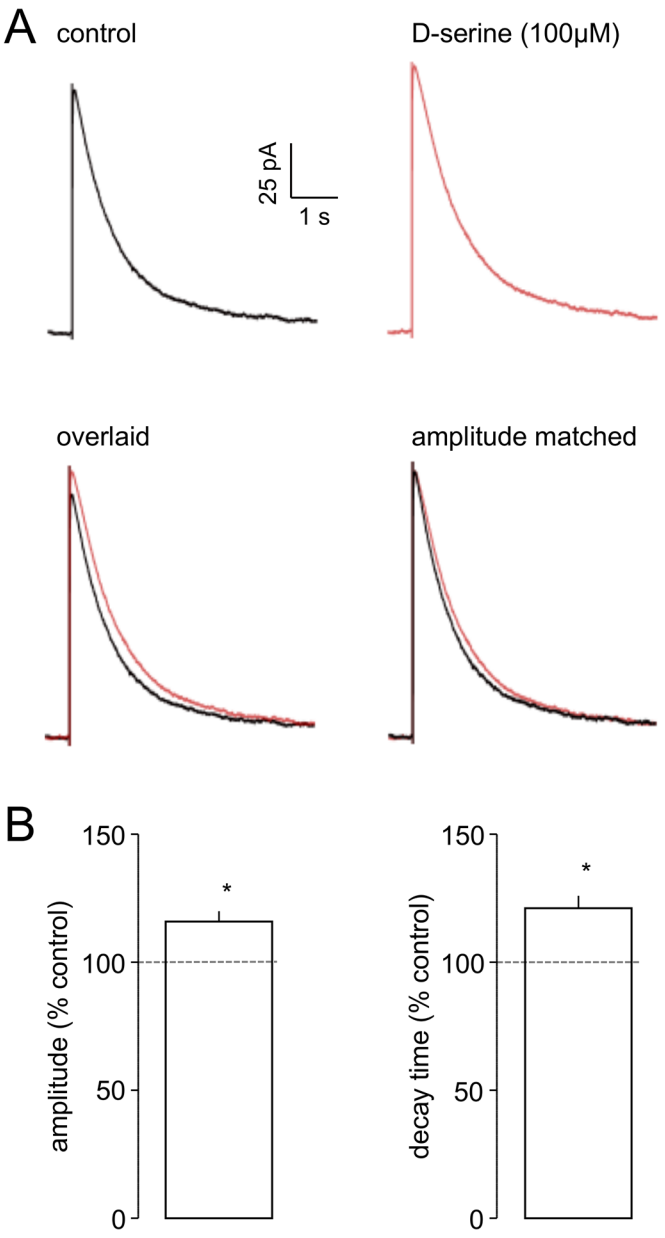

Fig 3. D-serine increases the amplitude and decay time of eNEPSC in EC neurones. A. The traces show averaged eNEPSCs recorded in one neurone. A small, but clear, increase in amplitude by D-serine can be seen when the responses are overlaid. When control and D-serine responses were scaled to the same amplitude and overlaid, the prolongation of decay time is also apparent. **B.** The histograms show pooled normalised data for eNEPSC amplitude and decay times in the presence of D-serine in six neurones. * $P<0.05$.

doi:10.1371/journal.pone.0133548.g003

agonist, D-serine (100 μM, n = 6), increased the mean peak amplitude of eNEPSCs, from 205.5±40.7 pA to 240.3±50.1 pA ($P<0.05$), a normalised increase of 15.9±4.0% (Fig 3). The averaged responses from one study are shown in Fig 3A, where an increase in peak amplitude is evident. In addition, D-serine prolonged the decay time of the eNEPSC from 381.3±105.0 ms to 450.5±112.3 ms (Fig 3B). Scaling the traces to match control and drug treated amplitudes

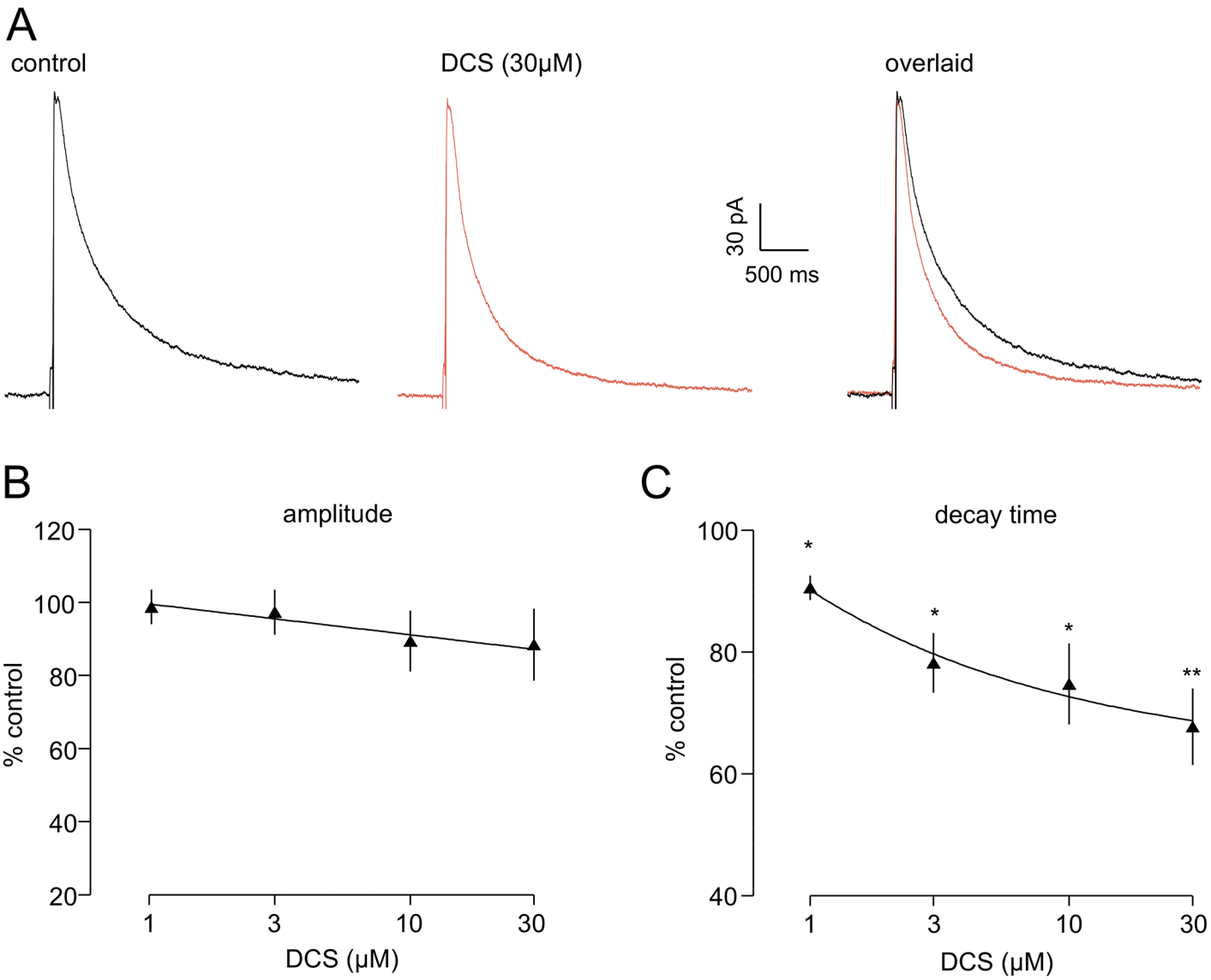

Fig 4. DCS decreases the decay time of eNEPSCs. A. Averaged traces for one neurone are shown for control and in the presence of 30 μM DCS. The overlaid traces clearly show that the amplitude of the eNEPSC is unaffected whereas the response decay is substantially accelerated. The graphs show pooled data of cumulative concentration response curves for normalised data in six neurones for peak amplitude **(B)** and decay time **(C)**. DCS failed to significantly alter peak amplitude at any concentration, but produced a concentration-dependent decrease in eNEPSC decay time. * $P<0.05$; ** $P<0.01$.

doi:10.1371/journal.pone.0133548.g004

shows this prolongation of decay. In contrast, the rise time of the eNEPSC in control recordings was 36.2±8.0 ms, and this was unaltered (33.4±6.3 ms) in the presence of D-serine.

Effects of DCS at postsynaptic NMDARs

We next examined the effect of DCS (1–30 μM), a partial agonist at the co-agonist site, on eNEPSCs in 6 neurones. In contrast to D-serine, DCS did not significantly alter the amplitude of eNEPSCs at any concentration tested, with a small reduction of around 8% recorded at the highest concentration (30 μM) tested (190.9±53.8 pA v 160.6±35.3 pA; Fig 4A and 4B). Likewise, DCS had no effect on rise time (44.7±9.3 ms v 52.3±15.1 ms at 30 μM) of eNEPSCs. However, the drug elicited a clear, concentration-dependent decrease in decay time (Fig 4A and 4C). This

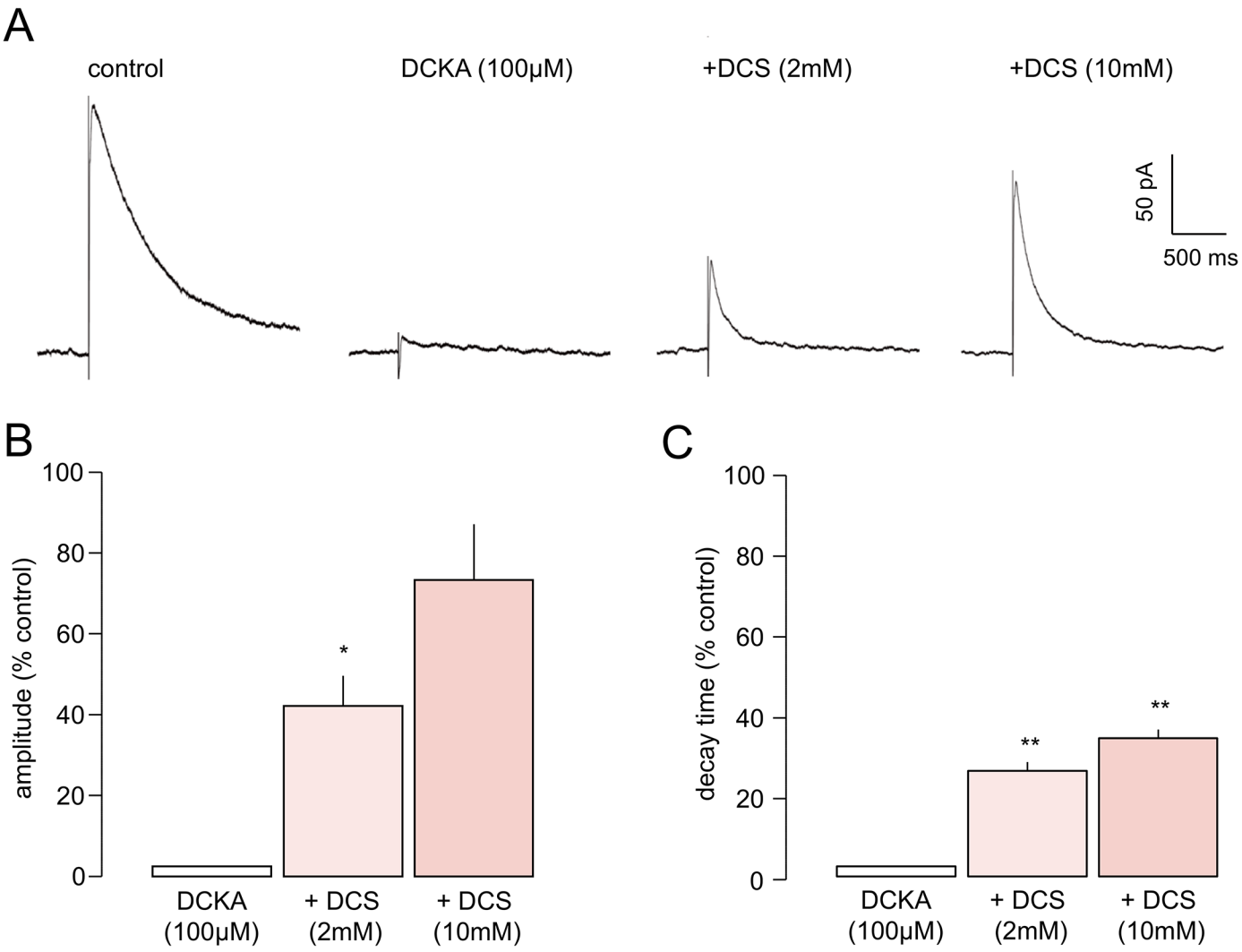

Fig 5. DCS rescues the abolition of the eNEPSC from inhibition by DCKA. A. Averaged synaptic responses from one neurone show abolition of the eNEPSC by the co-agonist site antagonist, DCKA. Subsequent addition of DCS at 2 mM partly restored the response; increasing the partial agonist concentration to 10 mM had a substantially greater restorative action. The histograms show the pooled normalised data for amplitude **(B)** and decay time **(C)** in 8 neurones. The restoration of the eNEPSC was partial, but it is noteworthy that the peak amplitude with DCKA plus DCS at 10 mM was not significantly different to that in control conditions. * $P<0.05$; ** $P<0.01$.

doi:10.1371/journal.pone.0133548.g005

was evident and significant even at low concentrations and the effect had an IC50 of 2.1 μM. The maximum normalised reduction (at 30 μM) was to 68.1±5.9% of control, corresponding to a decrease in mean decay time from 593.8±94.6 ms to 417.4±78.7 ms ($P<0.01$). The exemplar experiment shown in Fig 4A illustrates the lack of change in amplitude, but overlay of the records reveals the much faster decay in the presence of DCS.

To confirm that DCS was exerting its effects at the co-agonist site of the NMDAr we determined the effect of combined administration of the co-agonist site antagonist, DCKA. We showed earlier that DCKA applied at 100μM abolished eNEPSC and this is illustrated again in Fig 5A. In the presence of the antagonist, subsequent addition of 1 mM DCS (n = 3) had no restorative effects on the eNEPSC (not shown). However, at higher concentrations, DCS rescued eNEPSC amplitude in a concentration dependent manner (Fig 5A and 5B; n = 8). As before, eNEPSCs were essentially abolished by DCKA, but in its continued presence the

amplitude of the evoked response was increased by the partial agonist to reach a mean of 42.4 ±7.3% of control at 2 mM and 73.9±13.6% of control with cumulative addition to 10 mM (Fig 5A and 5B). The decay time of the restored responses was 26.1±2.9% of control (pre-DCKA) at 2 mM and 34.4±1.8% at 10 mM. Although the responses were not apparently fully recovered with 10 mM DCS, the eNEPSC at this concentration had a mean absolute amplitude of 188.4 ±101.9 pA, which was not significantly different to that before DCKA (217.6±64.5 pA). Thus, it seems likely that the effects of DCS alone on eNEPSCs were due to agonistic actions at the postNMDAr co-agonist binding site.

The effects of DCS are reversed by D-serine

To confirm whether the effect of DCS on eNEPSC kinetics was due to its partial agonist action we examined whether it was reversible by the full agonist. In these experiments a sub-maximal concentration (10 μM, n = 7) of DCS was applied, followed cumulatively by a saturating concentration of D-serine (1 mM). As noted above, DCS elicited a selective and significant decrease in decay time (to 84.7±2.9% of control). Following the addition of D-serine (Fig 6A and 6B), the reduction of eNEPSC decay time by DCS was reversed and increased to beyond control levels (109.8±2.1%; $P<0.05$). In addition, as with D-serine alone (see above), eNEPSC peak amplitude also increased (to 126.6±4.0%) in the presence of DCS plus D-serine (Fig 6A and 6C). The mean values for eNEPSC in control, DCS (10 μM) alone and DCS (10 μM) plus D-serine (1 mM) conditions were 391.0±26.6 ms, 333.0±28.7 ms and 430.1±31.5 ms, respectively, for decay time, and 123.5±23.9 pA, 124.8±26.2 pA and 160.1±34.3 pA, respectively, for amplitude.

These results indicated that the actions of DCS were indeed readily reversible by a full-agonist and indicated that the effects of DCS are likely to be due to a partial agonism at the co-agonist site.

Effects of ACBC at presynaptic NMDArs

DCS has a relatively high efficacy at the co-agonist binding site (~85%). To determine if efficacy was an important determinant of the actions of DCS we tested the effects of a partial agonist, ACBC, with a much lower efficacy (~40%; [43]) on both the preNMDAr and the post-NMDAr (see below). ACBC (1 mM) decreased the frequency of mEPSCs to 69.4±3.9%, from 1.7±0.3 Hz in control conditions to 1.2±0.2 Hz in the presence of the drug ($P<0.05$; n = 5; Fig 7A). Concurrently, there was no change in frequency distribution of event amplitudes (Fig 7B) or in mean amplitude (6.9±0.3 pA v 6.5±0.3 pA; see Fig 7C). Likewise, neither mEPSC rise time (2.18±0.14 ms v 2.38±0.06 ms) nor decay time (2.85±0.26 ms v 3.27±0.23 ms) was altered by ACBC, exemplified by the averaged (n = 20) events illustrated from one cell in Fig 7C.

Effects of ACBC at postsynaptic NMDArs

Like DCS, ACBC (0.03–1 mM, n = 7) substantially reduced the decay time of eNEPSCs (Fig 8A and 8C). The effect of ACBC was approaching maximal at 1 mM, where we recorded a mean reduction in eNEPSC decay time to 57.5±12.4% of control, with a change in mean from 524.8 ±102.96 ms to 249.0±26.5 ms ($P<0.05$). In contrast to DCS, however, ACBC also reduced the amplitude of eNEPSCs in a concentration-dependent manner (Fig 8A and 8B). The mean change in peak amplitude at 1 mM was to 62.0±5.9% of control (239.4±47.3 pA v 141.5±21.2 pA; $P<0.05$). Rise time was unaltered (31.3±4.2 ms v 30.3±5.3 ms). The averaged responses shown for one neurone in Fig 8A clearly show the change in amplitude, and when the responses were amplitude scaled and superimposed the reduced decay time was also obvious.

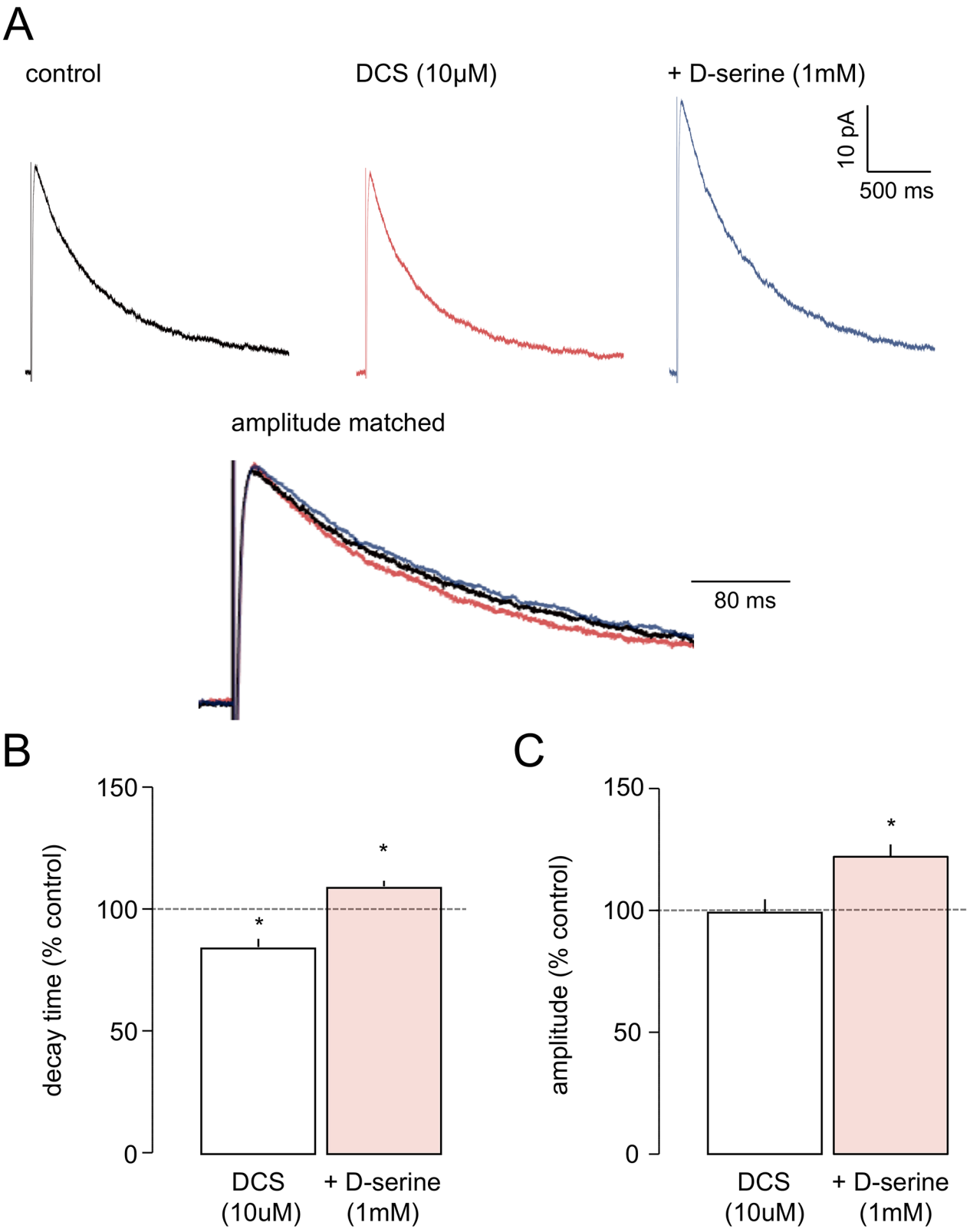

Fig 6. The effect of DCS on the eNEPSC is reversed by D-serine. A. Averaged responses in one neurone show little effect of DCS on amplitude but a decrease in decay time. Cumulative addition of D-serine reverses the effect of DCS and increases both parameters to beyond control levels. **B and C** show pooled data for the two parameters in 7 neurones. * $P<0.05$.

doi:10.1371/journal.pone.0133548.g006

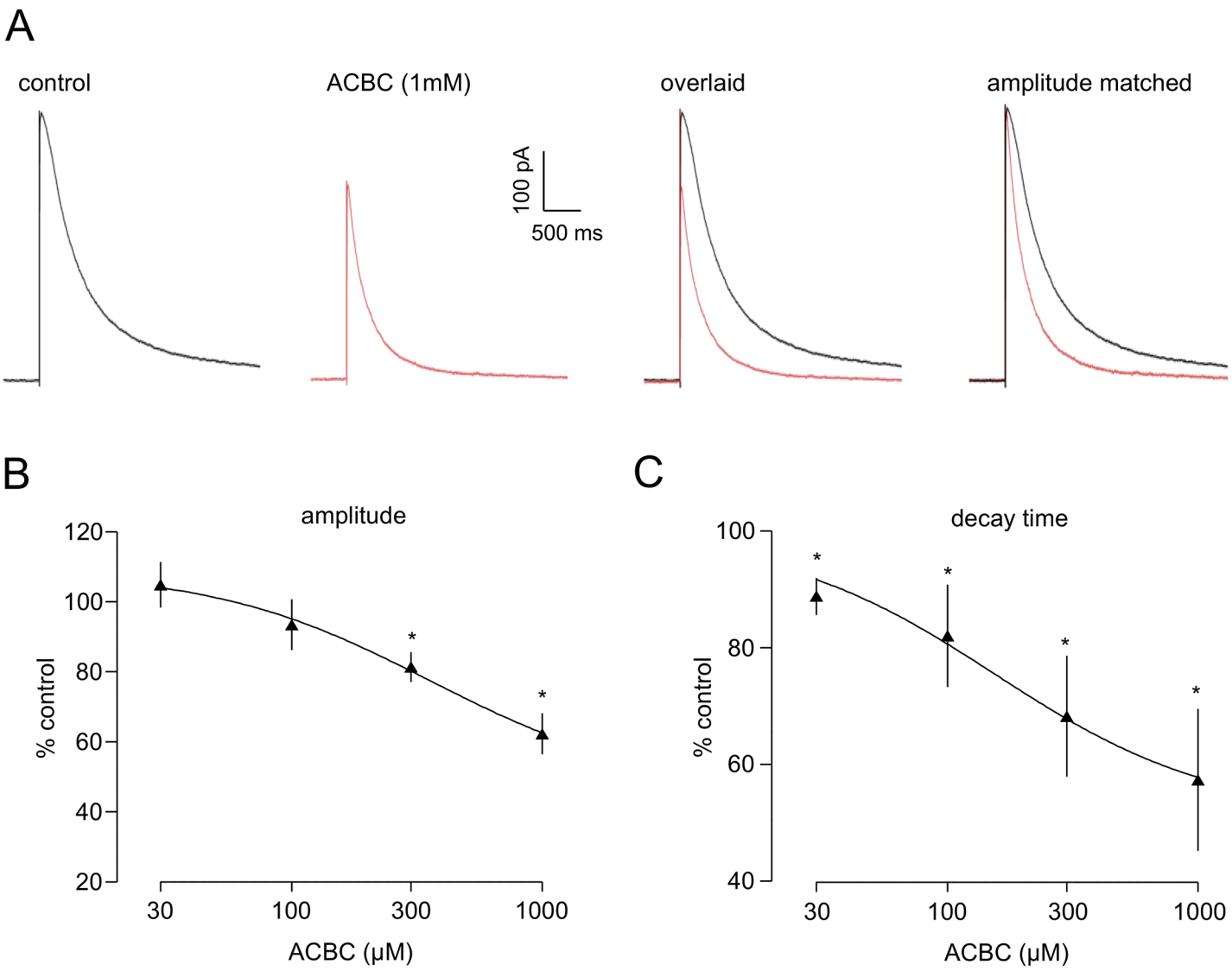

Fig 7. ACBC reduces preNMDAr activity. A. The histogram shows normalised frequency data for 5 neurones and indicates a significant decrease in frequency in the presence of the low-efficacy partial agonist. **B.** There was no concurrent change in frequency distribution of event amplitudes. **C.** The averaged mEPSCs recorded in one neurone illustrate that peak amplitude, rise and decay times of events was unaltered by ACBC. * $P<0.05$

doi:10.1371/journal.pone.0133548.g007

Discussion

DCS, the partial agonist at the NMDAr glycine/D-serine co-agonist binding site, had no detectable effect on the preNMDAr mediated tonic facilitation of glutamate release, whereas ACBC did induce a decrease in mEPSC frequency. This is explicable in terms of differences in efficacy of the two partial agonists. The preNMDAr is saturated, or very close to it, by endogenous D-serine [33], so the binding of a low efficacy partial agonist, ACBC, will substantially compete with the endogenous activation of the site. Since activation of the co-agonist site is obligatory for the receptor activation, ACBC will have a similar effect to a competitive antagonist at the site [33], and thereby reduce its activation by ambient glutamate. Thus, the tonic facilitation of glutamate release mediated by the preNMDArs will be reduced and mEPSC frequency will decline. DCS has a much higher efficacy (85%) than ACBC (40%), which means that its

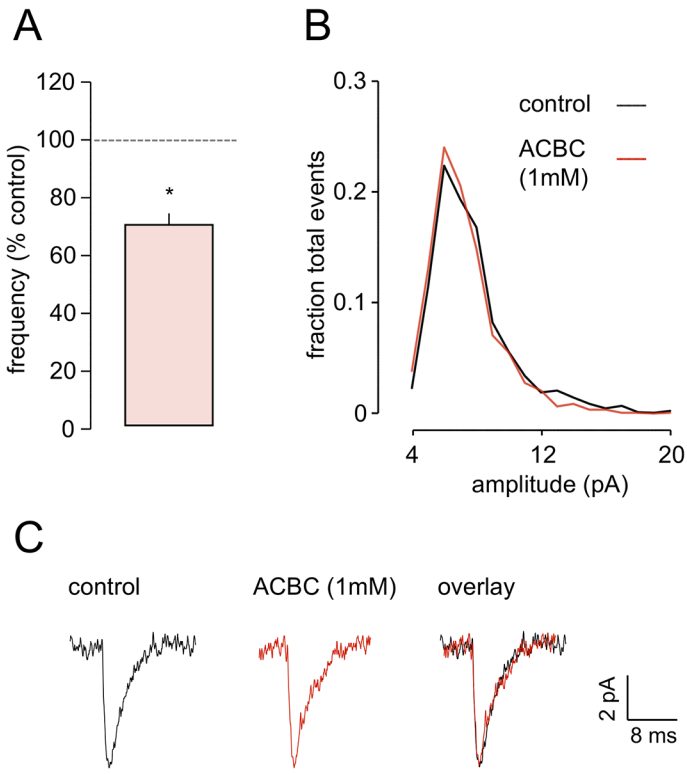

Fig 8. ACBC decreases both the amplitude and the decay time of the postsynaptic eNEPSC. A. Averaged responses for one neurone show a clear decrease in amplitude in the presence of ACBC, and the overlaid traces also indicate a substantial decrease in decay time. Amplitude scaling shows the latter effect very clearly. **B and C**. The graphs show pooled data for 7 neurones and illustrate the clear concentration-dependency for effects of ACBC on both parameters. * $P<0.05$.

doi:10.1371/journal.pone.0133548.g008

competition with endogenous D-serine will have a less deleterious effects on activation of the preNMDARs. Even complete blockade of preNMDAr activation with a competitive glutamate or co-agonist site antagonists only results in around 25–30% reduction in mEPSC frequency [30,31,33] it is not surprising that DCS did not elicit an obvious reduction in release.

It could also be that subunit specificity of the two partial agonists iis involved in the differential presynaptic effects of DCS and ACBC. There is evidence that although the action of partial agonists is due to binding at the co-agonist site on GluN1 subunits, efficacy may be determined by the identity of the GluN2 subunit. This certainly seems to be the case for DCS, which has a higher efficacy at GluN1-N2A (90%) than GluN1-N2B (65–70%) receptors [44]. PreNMDAr are comprised predominantly of GluN1-N2B diheteromers [31], whereas the postNMDAr are likely to be GluN1-N2A-N2B triheteromers [8]. Although the overall efficacy of ACBC is around 40% [43], comparative data at GluN1-N2A *v* GluN1-N2B receptors is not available. It is not inconceivable that it may have a much lower efficacy at the latter, and that this could contribute to why it is able to observably diminish the tonic facilitation of release whereas DCS does not.

In contrast to the preNMDAr, both partial agonists had significant effects on the response to postNMDAr activation. Following release, glutamate in the synaptic cleft rapidly peaks at approximately 1 mM, which is saturating at the postNMDAr, and is then cleared by reuptake with a time constant of 1 ms, approximately [45]. Activation of an NMDAr induces a series of openings that persist for a relatively long period due to a slow rate of glutamate unbinding.

Glutamate rebinding does not occur [42,45] indicating that the time course of postNMDAr currents is determined only by receptor gating between bound/open, bound/closed and unbound/closed conformations [46]. Several gating mechanisms have been proposed for NMDAr, commonly with at least 10 transitions, though these are not resolvable from macroscopic currents [47].

Partial agonists at ligand-gated ion channels characteristically elicit submaximal synaptic currents even at full occupancy due to a decrease in receptor open probability that results from a reduction in the efficiency of receptor gating. However, partial agonists of NMDAr also alter the decay of NMDAr synaptic currents. These properties were extensively studied by Priestley and Kemp [48] who demonstrated that relative to a full agonist, partial agonists at either the glutamate or the co-agonist binding site decrease the decay time in an extent proportional to their efficacy. The kinetic analysis of Kussius and Popescu [49] has indicated that inter-subunit coupling is central to the NMDAr gating process and that partial agonism at either site occurs through broad effects on multiple gating transitions which results in receptors spending more time in bound/closed states. Therefore, the reason why eNEPSC peak amplitude and decay time are both determined by agonist efficacy is likely to simply be that both are determined by the efficiency of gating transitions. This model also accurately predicts that partial agonists accelerate the decay of macroscopic currents resulting from prolonged glutamate application by increasing the time spent in bound/closed states, which can also transition to long-lived bound/closed (desensitized) states. More recently this kinetic scheme was seen to accurately predict changes in the decay time of synaptic-like macroscopic currents resulting from structural changes in NMDAr induced by site-directed mutagenesis [50]. These studies suggest that the faster decay time induced by NMDAr partial agonists in comparison to full agonists could result from the same broad reductions in channel gating efficiency that underlie lower amplitude responses, providing a simple explanation of why both are determined by efficacy.

In the current study we found that partial agonists at the co-agonist binding site had different effects on parameters of eNEPSCs in native tissue that may be related to efficacy. DCS selectively decreased the eNEPSC decay time without affecting peak amplitude whereas ACBC decreased both decay time and peak amplitude. A parsimonious explanation for the lack of effect of DCS on amplitude is that the postsynaptic receptor co-agonist site is bound by the endogenous full agonist (probably D-serine; e.g. [51]), which has a higher efficacy than DCS, but is present at a concentration such that the number of co-agonist sites bound and, hence, endogenous activation of these sites is matched to the efficacy of DCS. Thus, when DCS is present, the number of glutamate receptors activated in response to stimulation is essentially unchanged but the macroscopic decay is altered.

In contrast, ACBC decreased both amplitude and decay time. This result would support the above scheme, since the low efficacy (~40%) would mean that there was a mismatch between efficacy and number of sites bound by the endogenous agonist, so that when the partial agonist is added it would be predicted to reduce amplitude as well as the decay of the macroscopic response. The increase in amplitude seen with exogenous D-serine, alone or in combination with DCS, indicates that the co-agonist sites at these synapses are probably not saturated. A saturating concentration of D-serine elicited an increase in amplitude of 15–25%, which suggests a tonic activation of around 80–85%. This agrees with the efficacy of DCS reported by Priestly and Kemp [48] who also studied eNEPSCs (although in rat neuronal cultures). Subsequently, Dravid et al. [52] have showed that inter-subunit coupling is a key determinant of the efficacy of DCS at different NMDAr subtypes observing that the efficacy of DCS is 90% and 65% of maximum for GluN2A and GluN2B containing NMDA receptors, respectively. Interestingly, we have previously demonstrated that the postNMDAr in the EC is likely

to be a GluN1-N2A-N2B triheteromer [8]. In light of the findings of Dravid et al. [52] such a heterodimer could be anticipated to have the efficacy calculated by Priestly and Kemp [48].

Our data showing that D-serine increases the decay time of eNEPSCs warrants further discussion in light of evidence that D-serine is the endogenous co-agonist at synaptic NMDAr and, thus, already binding the receptor [51]. One explanation is the existence of partially-liganded NMDAr openings, which could cause a submaximal decay in the control condition but not when all sites are saturated by exogenous D-serine. Currently, partially-liganded NMDAr openings are not thought to occur, though evidence for this idea is largely reliant on expression systems, where regulation of the NMDA receptor may well be different. Our results with DCKA and DCS, where DCS rescued eNEPSC amplitude to a greater extent than decay time, may also support the existence of partially-liganded openings. A second explanation is that D-serine is not the sole endogenous ligand of the co-agonist site. Indeed, evidence for D-serine being the endogenous agonist at these receptors has been based on enzymatic depletion of D-serine, and typically this only produces a partial reduction of synaptic NMDAr currents [51]. Recently, endogenous activation of the postNMDAr coagonist site at hippocampal synapses has been shown to be due to a combination of both glycine and D-serine [53]; these may have different efficacies at the receptors in the EC, and this could account for a change in decay time when receptors become bound primarily by the exogenously applied D-serine. A further explanation is that D-serine is alters the contributions of different gating modes, which are argued to underlie the shape the synaptic response (see [54]). However, it would still be difficult to offer a molecular basis for this without either partially-liganded gated openings or the presence of another endogenous ligand.

An alternative explanation for the kinetic effects observed in this study is that the post-NMDAr population present consists of two or more subtypes with varying decay time. A change in kinetics could then occur through biased agonist effects on these subtypes, altering the contributions of the subtypes to the overall response and, thus, the kinetics. Our results with DCS, where a kinetic change was seen independent of a change in amplitude, are not consistent with such a scheme and may argue against this explanation. However, for the results with ACBC and D-serine this remains a plausible basis for the observed kinetic effects. Previous studies have indicated that the receptors underlying these responses are predominantly a GluN1-N2A-N2B triheteromer [8], though without the use of knockout animals it is difficult to conclusively rule out the possibility of multiple contributing receptor subtypes.

In contrast to effects at postNMDAr the lack of effect of DCS on frequency of mEPSCs indicates that the partial agonist does not noticeably modulate preNMDAr function. The lack of presynaptic effect could be related to the difference in subunit composition of the pre and post-NMDAr, as noted above. On the other hand, the preNMDAr appear to be saturated by endogenous D-serine [33], and even if this binding was completely replaced by DCS, we might expect only around a 20% reduction in function (see [52,54]), which may not be experimentally observable using the indirect reporting of receptor activity employed. This is supported by results with ACBC, which has a much lower efficacy and did decrease mEPSC frequency. Activation of preNMDArs does not appear to be restricted by saturation of the glutamate binding site, since blocking reuptake an increase the frequency of AMPAr mEPSCs [55]. Thus, extrapolating back from the postsynaptic site to presynaptic, it is possible that an unchanged strength of the current through the preNMDArs coupled with a moderately increased rate of closure in the presence of DCS would not affect physiological utility, as re-opening could quickly occur, and the tonic facilitatory effect would persist. With ACBC, both current strength and duration would be reduced and, thus, the facilitation would be compromised. Thus depending on the partial agonist, we may be able to differentially modulate the postsynaptic responses, but also exert site-specific (pre v post) modulation of NMDAr-mediated transmission.

In this study we have documented what is, superficially at least, a diminishing of post-NMDAr-mediated transmission by partial agonists, be it a decrease in duration alone or in both amplitude and duration; in the case of ACBC, we also report a decline in preNMDAr facilitation of glutamate release. However, there is good evidence for cognitive enhancement with DCS [16–25] and other co-agonist site partial agonists (e.g. GLYX-13 [56]). Cognitive enhancement is generally targeted at elevating NMDAr function (e.g. [57]), so these results would seem counterintuitive. However, in preliminary studies (Lench A.M. and Jones R.S.G., see S1 Fig) we have examined the effect of DCS on synchronized local field potential discharges induced by block of GABA-inhibition in EC slices. The effects were complex but generally characterised by increased inter and intra burst frequencies and amplitude of discharges with low doses of DCS. We have not yet investigated the cellular basis of this in detail. However, since DCS only increases the rate of closure of postNMDAr, at synapses where NMDAr-mediated transmission is operative this could permit more rapid and frequent reopening concurrent with a maintained peak amplitude of the signal. Conceptually, this could result in enhanced synchrony. As synchronous network oscillatory activity is likely to underlie many forms of cognitive processing [58–60], this could be a basis for cognitive enhancement. We are currently investigating the cellular basis for the prosynchronous effects of DCS and other partial agonists.

In this regard, it is interesting that low doses of DCS have been suggested to be a useful adjunct or treatment to enhance cognitive processing in schizophrenics through enhancement of NMDA mediated transmission [61,62]. Based originally on the observations that ketamine and phencyclidine can induce a schizophrenia-like psychosis [63,64], the disorder is increasingly being seen as involving a hypofunction of glutamatergic, particularly NMDAr-mediated, transmission [65–67]. There is also increasing evidence that the cognitive disruption associated with schizophrenia may involve alterations in the oscillatory activity (particularly gamma-oscillations) in cortical networks (see [68]) and experimental studies have shown that NMDAr dependent gamma rhythms [69] may be substantially decreased in the entorhinal cortex in schizophrenia and related animal models [68,70]. Thus, it may be tempting to suggest that the counterintuitive prosynchronous effect of DCS that we propose here may be a basis for restoring normal oscillatory effects in the EC in schizophrenia and amelioration of cognitive deficits associated with it.

It is also interesting to note that the non-competitive NMDAr antagonist, memantine, mildly enhances cognitive processing in people with Alzheimer's disease. This has been suggested to involve an increase in signal to noise ratio in cortical excitatory transmission signal, as a result of a reduction in NMDAr-mediated synaptic noise [71]. However, it is also the case that memantine can enhance both theta and gamma oscillations in cortical networks and reverse the deleterious effects on these rhythms induced by scopolamine [72]. We are not proposing that memantine and DCS share a common cellular mechanism for their prosynchronous effects, but it is clear that a negative effects on NMDAr mediated responses does not preclude a role as a cognitive enhancer, and the temporal and spatial location of these effects in network activity are likely to be determinant factors.

Supporting Information

S1 Fig. DCS enhances synchronised activity. Synchronised epileptiform bursts recorded extracellularly as local field potentials, were elicited in entorhinal slices by perfusion with bicuculline methiodide (20 μM), picrotoxin (50 μM) and strychnine (2 μM) to block both $GABA_A$ and glycine receptors. Application of DCS at 30 μM, increased burst frequency and increased the duration of individual bursts as well as the frequency of discharges within the bursts. In

some instances overall burst amplitude also increased. During washout, most parameters were rapidly reversed to control conditions although the intra-burst frequency increase was more persistent.
(TIF)

Acknowledgments

We thank the Medical Research Council and the Biotechnology and Biological Sciences Research Council for doctoral training awards to support Alex Lench and Emma Robson, respectively. We are grateful to the University of Bath for provision of laboratory and technical facilities.

Author Contributions

Conceived and designed the experiments: AML RSGJ. Performed the experiments: AML ER RSGJ. Analyzed the data: AML ER. Wrote the paper: AML ER RSGJ.

References

1. Eichenbaum H. The hippocampus and declarative memory: cognitive mechanisms and neural codes. Behav Brain Res. 2001; 127: 199–207. PMID: 11718892
2. Squire LR, Stark CE, Clark RE. The medial temporal lobe. Annu. Rev. Neurosci. 2004; 27: 279–306. PMID: 15217334
3. Witter MP, Moser EI. Spatial representation and the architecture of the entorhinal cortex. Trends Neurosci. 2006; 29: 671–678. PMID: 17069897
4. Coutureau E, Di Scala G. Entorhinal cortex and cognition. Prog Neuropsychopharmacol Biol Psychiat. 2009; 33: 753–761.
5. Igarashi KM, Lu L, Colgin LL, Moser MB, Moser EI. Coordination of entorhinal-hippocampal ensemble activity during associative learning. Nature. 2014; 510: 143–147. doi: 10.1038/nature13162 PMID: 24739966
6. Jones RSG, Woodhall GL. Background synaptic activity in rat entorhinal cortical neurones: differential control of transmitter release by presynaptic receptors. J Physiol. 2005; 562: 107–120. PMID: 15498804
7. Yang J, Woodhall GL, Jones RSG. Tonic facilitation of glutamate release by presynaptic NR2B-containing NMDA receptors is increased in the entorhinal cortex of chronically epileptic rats. J Neurosci. 2006; 26: 406–410. PMID: 16407536
8. Chamberlain SEL, Yang J, Jones RSG. The role of NMDA receptor subtypes in short-term plasticity in the rat entorhinal cortex. Neural Plasticity. 2008; http://www.hindawi.com/journals/np/2008/872456/.
9. Collingridge GL, Volianskis A, Bannister N, France G, Hanna L, Mercier M, et al. The NMDA receptor as a target for cognitive enhancement. Neuropharmacology. 2013; 64: 13–26. doi: 10.1016/j.neuropharm.2012.06.051 PMID: 22796429
10. Bortolato B, Carvalho AF, McIntyre RC. Cognitive Dysfunction in Major Depressive Disorder: A State-of-the-art Clinical Review. CNS Neurol Disord Drug Targets. 2014; 13: 1804–1818. PMID: 25470396
11. Brainin M, Tuomilehto J, Heiss WD, Bornstein NM, Bath PM, Teuschl Y, et al. Post-stroke cognitive decline: an update and perspectives for clinical research. Eur J Neurol. 2015; 22: 229–e16. doi: 10.1111/ene PMID: 25492161
12. Lehrner J, Kogler S, Lamm C, Moser D, Klug S, Pusswald G, et al. Awareness of memory deficits in subjective cognitive decline, mild cognitive impairment, Alzheimer's disease and Parkinson's disease. Int Psychogeriatr. 2015; 27: 357–366. doi: 10.1017/S1041610214002245 PMID: 25382659
13. Menlove L, Reilly C. Memory in children with epilepsy: A systematic review. Seizure. 2015; 25: 126–35. doi: 10.1016/j.seizure.2014.10.002 PMID: 25457449
14. Vinther-Jensen T, Larsen IU, Hjermind LE, Budtz-Jørgensen E, Nielsen TT, Nørremølle A, et al. A clinical classification acknowledging neuropsychiatric and cognitive impairment in Huntington's disease. Orphanet J Rare Dis. 2014; 9:114 doi: 10.1186/s13023-014-0114-8 PMID: 25026978
15. Bora E. Neurodevelopmental origin of cognitive impairment in schizophrenia. Psychol Med. 2015; 45: 1–9. doi: 10.1017/S0033291714001263 PMID: 25065902

16. Flood JF, Morley JE, Lanthorn TH. Effect on memory processing by D-cycloserine, an agonist of the NMDA/glycine receptor. Eur J Pharmacol. 1992; 221: 249–254. PMID: 1330624

17. Quartermain D, Mower J, Rafferty MF, Herting RL, Lanthorn TH. Acute but not chronic activation of the NMDA-coupled glycine receptor with D-cycloserine facilitates learning and retention. Eur J Pharmacol. 1994; 257; 7–12. PMID: 8082709

18. Goff DC, Tsai G, Manoach DS, Coyle JT. Dose-finding trial of D-cycloserine added to neuroleptics for negative symptoms in schizophrenia. Am J Psychiat. 1995; 152: 1213–1215. PMID: 7625475

19. van Berckel BN, Hijman R, van der Linden JA, Westenberg HG, van Ree JM, Kahn RS. Efficacy and tolerance of D-cycloserine in drug-free schizophrenic patients. Biol. Psychiat. 1996; 40: 1298–1300. PMID: 8959296

20. Ledgerwood L, Richardson R, Cranney J. Effects of D-cycloserine on extinction of conditioned freezing. Behav Neurosci. 2003; 117: 341–349. PMID: 12708530

21. Norberg MM, Krystal JH, Tolin DF. A meta-analysis of D-cycloserine and the facilitation of fear extinction and exposure therapy. Biol Psychiat. 2008; 63: 1118–1126. doi: 10.1016/j.biopsych.2008.01.012 PMID: 18313643

22. Myers KM, Carlezon WA. D-cycloserine effects on extinction of conditioned responses to drug-related cues. Biol Psychiat. 2012; 71: 947–955. doi: 10.1016/j.biopsych.2012.02.030 PMID: 22579305

23. Nave AM, Tolin DF, Stevens MC. Exposure therapy, D-cycloserine, and functional magnetic resonance imaging in patients with snake phobia: a randomized pilot study. J Clin Psychiat. 2012; 73: 1179–1186.

24. Feld GB, Lange T, Gais S, Born J. Sleep-dependent declarative memory consolidation—unaffected after blocking NMDA or AMPA receptors but enhanced by NMDA co-agonist D-cycloserine. Neuropsychopharmacology. 2013; 38: 2688–2697. doi: 10.1038/npp.2013.179 PMID: 23887151

25. Rodrigues H, Figueira I, Lopes A, Gonçalves R, Mendlowicz MV, Coutinho ES, et al. Does D-cycloserine enhance exposure therapy for anxiety disorders in humans? A meta-analysis. PLoS One. 2014; 9: e93519. doi: 10.1371/journal.pone.0093519 PMID: 24991926

26. De Sarro G, Gratteri S, Naccari F, Pasculli MP, De Sarro A. Influence of D-cycloserine on the anticonvulsant activity of some antiepileptic drugs against audiogenic seizures in DBA/2 mice. Epilepsy Res. 2000; 40: 109–21. PMID: 10863138

27. Ghasemi M, Schachter SC. The NMDA receptor complex as a therapeutic target in epilepsy: a review. Epilepsy Behav. 2011; 22: 617–40. doi: 10.1016/j.yebeh.2011.07.024 PMID: 22056342

28. Wla P, Poleszak E. Differential effects of glycine on the anticonvulsant activity of D-cycloserine and L-701,324 in mice. Pharmacol Rep. 2011; 63: 1231–1234. PMID: 22180366

29. Klatte K, Kirschstein T, Otte D, Pothmann L, Müller L, Tokay T, Kober M, Uebachs M, Zimmer A, Beck H. Impaired D-serine-mediated cotransmission mediates cognitive dysfunction in epilepsy. J Neurosci. 2013; 33: 13066–13080. doi: 10.1523/JNEUROSCI.5423-12.2013 PMID: 23926260

30. Berretta N, Jones RSG. Tonic facilitation of glutamate release by presynaptic N-methyl-D-aspartate autoreceptors in the entorhinal cortex. Neuroscience. 1996; 75: 339–344. PMID: 8931000

31. Woodhall G, Evans DI, Cunningham MO, Jones RSG. NR2B-containing NMDA autoreceptors at synapses on entorhinal cortical neurons. J Neurophysiol. 2001; 86: 1644–1651. PMID: 11600627

32. Yang J, Chamberlain SEL, Woodhall GL, Jones RSG. Mobility of NMDA autoreceptors but not postsynaptic receptors at glutamate synapses in the rat entorhinal cortex. J Physiol. 2008; 586: 4905–4924. doi: 10.1113/jphysiol.2008.157974 PMID: 18718983

33. Lench AM, Massey PV, Pollegioni L, Woodhall GL, Jones RSG. Astroglial d-serine is the endogenous co-agonist at the presynaptic NMDA receptor in rat entorhinal cortex. Neuropharmacology. 2014; 83: 118–127. doi: 10.1016/j.neuropharm.2014.04.004 PMID: 24747728

34. Jones RSG, Heinemann U. Synaptic and intrinsic responses of medical entorhinal cortical cells in normal and magnesium-free medium in vitro. J Neurophysiol. 1988; 59 1476–1496. PMID: 2898511

35. Sjöström PJ, Turrigiano GG, Nelson SB. Neocortical LTD via coincident activation of presynaptic NMDA and cannabinoid receptors. Neuron. 2003; 39; 641–654. PMID: 12925278

36. Samson RD, Paré D. Activity-dependent synaptic plasticity in the central nucleus of the amygdala. J Neurosci. 2005; 25: 1847–1855. PMID: 15716421

37. Bender VA, Bender KJ, Brasier DJ, Feldman DE. Two coincidence detectors for spike timing-dependent plasticity in somatosensory cortex. J Neurosci. 2006; 26: 4166–4177. PMID: 16624937

38. Jourdain P, Bergersen LH, Bhaukaurally K, Bezzi P, Santello M, Domercq M, et al. Glutamate exocytosis from astrocytes controls synaptic strength. Nat Neurosci. 2007; 10: 331–339. PMID: 17310248

39. Li YH, Han TZ. Glycine binding sites of presynaptic NMDA receptors may tonically regulate glutamate release in the rat visual cortex. J Neurophysiol. 2007; 97: 817–823. PMID: 17093111

40. Brasier DJ, Feldman DE. Synapse-specific expression of functional presynaptic NMDA receptors in rat somatosensory cortex. J Neurosci. 2008; 28: 2199–2211. doi: 10.1523/JNEUROSCI.3915-07.2008 PMID: 18305253

41. Woodhall GL, Bailey SJ, Thompson SE, Evans DIP, Stacey AE, Jones, RSG. Fundamental differences in spontaneous synaptic inhibition between deep and superficial layers of the rat entorhinal cortex Hippocampus. 2005;15: 232–245

42. Lester RA, Jahr CE. NMDA channel behaviour depends on agonist affinity. J Neurosci. 1992; 12: 635–643. PMID: 1346806

43. Inanobe A, Furukawa H, Gouaux E. Mechanism of partial agonist action at the NR1 subunit of NMDA receptors. Neuron. 2005; 47: 71–84. PMID: 15996549

44. Sheinin A, Shavit S, Benveniste M. Subunit specificity and mechanism of action of NMDA partial agonist D-cycloserine. Neuropharmacology. 2001; 41: 151–158. PMID: 11489451

45. Clements JD, Lester RA, Tong G, Jahr CE, Westbrook GL. The time course of glutamate in the synaptic cleft. Science 1992; 258: 1498–1501. PMID: 1359647

46. Lester RA, Clements JD, Westbrook GL, Jahr CE. Channel kinetics determine the time course of NMDA receptor-mediated synaptic currents. Nature. 1990: 346: 565–567. PMID: 1974037

47. Schorge S, Elenes S, Colquhoun D. Maximum likelihood fitting of single channel NMDA activity with a mechanism composed of independent dimers of subunits. J Physiol. 2005; 569: 395–418. PMID: 16223763

48. Priestley T, Kemp JA. Kinetic study of the interactions between the glutamate and glycine recognition sites on the N-methyl-D-aspartic acid receptor complex. Mol Pharmacol. 1994; 46: 1191–1196. PMID: 7808441

49. Kussius CL, Popescu GK. Kinetic basis of partial agonism at NMDA receptors. Nat Neurosci. 2009; 12: 1114–1120. doi: 10.1038/nn.2361 PMID: 19648915

50. Paganelli MA, Kussius CL, Popescu GK. Role of cross-cleft contacts in NMDA receptor gating. PLoS One 2013;21; 8:e80953. doi: 10.1371/journal.pone.0080953

51. Papouin T, Ladépêche L, Ruel J, Sacchi S, Labasque M, Hanini M, Groc L, et al. Synaptic and extrasynaptic NMDA receptors are gated by different endogenous co-agonists. Cell. 2012; 150: 633–646. doi: 10.1016/j.cell.2012.06.029 PMID: 22863013

52. Dravid SM, Burger PB, Prakash A, Geballe MT, Yadav R, Le P, Vellano K, et al. Structural determinants of D-cycloserine efficacy at the NR1/NR2C NMDA receptors. J Neurosci. 2010; 30: 2741–2754. doi: 10.1523/JNEUROSCI.5390-09.2010 PMID: 20164358

53. Le Bail M, Martineau M, Sacchi S, Yatsenko N, Radzishevsky I, Conrod S, et al. Identity of the NMDA receptor coagonist is synapse specific and developmentally regulated in the hippocampus. PNAS. 2015; 112: E204–13. doi: 10.1073/pnas.1416668112 PMID: 25550512

54. Popescu GK. Modes of glutamate receptor gating. J Physiol. 2012; 590: 73–91. doi: 10.1113/jphysiol.2011.223750 PMID: 22106181

55. Greenhill SD, Jones RSG. Diverse antiepileptic drugs increase the ratio of background synaptic inhibition to excitation and decrease neuronal excitability in neurones of the rat entorhinal cortex in vitro. Neuroscience. 2010; 167: 456–474. doi: 10.1016/j.neuroscience.2010.02.021 PMID: 20167261

56. Moskal JR, Burch R, Burgdorf JS, Kroes RA, Stanton PK, Disterhoft JF, Leander JD. GLYX-13, an NMDA receptor glycine site functional partial agonist enhances cognition and produces antidepressant effects without the psychotomimetic side effects of NMDA receptor antagonists. Expert Opin Investig Drugs. 2014; 23: 243–254. doi: 10.1517/13543784.2014.852536 PMID: 24251380

57. Collingridge GL, Volianskis A, Bannister N, France G, Hanna L, Mercier M, et al. The NMDA receptor as a target for cognitive enhancement. Neuropharmacology. 2013; 64: 13–26. doi: 10.1016/j.neuropharm.2012.06.051 PMID: 22796429

58. Singer W, Gray CM. Visual feature integration and the temporal correlation hypothesis. Annu Rev Neurosci. 1995; 18: 555–586. PMID: 7605074

59. Tiitinen H, Sinkkonen J, Reinikainen K, Alho K, Lavikainen J, Naatanen R. Selective attention enhances the auditory 40- Hz transient response in humans. Nature. 1993; 364: 59–60. PMID: 8316297

60. Tallon-Baudry C, Bertrand O, Peronnet F, Pernier J. Induced gamma-band activity during the delay of a visual short-term memory task in humans. J Neurosci. 1998; 18: 4244–4254. PMID: 9592102

61. Hashimoto K. Targeting of NMDA receptors in new treatments for schizophrenia. Expert Opin Ther Targets. 2014; 18: 1049–1063. doi: 10.1517/14728222.2014.934225 PMID: 24965576

62. Hashimoto K, Malchow B, Falkai P, Schmitt A.Glutamate modulators as potential therapeutic drugs in schizophrenia and affective disorders. Eur Arch Psychiatry Clin Neurosci. 2013; 263: 367–377. doi: 10.1007/s00406-013-0399-y PMID: 23455590

63. Javitt DC, Zukin SR. Recent advances in the phencyclidine model of schizophrenia. Am J Psychiatry. 1991; 148: 1301–1308. PMID: 1654746

64. Krystal JH, Karper LP, Seibyl JP, Freeman GK, Delaney R, Bremner JD, et al. Subanesthetic effects of the noncompetitive NMDA antagonist, ketamine, in humans. 24. Psychotomimetic, perceptual, cognitive, and neuroendocrine responses. Arch Gen Psychiatry 1994; 51: 199–214. PMID: 8122957

65. Weickert CS, Fung SJ, Catts VS, Schofield PR, Allen KM, Moore LT, et al. Molecular evidence of N-methyl-D-aspartate receptor hypofunction in schizophrenia. Mol Psychiatry. 2013; 18: 1185–1192. doi: 10.1038/mp.2012.137 PMID: 23070074

66. Harrison PJ, Owen MJ. Genes for schizophrenia? Recent findings and their pathophysiological implications. Lancet. 2003; 361: 417–419. PMID: 12573388

67. Schwartz TL, Sachdeva S, Stahl SM. Genetic data supporting the NMDA glutamate receptor hypothesis for schizophrenia. Curr Pharm Des 2012; 18: 1580–1592. PMID: 22280435

68. Roopun AK, Cunningham MO, Racca C, Alter K, Traub RD, Whittington MA. Region-specific changes in gamma and beta2 rhythms in NMDA receptor dysfunction models of schizophrenia. Schizophr Bull. 2008; 34: 962–973. doi: 10.1093/schbul/sbn059 PMID: 18544550

69. Middleton S, Jalics J, Kispersky T, Lebeau FE, Roopun AK, Kopell NJ, et al. NMDA receptor-dependent switching between different gamma rhythm-generating microcircuits in entorhinal cortex. PNAS. 2008; 105: 18572–18577. doi: 10.1073/pnas.0809302105 PMID: 18997013

70. Cunningham MO, Hunt J, Middleton S, LeBeau FE, Gillies MJ, Davies CH, Maycox PR, Whittington MA, Racca C. Region-specific reduction in entorhinal gamma oscillations and parvalbumin-immunoreactive neurons in animal models of psychiatric illness. J Neurosci. 2006; 26: 2767–2776. PMID: 16525056

71. Parsons CG, Danysz W, Dekundy A, Pulte I. Memantine and cholinesterase inhibitors: complementary mechanisms in the treatment of Alzheimer's disease. Neurotox Res. 2013; 24: 358–369. doi: 10.1007/s12640-013-9398-z PMID: 23657927

72. Ahnaou A, Huysmans H, Jacobs T, Drinkenburg WH. Cortical EEG oscillations and network connectivity as efficacy indices for assessing drugs with cognition enhancing potential. Neuropharmacology. 2014; 86: 362–377. doi: 10.1016/j.neuropharm.2014.08.015 PMID: 25181033